University of Bath

PHD

Ruthenium N-heterocyclic carbene complexes: C-H activation and catalysis

Paine, Belinda Marie

Award date:
2005

Awarding institution:
University of Bath

Link to publication

General rights
Copyright and moral rights for the publications made accessible in the public portal are retained by the authors and/or other copyright owners and it is a condition of accessing publications that users recognise and abide by the legal requirements associated with these rights.

- Users may download and print one copy of any publication from the public portal for the purpose of private study or research.
- You may not further distribute the material or use it for any profit-making activity or commercial gain
- You may freely distribute the URL identifying the publication in the public portal ?

Take down policy
If you believe that this document breaches copyright please contact us providing details, and we will remove access to the work immediately and investigate your claim.

Download date: 13. May. 2019

Ruthenium N-heterocyclic carbene complexes: C-H activation and catalysis

Belinda Marie Paine

A thesis submitted in partial fulfillment of the requirements for the degree of

Doctor of Philosophy

UNIVERSITY OF
BATH

University of Bath
Department of Chemistry

November 2005

Attention is drawn to the fact that copyright of this thesis rests with its author. This copy of the thesis has been supplied on condition that anyone who consults it is understood to recognise that its copyright rests with its author and that no quotation from the thesis and no information derived from it may be published without the prior written consent of the author.

This thesis may be made available for consultation within the University library and may be photocopied or lent to other libraries for the purposes of consultation.

UMI Number: U206773

All rights reserved

INFORMATION TO ALL USERS
The quality of this reproduction is dependent upon the quality of the copy submitted.

In the unlikely event that the author did not send a complete manuscript
and there are missing pages, these will be noted. Also, if material had to be removed,
a note will indicate the deletion.

UMI U206773
Published by ProQuest LLC 2013. Copyright in the Dissertation held by the Author.
Microform Edition © ProQuest LLC.
All rights reserved. This work is protected against
unauthorized copying under Title 17, United States Code.

ProQuest LLC
789 East Eisenhower Parkway
P.O. Box 1346
Ann Arbor, MI 48106-1346

30 15 MAR 2006
PhD

To
My Family

Contents

	Page no.
Acknowledgements	vi.
Abstract	viii.
Abbreviations	ix.
Chapter 1: Introduction	
1.1 Bonding of N-heterocyclic (NHC) ligands to transition metals	1.
1.1.1 Overview	1.
1.1.2 Steric and electronic effects of NHCs	2.
1.1.3 Basicity of NHCs	7.
1.2 NHCs as ligands in catalysis	9.
1.2.1 ROMP/RCM	9.
1.2.2 Cross-coupling reactions	11.
1.2.3 Hydrosilylation	15.
1.2.4 Hydrogenation reactions	17.
1.2.4.1 Overview	17.
1.2.4.2 Ruthenium-NHC catalysed hydrogenation reactions	20.
1.3 Tandem catalysis	25.
1.3.1 Classification	25.
1.3.2 Ruthenium-NHC complexes in tandem catalysis	26.
1.3.2.1 Metathesis/hydrogenation	26.
1.3.2.2 Metathesis/isomerisation	28.
1.4 Synopsis	29.
1.5 References	30.
Chapter 2: Synthesis and Characterisation of Ru-NHC Complexes	34.
2.1 General routes to metal-NHC complexes	34.
2.2 Syntheses of NHCs	36.
2.2.1 Syntheses of N-aryl substituted NHCs	36.
2.2.1.1 Synthesis of 1,3-bis(2,4,6-trimethylphenyl)imidazol-2-ylidene (IMes)	36.
2.2.1.2 Synthesis of 1,3-bis(2,4,6-trimethylphenyl)imidazolin-2-ylidene (SIMes)	37.

2.2.1.3 Synthesis of 1,3-di-(S)-1'-phenylethylimidazol-2-ylidene (I)* 37.
2.2.2 Syntheses of N-alkyl substituted NHCs 38.
2.2.2.1 Syntheses of tetraalkylimidazol-2-ylidenes 38.
2.2.2.2 Synthesis of 1,3-diisopropylimidazol-2-ylidene 39.
2.3 Syntheses of mono substituted Ru-NHCs 39.
2.3.1 Previous work 39.
2.3.2 Syntheses of N-aryl substituted Ru-NHC complexes 41.
2.3.2.1 Attempted synthesis of Ru(SIMes) 41.
2.3.3 Syntheses of N-alkyl substituted Ru-NHC complexes 43.
2.3.3.1 General procedure 43.
2.3.3.2 Syntheses of $Ru(IMe_4)$ complexes 45.
2.3.3.2.1 Synthesis of $RuH_2(CO)(PPh_3)_2(IMe_4)$ 45.
2.3.3.2.2 Synthesis of $RuH_2(CO)(PPh_3)(IMe_4)_2$ 46.
2.3.3.3 Syntheses of $Ru(IEt_2Me_2)$ complexes 49.
2.3.3.3.1 Synthesis of $RuH_2(CO)(PPh_3)_2(IEt_2Me_2)$ 49.
2.3.3.3.2 Synthesis of $RuH_2(CO)(PPh_3)(IEt_2Me_2)_2$ 51.
2.3.3.4 Syntheses of $Ru(^iPr_2Me_2)$ complexes 54.
2.3.3.4.1 Synthesis of $RuH_2(CO)(PPh_3)_2(I^iPr_2Me_2)$ 54.
2.3.3.4.2 Evidence for $RuH_2(CO)(PPh_3)(I^iPr_2Me_2)_2$ 55.
2.3.3.5 Synthesis of $RuH_2(CO)(PPh_3)_2(I^iPr)$ 55.
2.3.3.6 Synthesis of $RuH_2(CO)(PPh_3)_2(I^*)$ 57.
2.3.3.7 Other alkyl-substituted Ru-NHC complexes synthesised by the Whittlesey group 64.
2.4 Discussion 65.
2.5 Chapter summary 68.
2.6 References 69.

Chapter 3: C-H Bond Activations and Isomerisations of Ru-NHC Complexes 71.
3.1 C-H bond activation 71.
3.1.1 Introduction 71.
3.1.2 C-H bond activation involving NHC ligands 73.
3.1.2.1 Activation of N-aryl NHCs 74.
3.1.2.3 Activation of N-alkyl substituted NHCs 79.
3.2 Activation and Isomerisation of Ru-NHC complexes 81.

3.2.1 $RuH_2(CO)(PPh_3)_2(IEt_2Me_2)$ 82.
3.2.1.1 Activation 82.
3.2.1.2 Isomerisation 85.
3.2.2 $RuH_2(CO)(PPh_3)_2(I^iPr_2Me_2)$ 90.
3.2.2.1 Synthesis of $RuH(CO)(PPh_3)_2(I^iPr_2Me_2)$ 90.
3.2.3 $RuH_2(CO)(PPh_3)_2(I^iPr)$ 96.
3.2.4 $RuH_2(CO)(PPh_3)_2(I^nPr)$ 97.
3.2.5 $RuH_2(CO)(PPh_3)_2(I^*)$ 99.
3.2.6 $RuH_2(CO)(PPh_3)_2(IMe_4)$ 101.
3.3 Discussion 103.
3.3.1 Activation 103.
3.3.2 Isomerisation 104.
3.4 Chapter summary 106.
3.5 References 107.

Chapter 4: Ru-NHC Hydrogenation Reactions and their use in Tandem Catalysis 109.

4.1 Introduction 109.
4.2 Overview of C=C bond formation 109.
4.2.1 The Wittig reaction 110.
4.2.1.1 Mechanism of the Wittig reaction 110.
4.2.2 Preparation of phosphorane ylides 111.
4.3 Project overview 112.
4.4 Hydrogenations: proof of concept 115.
4.4.1 Direct hydrogenations 115.
4.4.2 Transfer hydrogenations 120.
4.4.3 Crossover transfer hydrogenations (CTH) 121.
4.5 Preparation of phosphorane ylides 123.
4.5.1 Phosphonium salt preparation 123.
4.5.2 Phosphorane ylide preparation 124.
4.6 Indirect Wittig reactions 125.
4.6.1 Initial results 125.
4.6.2 Oxidation of 4-fluoro-α-methylbenzylalcohol with acetone 126.
4.6.3 Reduction of trimethylvinylsilane 128.

4.6.4 Crossover transfer hydrogenations (CTH) 130.
4.7 One-pot tandem process 132.
4.7.1 Activity of Ru-NHC complexes 132.
4.7.2 *In situ* preparation of Ru-NHC catalysts 135.
4.7.3 Effect upon variation of ylide 136.
4.7.4 Effect upon variation of alcohol substrate 140.
4.8 Discussion 143.
4.9 Chapter summary 145.
4.10 References 146.

Chapter 5: Experimental 147.
5.1 General Procedures 147.
5.2 Physical and analytical measurements 147.
5.3 Syntheses of N-heterocylic carbenes 148.
5.3.1 Preparation of 1,3-bis(2,4,6-trimethylphenyl)imidazol-2-ylidene (IMes) 148.
5.3.2 Preparation of 1,3-bis(2,4,6-trimethylphenyl)imidazolin-2-ylidene (SIMes) 149.
5.3.3 Preparation of 1,3,4,5-tetramethylimidazol-2-ylidene (IMe_4) 150.
5.3.4 Preparation of 1,3-diethyl-4,5-dimethylimidazol-2-ylidene (IEt_2Me_2) 151.
5.3.5 Preparation of 1,3-diisopropyl-4,5-dimethylimidazol-2-ylidene ($I^iPr_2Me_2$) 152.
5.3.6 Preparation of 1,3-diisopropylimidazol-2-ylidene (I^iPr) 153.
5.3.7 Preparation of 1,3-bis((S)1-phenylethyl)imidazol-2-ylidene (I*) 154.
5.3.8 Preparation of 1,3-bis(cyclohexyl)-imidazol-2-ylidene (ICy) 155.
5.3.9 Synthesis of 1,3-bis(*n*-propyl)-imidazol-2-ylidene 156.
5.4 Syntheses of Ruthenium Precursors 158.
5.5 Syntheses of Ruthenium-NHC Complexes 158.
5.5.1 Syntheses of RuIMes Complexes 158.
5.5.2 Syntheses of $RuIMe_4$ Complexes 160.
5.5.3 Syntheses of $RuIEt_2Me_2$ Complexes 162.
5.5.4 Syntheses of $RuI^iPr_2Me_2$ Complexes 165.
5.5.5 Syntheses of RuI^iPr Complexes 167.
5.5.6 Syntheses of RuI* Complexes 169.
5.5.7 Syntheses of RuICy Complexes 170.
5.5.8 Synthesis of $RuH_2(CO)(PPh_3)_2(^nPr)$ 173.
5.6 Direct hydrogenations of alkenes and alkynes 173.

5.6.1 Direct hydrogenations in Young's NMR tubes: general procedure 1 173.
5.6.2 Direct hydrogenations using a autoclave: general procedure 2 176.
5.7 Transfer hydrogenations of alkenes and alkynes 177.
5.7.1 General procedure 3 177.
5.7.2 Transfer hydrogenations of alkenes and alkynes with two equivalents of IPA 177.
5.7.3 Transfer hydrogenations of alkenes and alkynes with five equivalents of IPA 178.
5.7.4 *In situ* transfer hydrogenation reactions monitored inside the 400 MHz NMR spectrometer 178.
5.8 Crossover transfer hydrogenations (CTH) 179.
5.8.1 General procedure 4 179.
5.8.2 Synthesis of benzyl dihydrocinnamate 179.
5.8.3 Synthesis of benzaldehyde 179.
5.8.4 Synthesis of acetophenone 179.
5.9 Syntheses of ylides 179.
5.9.1 Preparation of stabilised phosphorane ylides: general procedure 5 179.
5.9.2 Preparation of (triphenylphosphoranylidene)acetonitrile 180.
5.9.3 Preparation of benzyl (triphenylphosphoranylidene)acetate 181.
5.9.4 Preparation of *tert*-butyl (triphenylphosphoranylidene)acetate 182.
5.9.5 Preparation of ethyl (triphenylphosphoranylidene)pyruvate 183.
5.9.6 Preparation of *N,N*-dimethyl(triphenylphosphoranylidene)acetamide 184.
5.9.7 Preparation of *N*-methyl,*N*-methoxy(triphenylphosphoranylidene) acetamide 185.
5.9.8 Preparation of (triphenylphosphoranylidene)acetone 185.
5.10 Indirect Wittig reactions 186.
5.10.1 General procedure 6 186.
5.11 References 191.

Appendices 192.
Appendix 1: Crystallographic data, bond lengths and angles for 57. 192.
Appendix 2: Crystallographic data, bond lengths and angles for 85a. 196.
Appendix 3: Crystallographic data, bond lengths and angles for 58. 200.
Appendix 4: Crystallographic data, bond lengths and angles for 62a. 204.
Appendix 5: Crystallographic data, bond lengths and angles for 59a. 208.
Appendix 6: Crystallographic data, bond lengths and angles for 55. 214.
Appendix 7: Crystallographic data, bond lengths and angles for 60. 219.

Acknowledgements

Foremostly I would like to thank my supervisors, Mike Whittlesey and Jon Williams fosr giving me the opportunity to carry out this research on a project with such limitless potential. I have been very fortunate to have two supervisors who have both been very supportive and enthusiastic throughout the three years. Your advice and encouragement has ensured that the research has been very rewarding.

Throughout the last three years I have had the opportunity to work with some great lab mates. I especially want to thank Susie for being such a good friend over the last three years. It's been great to have someone to share the experience with right from the outset. Thank you for some unforgettable moments, my funniest memories from the PhD all seem to involve you! Also, Suzanne, who has not only been an excellent post-doc, but also a great friend. Thanks for your encouragement when things weren't always going to plan. And Sarah for always being cheery and, most importantly, for completing the all-female Whittlesey lab group! Boys are stupid, throw rocks at them! It has been great fun working with all of you; I couldn't have wished to work with nicer people.

I also want to thank Rudolph who taught me so much in the lab when I first arrived, and Mike E. who was very encouraging and gave me a lot of advice on the project. Their combined work efforts were the foundation to my research and the collaboration project between the Whittlesey and Williams groups. Thanks also to the boys in the Williams lab, especially Paul for his help on the organic side of the project.

I would also like to acknowledge Steve Bull who gave me the encouragement to start a PhD and has always been there for me if I needed him; John Lowe for your help with NMR spectroscopy and Mary Mahon for solving my crystal structures.

Over the past three years I have met some good friends. I won't mention everyone here but special thanks go to Dawn who has been a fantastic friend, Gillian, Marek, Carly, Purvi, Gemma and Nico, thank you all for making my experience at Bath a great one!

Most of all I want to thank my family who have all been amazing. I'm so lucky to have all of you and want to thank you for everything you have done for me. Thanks Mum and Dad for always being there for me, for your love and support and for giving me a place I can always call home. Also to Mark, Nigel and especially Carina for your constant "on-call" help, I am extremely thankful to all of you. Finally many thanks go to Biagio for giving me continued love, support and encouragement when things weren't going so well. Thanks for putting up with me. I've finally finished!

Abstract

This thesis describes the development of ruthenium N-heterocyclic carbene complexes, their C-H activation processes and applications in catalysis. The dihydride ruthenium N-heterocyclic carbene (NHC) complex $RuH_2(CO)(PPh_3)_2(IMes)$ has been established as an efficient catalyst for both the direct and transfer hydrogenation of alcohols, ketones and alkenes. The transfer hydrogenation capabilities have subsequently been exploited in a novel method for the formation of new C-C bonds from alcohols *via* an indirect Wittig reaction. The concept of catalytic electronic activation is utilised whereby hydrogen is borrowed from the alcohol to allow temporary oxidation to occur. A C=C bond forming reaction can then take place on the aldehyde before hydrogen is subsequently returned to obtain the target alkane.

A new series of N-alkyl substituted Ru-NHC complexes $RuH_2(CO)(PPh_3)_2(NHC)$ (NHC = IMe_4, IEt_2Me_2, $I^iPr_2Me_2$, I^iPr and I*) have been prepared. Addition of alkene to $RuH_2(CO)(PPh_3)_2(NHC)$ leads to C-H activation of the NHC ligand to afford $RuH(CO)(PPh_3)_2(NHC')$ for NHC = IEt_2Me_2, $I^iPr_2Me_2$, I^iPr and I*). The C-H activation reaction is reversible and reforms the dihydride precursors with either H_2 or alcohols. These have been fully characterised by multinuclear NMR spectroscopy and X-ray crystallography. The activity of these complexes has been investigated for the *in situ* Wittig reaction. A lowering of reaction times and temperatures occurs upon using the Ru-NHC complexes. Thus the reaction of benzyl alcohol with (triphenylphosphoranylidene)acetonitrile affords dihydro cinnamonitrile in 79% yield after 72 h at 150 °C with $[Ir(COD)Cl]_2$/dppf/Cs_2CO_3 but goes to 97% conversion in 3 h at 70 °C with $RuH_2(CO)(PPh_3)_2(I^iPr_2Me_2')$.

Abbreviations

Ar	Unspecified aryl group
atm	Atmospheres
Bn	Benzyl
CAE	Catalytic Electronic Activation
COD	Cyclooctadiene
COSY	Correlation Spectroscopy
Cp*	Pentamethylcyclopentadienyl
CTH	Crossover Transfer Hydrogenations
DCM	Dichloromethane
DMSO	Dimethylsulfoxide
ee	Enantiomeric excess
Et	Ethyl
Equiv.	Equivalents
g	Grams
GC	Gas chromatography
h	Hours
HMBC	Heteronuclear Multiple-Bond Correlation
HMQC	Heteronuclear Multiple Quantum Coherance
Hz	Hertz
i	*iso*
ICy	1,3-bis(cyclohexyl)-imidazol-2-ylidene
IEt_2Me_2	1,3-diethyl-4,5-dimethylimidazol-2-ylidene
I^nPr	1,3-bis(*normal*-propyl)-imidazol-2-ylidene
I^iPr	1,3-diisopropylimidazol-2-ylidene
$I^iPr_2Me_2$	1,3-diisopropyl-4,5-dimethylimidazol-2-ylidene
IMe_2	1,3-dimethylimidazol-2-ylidene
IMe_4	1,3,4,5-tetramethylimidazol-2-ylidene
IMes	1,3-bis(2,4,6-trimethylphenyl)imidazol-2-ylidene
IPA	Isopropanol (2-propanol)
^iPr	*iso*-propyl
IR	Infra-red

I*	1,3-bis((*S*)1-phenylethyl)imidazol-2-ylidene
J	Coupling constant
L	Generic metal ligand
m	*meta*
M	Molar
mmol	Millimoles
mol	Moles
Me	Methyl
MPV	Meerwein-Ponndorf-Verlay
MPVO	Meerwein-Ponndorf-Verlay-Oppenauer
n	*normal*
NMR	Nuclear Magnetic Resonance
NOESY	Nuclear Overhauser Enhancement Spectroscopy
o	*ortho*
p	*para*
Ph	Phenyl
ppm	Parts per million
Pr	Propyl
py	Pyridine
R	Unspecified generic group
rt	Room temperature
SIMes	1,3-bis(2,4,6-trimethylphenyl)imidazolin-2-ylidene
t	*tert*
*t*Bu	*tert*-butyl
THF	Tetrahydrofuran
VT	Variable Temperature

Chapter 1

Chapter 1: Introduction

1.1 Bonding of N-heterocyclic (NHC) ligands to transition metals

1.1.1 Overview

Since their first isolation by Arduengo in 1991,[1] N-heterocyclic carbenes (NHCs) have become popular ligands for transition metals. Their unique electronic properties, recent commercial availability, and the suggestions of increased stability of the metal complexes all contribute to their appeal.

Many studies have indicated that nucleophilic carbenes possess similar electronic properties to electron rich phosphine ligands, i.e. they are strong σ donors with negligible π-accepting ability. However, NHCs have been shown to have high thermal stability, whereas their phosphine counterparts suffer from P-C bond degradation at elevated temperatures. While in some systems carbenes have shown a higher *trans* effect than P-donor ligands,[2] other systems have shown this not to be the case.[3] In any case, NHC ligands confer different electronic properties onto the metal, and hence modify any potential catalytic behaviour.

As with phosphines, substituent groups can allow tuning of the steric and electronic properties of the NHC ligand. Subsequently, organometallic complexes containing NHCs have been used successfully for ruthenium catalysed alkene metathesis,[4-6] iridium catalysed hydrogenation and hydrogen transfer,[7,8] platinum[9,10] and rhodium[11] catalysed hydrosilylation, and palladium catalysed C-C coupling reactions.[12,13] The most commonly used NHCs for these reactions are represented in Table 1.1.

R	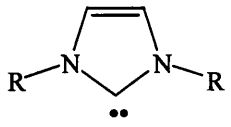	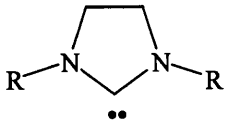
4-methylphenyl	ITol	-
2,4,6-trimethylphenyl	IMes	SIMes
2,6-diisopropylphenyl	IPr	SIPr
cyclohexyl	ICy	-
tert-butyl	I^{t}Bu	-
adamantyl	IAd	-

Table 1.1 *Most widely used NHCs in catalysis.*

1.1.2 Steric and electronic effects of NHCs

Pioneering studies on the phosphine ligand class by Tolman[14] in the 1970s led to the rapid development of new and improved phosphine ligands for catalysis. It is only recently that analogous binding studies on NHCs have begun.

In 1999 Nolan compared electronic and steric properties of bulky NHC ligands with the best phosphine donor ligands on an unsaturated ruthenium complex (Scheme 1.1, Cp*=η^5-C_5Me_5).[15] Bond dissociation energies (BDEs) were calculated by dividing the experimentally determined reaction enthalpies by the number of bonds formed (four) (Table 1.2). The results revealed that the NHCs studied were better donor ligands than the phosphines, with only the sterically demanding adamantyl NHC as an exception. These results were verified by performing ligand exchange reactions whereby NHCs were shown to displace the phosphines.

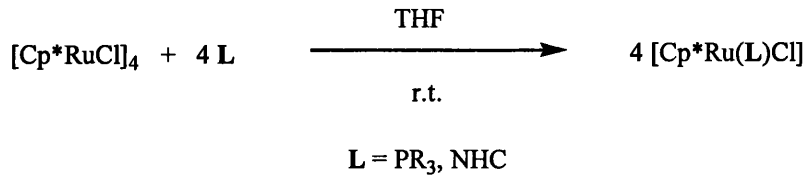

Scheme 1.1 *Ligand substitution with reactions of [Cp*RuCl]$_4$.*

L	R		$-\Delta H_{rxn}$ (kcal/mol)	relative BDE (kcal/mol)
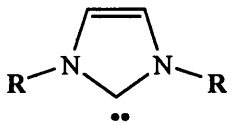	cyclohexyl	ICy	85.0(0.2)	21.2
	4-methylphenyl	ITol	75.3(0.4)	18.8
	4-chlorophenyl	IpCl	74.3(0.3)	18.6
	2,4,6-trimethylphenyl	IMes	62.6(0.2)	15.6
	adamantyl	IAd	27.4(0.4)	6.8
PCy_3			41.9(0.2)	10.5
P^iPr_3			37.4(0.3)	9.4

Table 1.2 *Experimental BDEs for NHCs and phosphines.*

The steric profile of phosphines is described by the cone angle, θ, a measure of the "cone" swept out by the ligand at the metal centre (Figure 1.1). The wider the angle of the cone the greater the steric influence of the ligand. A cone angle cannot be defined for the NHC system since NHC ligands are more two dimensional than phosphine ligands. Hence Nolan proposed a model whereby a sphere is imposed around the metal centre and the volume that the NHC occupies in that sphere is taken as the steric parameter, $\%V_{Bur}$ (Figure 1.1).[16] Their test calculations indicated that a radius of 3 Å is reasonable for the sphere centred on the metal, which so happens to be approximately the same distance as between the N atoms and the metal centre. This model now allows comparisons of steric factors between NHCs and phosphine ligands. Table 1.3 shows that on steric grounds SIPr and IPr are comparable to P^tBu_3 while the smaller ICy ligand is similar to PPh_3.

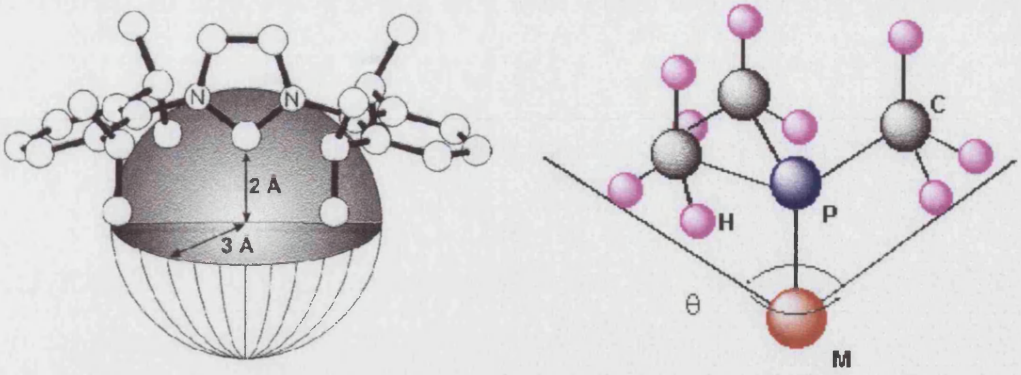

Figure 1.1 *Sphere dimensions for steric parameter determination ($\%V_{Bur}$) of NHC ligands and cone angle (θ) for phosphines.*[16]

Free Ligand	$\%V_{Bur}$	Free Ligand	$\%V_{Bur}$
SI^{t}Bu	38	SIMes	27
I^{t}Bu	37	IMes	26
IAd	37	ICy	23
P^{t}Bu$_3$	30	PPh_3	22
SIPr	30	PH_3	17
IPr	29		

Table 1.3 *Calculated $\%V_{Bur}$ of free NHC and PR_3 ligands.*

Nolan and co-workers also compared BDEs of saturated and unsaturated NHC ligands in Cp*Ru(L)Cl.[16] They concluded that saturated NHCs, in the absence of steric effects, do bind more strongly than their unsaturated analogues but by no more than 2-3 kcal mol^{-1}. Since shorter Ru-C bond lengths are predicted for saturated systems, steric effects are enhanced. For the bulky IPr systems, the unsaturated ligand actually binds more strongly than the saturated ligand by 0.7 kcal mol^{-1}. Results of experimental BDEs were plotted against calculated $\%V_{Bur}$ (Figure 1.2). A linear relationship was established indicating that BDEs are essentially controlled by steric requirements of the ligand and that $\%V_{Bur}$ does in fact capture the different steric requirements of the different ligands.

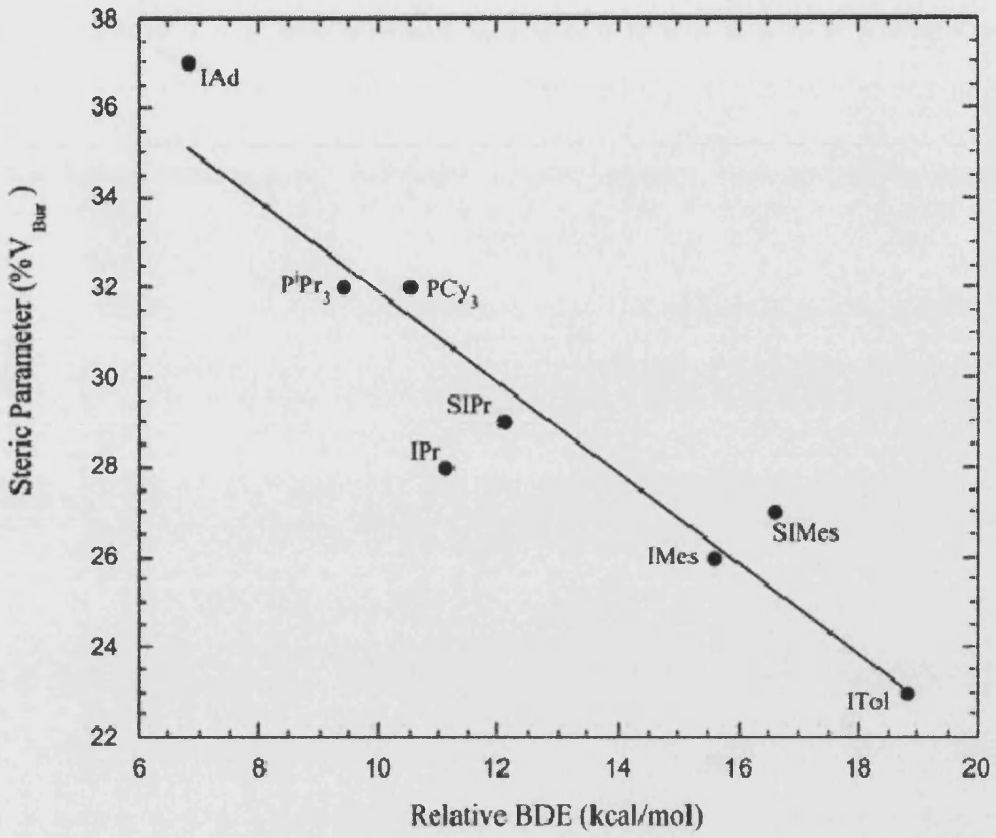

Figure 1.2 *Relative bond dissociation enthalpy (kcal/mol) vs. steric parameter (%V_{Bur}) in the Cp*Ru(L)Cl system.*[16]

NHC ligands are now thought to be electronically much more flexible than their phosphine counterparts and hence the electronic effects of NHC ligands are considered as important as their steric effects. The initial conception of NHC ligands being almost pure σ-donors was based on the "single-bond" character of the metal-NHC interactions deduced from crystallographically determined bond distances.[17] However, later studies have shown that filled and empty π, π* orbitals on the NHC imidazole ring can contribute to the metal-NHC bond. Their electronic flexibility enables stabilisation of electron rich metals through d → π* back-donation and stabilisation of electron deficient metals through π → d donation. The molecular orbitals involved in bonding from NHCs to metals are shown in Figure 1.3(a).

Evidence for π-bonding between metal ions and p-π orbitals of an NHC was found computationally for the first time by Meyer and co-workers in 2003.[18] Density functional theory calculations (DFT) were performed on a synthesised tridentate NHC-silver complex and visual inspection of the shape of the calculated molecular orbitals revealed evidence for significant π-interaction between the carbene ligands and the silver ions. The simplified d-π back-donation scheme is shown in Figure 1.3(c).

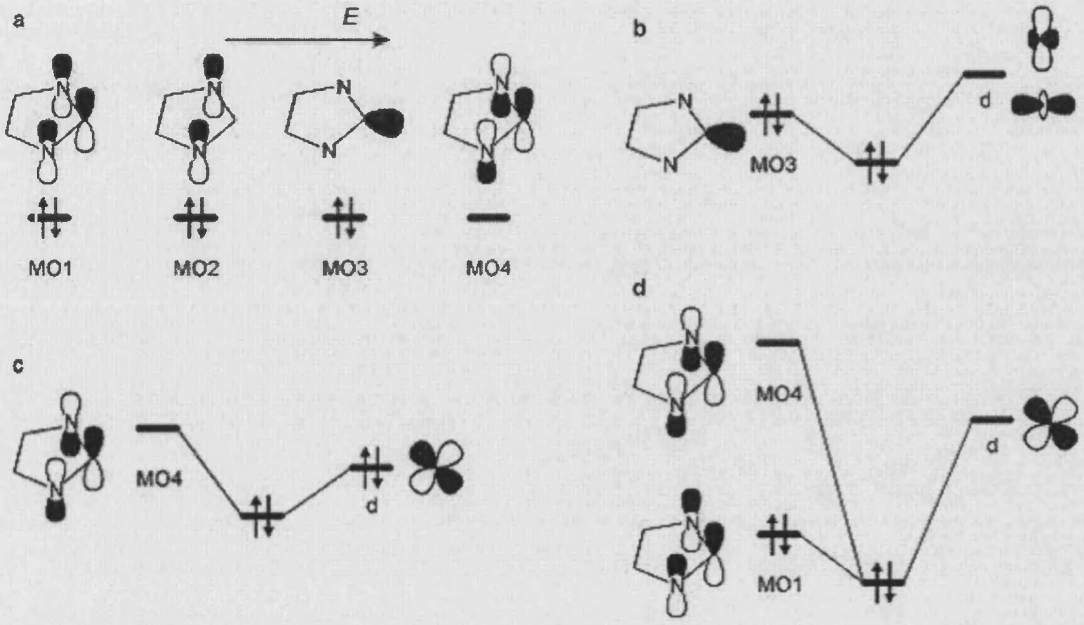

Figure 1.3 *Schematic representation of: (a) the most important NHC molecular orbitals (MO) involved in the NHC–metal bonding, (b) the NHC-to-metal σ → d donation, (c) the metal-to-NHC d → π* donation and (d) the NHC → metal π → d donation.*[18]

Cavallo and co-workers further studied the concept that NHC ligands are not just simple σ-donors.[17] They used molecular orbital analysis to study an iridium-NHC complex $[Ir(I^tBu')_2]PF_6$ (**1**), in which both the I^tBu ligands had undergone C-H bond activation. There was no evidence for agostic interactions into the two vacant coordination sites, despite the close proximity of the ^tBu C-H bonds. This is in agreement with X-ray structures of similar systems. The molecular orbital analysis revealed donation of electron density from the filled π-orbital of the NHC to the empty d-orbitals of the Ir

(Figure 1.3(d)), perhaps offering an explanation for the unusual stability exhibited by the 14-electron complex **1**.

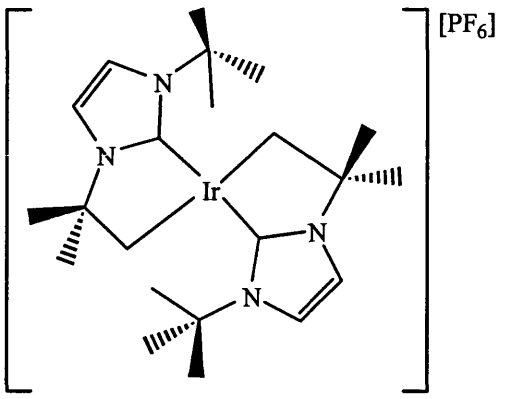

1

1.1.3 Basicity of NHCs

Cavell and co-workers made theoretical predictions of the basicity of nucleophilic carbenes in water and compared them to experimental values of common phosphines in aqueous solution (Table 1.4).[19] Even the most basic phosphine shown (P^tBu_3) is ~10 pK_a units less basic than the least basic carbene (**L12**). The high basicity predicted for the acyclic bis(dimethylamino)carbene **L11** reported along with the low wavenumber for the carbonyl stretching frequencies (2057 cm^{-1} and 1984 cm^{-1}) of the rhodium dicarbonyl(bis(diisopropylamino)) complex **2** reported by Herrmann and co-workers support the suggestion that the bis(diisopropylamino) carbene is the most basic carbene reported to date.[20] The CO stretching frequency is inversely related to the amount of backbonding from the metal centre. Therefore a strong σ-donor (i.e. basic) ligand, induces good π-back donation to the C≡O π* orbital, weakening the bond, thus resulting in a low frequency (wavenumber).

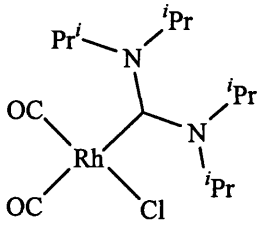

2

The thiazole–based carbene (**L12**) displayed the lowest pK_a out of the carbenes considered. Although nitrogen is more electronegative than sulphur, sulphur has the ability to absorb electron density and has a greater affinity to be polarised. It is well known that imidazolium ions are more basic than thiazolium ions.[19] The general trends of donor properties found by Cavell coincide with experimental data of Nolan, however Nolan reports that the electronic factors related to the σ-donor abilities of these ligands are unlikely to play a major role in the differences in catalytic activity for unsaturated versus saturated NHCs.[21]

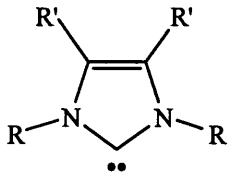

L1 R=Me, R'=H **L2** R=Me, R'=Me **L3** R=Me, R'=Cl
L4 R=^{i}Pr, R'=H **L5** R=^{t}Bu, R'=H **L6** R=^{i}Pr, R'=Me
L7 R=Ph, R'=H **L8** R=2,6-Xyl, R'=H

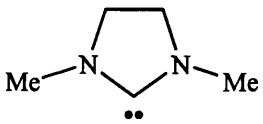

L9

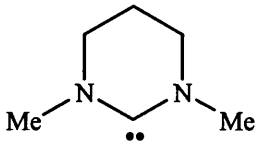

L10

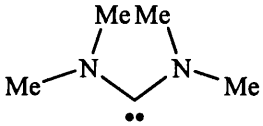

L11

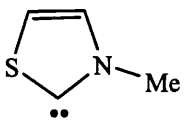

L12

Compound	pK_a (H_2O)	Compound	pK_a (H_2O)
L1	27.4 ± 0.4	**L11**	34.0 ± 0.3
L2	29.5 ± 0.3	**L12**	21.2 ± 0.2
L3	23.4 ± 0.2	P(*p*-ClC_6H_4)$_3$	1.03
L4	28.2 ± 0.3	PPh_3	2.73
L5	28.3 ± 0.1	P(*p*-MeC_6H_4)$_3$	3.84
L6	30.4 ± 0.3	PMe_3	8.65
L7	22.0 ± 0.1	PEt_3	8.69
L8	22.6 ± 0.1	PCy_3	9.70
L9	28.5 ± 0.4	P^{t}Bu$_3$	11.40
L10	33.7 ± 0.3		

Table 1.4 *Calculated basicities of NHCs **L1-L12** and common phosphines in aqueous solution.*

Overall, the introduction of NHC ligands should generate more electron rich metal centres, and this could have a significant effect on bond activation processes that are central to many catalytic schemes.

1.2 NHCs as ligands in catalysis

1.2.1 ROMP/RCM

The greater thermal stability of metal-NHC complexes compared with metal-phosphine complexes has led to the exploitation of NHCs in homogeneous catalysis. Replacement of phosphines by NHC ligands has also been shown to confer greater reactivity on transition metal catalysts. Perhaps the best example of the beneficial effect that NHCs can have comes from the later generation Grubbs alkene metathesis and ROMP/RCM catalysts.[6]

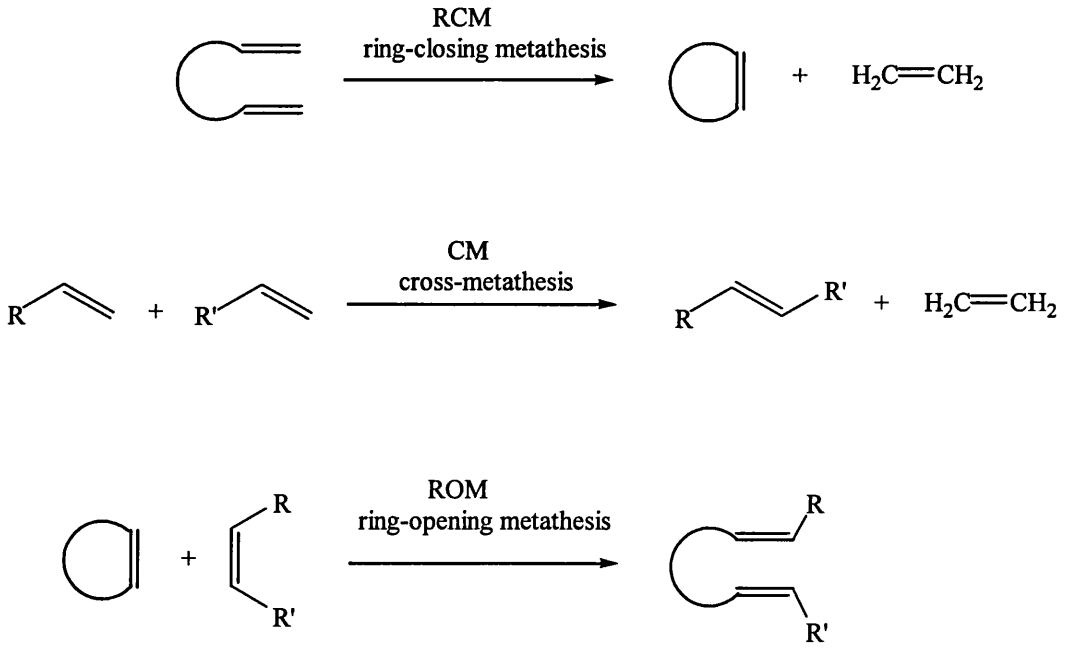

Scheme 1.2 *Three variants of Alkene Metathesis.*

Over the past two decades, alkene metathesis has emerged as a mild and efficient method for the formation of carbon-carbon double bonds as shown in Scheme 1.2.[22] Complexes **3** and **4** are routinely employed for these reactions. The Grubbs catalyst (**3**) is particularly useful because it is highly tolerant of organic functionality and has higher

moisture and atmospheric oxygen stability relative to those of the extremely sensitive molybdenum system (**4**).[15,22] However, despite excellent functional group compatibility, the substrates are limited to electron rich alkenes that are somewhat removed from heteroatom functionality.[23] This limitation was overcome by simple substitution of one PCy_3 group with an NHC producing new alkylidenes such as **5**. While maintaining the diverse functional group tolerance of **3**, **5** permits chemistry on a wider scope of substrates, in addition to permitting lower catalyst loadings and reaction times compared to the parent complex **3**.

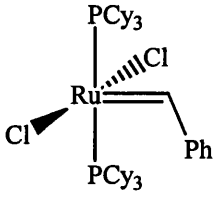

3

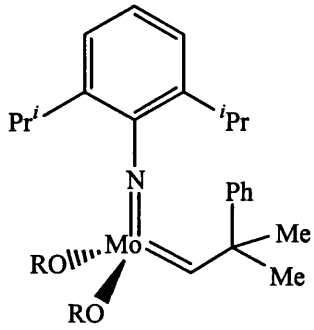

4 R = $CMe(CF_3)_2$

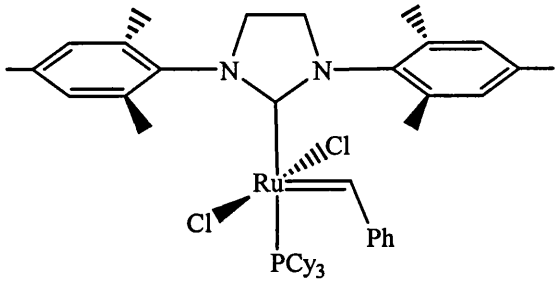

5

Several mechanistic studies of alkene metathesis reactions catalysed by complex **3** have been undertaken and shown that phosphine dissociation is a crucial step in the reaction pathway.[24] Subsequent studies by Grubbs and co-workers were carried out to better understand the differences in reactivity between **3** and **5**.[3,25] The mechanism of the ligand substitution of phosphine with alkene substrate was examined and it was found that phosphine exchange was in fact slower with **5** than **3**; an *inverse* relationship between phosphine exchange rate and alkene metathesis activity. Scheme 1.3 outlines the mechanism that **3** and **5** are thought to follow. The initial substitution of phosphine for alkene substrate in both cases proceeds in a dissociative fashion and involves a 14-electron intermediate which can either be trapped by PCy_3 to reform the starting alkylidene, or bind alkene substrate on the way to alkene metathesis. Hence the activity of the catalyst is dependent on the rate of alkene binding (k_2) versus recoordination of phosphine (k_{-1}) in addition to the initial phosphine dissociation rate (k_1). Differences in activity between **3** and **5** that had previously been attributed to faster phosphine dissociation with **5** instead proved to be due to the ability of **5** to bind alkenes more

rapidly in the presence of free phosphine. As such, the NHC complex performs multiple catalytic turnovers before being quenched.

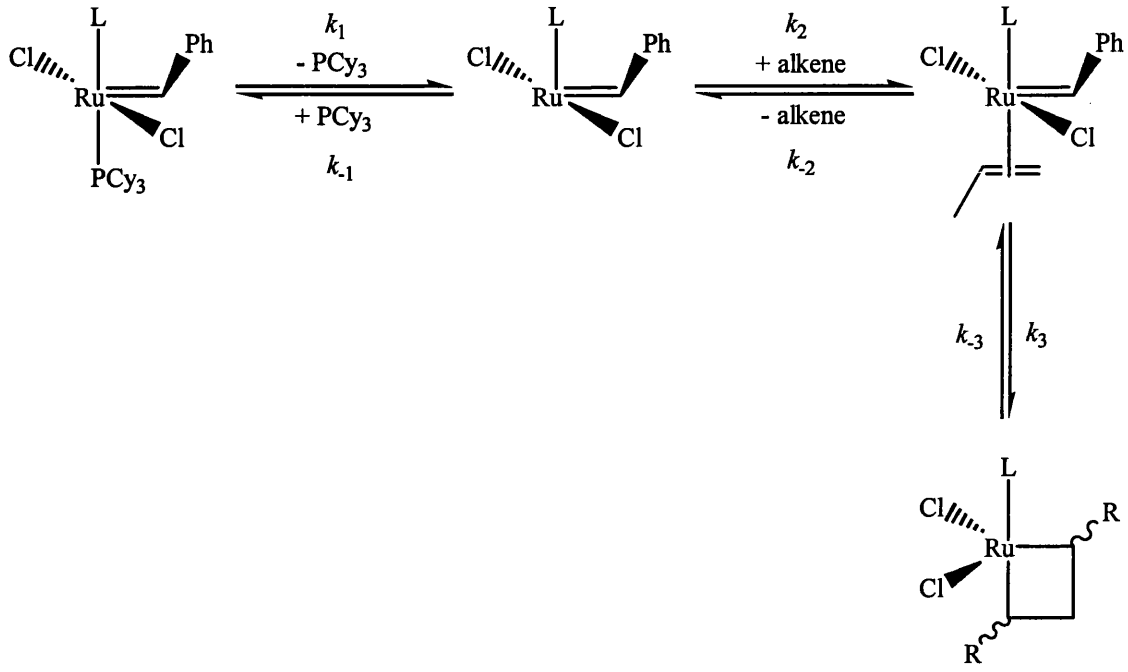

Scheme 1.3 *Mechanism of alkene metathesis reactions catalysed by 3 and 5.*

1.2.2 Cross-coupling reactions

The stability imparted by the NHC ligands to metal centres is further observed in palladium chemistry. Many NHC palladium-based complexes have displayed superior reactivity to their phosphine analogues in a variety of cross coupling reactions such as Heck,[26-29] Suzuki-Miyuara,[30-32] Stille,[32,33] Sonogoshira[32,34] and Kumada[32,35] reactions. The ability of NHCs to stabilise low valent Pd systems is probably responsible for the enhanced activity in these cases.[36]

The first report of NHCs being used as ligands in active C-C bond forming catalysts came from Herrmann and co-workers in 1995 where iodo palladium-carbene complexes were used as catalysts for the Heck reaction.[27] The Heck reaction couples an alkene with a halide or triflate to make a new alkene and is one of the most synthetically useful palladium-catalysed reactions (Scheme 1.4).[37] It is generally accepted that the reaction follows a catalytic pathway *via* a Pd(0)-Pd(II) cycle when it is catalysed by bis-phosphine complexes. Critical for the success of this reaction is the easy formation of

low-coordinate Pd(0) complexes. Studies by Herrmann revealed similar involvement of a Pd(0) species in catalysts bearing NHC ligands.[27] Herrmann found that there were short induction periods for Pd(II) catalysts, whereas Pd(0) complexes required no induction period. Induction periods were rapidly reduced upon addition of a reducing agent to the Pd(II) species.

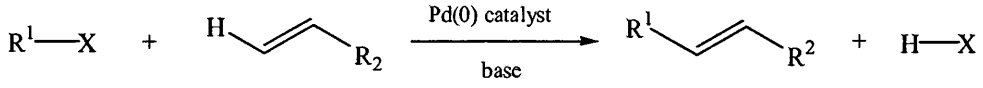

Scheme 1.4 *The Heck Reaction.*

Recent work by Nolan,[38] Hartwig[39,40] and Cloke[41] and co-workers on reactions involving R-X with a $Pd(NHC)_2$ precatalyst suggest formation of a PdL fragment which then undergoes oxidative addition of the R-X fragment, continuing along the same catalytic pathway as proposed for analogous Pd-phosphine complexes (Scheme 1.5).[32,41] Detailed kinetic studies by Cloke[42] suggest that oxidative addition reactions proceed via a 12-electron Pd(0)-NHC complex. Oxidative addition products of the type $Pd(4\text{-}RC_6H_4)Cl(I^tBu)_2$ (R = Me, CO_2Me, OMe) were shown to dissociate free carbene reversibly suggesting that the three-coordinate species was the most likely intermediate in these reactions.

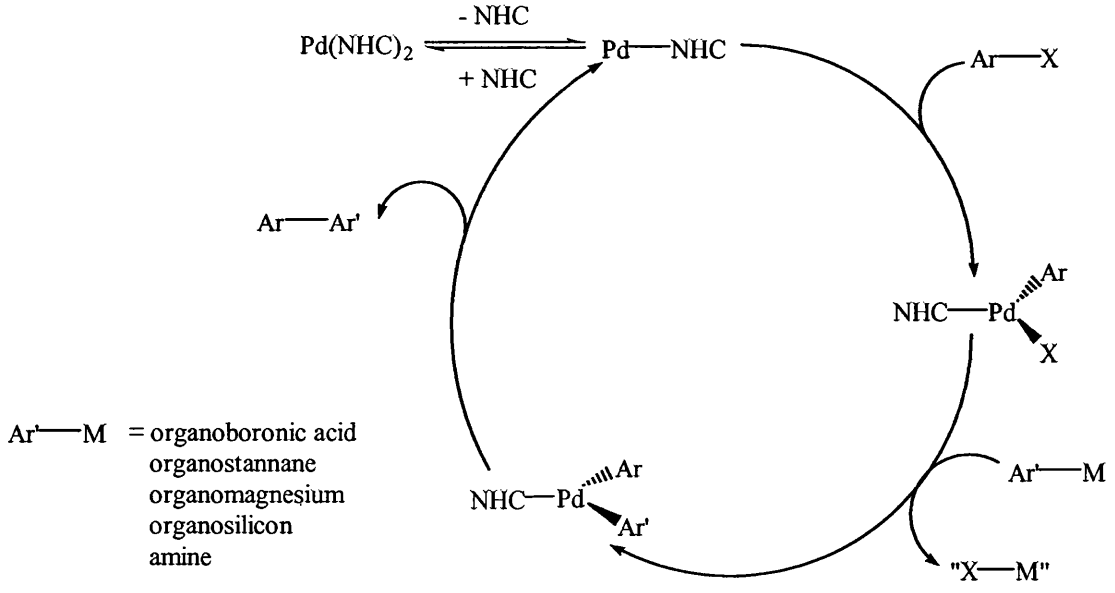

Scheme 1.5 *Proposed mechanism for palladium catalysed cross-coupling reactions.*

Cavell and co-workers have synthesised the bis-carbene complexes $Pd(MAH)(IMe_4)_2$ (**6**) and $Pd(TCNE)(IMe_4)_2$ (**7**) for studies of carbon-carbon coupling processes.[28] NMR and IR spectroscopic methods revealed significant Pd to alkene back-bonding in these species reflecting the electron density induced on the metal centre by the NHCs. Both complexes readily underwent oxidation reactions typical of Pd(0) and complex **7** was shown to be extremely reactive in Suzuki coupling reactions. Coupling of 4-bromo-acetophenone with phenylboronic acid catalysed by 1 x 10^{-3} mol% **7** gave a turnover number of > 55,000.

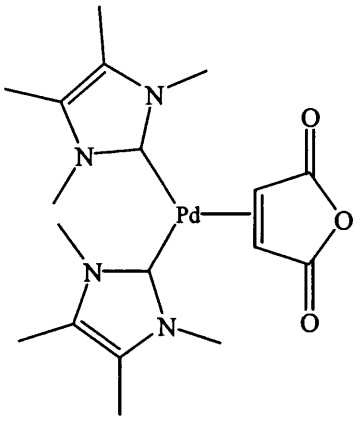

6

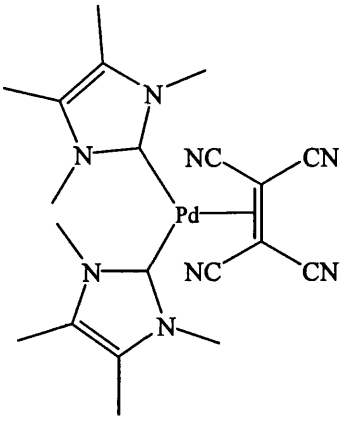

7

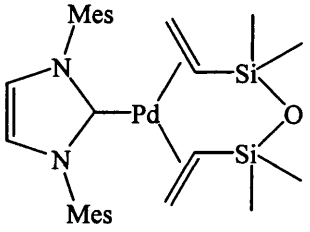

8

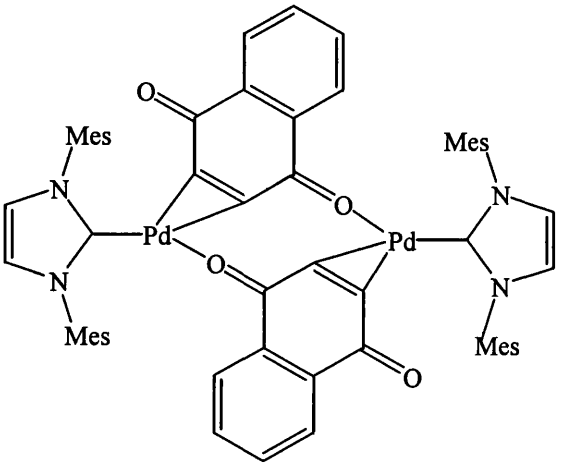

9

Beller and co-workers have synthesised a range of monocarbene(bisalkene)palladium(0) complexes for use in Heck and Suzuki reactions.[29,31] Addition of IMes to the known palladium complexes $[Pd_2(dae)_3]$ (dae = diallyl ether), [Pd(cod)(NQ)] (NQ = 1,4-naphthoquinone) and [Pd(cod)(BQ)] (BQ = *p*-benzoquinone) gave the complexes **8-10**

respectively. Complexes **8-10** were compared in the Heck reaction of both activated and non-activated chlorobenzenes with styrene (Scheme 1.6).[29] Complex **8** decomposed to palladium black when higher temperatures were applied, whereas no decomposition of either **9** or **10** was observed. Complexes **9** and **10** have subsequently shown remarkable activity and selectivity in a number of Heck reactions.[15] These results support the idea that the active species in NHC Pd-mediated organic transformations appears to be a Pd(0) centre. Some results are outlined in Table 1.5.[29]

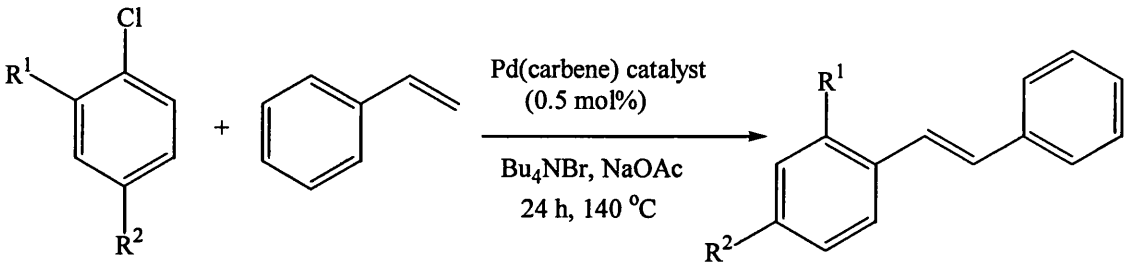

Scheme 1.6 *Pd-catalysed Heck reaction of aryl chlorides with styrene.*

Entry	R^1	R^2	Pd catalyst	Conversion(%)	Yield (%)
1	H	H	**8**	23	14
2	H	H	**9**	69	62
3	H	H	**10**	71	62
4	H	NO_2	**9**	100	92
5	H	NO_2	**10**	100	88
6	H	$COCH_3$	**9**	100	96
7	H	$COCH_3$	**10**	100	97
8	H	CF_3	**9**	88	86
9	H	CF_3	**10**	93	84
10	CN	H	**9**	100	94
11	CN	H	**10**	100	99

Table 1.5 *Pd-catalysed Heck reaction of aryl chlorides.*

1.2.3 Hydrosilylation

Hydrosilylation (Scheme 1.7) is a reaction of high commercial importance for the synthesis of silicon containing monomers.[22]

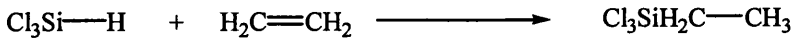

Scheme 1.7 *Alkene Hydrosilylation.*

The first tested example of NHC ligands used in catalysis to perform hydrosilylation reactions came from Herrmann and co-workers in 1996.[11] The enantiomerically pure rhodium complexes **11** and **12** catalysed the hydrosilylation of acetophenone with Ph_2SiH_2 without an induction period, even at low temperatures. Almost quantitative conversions were achieved with > 30 % ee.

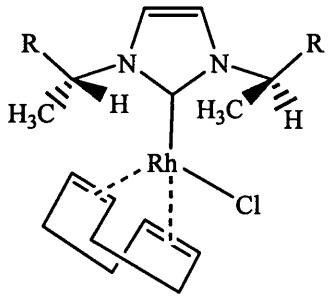

	R
11	C_6H_5
12	$C_{10}H_7$

There have been two recent examples in the literature of Ru-NHC catalysed hydrosilylation reactions. The first example reports the asymmetric addition of the Si-H bond to ketones.[43] Bis-paracyclophane based NHC ligands were generated from the corresponding imidazolium salts and silver triflate *in situ* to produce a catalyst for the hydrosilylation of arylmethylketones (Scheme 1.8). Representative results are given in Table 1.6.

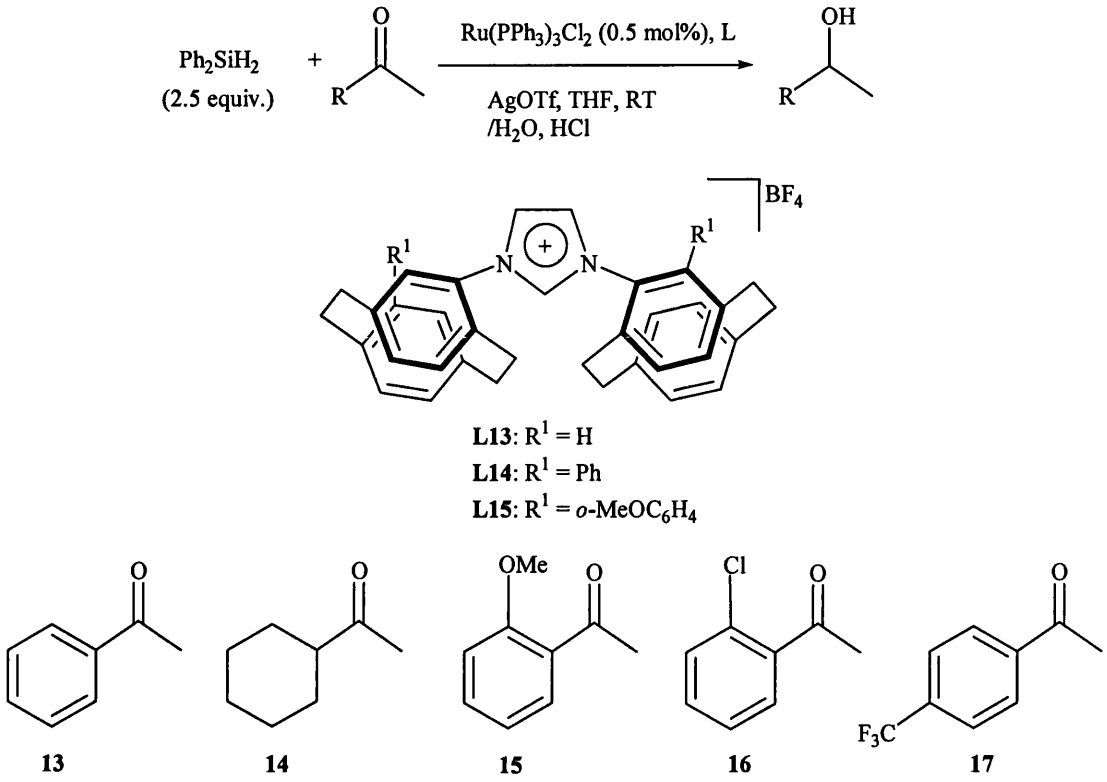

Scheme 1.8 *Ketone hydrosilylation reaction with Ru paracyclophane NHC complexes.*

Substrate	L	Ru:L	Time (h)	% yield	% ee
13	**L13**	1:2.4	16	98	90
13	**L14**	1:2.4	16	98	97
13	**L15**	1:2.4	16	98	97
13	**L15**	1:1	16	96	83
14	**L15**	1:2.4	36	93	58
15	**L15**	1:2.4	15	92	96
16	**L15**	1:2.4	20	90	97
17	**L15**	1:2.4	48	81	77

Table 1.6 *Yields and ee's of product alcohols following hydrosilylation of ketones by $Ru(PPh_3)_3Cl_2$: L (L = **L13/L14/L15**).*

The second Ru-NHC catalysed hydrosilylation reports the addition of silanes across terminal alkynes by $Ru(=CHPh)Cl_2(PCy_3)(SIMes)$ (**5**), $Ru(=CHPh)Cl_2(PCy_3)(IMes)$

(**18**) and the 3-phenylindenylid-1-ene analogue **19** (Scheme 1.9).[44] Reaction between phenylacetylene, triethylsilane and 1 mol% catalyst showed preferred formation of the *Z*-vinylsilane over the *E*-vinylsilane. Heating for 16 h showed total consumption of alkyne in all three cases, although only moderate yields were obtained due to the production of significant amounts of phenylacetylene dimer.

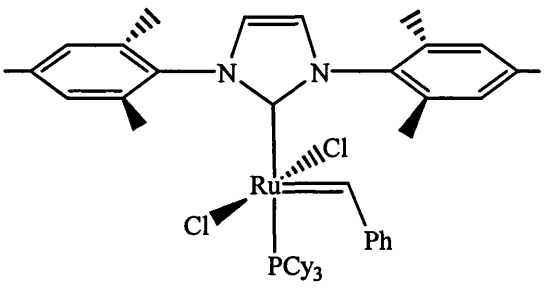

18

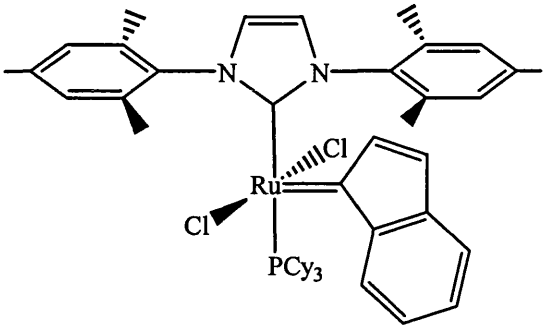

19

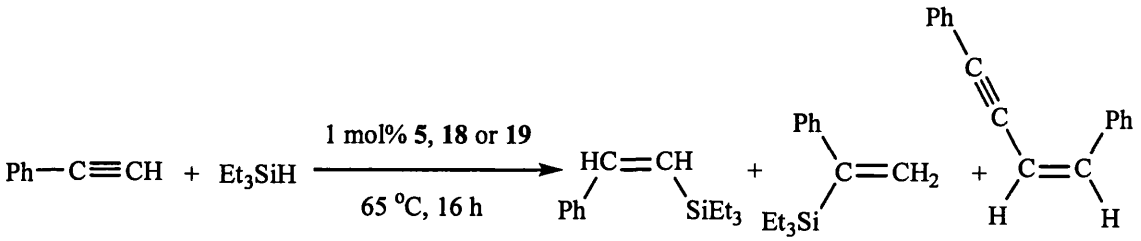

Scheme 1.9 *Hydrosilylation of styrene by 5, 18 and 19.*

1.2.4 Hydrogenation reactions

1.2.4.1 Overview

Ruthenium complexes for homogeneous hydrogenation catalysis have been known for around 40 years. Whilst good to excellent activities have been achieved with NHC complexes of rhodium, iridium, nickel and ruthenium for transfer hydrogenations (and in some cases direct hydrogenations), direct hydrogenations with employment of ruthenium-NHC complexes have been less successful.[45]

The importance of transfer hydrogenation arises from the ability to perform both oxidation and reduction reactions simultaneously. In order to develop successful

hydrogen transfer catalysts it is valuable to consider how the hydrogens are transferred from the alcohol to the ketone. Mechanistically, hydrogen transfer can proceed *via* one of two proposed pathways: (1) direct hydrogen transfer or (2) a hydridic route. Direct hydrogen transfer generally occurs with main group metals due to the combination of facile ligand exchange and Lewis acidity which enhances the carbonyl centre to hydride transfer. The hydridic route commonly arises with transition metal complexes and hydrogen transfer involves the intermediacy of either a monohydride or dihydride metal complex.

Bäckvall and co-workers have extensively studied the hydridic route and distinguished between two possible pathways by deuterium labelling studies (Scheme 1.10). The metal hydride species may arise purely from the C-H of the alcohol (Path A) or, alternatively, from *both* the O-H and C-H group (Path B). The monohydride route, therefore, gives selective carbon-to-carbon hydrogen transfer, whereas the dihydride route leads to non-selective hydrogen transfer involving both oxygen-to-carbon and carbon-to-carbon hydrogen transfer.

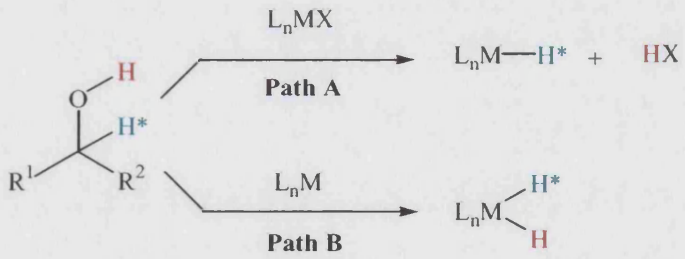

Scheme 1.10 *Proposed pathways for the hydridic route of hydrogen transfer.*

Bäckvall reported a dramatic rate acceleration upon addition of base in the $RuCl_2(PPh_3)_3$-catalysed transfer hydrogenation.[46] The effect of base indicated that $RuCl_2(PPh_3)_3$ was only the catalyst precursor. The base facilitated the formation of a ruthenium alkoxide species, which then underwent a β–elimination to form a Cl-Ru-H species. A second sequence of base promoted alkoxide formation-β-elimination to give a RuH_2 complex as the active species (Scheme 1.11). This was confirmed in a comparative study of $RuH_2(PPh_3)_3$, $Ru(H)Cl(PPh_3)_3$ and $RuH_2(PPh_3)_3$ in the hydrogen transfer from cyclopentanol to acetone. The dihydride species had no induction period

and had reached 50-60% conversion of cyclopentanol before either of the other two reactions had started.

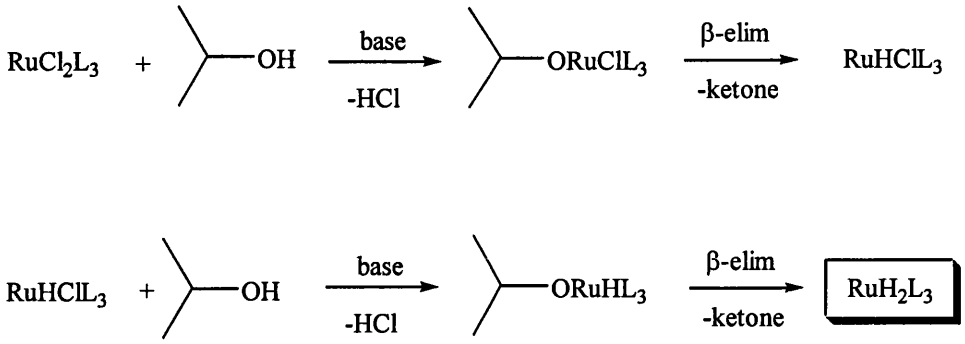

Scheme 1.11 *The role of base in the $RuCl_2L_3$-catalysed transfer hydrogenation of alcohols (L = PPh_3).*

The most widely used hydrogenation catalysts are Wilkinson's catalyst, $RhCl(PPh_3)_3$ and Crabtree's catalyst, $[Ir(COD)(py)(PCy_3)]PF_6$ (**20**). Despite the excellent activity of Crabtree's catalyst it has been shown to undergo an irreversible deactivation process involving the formation of a hydrogen bridged cluster, in addition to displaying poor thermal stability.[47] Nolan and co-workers replaced the phosphine ligand with SIMes to form a thermally stable analogue of Crabtree's catalyst (**21**). The catalytic performance of the two complexes was compared in simple alkene hydrogenations. Surprisingly, complex **21** was not as effective as **20** at room temperature. However, in contrast to **20** where activity drastically decreased, activity of **21** was significantly improved at elevated temperatures.[8]

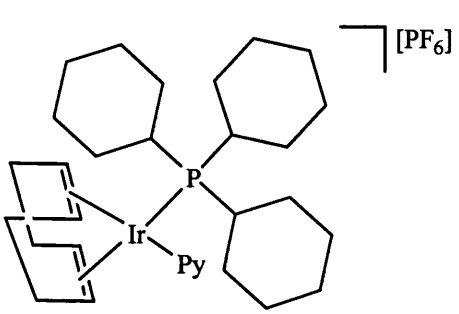

20

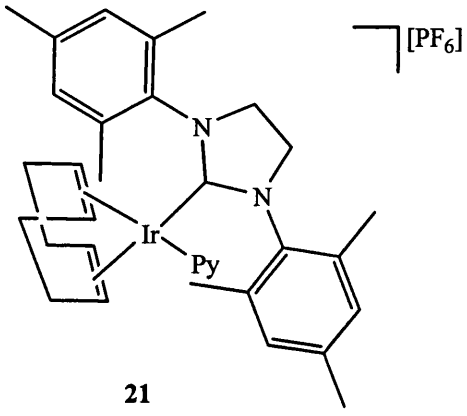

21

Buriak and co-workers performed similar substitution reactions on Crabtree's catalyst with IMes and 1,3-dimethylimidazol-2-ylidene (IMe_2) to yield NHC-phosphine complexes of iridium, in addition to the IMe_2 analogue of **21**.[7] Complexes having a combination of a phosphine and an NHC proved to be more reactive than those with a combination of a pyridine and an NHC (**21** and **22**). Furthermore the bulkier IMes complex **26** was more reactive for unhindered alkenes than the IMe_2 complexes **23-25**, whereas for tertiary and quaternary alkenes, the less hindered IMe_2 complexes were able to hydrogenate substrates considerably faster. Complex **25** hydrogenated alkenes with rates comparable to **20** at room temperature while rates of complexes **22-24** and **26** were reduced with respect to that of the parent compound **20**.

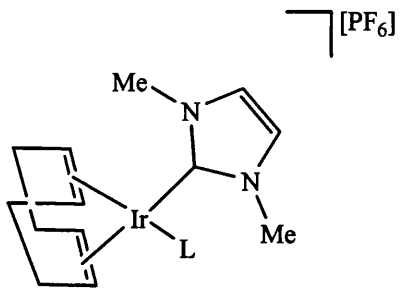

22 L = Py
23 L = PPh_3
24 L = PCy_3
25 L = $P(^nBu)_3$

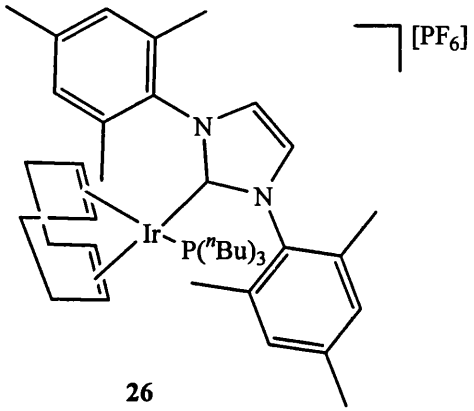

26

1.2.4.2 Ruthenium-NHC catalysed hydrogenation reactions

Nolan and co-workers also replaced PCy_3 for IMes in the ruthenium system $RuHCl(CO)(PCy_3)_2$ (**27**) to form $RuHCl(CO)(PCy_3)IMes$ (**28**).[48] Hydrogenation of 1-hexene at ambient temperature (0.1 mol% catalyst, 4 atm H_2) with **28** proved to be less efficient than with **27**. At elevated temperatures the two systems became comparable with TONs of 21,500 h^{-1} and 24,000 h^{-1} for **27** and **28** respectively. It is surprising that there is not more of a contrast in results between the systems since it might be expected that the more strongly donating NHC would favour alkene binding and H_2 oxidative addition.[49] For the ruthenium systems, it was suggested that dissociation of one of the PCy_3 ligands was essential for the formation of the active species.[48] This mechanism was supported when a more effective catalyst system was generated upon the addition of HBF_4, forming the reactive 14-electron species

$RuHCl(CO)(PCy_3)$ through loss of $[HPCy_3][BF_4]$. Hence lower activity of the NHC complexes might reflect stronger ligand coordination of PCy_3 *trans* to an NHC group, versus a second PCy_3 ligand. The increase in temperature facilitates ligand dissociation and thus improves catalytic activity.

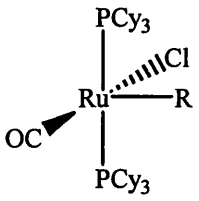

27 R = H
31 R = Ph

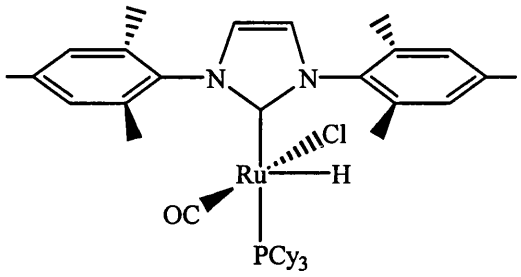

28

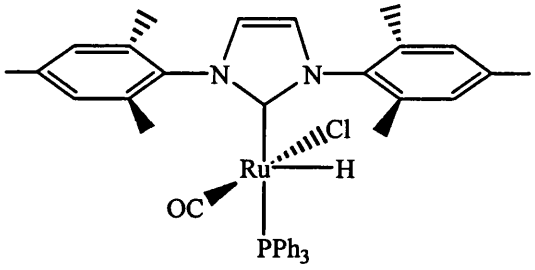

29

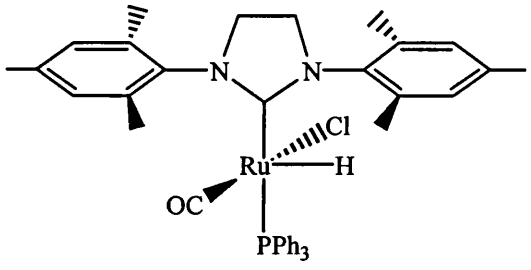

30

Nolan and Fogg subsequently investigated the effect of replacing the PCy_3 ligand with a more labile PPh_3 group to form $RuHCl(CO)(PPh_3)(NHC)$ (NHC = IMes, **29**; NHC = SIMes, **30**).[45] The results confirmed that the low lability of the PCy_3 phosphine donor had counteracted the activating effect of the NHC group. Compounds **29** and **30** exhibited much higher activity than **27** and **28** and displayed a much broader spectrum of catalytic activity, thus enabling reduction of much more sterically challenging alkenes. Reduction of both *cis*- and *trans*-cyclododecene (CDE) could be achieved with both **29** and **30**, whereas when employing **27** and **28**, *trans*-CDE showed resistance to hydrogenation and conversions were consequently affected (Table 1.7).

Catalyst	Substrate	TOF[b](h^{-1})	Time (min)	Conversion[c]
27	CDE	740	60	33
28	CDE	235	60	8
29	CDE	3,228	60	96[d]
30	CDE	3,280	60	97[d]

[a] Conditions: 0.05 mol % [Ru], 9.3 atm H_2, 80 °C, toluene. [b] Turnover frequency calculated at 30 min. [c] Conversions determined by GC; ±3% in replicate runs. [d] The conversion was 100% within 2 h.

Table 1.7 *Hydrogenation of cyclododecene(CDE).*

Dinger and Mol tested the efficiency of $Ru(Ph)Cl(CO)(PCy_3)_2$ (**31**) and $Ru(Ph)Cl(CO)(PCy_3)(SIMes)$ (**32**) for the hydrogenation of 1-octene, and compared the results with those of **27**.[50] Data comparable to those of Nolan and co-workers were found. At room temperature only **27** displayed appreciable hydrogenation activity; the temperature was raised to 100 °C before comparable activities of the three catalysts were seen. However, when lower catalyst loadings were examined (1:350,000 **32**:1-octene), **32** showed poorer selectivity for conversion to octane than either **31** or **27**. A later report revealed that the hydrogenation activity of the related mono carbene species $Ru(H)Cl(CO)(PCy_3)(SIPr)$ (**33**) is compromised by the ability to isomerise alkenes.[51]

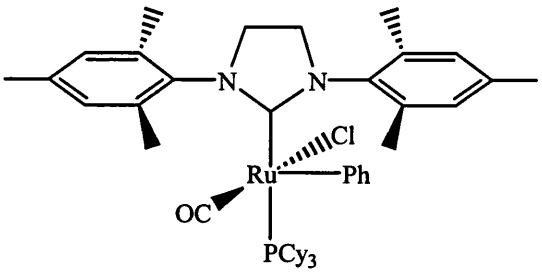

32

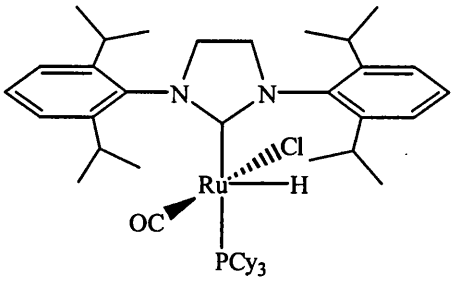

33

Water-soluble complexes Ru(II)-NHC complexes **34** and **35** catalyse the hydrogenation of C=O as well as C=C bonds in aqueous solution.[52] Reduction of acetone, acetophenone, cinnamaldehyde and benzylideneacetone was catalysed by both **34** and **35**, although **35** gave significantly higher conversions under the reaction conditions (10 atm H_2, 80 °C). Preferential C=C bond reduction was observed in cinnamaldehyde and benzylideneacetone. Hydrogenation of allyl alcohol gave 1-propanol and propanal as

products and rate data suggested that 1-propanol was formed *via* two different reaction pathways: reduction of propanal and a second redox isomerisation pathway.

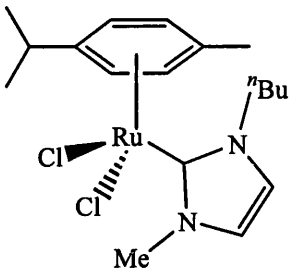

34

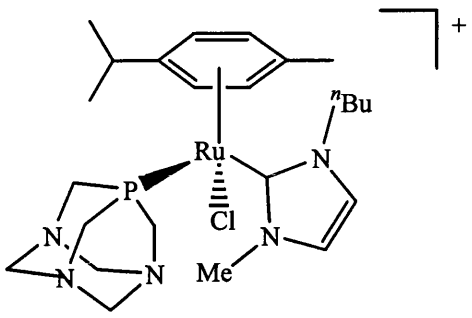

35

Herrmann and co-workers have recently reported transfer hydrogenation of ketones with alcohols with TOF values that are among the highest reported in the literature.[53] Their catalyst combines the commercially available free carbene 1,3,4-triphenyl-4,5-dihydro-1*H*-1,2,4-triazol-5-ylidene with a monohydride, diphosphine complex bearing 2-(aminomethyl)pyridine (ampy) (**36**). Displacement of one of the phosphines occurs with simultaneous orthometallation of a phenyl group and elimination of dihydrogen. The formation of the five-membered ring is thought to contribute stability to the ruthenium centre, preventing oxidation or degradation of the catalytic species.

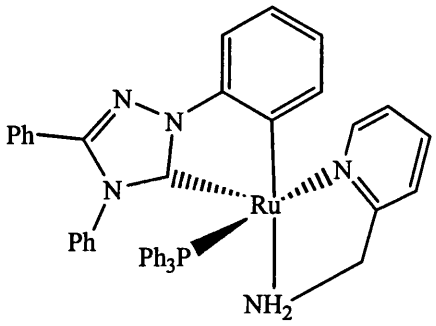

36

Complex **36** has been shown to catalyse reduction of a number of different ketones, including alkylaryl, cyclic and dialkyl substrates, to their corresponding alcohols within minutes with TOF of up to 120,000 h^{-1}. For example, cyclohexanone is converted into cyclohexanol in less than 2 min with a TOF of 100,000 h^{-1}.

Whilst monodentate carbene systems have been the focus of many studies, the carbene analogues of chelating diphosphines have received less attention. This is most likely due to the lack of known synthetic routes that can be transferred from the monodentate case. The precursor imidazolium salts are often converted to the free carbene by deprotonation using strong bases that could possibly attack -CH_2- linkers between the carbene units or other sensitive sites. It has also been found that this deprotonation route often affords bimetallic species with a monodentate carbene coordinated to each metal centre. However, the successful synthesis of chelating carbenes would probably yield metal complexes of increased stability by, for example, slowing down decomposition reactions such as reductive elimination of the carbene.

Combining the stability of late transition metal carbenes with a high entropic chelate effect, chelate and pincer carbene ligands are among the most challenging compounds to obtain. Their syntheses provide a new family of highly stable compounds with interesting chemical properties.[2]

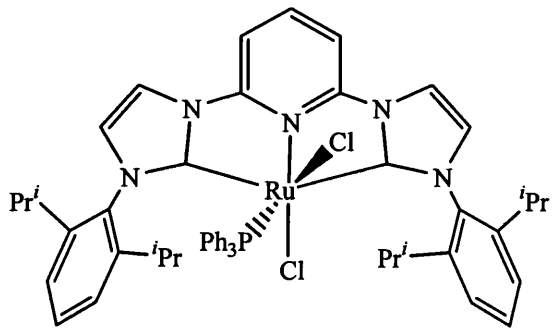

37

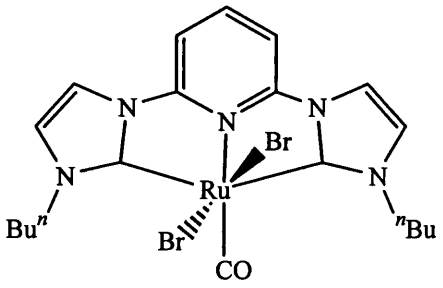

38

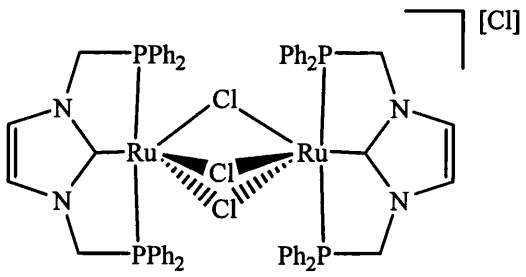

39

The pincer bis(carbene) complex **37** catalyses reduction of ketones *via* hydrogen transfer from IPA/KOH at 55-80 °C in quantitative yields.[54] The related pincer bis(carbene) complex **38** displayed higher turnovers at lower catalyst loadings than **37**,

although higher temperatures were employed.[2] The high stability of **38** allowed the reactions to be carried out in air with no special precautions taken concerning moisture. The activities of **38** and **37** are summarised in Table 1.8. More recently the pincer carbene based cationic dimer **39** has been shown to catalyse the hydrogenation of ketones *via* hydrogen transfer from IPA in the presence of base.[55]

Substrate	Catalyst	Loading (mol%)	Temp (°C)	Time (h)	TON
cyclohexanone	**38**	0.07[a]	80	3	8800
cyclohexanone	**38**	0.07[a]	80	20	12600
cyclohexanone	**38**	0.0007[a]	80	20	126000
cyclohexanone	**37**	0.01[b]	55	20	8800
acetophenone	**38**	0.07[a]	80	6	700
acetophenone	**37**	0.015[b]	80	12	4000
benzophenone	**38**	0.07[a]	80	3	1400

[a] Conditions: 2 mmol substrate, 10 mL 0.1M KOH in ^{i}PrOH. [b] Conditions: 50 mmol substrate, 4.5 mmol KO^{t}Bu in ^{i}PrOH.

Table 1.8 *Transfer hydrogenation of ketones by 37 and 38.*

1.3 Tandem catalysis

1.3.1 Classification

Transition metal catalysed processes have enabled vast transformative developments in organic synthesis. Ideally the synthesis of any target molecule would proceed in the shortest number of steps. It is therefore not surprising that the idea of coupling such highly selective transformations has gained much interest. Many "one-pot" processes involving multiple catalytic transformations, rather than focusing on chemical reactions as discrete events, have been developed. Intermediate work-up steps are eliminated thus increasing the efficiency of the processes.

One pot procedures can be classified into separate classes including domino, cascade or tandem reactions. All of these terms are used to describe transformations of an organic

substrate through two or more individual elaborations with a single workup step. The flowchart shown classifies the one pot processes (Figure 1.4).[56]

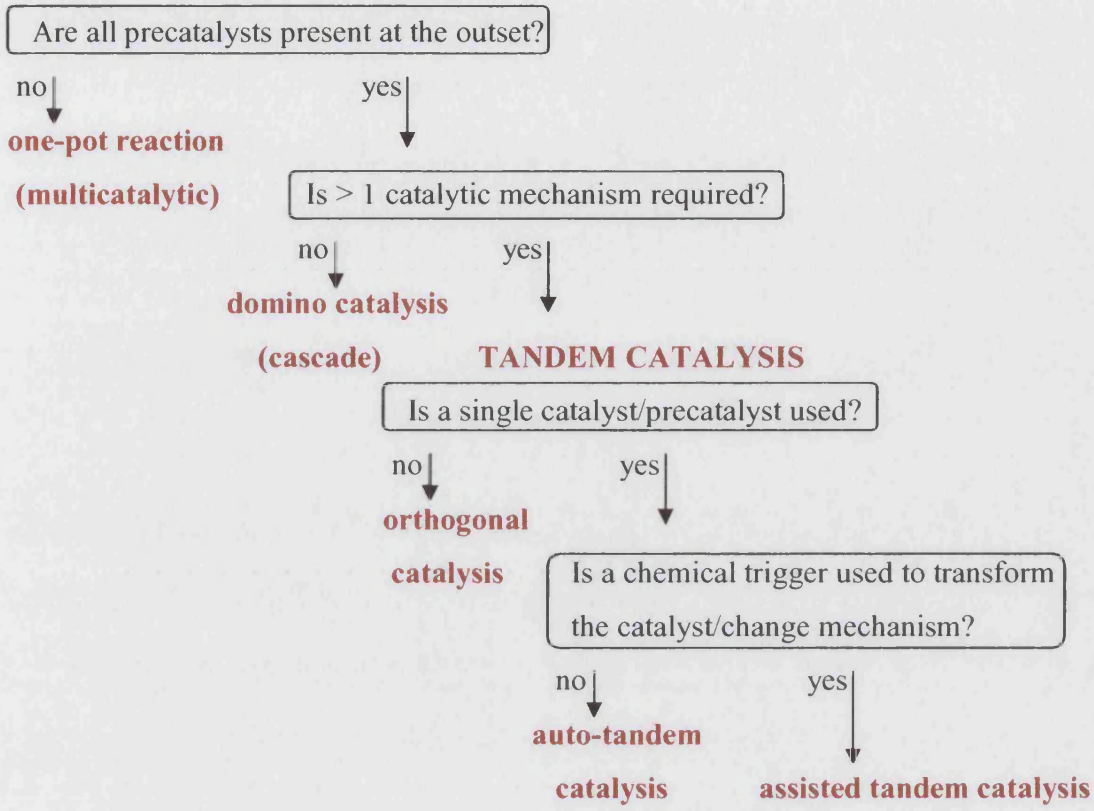

Figure 1.4 *Flowchart for classification of one-pot processes involving sequential elaboration of an organic substrate via multiple catalytic transformations.*[56]

Significant advances have been made in tandem catalysis over the last five years, including some utilising M-NHC complexes.

1.3.2 Ruthenium-NHC complexes in tandem catalysis

1.3.2.1 Metathesis/hydrogenation

Grubbs' second generation catalyst Ru(=CHPh)Cl_2(PCy_3)(SIMes) (**5**) has recently been shown to be an effective catalyst for hydrogenation reactions as well as its use in alkene metathesis. This catalyst has subsequently been applied to a number of one-pot tandem metathesis-hydrogenation procedures,[57] giving a more convenient procedure to the conventional approach where Pd/C or Rh hydrogenation catalysts are used after the

alkene metathesis product has been isolated. Grubbs and co-workers have shown **5** to be tolerant of a wide range of functionality without loss in activity.[58] In addition **5** proved to be effective for the regiospecific reduction of ketones and also for transfer hydrogenation catalysts. These methods were combined for the construction of (*R*)-(-)-Muscone (Scheme 1.12). This same approach was used for the synthesis of phosphotriester based cyclic dinucleotides.[59]

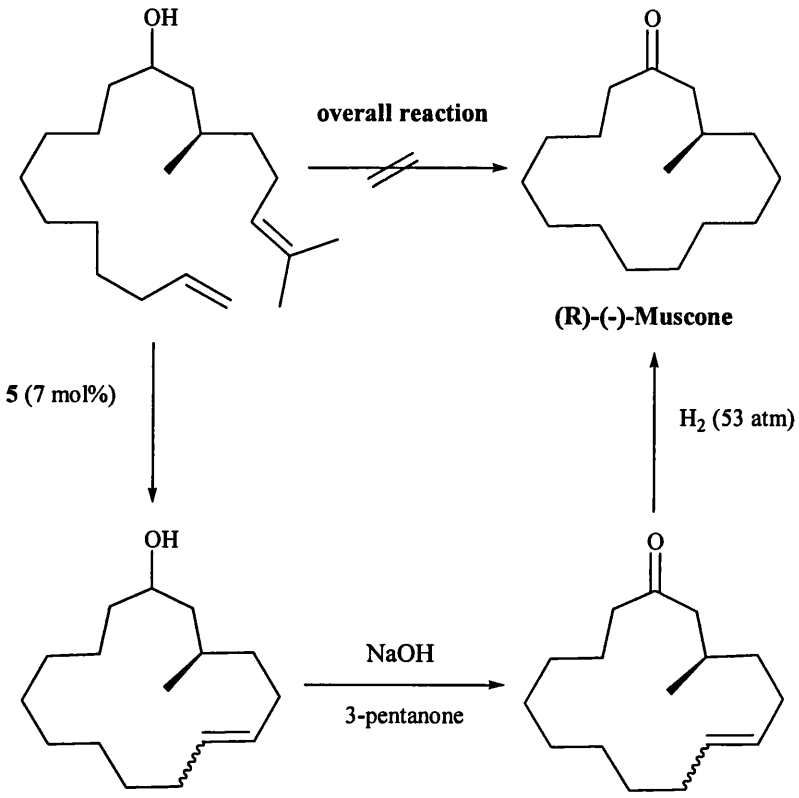

Scheme 1.12 *Synthesis of (R)-(-)-Muscone via a tandem RCM hydrogenation pathway.*

Schmidt and co-workers attempted to apply the same methodology for the synthesis of 1-*tert*-butyl-cyclopentanol but only the primary metathesis product was detected in the crude reaction mixture.[60] However, upon addition of catalytic amounts of inorganic hydrides such as NaH, the catalyst was activated to a dihydride species for the hydrogenation step. By employing an excess of NaH with protic functional groups or water the hydrogen was generated *in situ* without the need for external pressures of H_2. Thus substrates **40** and **41** were converted to cyclopentanols **42** and **43** respectively (Scheme 1.13).

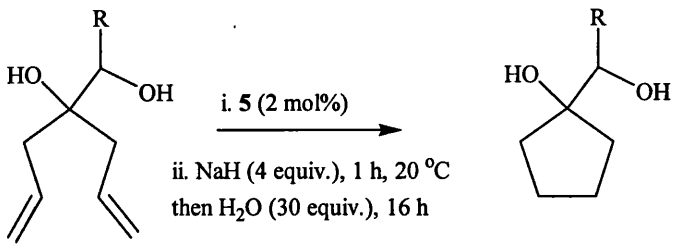

40 R = Ph
41 R = Me

42 R = Ph
43 R = Me

Scheme 1.13 *Hydride enhanced RCM/hydrogenation catalysis.*

1.3.2.2 Metathesis/isomerisation

Alkene isomerisation, a reaction that has the net effect of moving the C=C group along the chain of the molecule, has been noted to interfere with the metathesis process occasionally.[61] Ruthenium NHC complexes can be converted into ruthenium hydride complexes by reaction with hydrogen or by decomposition, leading to unwanted side reactions. For example, Nolan and co-workers have observed how **5** catalyses the competing reaction of RCM versus alkene isomerisation depending on solvent.[62] However, alkene isomerisation is not necessarily undesirable since it opens up new applications for ruthenium hydride-mediated catalysis.

Ru-NHC catalysed metathesis has been used in conjunction with isomerisation for the synthesis of indoles,[63] heterocycles[64-66] and cyclic enol ethers.[67] RCM of enol ethers or enamines is sometimes disadvantageous since more active, less conventional catalysts are required and high dilutions have to be applied to limit intermolecular metathesis. Snapper and co-workers have employed this methodology for the synthesis of five-, six- and seven-membered ring cyclic enol ethers using **5** in the presence of a 95:5 mixture of N_2 and H_2 (Scheme 1.14).[67]

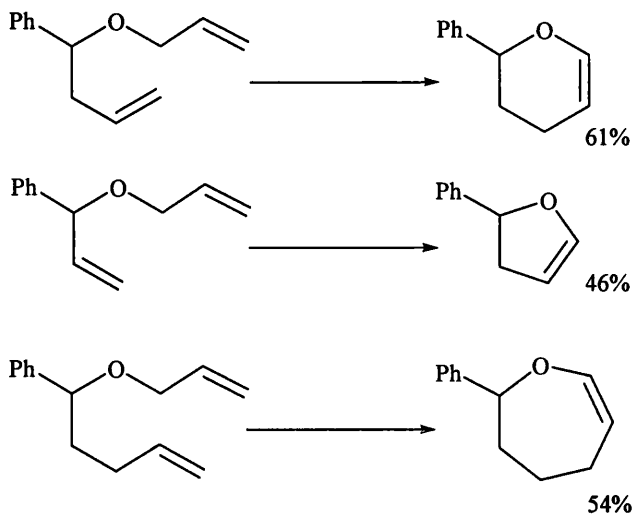

General conditions: **5** (10 mol%), 45-70 °C, CH_2Cl_2, 95:5 N_2:H_2

Scheme 1.14 *Tandem RCM/isomerisation route to cyclic enol ethers.*

1.4 Synopsis

This thesis describes the development of ruthenium-NHC complexes for their use as catalysts in a novel one-pot tandem process converting alcohols into alkanes.

Chapter 2 describes the synthesis and characterisation of the mono substituted Ru-NHC complexes. N-aryl substituted and N-alkyl substituted NHCs are synthesised and complexed to ruthenium. The structural properties of the ruthenium complexes with varied NHC ligands are compared.

The C-H bond activation and isomerisation processes of each of the Ru-NHC complexes are investigated in **Chapter 3**. C-H activation and isomerisation products are isolated and characterised and comparisons between the complexes are made.

The final chapter, **Chapter 4**, explores the catalytic activity of the Ru-NHC complexes. Their potential in both direct and transfer hydrogenation catalysis is explored in addition to their subsequent application to the one-pot tandem process involving an *in situ* Wittig reaction.

1.5 References

[1]Arduengo, A. J.; Harlow, R. L.; Kline, M. *J. Am. Chem. Soc.* **1991**, *113*, 361-363.

[2]Poyatos, M.; Mata, J. A.; Falomir, E.; Crabtree, R. H.; Peris, E. *Organometallics* **2003**, *22*, 1110-1114.

[3]Sanford, M. S.; Grubbs, R. H.; Love, J. A. *J. Am. Chem. Soc.* **2001**, *123*, 6543-6554.

[4]Weskamp, T.; Schattenmann, W. C.; Spiegler, M.; Herrmann, W. A. *Angew. Chem. Int. Edit.* **1998**, *37*, 2490-2493.

[5]Huang, J.; Stevens, E. D.; Nolan, S. P.; Petersen, J. L. *J. Am. Chem. Soc.* **1999**, *121*, 2674-2678.

[6]Scholl, M.; Ding, S.; Lee, C. W.; Grubbs, R. H. *Org. Lett.* **1999**, *1*, 953-956.

[7]Vasquez-Serrano, L. D.; Owens, B. T.; Buriak, J. M. *Chem. Commun.* **2002**, 2518-2519.

[8]Lee, H. M.; Jiang, T.; Stevens, E. D.; Nolan, S. P. *Organometallics* **2001**, *20*, 1255-1258.

[9]Marko, I. E.; Sterin, S.; Buisine, O.; Mignani, R.; Branlard, P.; Tinant, B.; Declercq, J. P. *Science* **2002**, *298*, 204-206.

[10]Buisine, O.; Berthon-Gelloz, G.; Briere, J. F.; Sterin, S.; Mignani, G.; Branlard, P.; Tinant, B.; Declercq, J. P.; Marko, I. E. *Chem. Commun.* **2005**, 3856-3858.

[11]Herrmann, W. A.; Goossen, L. J.; Kocher, C.; Artus, G. R. J. *Angew. Chem. Int. Edit. Engl.* **1996**, *35*, 2805-2807.

[12]Viciu, M. S.; Germaneau, R. F.; Nolan, S. P. *Org. Lett.* **2002**, *4*, 4053-4056.

[13]Navarro, O.; Kelly, R. A.; Nolan, S. P. *J. Am. Chem. Soc.* **2003**, *125*, 16194-16195.

[14]Tolman, C. A. *Chem. Rev.* **1977**, *77*, 313-324.

[15]Scott, N. M.; Nolan, S. P. *Eur. J. Inorg. Chem.* **2005**, 1815-1828.

[16]Hillier, A. C.; Sommer, W. J.; Yong, B. S.; Petersen, J. L.; Cavallo, L.; Nolan, S. P. *Organometallics* **2003**, *22*, 4322-4326.

[17]Cavallo, L.; Correa, A.; Costabile, C.; Jacobsen, H. *J. Organomet. Chem.* **2005**, *690*, 5407-5413.

[18]Hu, X. L.; Tang, Y. J.; Gantzel, P.; Meyer, K. *Organometallics* **2003**, *22*, 612-614.

[19]Magill, A. M.; Cavell, K. J.; Yates, B. F. *J. Am. Chem. Soc.* **2004**, *126*, 8717-8724.

[20]Denk, K.; Sirsch, P.; Herrmann, W. A. *J. Organomet. Chem.* **2002**, *649*, 219-224.

[21]Dorta, R.; Stevens, E. D.; Scott, N. M.; Costabile, C.; Cavallo, L.; Hoff, C. D.; Nolan, S. P. *J. Am. Chem. Soc.* **2005**, *127*, 2485-2495.

[22]Crabtree, R. H. *The Organometallic Chemistry of the Transition Metals*; 3rd ed.; Wiley-Interscience, 2001.

[23]Grubbs, R. H.; Morgan, J. P. *Org. Lett.* **2000**, *2*, 3153-3155.

[24]Dias, E. L.; Nguyen, S. T.; Grubbs, R. H. *J. Am. Chem. Soc.* **1997**, *119*, 3887-3897.

[25]Grubbs, R. H.; Sanford, M. S.; Ulman, M. *J. Am. Chem. Soc.* **2001**, *123*, 749-750.

[26]Herrmann, W. A.; Weskamp, T.; Bohm, V. P. W. *Adv. Organomet. Chem.* **2001**, *48*, 1-69.

[27]Herrmann, W. A.; Elison, M.; Fischer, J.; Kocher, C.; Artus, G. R. J. *Angew. Chem. Int. Edit. Eng.* **1995**, *34*, 2371-2374.

[28]McGuinness, D. S.; Cavell, K. J.; Skeleton, B. W.; White, A. H. *Organometallics* **1999**, *18*, 1596-1605.

[29]Selvakumar, K.; Zapf, A.; Beller, M. *Org. Lett.* **2002**, *4*, 3031-3033.

[30]Zhang, C.; Huang, J.; Trudell, M. L.; Nolan, S. P. *J. Org. Chem.* **1999**, *64*, 3804-3805.

[31]Selvakumar, K.; Zapf, A.; Spannenberg, A.; Beller, M. *Chem. Eur. J.* **2002**, *8*, 3901-3906.

[32]Hillier, A. C.; Grasa, G.; Viciu, M. S.; Lee, H. M.; Yang, C.; Nolan, S. P. *J. Organomet. Chem.* **2002**, *653*, 69-82.

[33]Weskamp, T.; Bohm, V. P. W.; Herrmann, W. A. *J. Organomet. Chem.* **1999**, *585*, 348.

[34]Kuhl, S.; Schneider, R.; Fort, Y. *Organometallics* **2003**, *22*, 4184-4186.

[35]Ozedemir, I.; Demir, S.; Cetinkaya, B. *Tetrahedron* **2005**, *61*, 9791-9798.

[36]Crudden, C. M.; Allen, D. P. *Coord. Chem. Rev.* **2004**, *248*, 2247-2273.

[37]Clayden, J.; Greeves, N.; Warren, S.; Wothers, P. *Organic Chemistry*; Oxford University Press Inc., 2001.

[38]Huang, J.; Grasa, G.; Nolan, S. P. *Org. Lett.* **1999**, *1*, 1307-1309.

[39]Stambuli, J. P.; Buhl, M.; Hartwig, J. F. *J. Am. Chem. Soc.* **2002**, *124*, 9346-9347.

[40]Stauffer, S. R.; Lee, S.; Stambuli, J. P.; Hauck, S. I.; Hartwig, J. F. *Org. Lett.* **2000**, *2*, 1423-1426.

[41]Caddick, S.; Cloke, F. G. N.; Hitchcock, P. B.; Leonard, J.; Lewis, A. K. D.; McKerrecher, D.; Titcomb, L. R. *Organometallics* **2002**, *21*, 4318-4319.

[42]Lewis, A. K. D.; Caddick, S.; Cloke, F. G. N.; Billingham, N. C.; Hitchcock, P. B.; Leonard, J. *J. Am. Chem. Soc.* **2003**, *125*, 10066-10073.

[43]Song, C.; Ma, C. Q.; Ma, Y. D.; Feng, W. H.; Ma, S. T.; Chai, Q.; Andrus, M. B. *Tetrahedron Lett.* **2005**, *46*, 3241-3244.

[44]Maifield, S. V.; Tran, M. N.; Lee, D. *Tetrahedron Lett.* **2005**, *46*, 105-108.

[45]Dharmasena, U. L.; Foucault, H. M.; dos Santos, E. N.; Fogg, D. E.; Nolan, S. P. *Organometallics* **2005**, *24*, 1056-1058.

[46]Backvall, J. E. *J. Organomet. Chem.* **2002**, *652*, 105-111.

[47]Crabtree, R. H.; Felkin, H.; Morris, G. E. *J. Organomet. Chem.* **1977**, *135*, 205-215.

[48]Lee, H. M.; Smith, D. C.; He, Z. J.; Stevens, E. D.; Yi, C. S.; Nolan, S. P. *Organometallics* **2001**, *20*, 794-797.

[49]Diggle, R. A.; Macgregor, S. A.; Whittlesey, M. K. *Organometallics* **2004**, *23*, 1857-1865.

[50]Dinger, M. B.; Mol, J. C. *Eur. J. Inorg. Chem.* **2003**, 2827-2833.

[51]Banti, D.; Mol, J. C. *J. Organomet. Chem.* **2004**, *689*, 3113-3116.

[52]Csabai, P.; Joo, F. *Organometallics* **2004**, *23*, 5640-5643.

[53]Baratta, W.; Schutz; Herdtweck, E.; Herrmann, W. A.; Rigo, P. *J. Organomet. Chem.* **2005**, *in press*.

[54]Danopoulos, A. A.; Winston, S.; Motherwell, W. B. *Chem. Commun.* **2002**, 1376-1377.

[55]Chiu, P. L.; Lee, H. M. *Organometallics* **2005**, *24*, 1692-1702.

[56]Fogg, D. E.; dos Santos, E. N. *Coord. Chem. Rev.* **2004**, *248*, 2365-2379.

[57]Schmidt, B. *Eur. J. Org. Chem.* **2004**, 1865-1880.

[58]Louie, J.; Bielawski, C. W.; Grubbs, R. H. *J. Am. Chem. Soc.* **2001**, *123*, 11312-11313.

[59]Borsting, P.; Nielsen, P. *Chem. Commun.* **2002**, 2140-2141.

[60]Schmidt, B.; Pohler, M. *Org. Biomol. Chem.* **2003**, *1*, 2512-2517.

[61]Maynard, H. D.; Grubbs, R. H. *Tetrahedron Lett.* **1999**, *40*, 4137-4140.

[62]Bourgeouis, D.; Pancrazi, A.; Nolan, S. P.; Prunet, J. *J. Organomet. Chem.* **2002**, *643-644*, 247-252.

[63]Arisawa, M.; Terada, Y.; Nakagawa, M.; Nishida, A. *Angew. Chem. Int. Edit.* **2002**, *41*, 4732-4734.

[64]van Otterlo, W. A. L.; Pathak, R.; de Koning, C. B. *Synlett* **2003**, 1859-1861.

[65]van Otterlo, W. A. L.; Morgans, G. L.; Khanye, S. D.; Aderibigbe, B. A. A.; Michael, J. P.; Billing, D. G. *Tetrahedron Lett.* **2004**, *45*, 9171-9175.

[66]van Otterlo, W. A. L.; Ngidi, E. L.; de Koning, C. B. *Tetrahedron Lett.* **2003**, *44*, 6483-6486.

[67]Sutton, A. E.; Seigal, B. A.; Finnegan, D. F.; Snapper, M. L. *J. Am. Chem. Soc.* **2002**, *124*, 13390-13391.

Chapter 2

Chapter 2: Syntheses and Characterisation of Ru-NHC Complexes

2.1 General routes to metal-NHC complexes

Enormous interest has been focused on the use of N-heterocyclic carbene ligands in homogeneous catalysis and as a result a large number of metal-NHC complexes are now known. Three main methods are used for the synthesis of such species:

- Direct complexation of a metal to a free NHC.
- *In-situ* deprotonation of an NHC precursor in the presence of a metal precursor.
- Silver transmetallation.

Perhaps the most widely used of these routes is *via* complexation of preformed, free NHCs to metal complexes or salts. The obvious requirement of this is to have stable, isolable carbenes, which was first shown by Arduengo in 1991.[1] The isolation of 1,3-(diadamantyl)imidazol-2-ylidine (**L16**), was initially thought to be a consequence of the steric protection offered by the adamantyl groups. Since then, however, it has been shown that electronic stabilisation of the carbene centre in imidazol-2-ylidines provides stable carbenes even in the absence of steric shielding.[2] However, for the synthesis of stable saturated NHCs it is essential to have sterically demanding substituents on the nitrogen atoms in order to prevent dimerisation.[3]

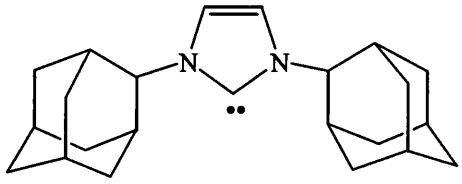

L16

The general route for preparing free NHCs is *via* the deprotonation of their imidazolium salts. The synthesis of imidazoles and imidazolium ions has been extensively developed and numerous imidazolium precursors can be made along various reliable routes.[4] The starting imidazole can be alkylated or the whole imidazolium ring can be constructed in a multicomponent reaction, usually from an arylamine, formaldehyde and glyoxal. This introduces the possibility of developing a vast array of functionalised imidazole rings to

enhance catalytic activity. With the imidazolium ring built up, subsequent deprotonation by use of a strong base generates the free NHC.

Direct metallation of the imidazolium salt by a metal precursor is not so widely applicable. *In situ* preparation of the free carbene is advantageous in cases where the carbene is particularly unstable or difficult to handle. Deprotonation of the imidazolium salt can be achieved by use of basic metallates, basic anions or by an external base.[5] These methods are not applicable where catalysts of high purity are required. For example, alkene metathesis reactions are inhibited by an excess of free phosphine and therefore generation of **44** *in situ* would require the use of a phosphine scavenger in further reactions (Scheme 2.1).[6]

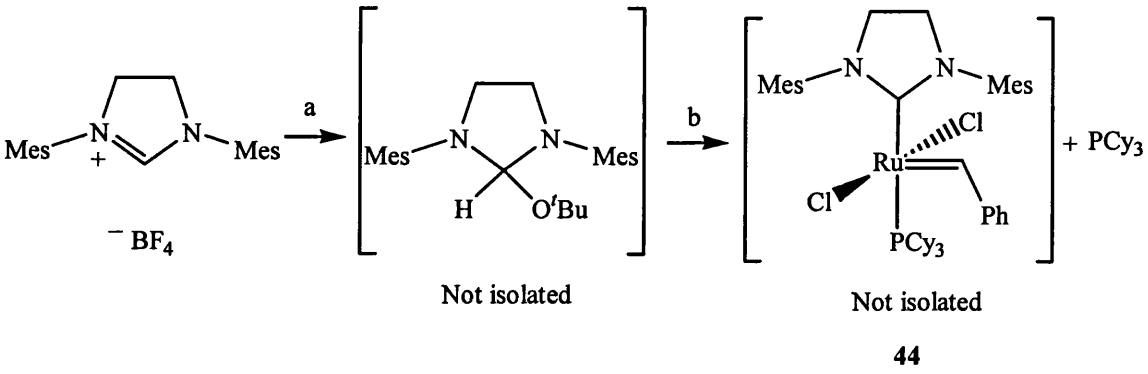

Scheme 2.1 *In situ catalyst synthesis by the alkoxide route. (a) KO^{t}Bu, THF, less than 1 min at 25 °C; (b) $RuCl_2(=CHPh)(PCy_3)_2$, 80 °C, 30 min.*

An advance was made by Lin in the use of Ag_2O as a metallating agent (Scheme 2.2).[7-9] Generation of the free NHC is totally avoided. The synthesis works well even in the presence of air and water; water can even be used as solvent. The resulting Ag-NHC complex can then be reacted with a variety of organometallic precursors and metal salts to give a range of NHC complexes. However the Ag_2O or transmetallation reactions can sometimes be very low yielding or may not proceed at all.[9]

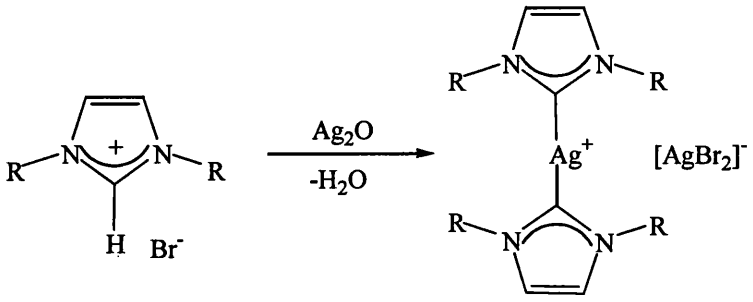

Scheme 2.2 *Formation of an Ag-NHC complex.*

2.2 Syntheses of NHCs

The method we have used to prepare metal-NHC complexes is *via* isolation of free NHCs followed by direct substitution with ruthenium complexes bearing relatively labile phosphine ligands. A number of groups have adopted this route to prepare metal-NHC complexes.

2.2.1 Syntheses of N-aryl substituted NHCs

2.2.1.1 Synthesis of 1,3-bis-(2,4,6-trimethylphenyl)imidazol-2-ylidene (IMes) (L17)

A route previously reported by Arduengo[3] *et al.* was adapted to synthesise the unsaturated aryl substituted NHC IMes (Scheme 2.3). It was essential that the precursor imidazolium salt was completely dry prior to deprotonation for the successful production of the carbene. IMes was synthesised in good yields (73%) and was characterised by ^{1}H and $^{13}C\{^{1}H\}$ NMR spectroscopy, in good agreement with the literature.[3]

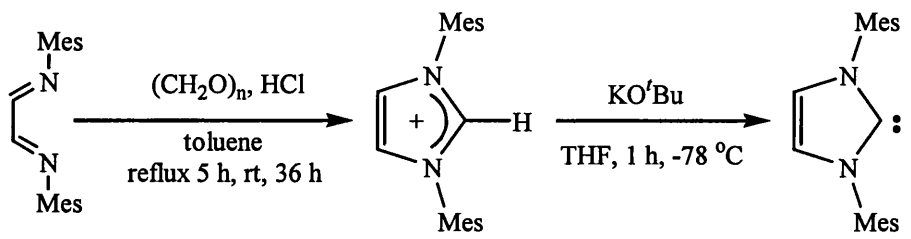

L17

Scheme 2.3 *Synthesis of IMes (L17).*

2.2.1.2 Synthesis of 1,3-bis-(2,4,6-trimethylphenyl)imidazolin-2-ylidene (SIMes) (L18)

A route adapted from the literature was used to prepare the saturated NHC SIMes.[3] The synthesis also involved the deprotonation of the precursor imidazolium salt, although different reaction conditions were required compared to those used to synthesise IMes (Scheme 2.4).

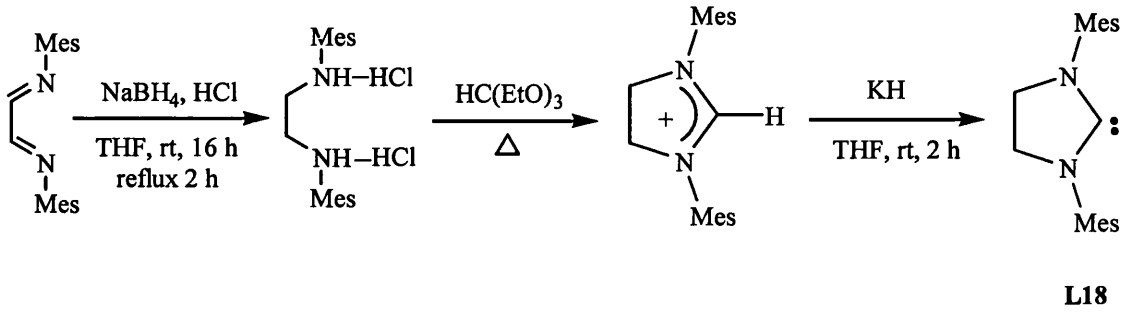

Scheme 2.4 *Synthesis of SIMes (L18).*

It was found that the precursor imidazolium salt had to be recrystallised under inert conditions and stored in the glove box prior to use to ensure successful synthesis of the carbene. The saturated carbene proved to be much more unstable than its unsaturated analogue IMes. Once the reaction conditions had been optimised, reasonably good yields were obtained (up to 58%). The formation of SIMes was confirmed by analyses of the ^{1}H and $^{13}C\{^{1}H\}$ NMR spectra, which were in agreement with the literature.[3]

2.2.1.3 Synthesis of 1,3-di-(*S*)-1'-phenylethylimidazol-2-ylidene (I*) (L19)

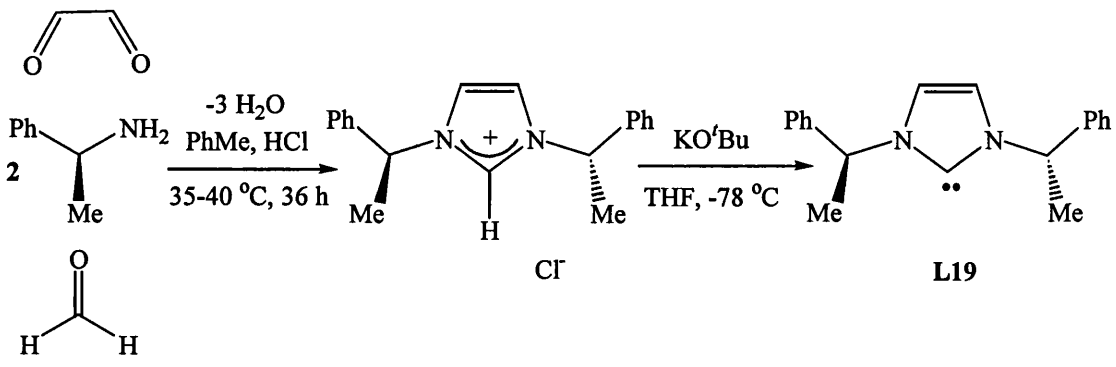

Scheme 2.5 *Synthesis of the chiral carbene I* (L19).*

A chiral imidazolium salt was synthesised *via* a one-pot method adapted from the literature (Scheme 2.5),[3,10] starting from the enantiomerically pure (*S*)-1-phenylethylamine. The salt was obtained as an extremely hygroscopic pale brown solid and deprotonated with the addition of KO^{t}Bu (Scheme 2.5).[13] The carbene was isolated in 83% yield as a yellow solid.

2.2.2 Syntheses of N-alkyl substituted NHCs

2.2.2.1 Syntheses of tetraalkylimidazol-2-ylidenes (L2, L6 and L20)

A different approach was taken to synthesise NHCs with alkyl groups on the nitrogen atoms and methyl groups on the backbone of the imidazole ring. A method was adapted from the literature.[11] The condensation reaction between thioureas **45-47** and 3-hydroxy-2-butanone in boiling hexanol yielded the tetraalkylimidazole-2(3H)-thiones **48-50**. Reduction of the thiones took place with potassium in THF affording the NHCs **L2, L6 and L20** in almost quantitative yields (Scheme 2.6). The carbenes were characterised by ^{1}H and ^{13}C{^{1}H} NMR spectroscopy. The ^{13}C{^{1}H} NMR spectra were essential for verification since the ^{1}H NMR spectra of the thiones and carbenes display essentially the same signals with only a slight shift upfield upon formation of the carbene. The ^{13}C{^{1}H} NMR spectra, however, display a significant downfield shift (about 50 ppm to approximately δ 210) upon comparison of the C=S carbon to the N-C-N carbon of the free carbene.

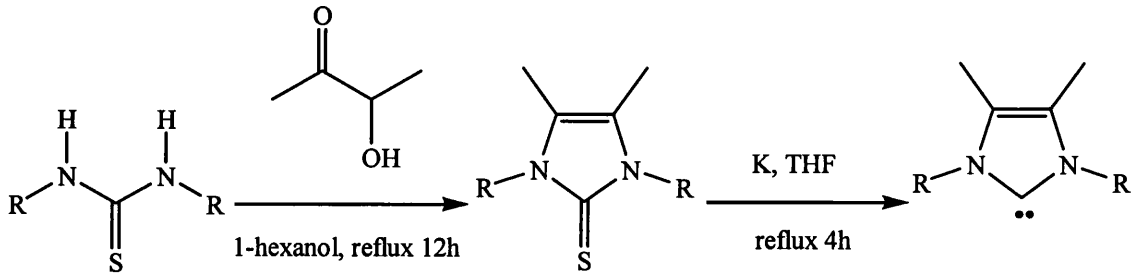

45 R = Me
46 R = Et
47 R = ^{i}Pr

48 R = Me
49 R = Et
50 R = ^{i}Pr

L2 R = Me
L20 R = Et
L6 R = ^{i}Pr

Scheme 2.6 *Syntheses of tetraalkylimidazol-2-ylidenes (L2, L6 and L20).*

2.2.2.2 Synthesis of 1,3-diisopropylimidazol-2-ylidene (I^iPr) (L4)

One further alkyl substituted carbene, where methyl groups on the backbone of the imidazole were not desired, was synthesised. A one-pot procedure adapted from the literature was used to prepare the imidazolium salt with isopropyl substituents on the nitrogen atoms (Scheme 2.7).[3,10] The imidazolium salt was obtained as a hygroscopic solid. The salt was deprotonated using KO^{t}Bu to give the free carbene **L4** as a yellow oil in 81% yield (Scheme 2.7)[13]

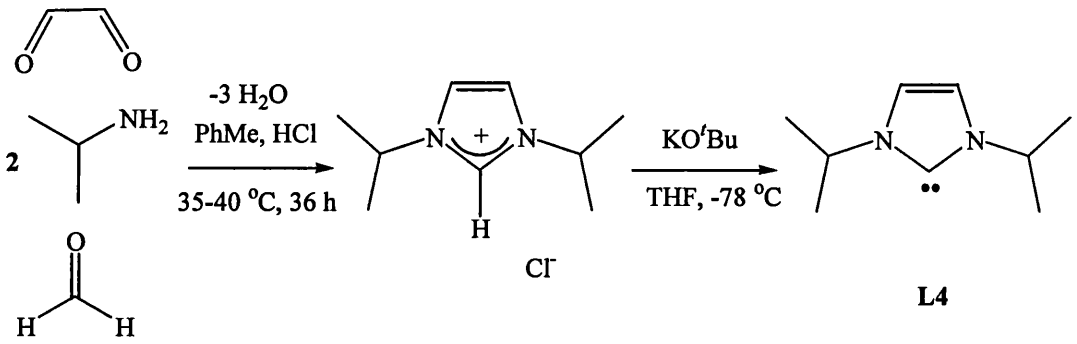

Scheme 2.7 *A one pot synthesis to yield free carbenes.*

2.3 Syntheses of mono substituted Ru-NHC complexes

2.3.1 Previous work

The synthesis of the Ru-NHC complex $RuH_2(CO)(PPh_3)_2$(IMes), **51**, was developed by a previous member of the Whittlesey group, Rudolf Jazzar.[12] The aryl NHC, IMes, was complexed to Ru *via* the addition of excess free carbene (three equivalents) to the ruthenium precursor $RuH_2(CO)(PPh_3)_3$, **52**, upon stirring at 70 °C for 2 weeks. Small traces of the bis-substituted carbene complex could be detected by ^{1}H NMR spectroscopy. This bis carbene complex could not be isolated and was removed upon work up. The mono carbene complex **51** (Figure 2.1) contained two inequivalent *cis* phosphines and *cis* hydrides. This was apparent from the ^{1}H NMR spectrum by the appearance of two doublet of doublet of doublets at δ -6.36 (J_{HP} = 26.8, J_{HP} = 23.6, J_{HH} = 6.0 Hz) and -8.08 (J_{HP} = 81.2, J_{HP} = 33.6, J_{HH} = 6.0 Hz) for the hydrides arising from coupling to two inequivalent phosphorus nuclei and the other inequivalent hydride (Figure 2.1). The smallest coupling constant was assigned to the H-H coupling and the largest to the *trans* H-P coupling. The ^{31}P{^{1}H} NMR spectrum further verified the

formation of **51** with two doublets at δ 59.0 (J_{PP} = 14.8 Hz) and 47.8 (J_{PP} = 14.8 Hz). The signal at δ 47.8 represents the phosphorus *trans* to the hydride, the signal shifted further upfield represents the phosphorus *trans* to the carbene.

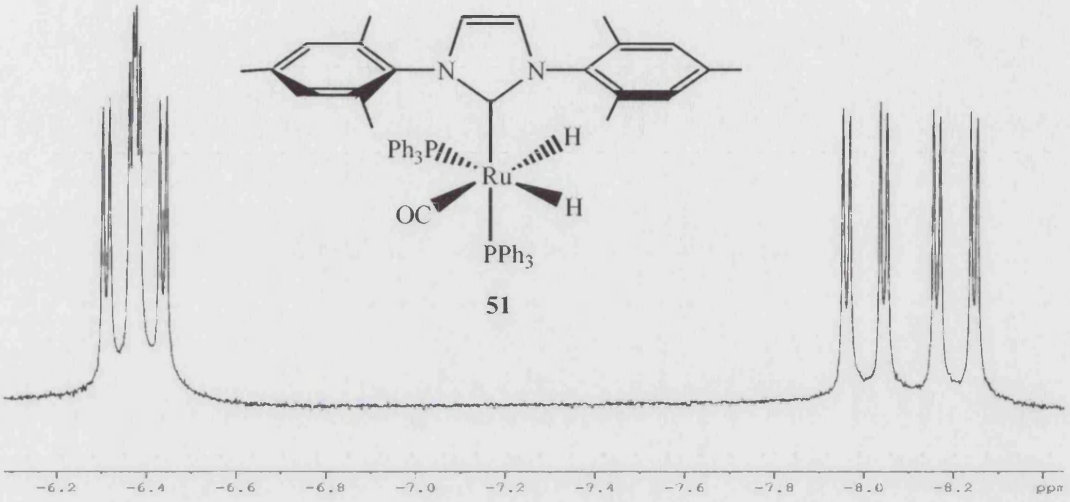

Figure 2.1 *Hydride region of the ^{1}H NMR spectrum (benzene-d_6, 400 MHz, 298 K) of $RuH_2(CO)(PPh_3)_2(IMes)$, **51**.*

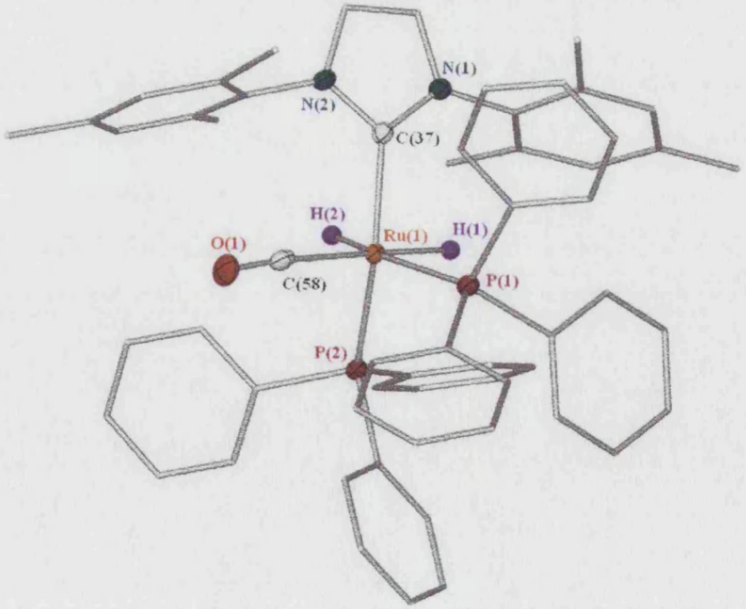

Figure 2.2 *X-ray structure of **51**.*

The X-ray structure was determined (Figure 2.2) to confirm the geometry of **51**. The C(37)-Ru-P(2) angle (146.33(5) °) showed that the complex is distorted from regular octahedral due to the bulky PPh_3 ligands and mesityl groups.

The Whittlesey group also attempted the synthesis of the analogous complex with the NHC 1,3-bis(2,6-diisopropylphenyl)imidazol-2-ylidene (IPr) but this ligand proved to be too sterically demanding to complex to the ruthenium. After prolonged heating, only trace amounts of the mono substituted Ru-NHC complex, could be detected by ^1H and $^{31}P\{^1H\}$ NMR spectroscopy.

2.3.2 Syntheses of N-aryl substituted Ru-NHC complexes

2.3.2.1 Attempted synthesis of $RuH_2(CO)(PPh_3)_2$(SIMes) (53)

The saturated analogue of IMes was synthesised (section 2.1.1.2) in order to compare the effects of a saturated carbene system with that of an unsaturated system. Initially we had thought that the saturated carbene would be more nucleophilic than IMes caused by the absence of delocalised electrons across the backbone double bond but it has been shown since that there is little difference between the two ligands.[13] Our attempts to complex SIMes to $RuH_2(CO)(PPh_3)_3$ (**52**) were unsuccessful. Following the experimental procedure used to synthesise **51** (heating an excess of carbene with **52** at 70 °C) we found no evidence for ligand exchange between **52** and SIMes; prolonged reaction times and/or higher temperatures resulted in the eventual decomposition of the carbene. Various quantities of carbene (1-10 equivalents) and different reaction temperatures (rt-100 °C) and solvents (benzene, toluene and THF) were tested but it was only when the reaction temperature was decreased to 40 °C that small amounts of the mono Ru-NHC complex **53** could be detected by ^1H and $^{31}P\{^1H\}$ NMR spectroscopy (Figure 2.3). However, no further complexation occurred even after prolonged periods of time.

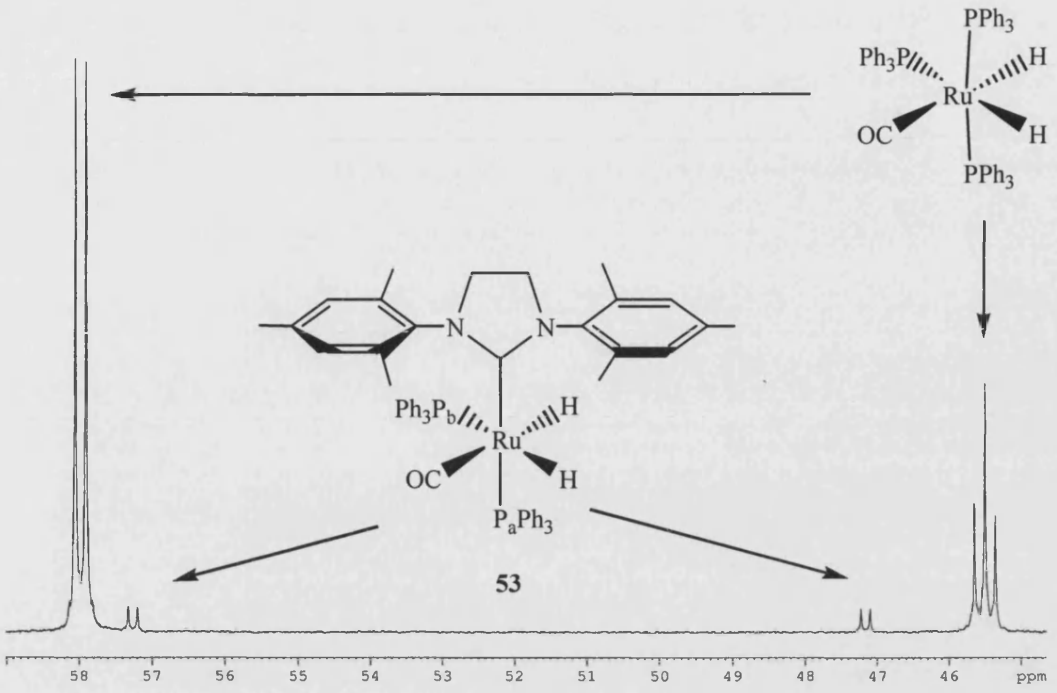

Figure 2.3 *$^{31}P\{^{1}H\}$ NMR spectrum (benzene-d_6, 121 MHz, 298 K) following the reaction of* ***52*** *with SIMes at 40 °C after 5 days.*

Nolan has attributed differences between IMes and SIMes when complexed to palladium to the presence of the two sp^3 carbon atoms on SIMes causing deformation of the imidazole ring and subsequent rotation of the N-substituted aryl groups.[14] In our case the aryl groups could now be directed towards the bulky equatorial PPh_3 inhibiting complexation to the ruthenium. In addition, shorter Ru-C distances are predicted for saturated NHC complexes, which also enhance steric effects.[14]

We have observed that $RuH_2(CO)(PPh_3)_2$(IMes) (**51**) loses IMes at high temperatures (≥70 °C) to reform **52**. It is possible that $RuH_2(CO)(PPh_3)_2$(SIMes) (**53**) undergoes the same decomposition pathway but at lower temperatures due to the enhanced steric effects as previously discussed. Thus the failure to form **53** could be due to (a) incompatibility of the NHC in bonding to ruthenium or (b) facile decomposition of the product by loss of SIMes.

2.3.3 Syntheses of N-alkyl substituted Ru-NHC complexes

2.3.3.1 General Procedure

Coordination of the N-alkyl substituted NHCs to ruthenium proved to be quite facile and complexation to ruthenium was much more rapid than with IMes, presumably due to their reduced steric bulk and increased nucleophilicity. In all cases, the reaction of an excess of free carbene with $RuH_2(CO)(PPh_3)_3$ (**52**) at 70 °C for a minimum of 20 h led to displacement of PPh_3 ligands as monitored by ^1H and $^{31}P\{^1H\}$ NMR spectroscopy. Because complexation was so rapid, varied mixtures of mono, bis and tris Ru-NHC complexes were formed. For R = Me, Et, ^{i}Pr and CH(Me)Ph we found that the mono-NHC complexes could not be synthesised cleanly without unreacted **52**. Therefore in most cases, the syntheses involved the formation of all three mono-, bis- and tris-NHC complexes; after work-up the mono-NHC complexes could be isolated as white solids in 46% – 66% yields. Interestingly, all alkyl carbenes substituted *trans* to a hydride, rather than *trans* to a phosphine, as with $RuH_2(CO)(PPh_3)_2$(IMes) **51**. This is presumably the preferred location of substitution and reflects the reduced steric bulk of the N-alkyl substituted NHCs compared to that of the N-aryl substituted NHCs. Attempts to isomerise these complexes thermally in order to place the NHCs *trans* to PPh_3 were unsuccessful. However, it was found that isomerisation could be achieved photochemically.[15]

Synthesis of the bis-carbene complexes $RuH_2(CO)(PPh_3)(NHC)_2$ required the same experimental method as with the mono-carbene complexes, but with different work up procedures. In order to form a greater quantity of the bis-carbene complexes, a larger excess of carbene (six equivalents) was heated at 70 °C with **52** for a minimum of 20 h. The carbenes substituted, as with the mono-carbene complexes, *trans* to hydride, in addition to substitution *trans* to a phosphine to give complexes of the form shown in Scheme 2.8. These differ from the bis-carbene complex observed for IMes where the carbenes reside *trans* to each other, presumably due to the bulk of the bulky mesityl rings.[16]

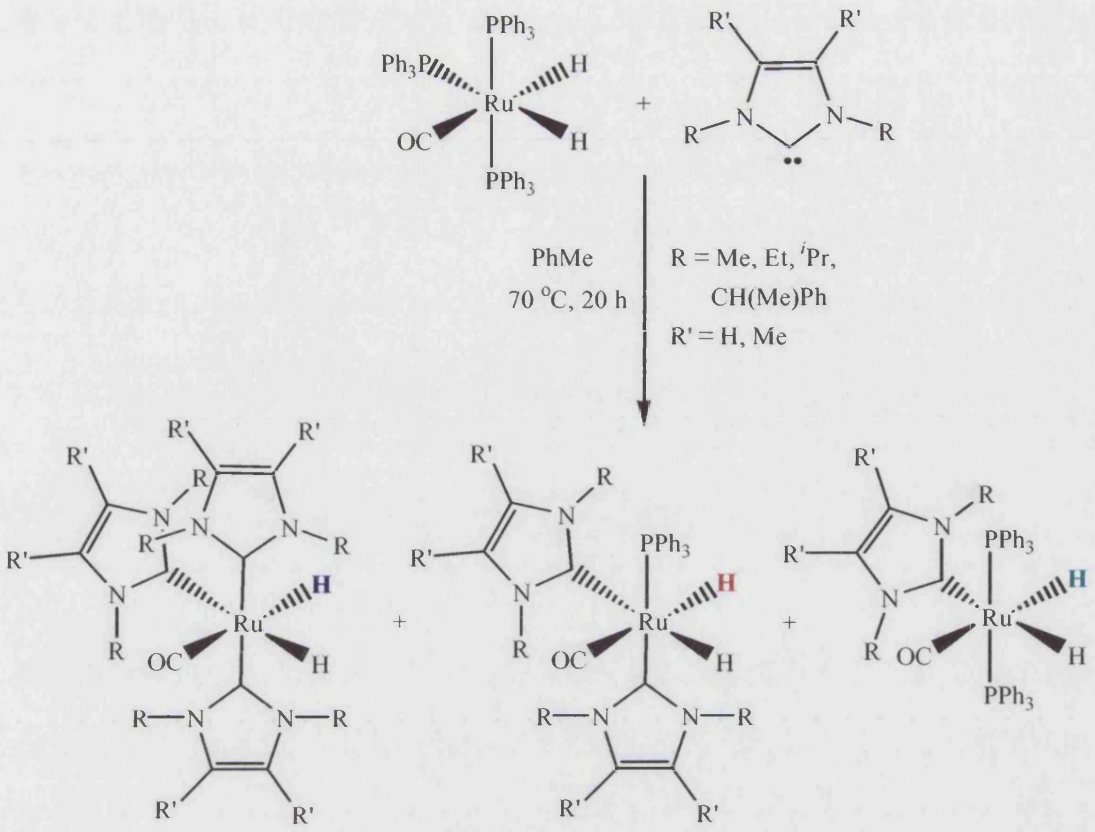

Scheme 2.8 *Synthesis of N-alkyl Ru-NHC complexes.*

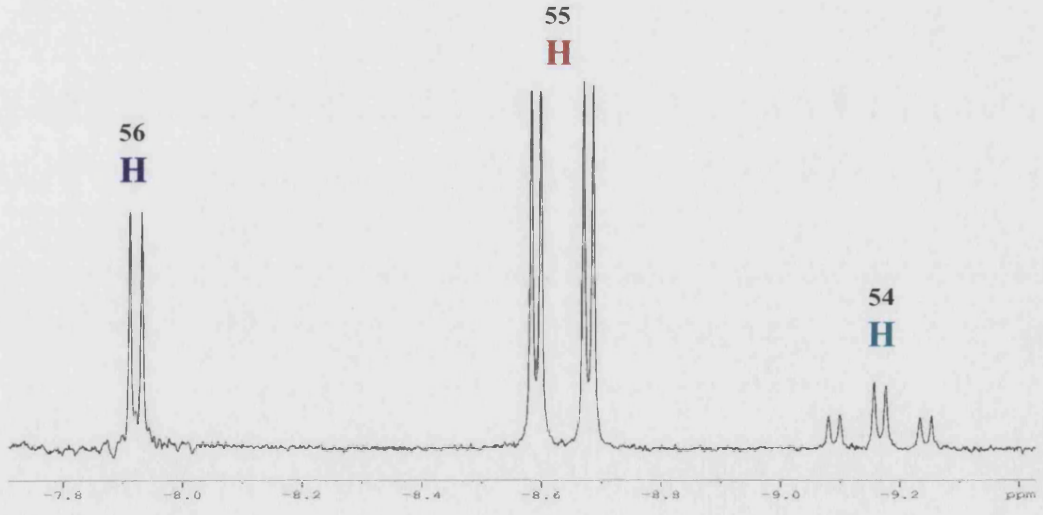

Figure 2.4 *^{1}H NMR (400 MHz, benzene-d_6, 298 K) showing some of the hydride resonances from $RuH_2(CO)(PPh_3)_2(IMe_4)$ (**54**), $RuH_2(CO)(PPh_3)(IMe_4)_2$ (**55**) and $RuH_2(CO)(IMe_4)_3$ (**56**).*

2.3.3.2 Syntheses of Ru(IMe$_4$) Complexes

2.3.3.2.1 Synthesis of RuH$_2$(CO)(PPh$_3$)$_2$(IMe$_4$) (54)

An excess of IMe$_4$ (three equivalents) was added to the ruthenium precursor, **52**, and the mixture heated in toluene at 70 °C for 3 days. The ^{1}H NMR spectrum revealed the complete loss of **52** and formation of the mono-, bis- and tris-(IMe$_4$) complexes, RuH$_2$(CO)(PPh$_3$)$_2$(IMe$_4$) (**54**), RuH$_2$(CO)(PPh$_3$)(IMe$_4$)$_2$ (**55**), and RuH$_2$(CO)(IMe$_4$)$_3$ (**56**). The excess of carbene was required since the formation of the bis- and tris-carbene complexes was rapid and the addition of fewer equivalents of carbene resulted in residual **52**. Removal of the solvent *in vacuo* and dissolution of the residue in ethanol, followed by stirring overnight gave a white precipitate of **54** in 51% yield. The ^{1}H NMR spectrum of the complex in benzene-d_6 showed two doublet of triplet resonances at δ -5.92 (J_{HP} = 26.9 Hz, J_{HH} = 5.5 Hz) and -9.03 (J_{HP} = 23.1 Hz, J_{HH} = 5.5 Hz), each coupled to two *cis* ^{31}P nuclei and the other inequivalent hydride (Figure 2.5). Four methyl signals suggest that there is restricted rotation of the carbene at room temperature. The N-CH$_3$ resonances (δ 3.10 and 2.69) were assigned *via* a ^{13}C{^{1}H}-^{1}H HMBC experiment where correlations could be seen to the carbenic carbon. Correlations from the imidazole backbone methyls (δ 1.37 and 1.17) to this carbon, as expected, could not be seen. In addition, correlations from the imidazole backbone methyls to the quaternary backbone carbons were stronger than those seen from the N-CH$_3$ protons confirming the correct identification of these signals. The ^{31}P{^{1}H} NMR spectrum displayed a singlet at δ 65.0 confirming the equivalent nature of the phosphines.

The IR spectrum (in benzene-d_6) displayed a carbonyl bond of 1922 cm^{-1} lower in frequency than that given for **51** (1941 cm^{-1}), indicating that IMe$_4$ is a better electron donor than IMes. The methyl groups on the backbone of the IMe$_4$ carbene add to the electron donating ability of the carbene while the presence of N-alkyl substituents also enhances the donor power. Nolan has found this with the Ni-NHC complexes [Ni(CO)$_3$(NHC)] in which the trend of alkyl substituents making the NHC ligand more donating is followed (Ni(CO)$_3$(IMes): 2051, 1970 cm^{-1}; Ni(CO)$_3$(ICy): 2050, 1965 cm^{-1}). However, the overall range in values of NHC data was relatively small (Table 2.1).[14] In fact there have been some contradictions to these data with experimentally determined and calculated IR data for Cr, Rh and Ir complexes.[17-20] Hence, there is still

some uncertainty as to whether N-alkyl substituents strengthen or weaken the donor power of the carbene relative to N-aryl groups.

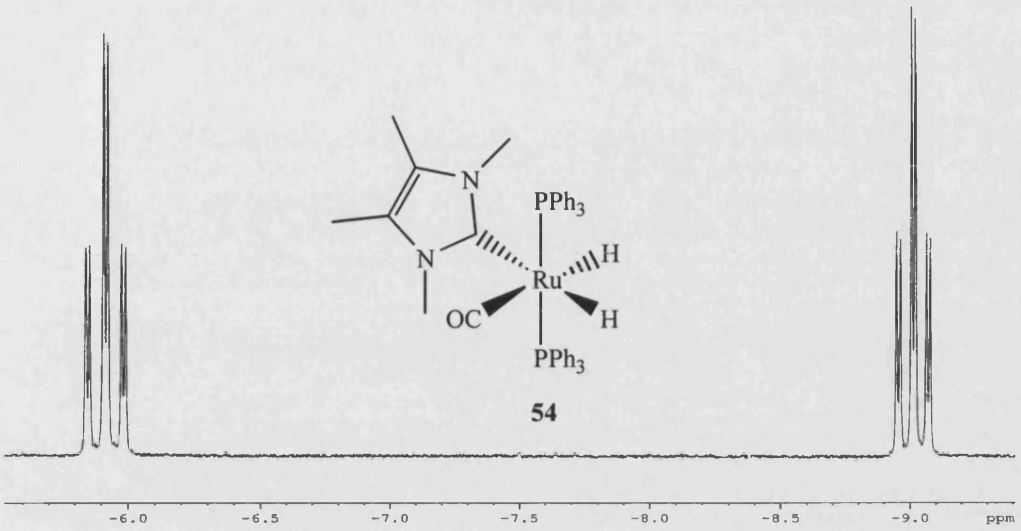

Figure 2.5 *Hydride region of the ^{1}H NMR spectrum (benzene d_6, 400 MHz, 298 K) of* ***54****.*

Complex	ν_{CO} [(cm^{-1})] CH_2Cl_2	ν_{CO} [(cm^{-1})] CH_2Cl_2
[Ni(CO)$_3$(IMes)]	2050.7	1969.8
[Ni(CO)$_3$(SIMes)]	2051.5	1970.6
[Ni(CO)$_3$(IPr)]	2051.5	1970.0
[Ni(CO)$_3$(SIPr)]	2052.2	1971.3
[Ni(CO)$_3$(ICy)]	2049.6	1964.6
[Ni(CO)$_3$(P^{t}Bu$_3$)]	2056.1	1971
[Ni(CO)$_3$(P^{i}Pr$_3$)]	2059.2	1977
[Ni(CO)$_3$(PPh$_3$)]	2068.9	1990

Table 2.1 *IR stretching frequencies in [Ni(CO)$_3$(L)].*[14]

2.3.3.2.2 Synthesis of $RuH_2(CO)(PPh_3)(IMe_4)_2$ (55)

Rather than stirring in ethanol which afforded $RuH_2(CO)(PPh_3)_2(IMe_4)$ **54** in pure form, concentration of the toluene solvent from a heated solution of **52** and IMe_4 allowed

isolation of a yellow precipitate of **55** in 43% yield. Since **55** was insoluble in toluene and benzene, THF solutions were made up to obtain NMR data. The ^{1}H NMR spectrum displayed two doublet of doublets at δ -6.37 (J_{HP} = 37.3 Hz, J_{HH} = 4.9 Hz) and -9.75 (J_{HP} = 26.3 Hz, J_{HH} = 4.9 Hz) arising from the inequivalent hydrides present (Figure 2.6). Lower field signals associated with the IMe_4 ligands showed the carbene *trans* to the phosphine was free to rotate since there were only two sets of methyl resonances, one for the methyls on the imidazole backbone (δ 1.66) and one for the methyls on the nitrogens (δ 3.17). These shifts were associated with the axial IMe_4 ligand, *trans* to phosphine, by $^{13}C\{^{1}H\}$ NMR and $^{13}C\{^{1}H\}$-^{1}H HMBC experiments. The carbenic carbons were assigned in the $^{13}C\{^{1}H\}$ NMR spectrum according to their coupling constants: the axial carbene has a large *trans* coupling to phosphine. This carbon was then correlated in the $^{13}C\{^{1}H\}$-^{1}H HMBC to the N-CH_3 groups. However, the carbene residing *trans* to the hydride displayed four sets of methyl resonances, one for each methyl group (δ 3.00, 2.62, 1.47, 1.45), suggesting that the carbene does not freely rotate at room temperature. This is presumably due to the increased steric crowding in the position *cis* to the bulky phosphine ligand.

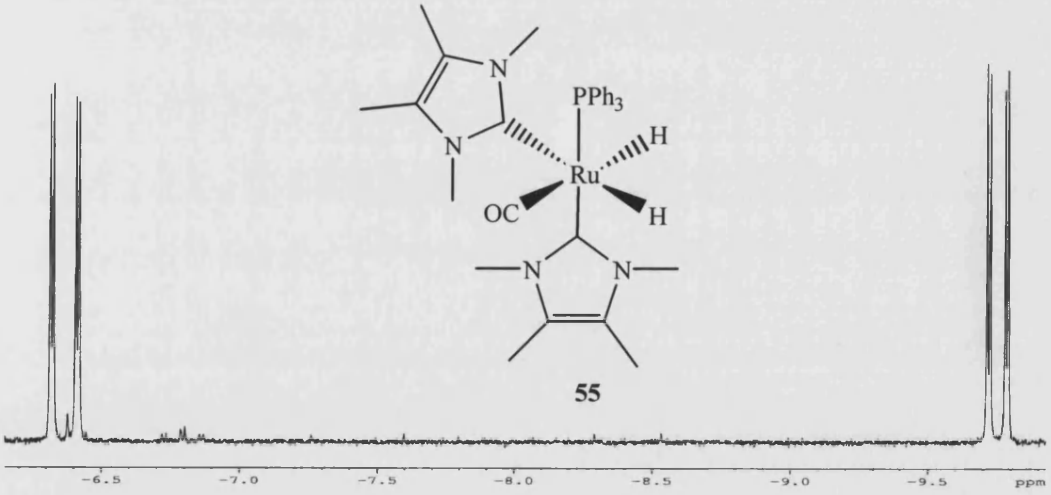

Figure 2.6 *Hydride region of the ^{1}H NMR spectrum (THF-d_8, 400 MHz, 298 K) of* ***55****.*

To prove the formation of **55** beyond doubt, X-ray quality crystals were grown by layering a THF solution with hexane and the crystal structure was recorded at -123 °C (Figure 2.7). The Ru-C(carbene) bond lengths are shorter than for the mono-substituted

carbene complexes, $RuH_2(CO)(PPh_3)_2(IEt_2Me_2)$ (**57**) (2.171(3) Å), $RuH_2(CO)(PPh_3)_2(I^iPr)$ (**58**) (2.1604(19) Å) and $RuH_2(CO)(PPh_3)_2(I^*)$ (**59a**) (2.136(3) Å), perhaps due to the small methyl groups allowing closer approach of the NHC ligands to the ruthenium centre. The carbene residing in the axial position, *trans* to phosphine, has a shorter Ru-C(carbene) bond length (2.086(4)Å) than that *cis* to phosphine (2.122(4) Å), presumably due to the larger *trans* influence of hydride compared to PPh_3. The P(1)-Ru-C(2) angle is distorted from regular octahedral (166.91(10)°) but less so than in the other mono-carbene complexes, **57**, **58** and **59a**, due to the reduction in steric bulk with the replacement of another phosphine. In fact, the C(2)-Ru-C(9) angle is not distorted at all (90.32(13)°).

The Ru-CO bond length (1.867(4) Å) is also slightly shorter than in the mono-carbene complexes (1.880(4) Å, 1.900(2) Å, and 1.884(4) Å for **57**, **58** and **59a** respectively). The C≡O stretching frequency drops 38 cm^{-1} from 1922 cm^{-1} in the mono-carbene complex **54** to 1884 cm^{-1} in the bis-carbene complex **55** indicating an increase in backbonding from the metal to the carbonyl. This is due to the increased σ-donor ability of the two carbenes compared to the coordination of one carbene and one phosphine.

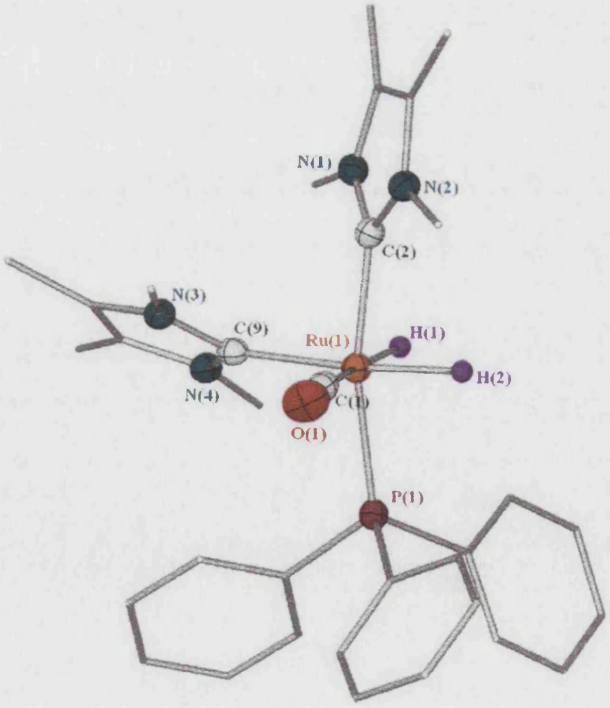

Figure 2.7 *X-ray structure of 55.*

Selected Bond Lengths (Å)		Selected Bond Angles (°)	
Ru-C(1)	1.867(4)	P(1)-Ru-C(2)	166.91(10)
Ru-C(2)	2.086(4)	C(9)-Ru-P(1)	98.77(10)
Ru-C(9)	2.122(4)	C(2)-Ru-C(9)	90.32(13)
Ru-P(1)	2.2930(10)	C(1)-Ru-C(2)	96.42(15)
		C(1)-Ru-P(1)	91.33(12)
		C(1)-Ru-C(9)	99.68(15)

Table 2.2 *Selected bond lengths and angles for* ***55****.*

2.3.3.3 Syntheses of Ru(IEt$_2$Me$_2$) complexes

2.3.3.3.1 Synthesis of RuH$_2$(CO)(PPh$_3$)$_2$(IEt$_2$Me$_2$) (57)

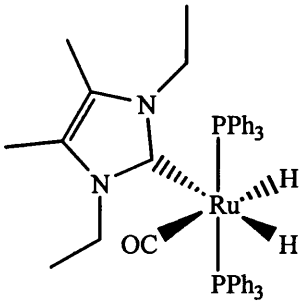

57

The reaction of four equivalents of IEt$_2$Me$_2$ with **52** at 70 °C for 20 h resulted in displacement of PPh$_3$ ligands to yield a mixture of the mono and bis-carbene complexes in a 1:1 ratio based on ^{1}H NMR spectroscopy. Removal of solvent gave a brown residue which upon addition of ethanol immediately afforded somewhat surprisingly a bright red solution with the evolution of a gas (presumably H$_2$). It is noted that Morris and co-workers have also witnessed an extremely reactive red solution in the reaction of RuHCl(PPh$_3$)$_3$ with I^{t}Bu that they proposed to result from a coordinatively unsaturated Ru(I^{t}Bu)(PPh$_3$)$_2$ species. Upon addition of H$_2$, this complex gave the mono carbene dihydride species RuH$_2$(PPh$_3$)$_2$(I^{t}Bu).[21] In the case of **57**, stirring the red solution overnight produced a white precipitate. The mixture was subsequently filtered and the precipitate dissolved in benzene and heated at 70 °C for 1 h. Removal of solvent *in*

vacuo and recrystallisation from THF/hexane gave the monocarbene complex $RuH_2(CO)(PPh_3)_2(IEt_2Me_2)$ (**57**) as colourless crystals in 48% yield.[22] The ^1H NMR spectrum of the complex in benzene-d_6 showed two doublet of triplets at δ -6.38 (J_{HP} = 26.3 Hz, J_{HH} = 5.5 Hz) and -9.99 (J_{HP} = 24.7 Hz, J_{HH} = 5.5 Hz), each coupled to two *cis* ^{31}P nuclei and the other inequivalent hydride. Two sets of ethyl signals are testimony to the fact that the carbene ligand does not freely rotate at room temperature. The equivalent nature of the phosphines was confirmed by the appearance of a singlet in the $^{31}P\{^1H\}$ NMR spectrum at δ 63.7. To confirm the geometry of **57**, the X-ray crystal structure was determined, as depicted in Figure 2.8. Despite the disorder in **57**, the crystal structure is unambiguous. Concentrating on the major disordered component (80 % occupancy), it is clear that the geometry at ruthenium is distorted from regular octahedral with a *trans* P(1)-Ru-P(2) angle of 164.32(4)°. The small P(1)-Ru-P(2) angle is mainly due to steric effects of the carbene ligand. Leaning of the PPh_3 ligands towards the small hydride ligands is a common feature of dihydride complexes.[21] The Ru-C(2) bond distance (2.171(3) Å) is considerably longer than the Ru-IMes distance in **51** (2.0956(17) Å). This presumably reflects both the longer M-C(alkyl NHC) versus M-C(aryl NHC) bond found by others[23] and the orientation of the IEt_2Me_2 ligand *trans* to the labilising hydride ligand.

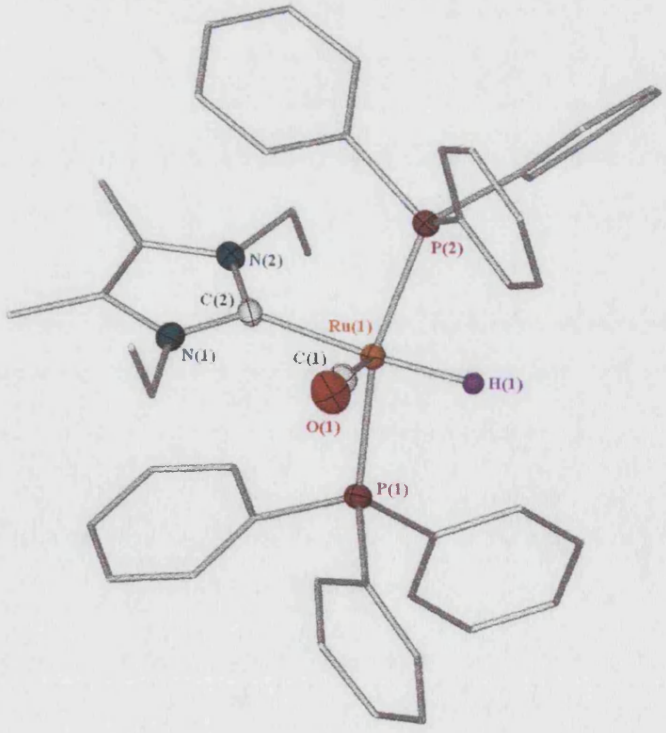

Figure 2.8 *X-ray structure of* ***57****.*

Selected Bond Lengths (Å)		Selected Bond Angles (°)	
Ru-C(2)	2.171(3)	P(1)-Ru-P(2)	164.32(4)
Ru-C(1)	1.880(4)	C(2)-Ru-P(1)	94.87(18)
Ru-P(1)	2.3313(13)	C(2)-Ru-P(2)	96.84(18)
Ru-P(2)	2.3048(13)	C(1)-Ru-C(2)	99.7(2)
		C(1)-Ru-P(1)	98.29(17)
		C(1)-Ru-P(2)	89.99(17)

Table 2.3 *Selected bond lengths and angles for 57.*

2.3.3.3.2 Synthesis of $RuH_2(CO)(PPh_3)(IEt_2Me_2)_2$ (60)

An excess of IEt_2Me_2 (six equivalents) was heated at 70 °C with **52** in toluene for 20 h. Removal of the solvent gave a brown residue which was washed with hexane affording, $RuH_2(CO)(PPh_3)(IEt_2Me_2)_2$ (**60**) as a purple precipitate. The complex was isolated as a pale purple solid in 29% yield and characterised by ^1H, $^{31}P\{^1H\}$ and $^{13}C\{^1H\}$ NMR spectroscopy. The ^1H NMR spectrum displayed two doublet of doublet hydride resonances at δ -5.52 (J_{HP} = 39.5 Hz, J_{HH} = 4.9 Hz) and -8.93 (J_{HP} = 26.9 Hz, J_{HH} = 4.9 Hz) arising from the coupling of each hydride to the *cis*-phosphorus and also to the other inequivalent hydride. From the ^1H NMR spectrum it is clear that, as with the **55**, the carbene *trans* to the PPh_3 is freely rotating whereas the carbene *cis* to the PPh_3 has restricted rotation. However, rather than observing the expected quartet resonances for the N-methylene protons, the couplings are more complicated implying that these CH_2 protons are diastereotopic due to the restricted rotation about the N-CH_2 bond (Figure 2.9 resonances A and B). However, ethyl CH_3 groups show similar couplings to the two methylene protons and they appear as triplets. Thus, for the ethyl substituents, one triplet and one multiplet are observed for the carbene *trans* to the phosphine (rotating) (Figure 2.9 resonance A), and two triplets and four multiplets are observed for the carbene *trans* to the hydride (fixed) (Figure 2.9 resonance B).

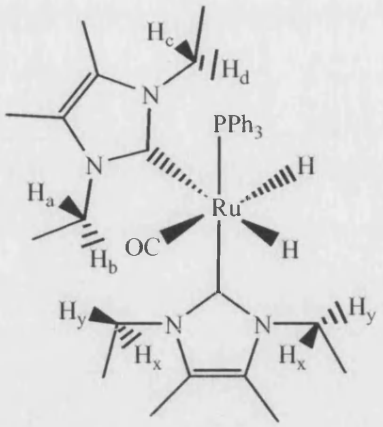

60

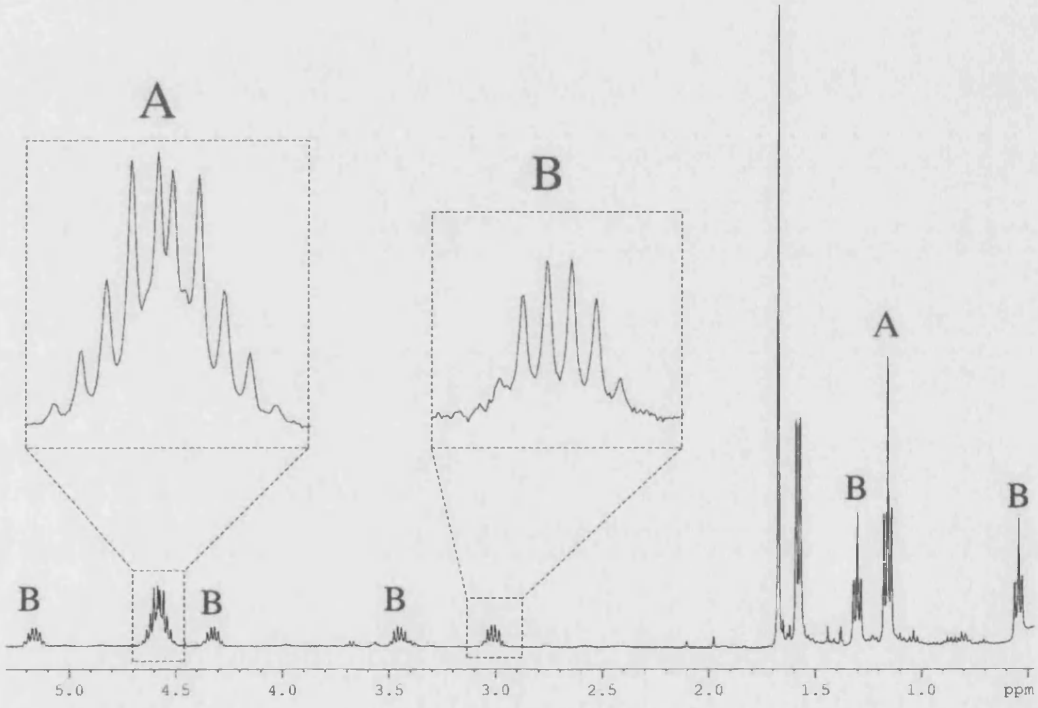

Figure 2.9 *^{1}H NMR spectrum of $RuH_2(CO)(PPh_3)(IEt_2Me_2)_2$ (**60**) (benzene-d_6, 400 MHz, 298 K) showing the signals for the ethyl groups of the two NHC ligands.*

The X-ray structure was determined to confirm the structure of **60** (Figure 2.10). The Ru-C(carbene) bond lengths (2.0951(18) Å and 2.145(2) Å) were slightly shorter than in the mono-IEt_2Me_2 carbene complex **57**. As with the bis-IMe_4 carbene complex **55**, the shortest Ru-C(carbene) bond length arises from the carbene *trans* to phosphine rather than the one *cis* to phosphine, *trans* to hydride. The carbene *trans* to phosphine

can gain a closer approach to the metal centre with no obstruction from the bulky PPh_3 ligand in addition to the *trans* influence of the hydride lengthening the Ru-C bond of the carbene *cis* to phosphine. The Ru-CO bond distance is also slightly reduced from the mono-IEt_2Me_2 complex **57** (1.880(4) Å) to the bis-IEt_2Me_2 complex **60** (1.8615(19) Å). The CO stretching frequency drops 37 cm^{-1} from 1921 cm^{-1} in complex **57** to 1884 cm^{-1} in complex **60**. These values are almost identical to the Ru-IMe_4 complexes **54** and **55** indicating that the difference in donor effects of these carbenes is negligible.

The C(30)-Ru-C(20) angle (89.90(7) °) is as expected for octahedral geometry but the P-Ru-C(30) angle (163.30(5) °) is more acute than regular octahedral indicating the leaning of the bulky ligands towards the small hydrides.

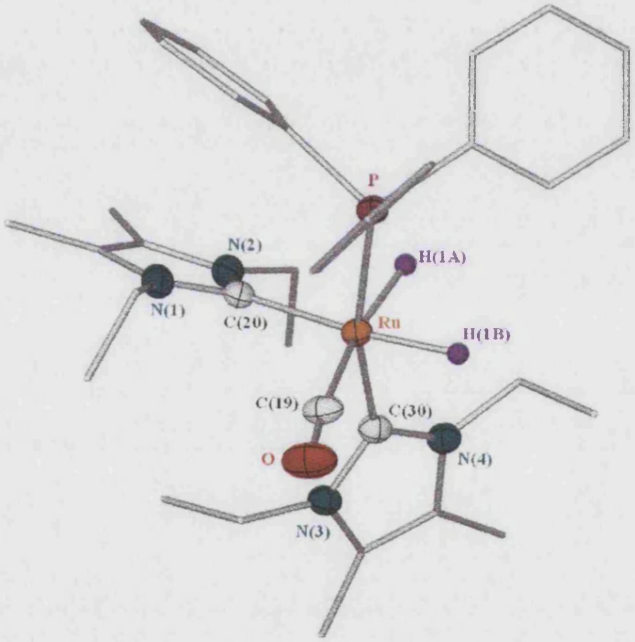

Figure 2.10 *X-ray structure of $RuH_2(CO)(PPh_3)(IEt_2Me_2)_2$ (**60**).*

Selected Bond Lengths (Å)		Selected Bond Angles (°)	
Ru-C(19)	1.8615(19)	P-Ru-C(30)	163.30(5)
Ru-C(30)	2.0951(18)	C(20)-Ru-P	96.54(5)
Ru-C(20)	2.145(2)	C(30)-Ru-C(20)	89.90(7)
Ru-P	2.3000(5)	C(19)-Ru-C(30)	93.72(8)
		C(19)-Ru-P	99.36(6)
		C(19)-Ru-C(20)	105.40(9)

Table 2.4 *Selected bond lengths and angles for $RuH_2(CO)(PPh_3)(IEt_2Me_2)_2$ (60).*

2.3.3.4 Syntheses of Ru(I^{i}Pr$_2$Me$_2$) complexes

2.3.3.4.1 Synthesis of $RuH_2(CO)(PPh_3)_2(I^iPr_2Me_2)$ (61)

Attempts to produce the mono-I^{i}Pr$_2$Me$_2$ dihydride complex **61** by the same general method (section 2.3.1.1) were unsuccessful. Instead, the C-H activated complex RuH(CO)(PPh$_3$)$_2$(I^{i}Pr$_2$Me$_2$') **62a** was isolated in good yield (see Chapter 3). The mono – NHC dihydride complex **61** could be synthesised by addition of either alcohol or, most cleanly, by bubbling hydrogen through a benzene solution of **62a** at 50 °C for 3 h (Scheme 2.9). Once the solution had cooled to room temperature, **61** precipitated out of solution. The mixture was filtered giving clean dihydride product in high yield (93%). The ^{1}H NMR spectrum of **61** displays two doublet of triplet hydride resonances at δ -5.79 (J_{HH} = 6.0 Hz, J_{HP} = 26.9 Hz) and -9.98 (J_{HH} = 6.0 Hz, J_{HP} = 26.9 Hz). Only two sets of resonances were observed for the isopropyl methyl groups and backbone methyl groups suggesting that the two isopropyl N-substituents are inequivalent, implying that the carbene is not freely rotating at room temperature. The fact that there are only two sets of signals also indicates that there is free rotation about the N-CHMe$_2$ bond at room temperature.

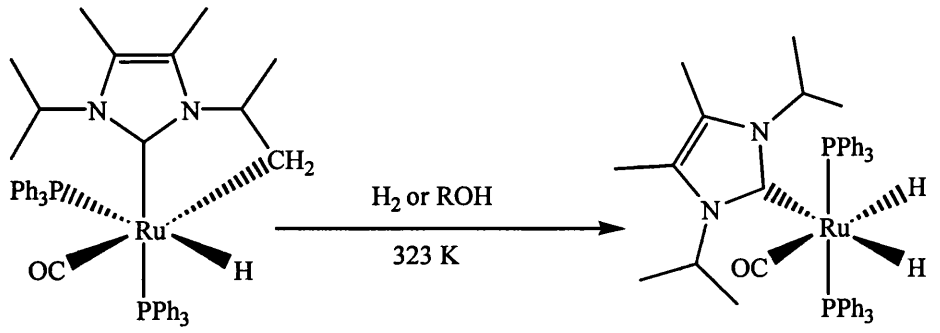

Scheme 2.9 *Formation of the mono dihydride complex of* ***61*** *from* ***62a.***

The CO stretching frequency (1917 cm^{-1}) was slightly lower than for the mono Ru-NHC complexes, **54**, **57**, **58** and **59a** (1922, 1921, 1922 and 1937 cm^{-1} respectively) suggesting that this alkyl carbene is the strongest σ-donor. This is in agreement with Cavell's calculated basicities of carbenes where he suggests that $I^iPr_2Me_2$ is the most basic NHC there is with a p*K*a of 30.4 ± 0.3 in aqueous solution.[24] Alder *et al.* measured the p*K*a in DMSO-d_6 as 24.0.[25]

2.3.3.4.2 Evidence for $RuH_2(CO)(PPh_3)(I^iPr_2Me_2)_2$ (63)

Evidence for the formation of the bis-carbene complex of $I^iPr_2Me_2$ was seen in the ^1H NMR spectrum upon addition of excess $I^iPr_2Me_2$ to **52**. The resonances were very similar to those seen for $RuH_2(CO)(PPh_3)(IMe_4)_2$ (**55**) and $RuH_2(CO)(PPh_3)(IEt_2Me_2)_2$ (**60**). However, this complex was not isolated due to its high solubility in all solvents preventing separation from free phosphine and carbene remaining in the reaction mixture.

2.3.3.5 Synthesis of $RuH_2(CO)(PPh_3)_2(I^iPr)$ (58)

Complex **58** was prepared as a comparison to **61** to establish what effects methyl groups on the backbone of the carbene have on the relative properties of the two complexes. A mixture of I^iPr and **52** (ratio 4:1) was heated at 70 °C in toluene for 20 h. Removal of the toluene and dissolution of the brown residue in ethanol gave a red solution and evolution of gas. The solution was stirred overnight to yield a white precipitate which was filtered and washed with hexane to give the desired dihydride mono-carbene product **58** in a 55% yield. The ^1H NMR spectrum of **58** in benzene-d_6 displayed two doublet of triplet resonances at δ -5.89 (J_{HP} = 26.9 Hz, J_{HH} = 6.0 Hz) and -9.46 (J_{HP} =

26.9 Hz, J_{HH} = 6.0 Hz) shifted slightly from the corresponding signals for **62a**. To confirm the geometry of **58**, crystals suitable for X-ray diffraction were grown from a benzene/hexane solution. The X-ray structure obtained is depicted in Figure 2.11. The Ru-C(carbene) bond length (2.1604(19) Å) is similar to that of $RuH_2(CO)(PPh_3)_2(IEt_2Me_2)$ (**57**) (2.171(3) Å). The Ru-CO bond lengths are also similar (1.900(2) Å for **58** compared to 1.880(4) Å for **57**), consistent with the findings of Nolan that CO bond lengths do not alter significantly with different NHC donor ligands.[14] The P(1)-Ru-P(2) angle (155.549(19) °) shows the distortion from regular octahedral at the metal, slightly more so than with **57** reflecting the increased steric bulk of ^{i}Pr compared to Et.

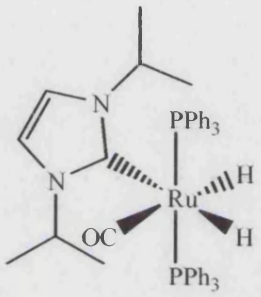

58

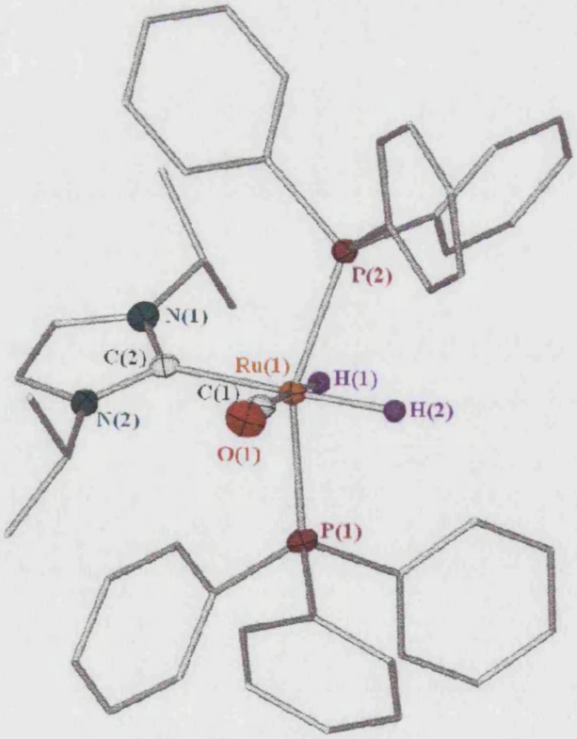

Figure 2.11 *X-ray structure of $RuH_2(CO)(PPh_3)_2(I^iPr)$ (**58**).*

Selected Bond Lengths (Å)		Selected Bond Angles (°)	
Ru-C(2)	2.1604(19)	P(1)-Ru-P(2)	155.549(19)
Ru-C(1)	1.900(2)	C(2)-Ru-P(1)	99.03(5)
Ru-P(1)	2.2982(5)	C(2)-Ru-P(2)	100.42(5)
Ru-P(2)	2.3075(5)	C(1)-Ru-C(2)	100.10(8)
		C(1)-Ru-P(1)	96.90(6)
		C(1)-Ru-P(2)	94.13(6)

Table 2.5 *Selected bond lengths and angles for $RuH_2(CO)(PPh_3)_2(I^iPr)$ (58).*

2.3.3.6 Synthesis of $RuH_2(CO)(PPh_3)_2(I^*)$ (59a)

An excess of the (*S,S*)-I* carbene to **52** (ratio 4:1) was heated in toluene for 20 h at which time resonances due to **52** had completely disappeared. The solvent was removed and the residue washed with ethanol. Upon addition of ethanol the solution immediately turned red as with the other complexes. However, precipitation was much slower and so the solution was left to stir for 1 week at which point sufficient solid had precipitated. The solution was filtered and the remaining solid washed with hexane to yield **59a** as a white solid. Interestingly, sets of major and minor resonances could be seen in the ^1H (Figure 2.12) and $^{31}P\{^1H\}$ NMR spectra. Variable temperature (VT) ^1H NMR experiments revealed that there was no interconversion between the two compounds **59a** and **59b**. It was thought that these two complexes could perhaps be diastereomers.

To obtain **59a** with (*S,S*)-stereochemistry alone, the solid was recrystallised from a layered solution of benzene with hexane. The ^1H NMR spectrum of the recrystallised product showed loss of the minor component **59b** with only the major component **59a** remaining.

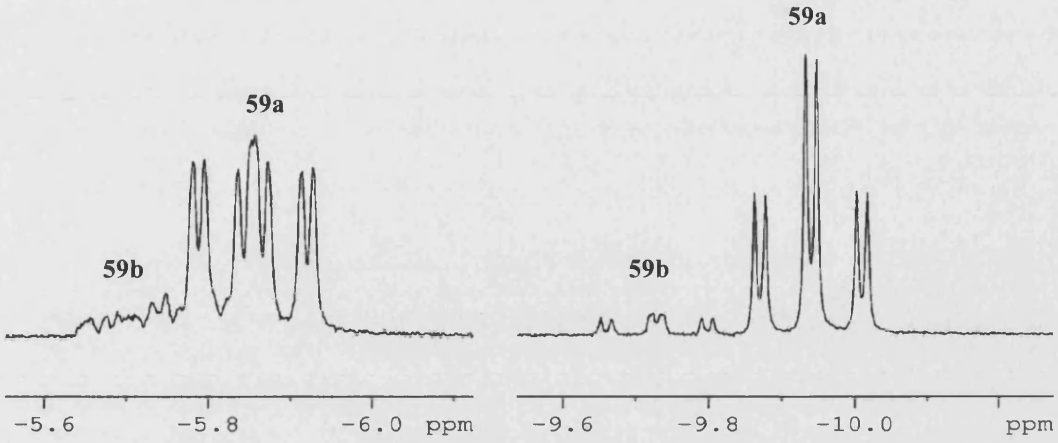

Figure 2.12 *^{1}H NMR spectrum (benzene-$_{d6}$, 400 MHz, 298 K) of $RuH_2(CO)(PPh_3)_2$(I*) showing the presence of major (**59a**) and minor(**59b**) resonances.*

The purified chiral carbene complex **59a** was fully characterised by multinuclear 1-D NMR and 2-D NMR correlations. Two multiplets furthest downfield in the ^{1}H NMR spectrum at δ 7.83-7.72 and 7.68-7.50 were initially thought to arise from the phenyl groups of the carbene. However, 2-D COSY and HMQC experiments showed correlations from these peaks to other multiplets in the aromatic region proving that they in fact belonged to PPh_3 (Figure 2.13 peak A). A $^1H\{^{31}P\}$ experiment confirmed this with the multiplets furthest downfield being simplified due to the absence of phosphorus couplings. The Ph groups of the carbene could therefore not be assigned precisely as they were hidden underneath the other aromatic PPh_3 peaks.

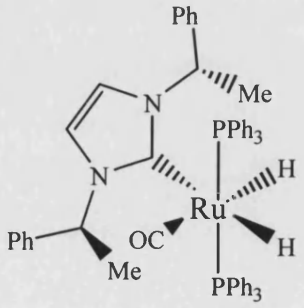

59a

The substituent N-CH protons were identified by $^{13}C\{^1H\}$-^1H HMQC/HMBC experiments (Figure 2.13 peak B) and were shifted all the way up to the aromatic region

(δ 7.05 and 6.84), presumably due to the presence of the adjacent phenyl group causing additional deshielding of the C-H group. Herrmann and co-workers report similar shifts for these protons in the complexes $Ni(CO)_3(I^*)$ (δ 6.08) and $W(CO)_5(I^*)$ (δ 6.48).[26]

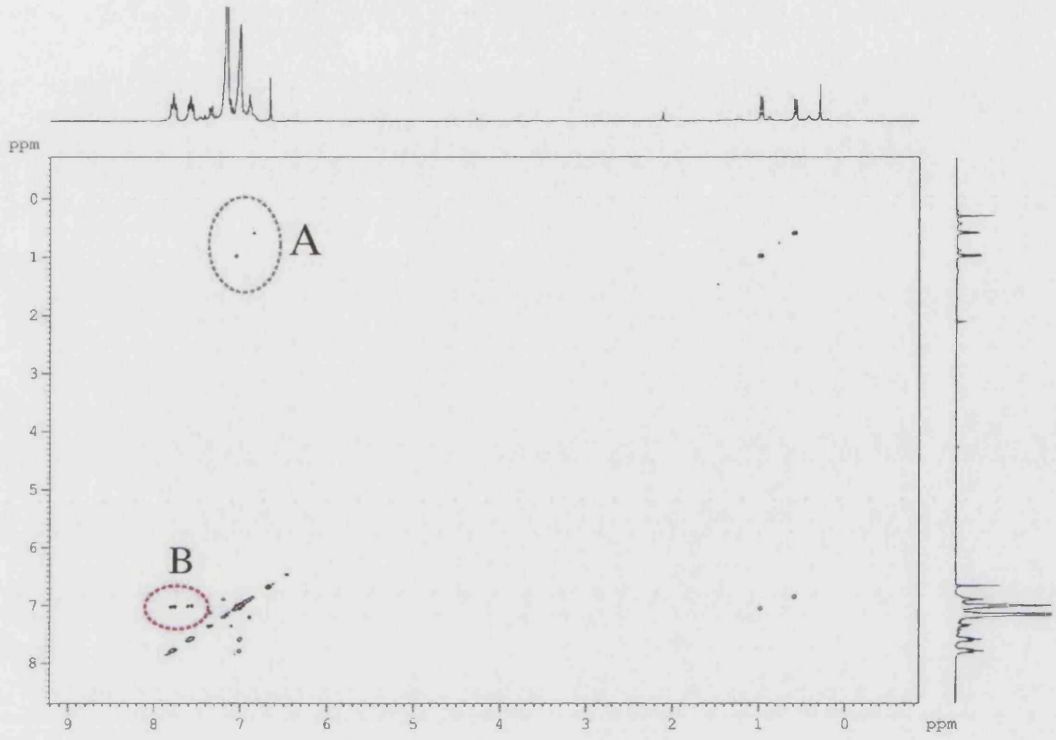

Figure 2.13 *COSY 2-D NMR (400 MHz, benzene-d_6, 298 K) of* ***59a****.*

The hydride region of the proton NMR spectrum revealed that the phosphines were very slightly inequivalent. While in one case the hydride appeared as the expected doublet of triplets (δ -9.81, J_{HP} = 28.0 Hz, J_{HH} = 5.5 Hz), the second hydride signal appeared as a doublet of doublet of doublets (δ -5.72, J_{HP} = 28.0 Hz, J_{HP} = 22.0 Hz, J_{HH} = 5.5 Hz) (Figure 2.14). The inequivalent nature of the phosphines was more apparent in the $^{31}P\{^1H\}$ NMR spectrum where a clear AB type system could be seen (Figure 2.15).

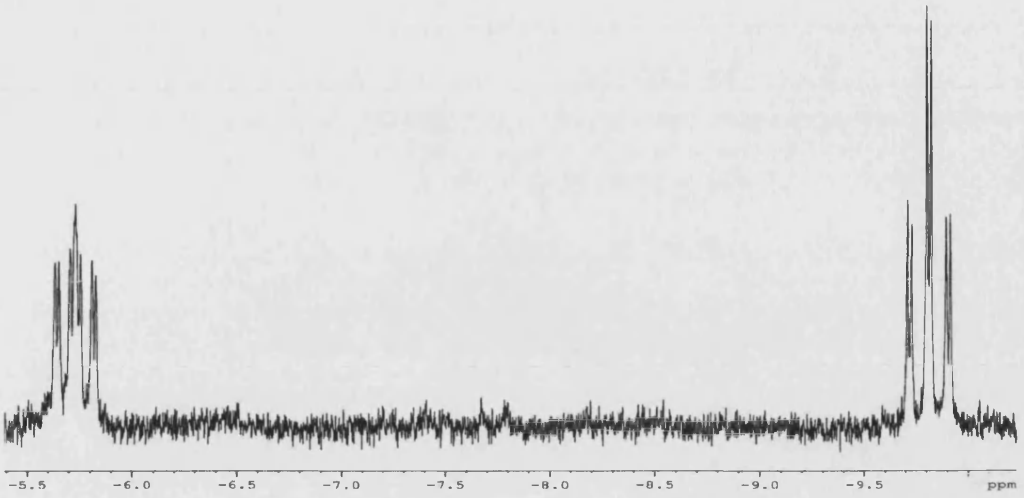

Figure 2.14 *Hydride region of the ^{1}H NMR spectrum of* ***59a*** *(benzene-d_6, 300 MHz, 298 K).*

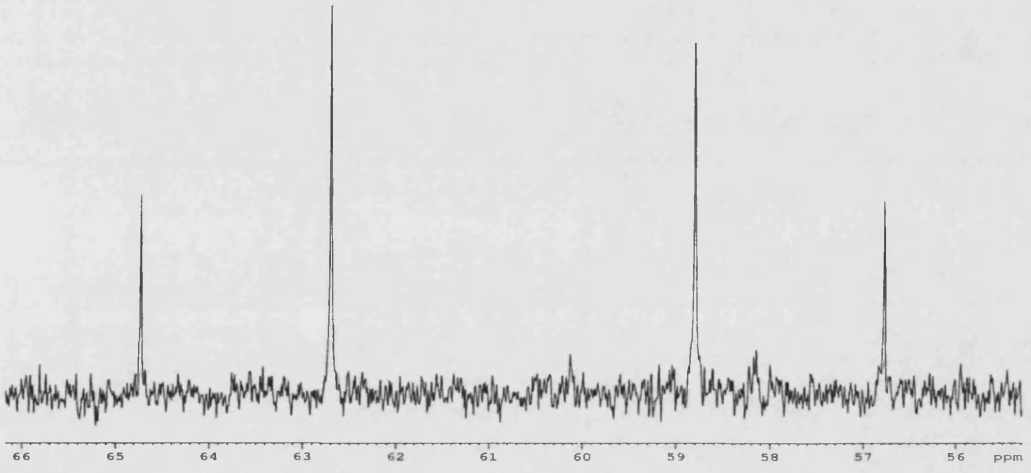

Figure 2.15 *$^{31}P\{^{1}H\}$ spectrum of* ***59a*** *(benzene-d_6, 121 MHz, 298 K).*

An X-ray structure was obtained as depicted in Figure 2.16. The Ru-C(carbene) bond length in **59a** (2.136(3) Å) is shorter than those of the alkyl substituted Ru-NHC complexes but longer than in the aryl substituted NHC complex **51**. The averaged bond length given for **59a**, which comprises an NHC with mixed alkyl/aryl character, supports the findings by others of shorter M-C(alkyl) bond lengths compared to M-C(aryl) bond lengths.[23]

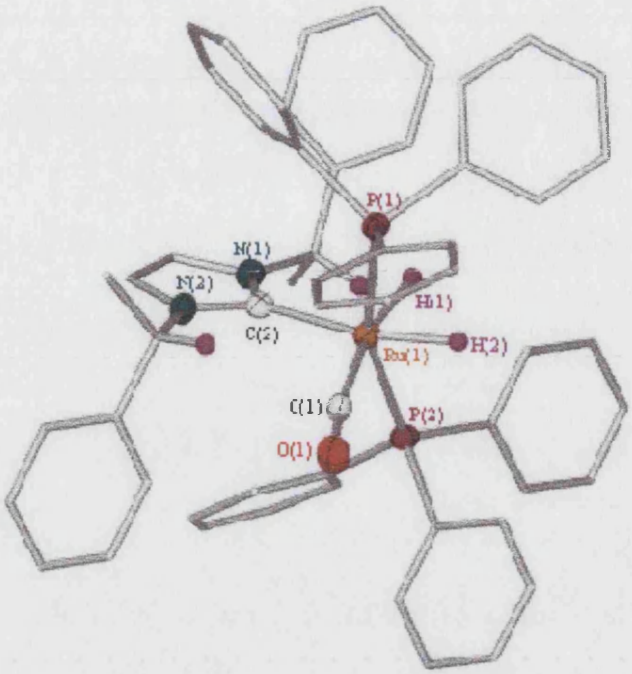

Figure 2.16 *X-ray structure of $RuH_2(CO)(PPh_3)_2$(I*) (**59a**).*

Selected Bond Lengths (Å)		Selected Bond Angles (°)	
Ru-C(2)	2.136(3)	P(1)-Ru-P(2)	160.24(3)
Ru-C(1)	1.884(4)	C(2)-Ru-P(1)	98.09(9)
Ru-P(1)	2.3084(9)	C(2)-Ru-P(2)	97.93(9)
Ru-P(2)	2.3028(9)	C(1)-Ru-C(2)	105.87(13)
		C(1)-Ru-P(1)	96.53(11)
		C(1)-Ru-P(2)	90.13(11)

Table 2.6 *Selected bond lengths and angles for $RuH_2(CO)(PPh_3)_2$(I*) (**59a**).*

Close inspection of the crystal structure revealed no evidence for π-stacking between the phenyl rings of the carbene and phosphines. The methyl groups of the carbene appear to point into the phenyl rings of the PPh_3 groups but distances between the methyl and π-cloud centroid were too long to suggest any CH-π interaction.

When resolving the crystal structure, there were two structures within the lattice. Initially we had thought that this was perhaps the unidentified second "diastereomeric"

complex **59b** but upon further inspection the two crystals both contained the *S,S*-enantiomer of the carbene. All aspects of the crystal structures overlap save the phenyl rings of the N-substituents which were slightly twisted compared to each other. This is displayed in Figure 2.17 below. The phenyl rings have been simplified for clarity.

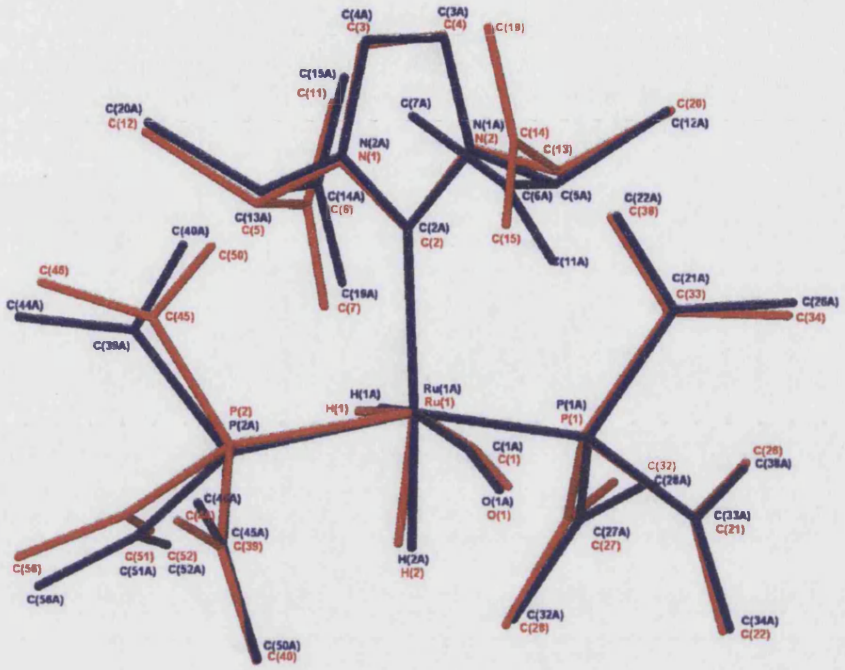

Figure 2.17 *X-ray structure of $RuH_2(CO)(PPh_3)_2$(I*) (**59a**) displaying twisted Ph rings.*

To confirm whether the two compounds seen in the ^{1}H NMR spectrum consisted of diastereotopic NHC ligands, the carbene was resynthesised but starting from the racemic amine rather than the enantiopure *S,S*-amine (see Section 2.2.1.3). This carbene was complexed to the ruthenium and it was anticipated that if the separate signals shown were in fact due to diastereomers, a 1:1 ratio of the two compounds would be seen. However, unexpectedly, the same ratio of the two compounds was exhibited. This meant that either (a) when forming the carbene, formation of one set of diastereomers (*R,R* and *S,S*) is favoured, (b) both sets of diastereomers are formed but one set is favoured for complexation over the other due to sterics around the ruthenium, (c) the carbene epimerises once complexed or, (d) the two NMR resonances do not arise from differences in the carbene ligand.

The ^{1}H NMR spectra of both the enantiopure free carbene I* and the racemic free carbene I* were compared. The spectra were identical with only one set of signals exhibited for the CH_3 and CH N-substituents (Figure 2.18) indicating the presence of only one diastereomer at this stage.

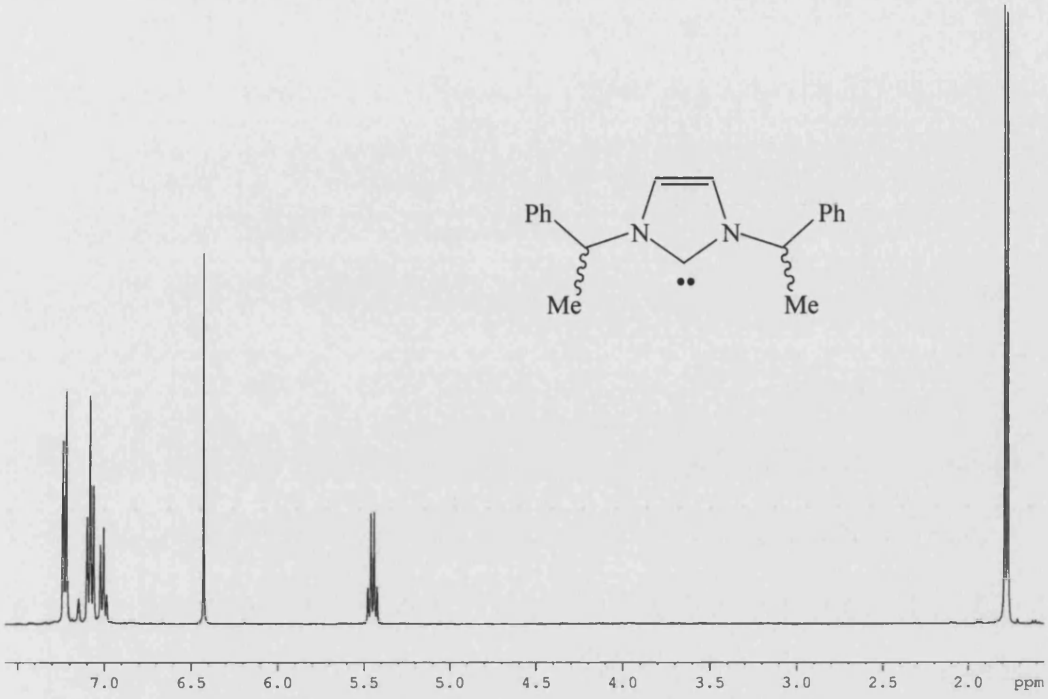

Figure 2.18 *^{1}H NMR spectrum (benzene-d_6, 400 MHz, 298 K) of I* synthesised from both racemic and enantiopure 1-phenethylamine.*

If the two compounds observed are not due to the carbene ligands it is possible that the coordinated PPh_3 ligands have opposite propeller configurations so that the complexes exist as conformational diastereoisomers. Solid-state enantiomeric conformations of metal coordinated PPh_3, **P** and **M**, are known and have been characterised (Figure 2.19).[27-29]

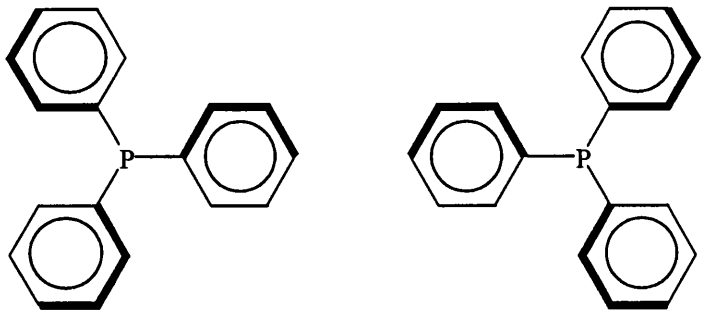

P M

Figure 2.19 *Stereogenic propeller configurations (P or M) of coordinated PPh_3.*

To definitively confirm the structure of the minor compound, a crystal structure of the second complex would be necessary but unfortunately, attempts to obtain crystals were unsuccessful.

2.3.3.7 Other alkyl-substituted Ru-NHC complexes synthesised by the Whittlesey group

Analogous mono-NHC complexes bearing ICy[30] and I^{n}Pr[31] carbenes were prepared by other members in the Whittlesey Group (complexes **64** and **65** respectively). These have been utilised and compared to the other complexes in catalysis (see Chapter 4). I^{t}Bu was also synthesised but proved too sterically demanding to complex to $RuH_2(CO)(PPh_3)_3$ **52**. Morris and co-workers have isolated compounds of the type $RuH_2(PPh_3)_2$(I^{t}Bu) but they are five coordinate and thus less sterically encumbered.[21] However, their attempts to form a bis-carbene complex failed presumably for steric reasons, as Nolan has reported I^{t}Bu to be more bulky than sterically demanding phosphine ligands such as P^{t}Bu$_3$.[32]

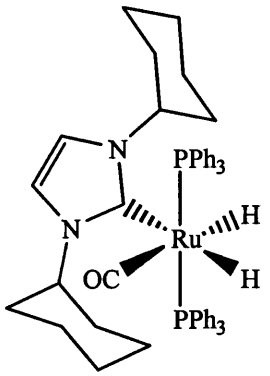

64

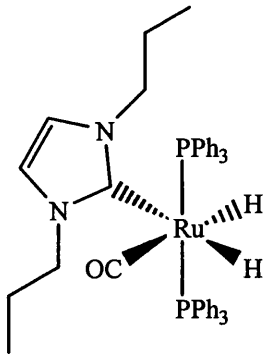

65

The bis-ICy complex (**66**) was also synthesised in the group by Suzanne Burling[30] and shows the same pattern of substitution as for $RuH_2(CO)(PPh_3)(IMe_4)_2$ (**55**) and $RuH_2(CO)(PPh_3)(IEt_2Me_2)_2$ (**60**). This complex has been utilised in Chapter 4.

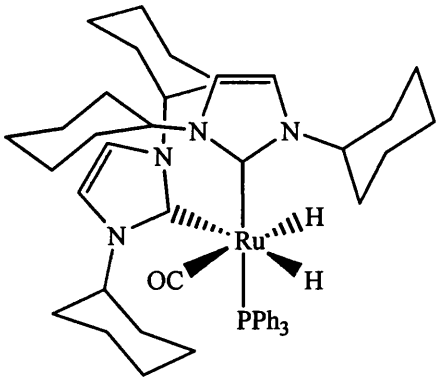

66

2.4 Discussion

Synthesis of dihydride ruthenium complexes bearing alkyl carbenes resulted in substitution *trans* to hydride, unlike the bulkier aryl carbene IMes which substituted *trans* to phosphine. Chemical shifts of the hydrides in the ^1H NMR spectra and phosphines in the $^{31}P\{^1H\}$ NMR spectra were remarkably similar for all alkyl carbene complexes. Coupling patterns were also similar, with the exception of **59a** which exhibited coupling due to chemically inequivalent phosphines, presumably caused by the bulkier nature of the I* NHC.

Table 2.7 below highlights the key data obtained for the range of synthesised Ru-NHC complexes. The first consideration is the IR CO stretching frequencies. Comparing the mono Ru-NHC complexes it is apparent that the complex **61** (Entry 5) has the lowest stretching frequency suggesting that $I^iPr_2Me_2$ is the strongest donor ligand of those considered. Complex **51** (Entry 1) has the highest stretching frequency (1941 cm^{-1}) suggesting that IMes is the poorest donor ligand. The remaining alkyl substituted NHC complexes (Entries 3-8) give similar stretching frequencies suggesting negligible difference in their donor abilities.

Complex **59a** (Entry 2) has aryl N-substituents further removed from the N atoms. This is reflected in the CO stretching frequency given (1937 cm^{-1}), which is lower than the aryl NHC complex but higher than all the alkyl NHC complexes (1917-1922 cm^{-1}).

The Ru-CO bond lengths generally correlate to the IR CO stretching frequencies. The lengths range from 1.9145(17) Å (entry 2) to 1.8615(19) Å (Entry 11) correlating to stretching frequencies 1941 cm^{-1} to 1884 cm^{-1} respectively.

The Ru-C(carbene) bond lengths follow the pattern seen by others in that M-C(alkyl) bond lengths are longer than M-C(aryl) bond lengths. Hence in order from longest to shortest bond lengths for Ru-C(carbene) bonds IMes>I*>ICy>I^nPr>I^iPr>IEt. In addition, Ru-C(carbene) bond lengths *trans* to phosphine are shorter than those *trans* to hydride due to the larger *trans* influence of hydride compared to phosphine.

Comparing the *trans* L(ax)-Ru-L(ax) bond angles (Ph_3P-Ru-PPh_3 or Ph_3P-Ru-NHC) it would be expected that smaller angles, i.e. a greater distortion from octahedral geometry would be exhibited for complexes bearing the most bulky NHC ligands. In fact the greatest distortion does occur with **51** (146.33(5) °), and the least with the bis-IMe_4 carbene complex **55** (166.91(10) °). However, there is a bit of overlap in between. In all probability, electronic factors play an equally important role in this distortion as do steric factors.

Entry	Complex	ν_{CO} (cm^{-1})[a]	Ru-CO (Å)	Ru-C(*trans* to H) (Å)	Ru-C(*trans* to P) (Å)	L(ax)-Ru-L(ax) (°)
1	$RuH_2(CO)(PPh_3)_2$(IMes)	1941	1.9145(17)	-	2.0956(17)	146.33(5)
2	$RuH_2(CO)(PPh_3)_2$(I*)	1937	1.884(4)	2.136(3)	-	160.24(3)
3	$RuH_2(CO)(PPh_3)_2$(IMe_4)	1922	-	-	-	-
4	$RuH_2(CO)(PPh_3)_2$(IEt_2Me	1921	1.880(4)	2.171(3)	-	164.32(4)
5	$RuH_2(CO)(PPh_3)_2$($IiPr_2M$	1917	-	-	-	
6	$RuH_2(CO)(PPh_3)_2$(I^iPr)	1922	1.900(2)	2.1604(19)	-	155.549(19)
7	$RuH_2(CO)(PPh_3)_2$(I^nPr)	1920	1.864(3)	2.142(6)	-	162.78(3)
8	$RuH_2(CO)(PPh_3)_2$(ICy)	1922	1.833(6)	2.140(4)	-	157.59(6)
9	$RuH_2(CO)(PPh_3)(IMe_4)_2$	1884	1.867(4)	2.122(4)	2.086(4)	166.91(10)
10	$RuH_2(CO)(PPh_3)(IEt_2Me_2$	1884	1.8615(19)	2.145(2)	2.0951(18)	163.30(5)
11	$RuH_2(CO)(PPh_3)(ICy)_2$	1885	1.865(4)	2.147(3)	2.099(3)	161.75(13)

[a] all recorded in benzene-d_6

Table 2.7 *Selected data obtained for synthesised Ru-NHC complexes.*

2.5 Chapter summary

- A new range of alkyl Ru-NHC complexes has been synthesised and fully characterised with the use of multinuclear 1- and 2-D NMR experiments, X-ray crystallography, IR spectrometry and CHN analysis.

- All alkyl substituted NHCs coordinated *trans* to hydride. This is different to the initial N-aryl substituted NHC complex $RuH_2(CO)(PPh_3)_2(IMes)$ (**51**) where substitution occurred *trans* to phosphine.

- Alkyl substituted NHCs complex more rapidly to ruthenium than aryl substituted NHCs.

- IR CO stretching frequency data suggest that there is little difference in the donation abilities of the alkyl substituted NHCs, but that they are better donors than aryl substituted NHCs.

2.6 References

[1]Arduengo, A. J.; Harlow, R. L.; Kline, M. *J. Am. Chem. Soc.* **1991**, *113*, 361-363.

[2]Arduengo, A. J.; Dias, H. V. R.; Harlow, R. L.; Kline, M. *J. Am. Chem. Soc.* **1992**, *114*, 5530-5534.

[3]Arduengo, A. J.; Krafczyk, R.; Schmutzler, R.; Craig, H. A.; Goerlich, J. R.; Marshall, W. J.; Unverzagt, M. *Tetrahedron* **1999**, *55*, 14523-14534.

[4]Denk, K.; Fridgen, J.; Herrmann, W. A. *Adv. Synth. Catal.* **2002**, *344*, 666-670.

[5]Herrmann, W. A.; Weskamp, T.; Bohm, V. P. W. *Adv. Organomet. Chem.* **2001**, *48*, 1-69.

[6]Grubbs, R. H.; Morgan, J. P. *Org. Lett.* **2000**, *2*, 3153-3155.

[7]Wang, H. M. J.; Lin, I. J. B. *Organometallics* **1998**, *17*, 972-975.

[8]Wanniarachchi, Y. A.; Khan, M. A.; Slaughter, L. M. *Organometallics* **2004**, *23*, 5881-5884.

[9]Crabtree, R. H. *J. Organomet. Chem.* **2005**, *690*, 5451-5457.

[10]Herrmann, W. A.; Kocher, C.; Goossen, L. J.; Artus, G. R. J. *Chem. Eur. J.* **1996**, *2*, 1627-1636.

[11]Kuhn, N.; Kratz, T. *Synthesis-Stuttgart* **1993**, 561-562.

[12]Jazzar, R. F. R. "PhD thesis," University of Bath, **2003**.

[13]Hillier, A. C.; Sommer, W. J.; Yong, B. S.; Petersen, J. L.; Cavallo, L.; Nolan, S. P. *Organometallics* **2003**, *22*, 4322-4326.

[14]Scott, N. M.; Nolan, S. P. *Eur. J. Inorg. Chem.* **2005**, 1815-1828.

[15]Douglas, S. R.; Unpublished results: University of Bath, **2005**.

[16]Jazzar, R. F. R.; Macgregor, S. A.; Mahon, M. F.; Richards, S. P.; Whittlesey, M. K. *J. Am. Chem. Soc.* **2002**, *124*, 4944-4945.

[17]Lee, M. T.; Hu, C. H. *Organometallics* **2004**, *23*, 976-983.

[18]Martin, H.; James, N. H.; Aitken, J.; Gaunt, J. A.; Adams, H.; Haynes, A. *Organometallics* **2003**, *23*, 4451-4458.

[19]Doyle, M. J.; Lappert, M. F.; Pye, P. L.; Terreros, P. *J. Chem. Soc. Dalton Trans.* **1984**, 2355.

[20]Chianese, A. R.; Li, X.; Janzen, M. C.; Faller, J. W.; Crabtree, R. H. *Organometallics* **2003**, *22*, 1663-1667.

[21]Abdur-Rashid, K.; Fedorkiw, T.; Lough, A. J.; Morris, R. H. *Organometallics* **2004**, *23*, 86-94.

[22]Burling, S.; Mahon, M. F.; Paine, B. M.; Whittlesey, M. K.; Williams, J. M. J. *Organometallics* **2004**, *23*, 4537-4539.

[23]Viciu, M. S.; Navarro, O.; Germaneau, R. F.; Kelly, R. A.; Sommer, W.; Marion, N.; Stevens, E. D.; Cavallo, L.; Nolan, S. P. *Organometallics* **2004**, *23*, 1629-1635.

[24]Magill, A. M.; Cavell, K. J.; Yates, B. F. *J. Am. Chem. Soc.* **2004**, *126*, 8717-8724.

[25]Alder, R. W.; Allen, P. R.; Williams, S. J. *J. Chem. Soc. Chem. Commun.* **1995**, 1267-1268.

[26]Herrmann, W. A.; Goossen, L. J.; Artus, G. R. J.; Kocher, C. *Organometallics* **1997**, *16*, 2472-2477.

[27]Ayscough, A. P.; Davies, S. G. *J. Chem. Soc. Chem. Commun.* **1986**, 1648-1649.

[28]Ayscough, A. P.; Costello, J. F.; Davies, S. G. *Tetrahedron Asymm.* **2001**, *12*, 1621-1624.

[29]Dance, I.; Scudder, M. *J. Am. Chem. Soc. Dalton Trans.* **2000**, *10*, 1579-1585.

[30]Burling, S.; Kociok-Kohn, G.; Mahon, M. F.; Whittlesey, M. K.; Williams, J. M. J. *Organometallics* **2005**, *24*, 5868-5878.

[31]Brown, V. "M. Chem. Report.," University of Bath, **2005**.

[32]Dorta, R.; Stevens, E. D.; Nolan, S. P. *J. Am. Chem. Soc.* **2004**, *126*, 5054-5055.

Chapter 3

Chapter 3: C-H Bond Activations and Isomerisations of Complexes

3.1 C-H bond activation

3.1.1 Introduction

The field of C-H bond activation has been the subject of intense study since the 1960s in both stoichiometric and catalytic reactions.[1] C-H bond activation arises from the weakening and subsequent cleavage of the C-H σ-bond, which can be induced by coordination of the substrate to a metal centre.[2] The scope of these reactions is too vast to discuss exhaustively for the purpose of this thesis. However, the area has been the subject of several comprehensive reviews[1,3-7] and a number of representative examples of both catalytic and stoichiometric C-H bond activation reactions are shown in Scheme 3.1.

Oxidative addition of alkanes to form alkyl hydride complexes was first directly observed by Janowicz and Bergman in 1982 using iridium complexes.[8] The iridium dihydride complex $Cp^*Ir(H)_2PMe_3$ (Cp^* = pentamethylcyclopentadienyl) was irradiated in cyclohexane and neopentane to give the complexes $Cp^*Ir(H)(C_6H_{11})(PMe_3)$ and $Cp^*Ir(H)(CH_2CMe_3)(PMe_3)$ respectively. Other saturated hydrocarbons and benzene also readily added to this complex. Subsequent syntheses of indenyliridium complexes were shown to parallel the chemistry of the Cp^* systems but with increased reactivity.[9] Scheme 3.1 illustrates how (η^5-C_9H_7)Ir(*p*-tolyl)(H)(PMe_3) (**67**) thermally eliminates toluene in benzene to give (η^5-C_9H_7)Ir(Ph)(H)(PMe_3) (**68**). Jones and co-workers observed similar C-H oxidative addition products of analogous complexes of Rh.[10,11]

Similar reactions were further observed by Field and co-workers in the first example of alkane C-H activation involving a complex of a first row transition metal.[12] The dihydride complex $FeH_2(dmpe)_2$ (**69**) (dmpe = 1,2-bis(dimethylphosphino)ethane) was irradiated at low temperature (<-90 °C) in *n*-pentane solution resulting in elimination of dihydrogen and formation of $Fe(H)(dmpe)_2(C_5H_{11})$ (**70**) (Scheme 3.1). Complex **70** decomposed at temperatures above -20 °C and therefore could not be isolated.

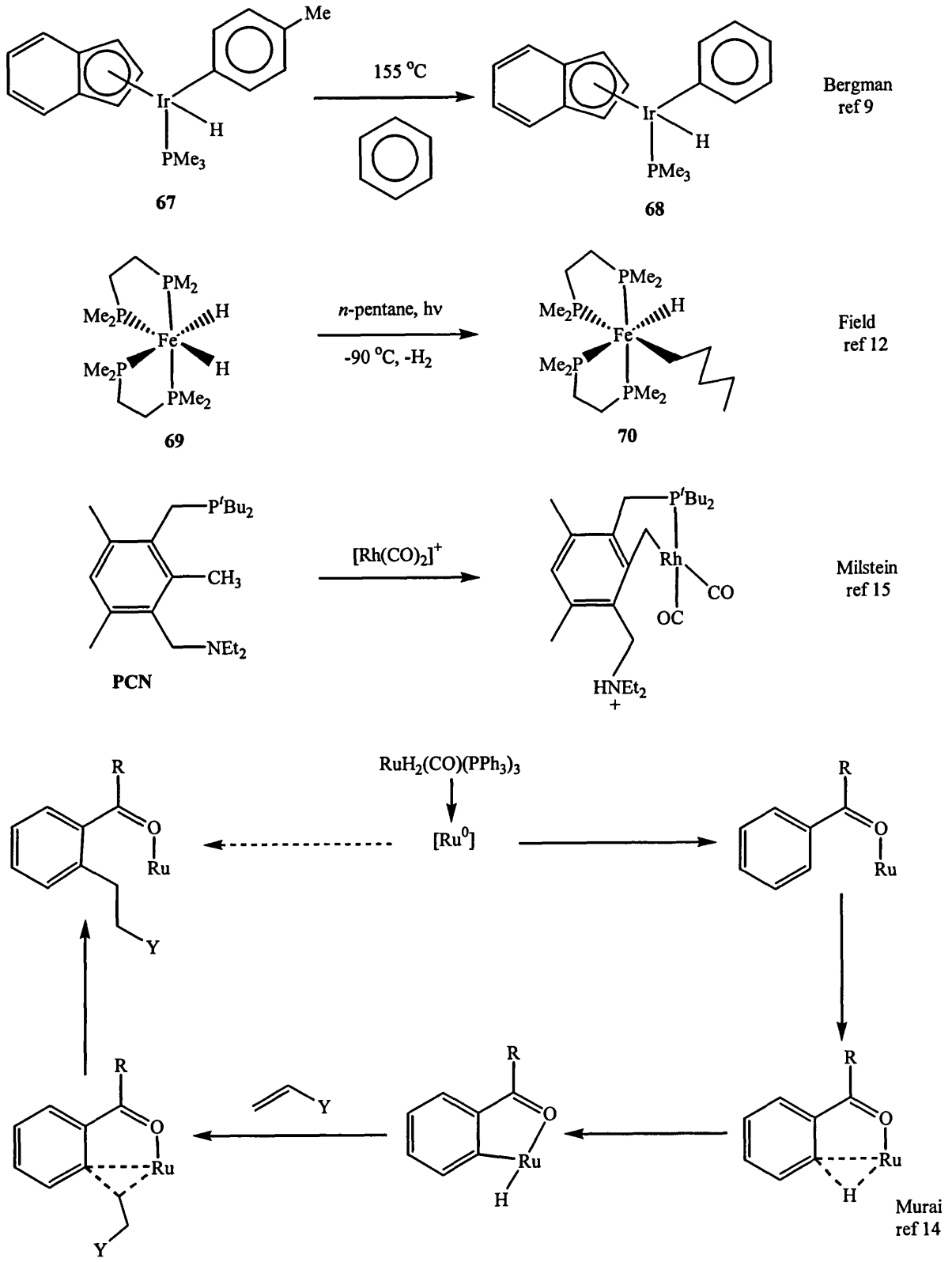

Scheme 3.1 *Stoichiometric and catalytic C-H bond activation.*

Ruthenium is a prime choice for C-H bond activation in general as shown by the Murai reaction where an *ortho*-C-H of an aromatic ketone is replaced by an alkyl group following alkene insertion into a C-H bond (Scheme 3.1).[13,14] The reaction proceeds *via* cyclometallation, followed by alkene insertion into Ru-H and subsequent reductive elimination of the alkylated ketone. The course of the catalytic reaction is outlined in Scheme 3.1.

Milstein and co-workers have observed intramolecular C-H activation of the PCN ligand at Rh (Scheme 3.1).[15] It was found that formation of either a C-C activated complex, a C-H activated complex or an agostic C-C complex could be controlled by simple choice of $Rh(CO)_n$-based precursors, demonstrating the influence of π-accepting ligands on C-H activation. Thus reaction of $[Rh(CO)_2(solv)_n]^+BF_4^-$ with PCN resulted in activation of the methyl group between the two ligand arms of PCN (Scheme 3.1).

The intramolecular cleavage of a C-H bond is more facile than intermolecular activation.[1] Cyclometallation of ligand aryl groups was discovered early and ultimately found to be quite common. The intramolecular activations can be assisted by interaction of the π-orbitals of aromatic C-H bonds as shown in an early example by Bennett and Milner (Scheme 3.2).[16]

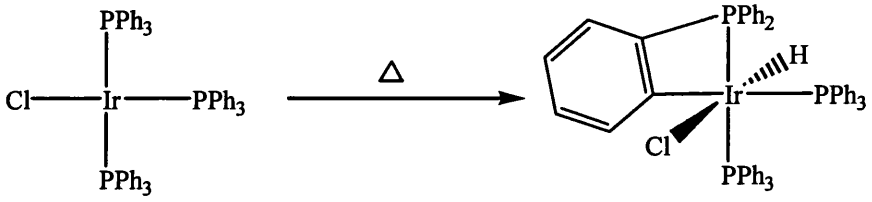

Scheme 3.2 *Intramolecular C-H activation of a phosphine ligand.*

3.1.2 C-H Bond activation involving NHC ligands

It is now apparent that N-heterocyclic carbenes (NHCs) are not necessarily innocent, inert ligands that simply help to stabilise reactive and potentially catalytically useful metal complexes. In a number of cases with late transition metals, NHCs have been found to undergo facile intramolecular C-H bond activation[17] and, in one case reported by the Whittlesey group under more forcing conditions, C-C bond activation.[18] These activations can be explained by the increased electron density on the metal centre

arising as a consequence of the strongly electron donating carbene, in addition to the steric bulk of the NHCs forcing C-H and C-C bonds into close proximity of the metal centre.[19]

3.1.2.1 Activation of N-aryl substituted NHCs

Lappert and co-workers were the first to describe aryl C-H bond activation of the N substituents on NHCs.[20] Treatment of coordinatively unsaturated Ru(II) and Ir(I) precursors with electron rich carbene dimers produced NHC complexes with metallated N-aryl substituents (Scheme 3.3). Lappert proposed that the excess enetetramine act as a proton acceptor.[21]

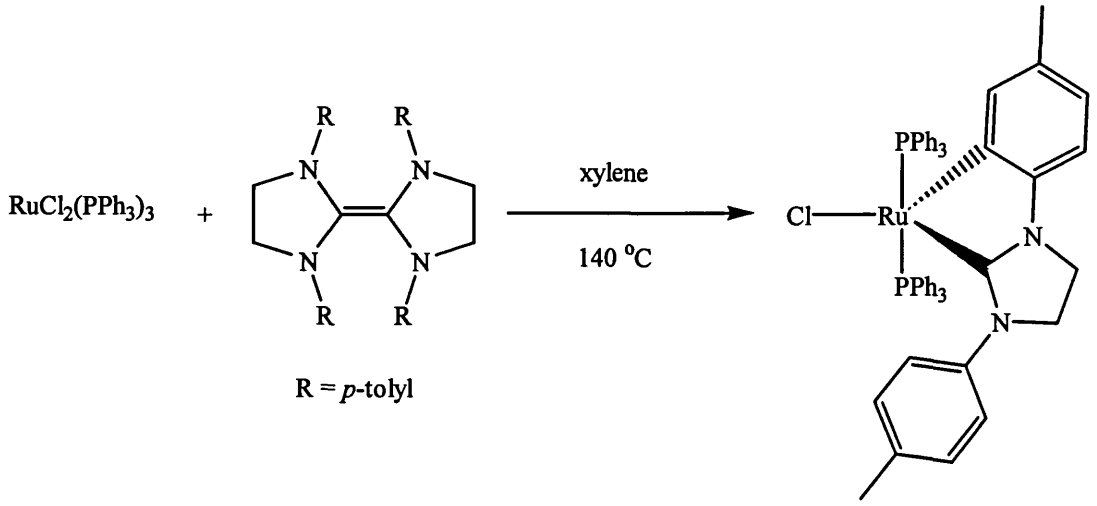

Scheme 3.3 *First example of C-H activation of NHCs.*

More recently, aryl CH_2-H activation of IMes and SIMes has been reported in Rh- and Ru-NHC complexes. Grubbs and co-workers have observed C-H activation in their second generation alkene metathesis catalysts as a result of C-H oxidative addition and loss of the alkylidene ligand when air was not rigorously excluded from the reaction conditions (Scheme 3.4).[19,22] Thus complex **71** was isolated rather than the expected direct substitution product $Ru(=CHPh)Cl_2(PCy_3)(SIMes)$.

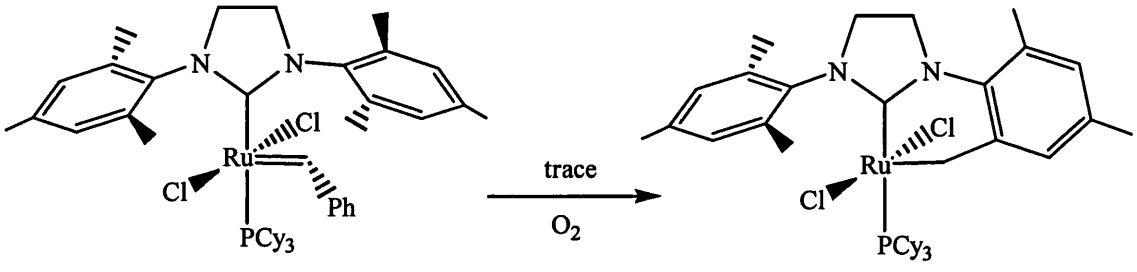

5 71

Scheme 3.4 *C-H activation of the Grubbs second generation metathesis catalyst.*[19,22]

Nolan also described the formation of a cyclometallated IMes complex of Rh.[23] Upon reaction of $[Rh(COE)_2Cl]_2$ with IMes at room temperature, total displacement of the COE ligands was observed, in addition to the splitting of the dimer and simultaneous C-H activation of one of the IMes methyl groups (Scheme 3.5). This metallation was effectively reversible by rapid room temperature reaction with either H_2, to form the trigonal bipyramidal dihydride $RhH_2Cl(IMes)_2$, or CO, to produce the square planar $RhCl(CO)(IMes)_2$. Herrmann previously reported a related ligand substitution of $[Rh(COD)Cl]_2$ with NHCs without the bulky mesityl substituent.[24] The reactions yielded the simple substitution of one COD ligand with no observed C-H activation, indicating that both the increased lability of COE versus COD and the bulk of the mesityl groups assist activation.

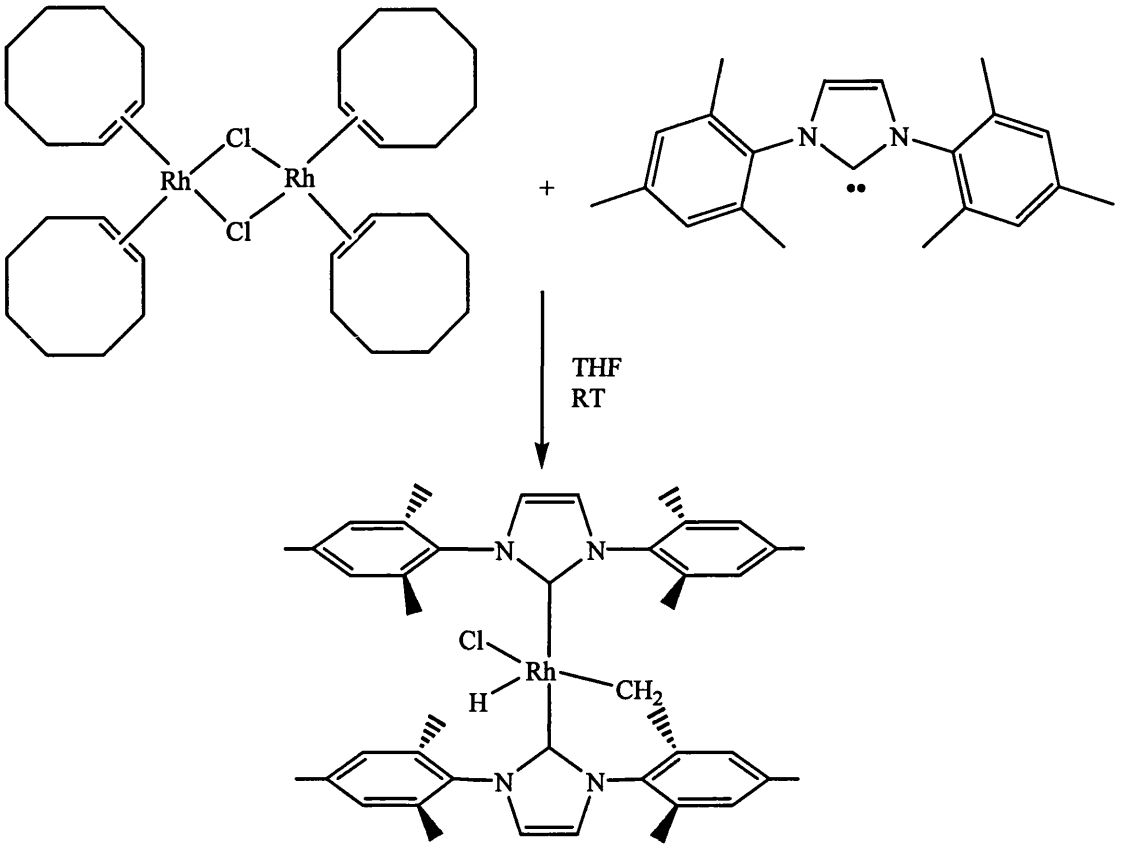

Scheme 3.5 *Simultaneous complexation and C-H activation of IMes to Rh.*[23]

The Whittlesey group have observed a similar activation process to Grubbs and Nolan in the Ru-IMes complex, **51**.[18] Addition of the hydrogen acceptor H_2C=$CHSiMe_3$ to **51** resulted in the C-H bond cleavage of an aryl CH_2-H bond and the formation of the metallated $RuH(CO)(PPh_3)_2$(IMes'), **72** (Scheme 3.6). The C-H activated product has been calculated to be 11.3 kcalmol^{-1} higher in energy than **51** explaining the need for a hydrogen acceptor for the formation of **72**.

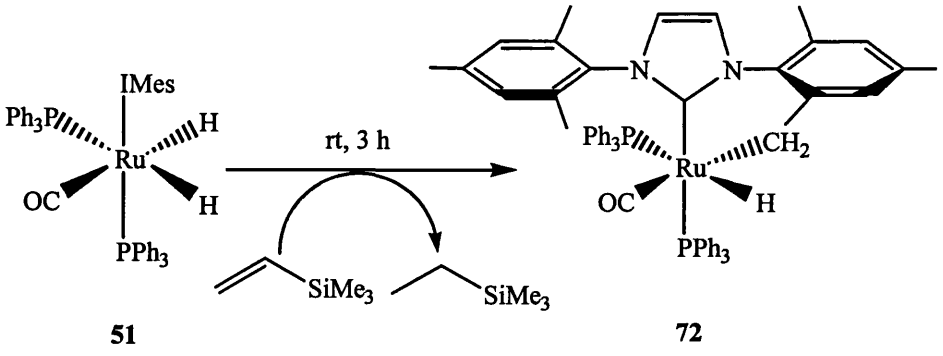

51 **72**

Scheme 3.6 *C-H activation of 51.*

To investigate the influence of ancillary ligands on the C-H activation process, the bidentate phosphine and phosphine-arsine precursors $RuH_2(CO)(dppp)(IMes)$ (**73**) $RuH_2(CO)(arphos)(IMes)$ (**74**) were prepared.[25] Complex **73** did not react with $H_2C{=}CHSiMe_3$ at room temperature, but upon heating to 100 °C afforded the C-H activated complex RuH(CO)(dppp)(IMes′) **75** (Scheme 3.7). The potentially hemilabile system **74** gave three isomeric products **76**, **77** and **78** in a ratio 1:1:0.7 upon heating to 85 °C with $H_2C{=}CHSiMe_3$.

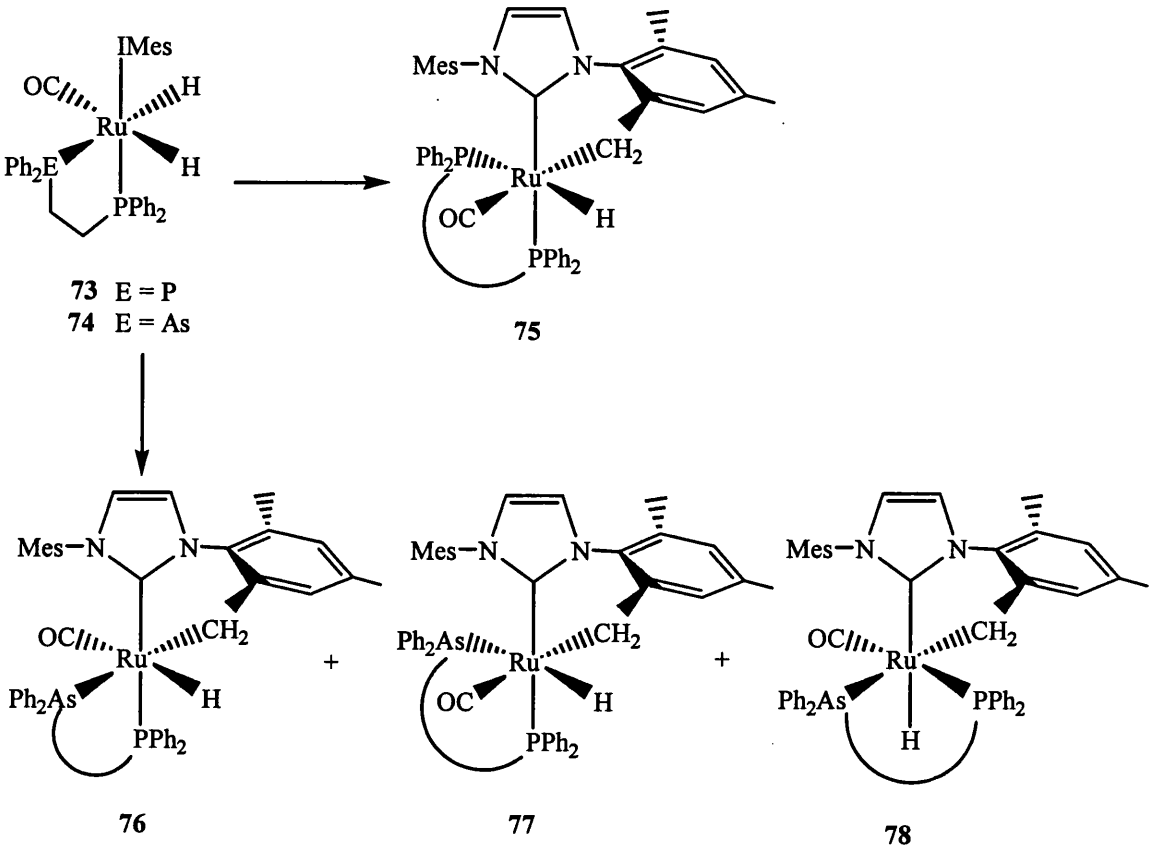

Scheme 3.7 *Ancillary Ligand Effect on C-H activation of IMes.*

Morris and co-workers have synthesised a similar complex to **72**, but with an alternate stereochemistry.[17] Reaction of $RuH(Cl)(PPh_3)_3$ with the two related carbenes IMes and SIMes gave the two C-H insertion products $RuH(PPh_3)_2(IMes')$ **79** and $RuH(PPh_3)_2(SIMes')$ **80**. Subsequent addition of CO to the IMes C-H insertion product **79** yielded a different isomer to **72** (Scheme 3.8)[17]

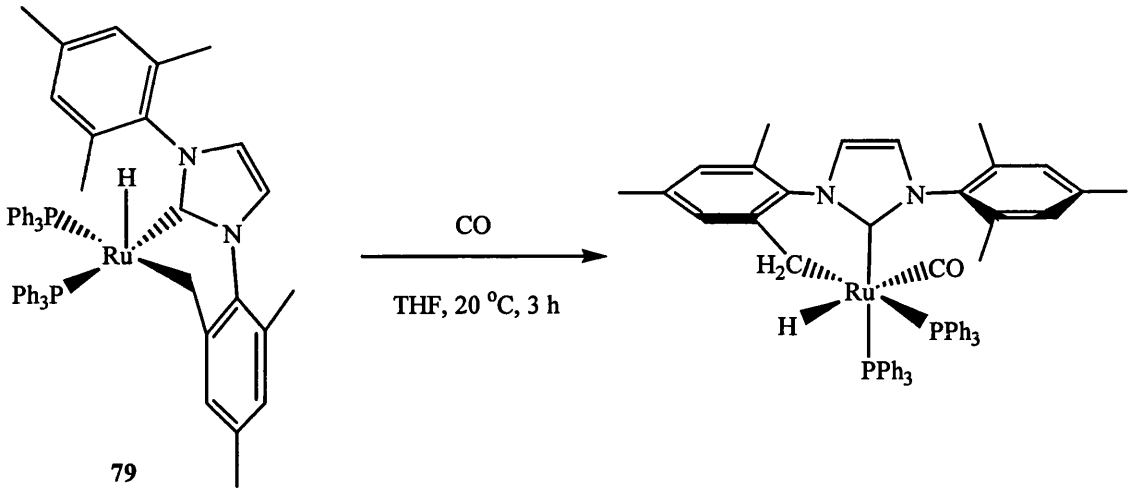

Scheme 3.8 *Reaction of $RuH(PPh_3)_2(IMes')$ (79) with carbon monoxide.*

The first example involving C-H activation of an *N*-pyridine functionalised NHC came from Danopoulos.[26] Room temperature reaction of 1-[2-(6-trimethylsilyl)pyridyl]-3-[2,6-di-iso-propyl)phenyl]imidazol-2-ylidene (py-NHC) with $[IrCl(COD)]_2$ resulted in isolation of the air stable C-H insertion product **81**. In contrast, reaction of the same carbene with $[RhCl(COD)]_2$ under the same conditions gave **82** (Scheme 3.9), which NMR data showed contained a close contact between an *ortho* hydrogen with the Rh centre. The difference in reactivity presumably reflects the tendency of 3rd row transition metals to form stronger bonds than their 2nd row congeners.

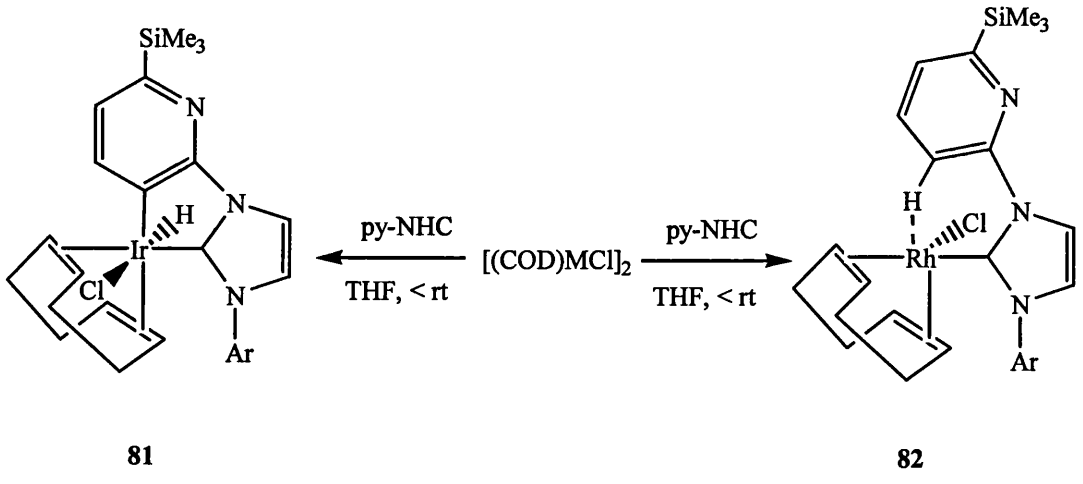

Scheme 3.9 *C-H activation of a functionalised NHC.*

3.1.2.3 Activation of N-alkyl substituted NHCs

Arenes are much more reactive than alkanes in C-H bond cleavage reactions in spite of the greater strength of aryl versus alkyl C-H bonds.[27] Arene C-H bond cleavage is favourable thermodynamically because of the stronger bonds formed in the product: M-aryl bonds are much stronger than M-alkyl ones. This is due to the stronger bonding made possible with an sp^2 carbon, in addition to favourable π-bonding. Arenes are also probably more reactive kinetically since the arene C-H bond is less hindered and the metal can interact with the ring π system prior to bonding.[28]

Morris also attempted analogous reactions to his previous IMes and SIMes systems with 1,3-bis-(*tert*-butyl)-imidazole-2-ylidene (I^tBu).[17] Unlike with IMes and SIMes, a cyclometallated product was not observed. Thermolysis of I^tBu with $Ru(H)Cl(PPh_3)_3$ in THF gave a species which behaved as "$Ru(PPh_3)_2(I^tBu)$" in that it reacted with H_2 to form a mixture of isomers of the structurally characterised dihydride $RuH_2(PPh_3)_2(I^tBu)$. Both isomers contained an agostic interaction with a methyl hydrogen from one of the *tert*-butyl groups of the NHC ligand.

To date, there have only been four examples of intramolecular C-H bond activation of N-substituted alkyl carbenes. Herrmann[29] has reported the C-H bond cleavage of 1,3-bis(cyclohexyl)imidazol-2-ylidene (ICy) by $[(\eta^5\text{-}C_5Me_5)IrCl_2]_2$. The direct activation product was not observed, since rapid β-hydrogen elimination afforded a 1-(2-cyclohexenyl)-3-cylclohexylimidazol-2-ylidene ligand in the ultimate product (Scheme 3.10).[19] The second example of N-alkyl C-H bond activation was described recently by Nolan and co-workers. Double C-H activation of I^tBu was observed at both rhodium and iridium (Scheme 3.11).[30,31] Interestingly, these products were only observed when using benzene as a solvent. Simple change of solvent (for Rh) or of reaction times (for Ir) gave several precursors, most notably the hydride species where activation of only one of the NHC *tert*-butyl substituents was observed.

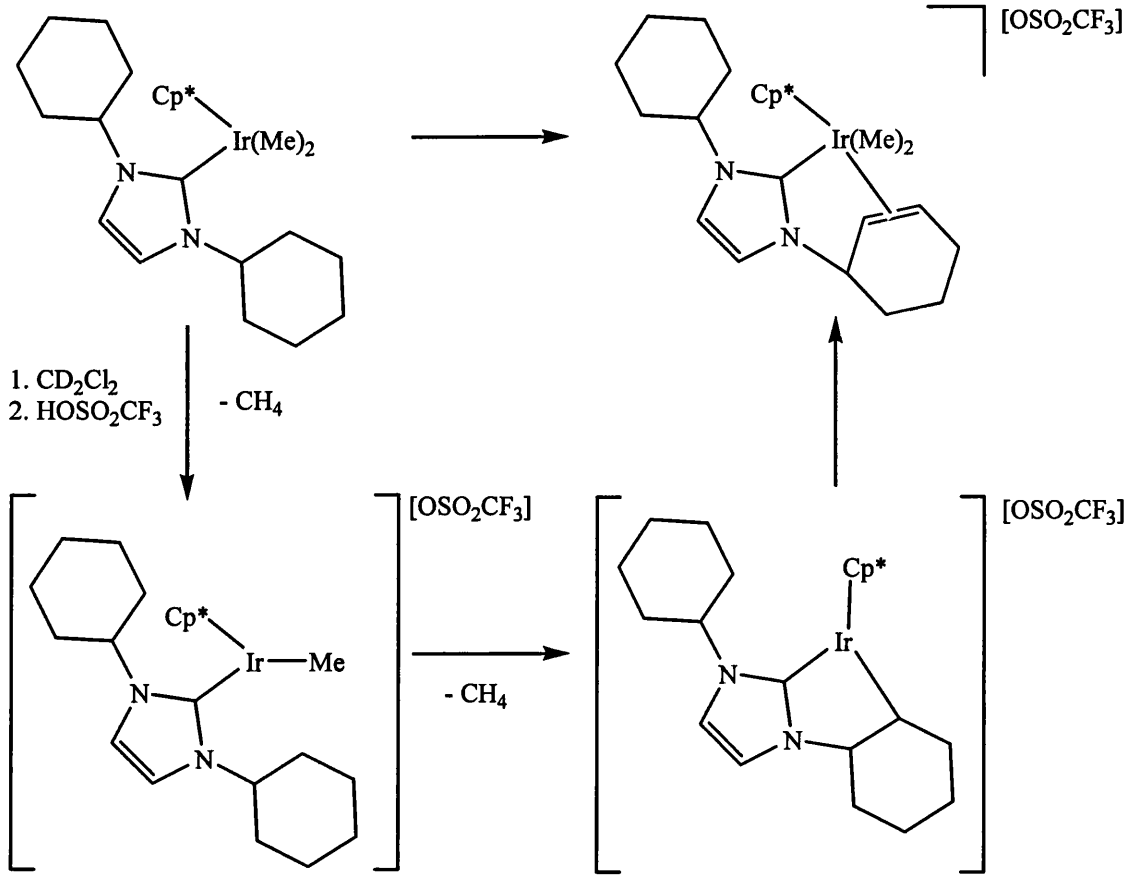

Scheme 3.10 *C-H activation of an alkyl NHC on iridium.*

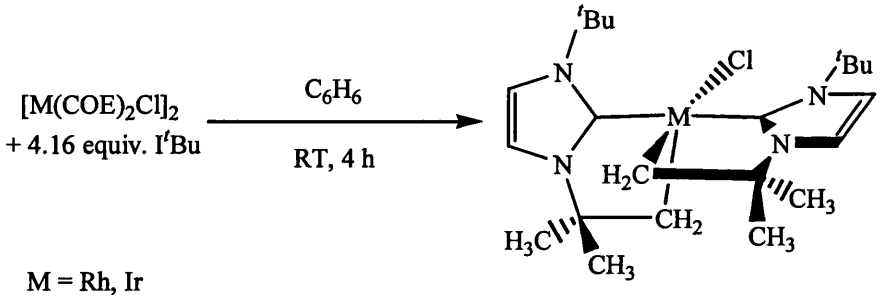

Scheme 3.11 *Double C-H activation in Rh- and Ir-NHC complexes.*

The first cluster complex containing NHC ligands has very recently been reported by Cabeza and co-workers and leads to activation of two C-H bonds of a methyl group attached to a nitrogen of an NHC (Scheme 3.12).[32] The trinuclear NHC derivative $Ru_3(IMe_2)(CO)_{11}$ (**83**) (IMe_2 = 1,3-dimethylimidazol-2-ylidene) was prepared *via*

deprotonation of 1,3-dimethylimidazolium iodide by KO^{t}Bu followed by addition of $Ru_3(CO)_{12}$ at room temperature in THF. Refluxing a THF solution of **83** resulted in the uncommon oxidative addition of two C-H bonds of the nitrogen bound methyl group to yield $Ru_3(\mu\text{-}H)_2(\mu_3\text{-}IMeCH)(CO)_9$ (**84**). Interestingly, this process was fully reversible upon addition of CO to a solution of **84**, implying that both C-H activation steps should have small activation barriers.

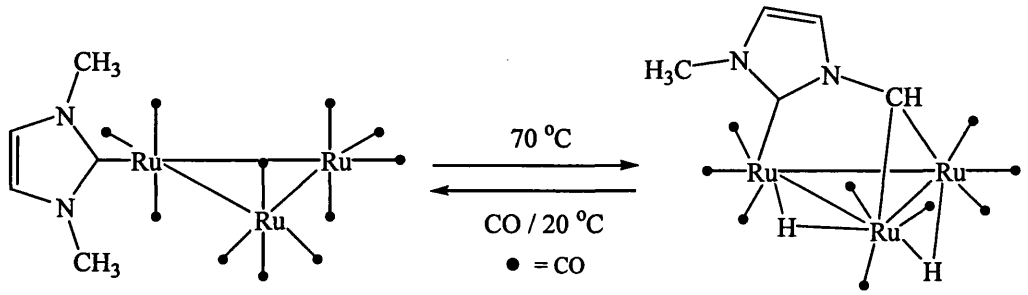

83 **84**

Scheme 3.12 *Double C-H activation of an NHC N-CH$_3$ group.*

3.2 Activation and isomerisation of Ru-NHC complexes

As previously discussed, the Ru-NHC complex **51** has been shown to undergo C-H activation upon addition of the hydrogen acceptor, H_2C=CHSiMe$_3$. In this process the alkene gets reduced to $CH_3CH_2SiMe_3$. This C-H activation process was fully reversible upon addition of H_2 or alcohol. Thus, with regeneration of the starting dihydride ruthenium species, the system showed promise for catalytic hydrogenation chemistry. This is discussed in further detail in Chapter 4.

With the importance of C-H activation for the synthesis of organic molecules, in addition to the susceptibility for carbenes to undergo metal induced bond activation reactions, activation of the new range of alkyl substituted Ru-NHC complexes synthesised in Chapter 2 has been explored. They will be discussed in a different order to that of Chapter 2 according to their activities. Some interesting isomerisation reactions are also discussed.

3.2.1 $RuH_2(CO)(PPh_3)_2(IEt_2Me_2)$ (57)

3.2.1.1 Activation

Thermolysis of $RuH_2(CO)(PPh_3)_2(IEt_2Me_2)$ (**57**) in benzene-d_6 at 50 °C with an excess of H_2C=$CHSiMe_3$ results in C-H activation of the NCH_2CH_2-H bond affording $RuH(CO)(PPh_3)_3(IEt_2Me_2')$ (**85a**) (Scheme 3.13). Compelling evidence for the C-H bond cleavage was provided by the ^1H NMR spectrum of **85a** which shows one hydride triplet (δ -7.01, J_{HP} = 23.1 Hz), and the $^{13}C\{^1H\}$ NMR spectrum, which exhibited four distinct ethyl resonances, most tellingly a triplet at δ 8.3 (J_{CP} = 11.0 Hz) arising from the metallated carbon of the N-CH_2-CH_2 group coupling to the two equivalent phosphines. In addition to this major C-H insertion product where the carbene remained *trans* to hydride upon activation, minor amounts of the C-H activated isomer **85b** where the carbene resides in the axial position, *trans* to phosphine, were also detected by NMR spectroscopy, despite the absence of the corresponding geometry of the dihydride species. This species was represented as a doublet of doublets at a very similar shift to **72** (δ -7.97) due to *cis* and *trans* couplings to inequivalent phosphines. The reason for this isomerisation is most likely steric effects. As discussed in Chapter 2, syntheses of complexes with bulky aryl ligands were found to substitute *trans* to phosphine rather than *trans* to hydride as with the alkyl carbenes. Upon activation a carbene is brought closer to the metal centre increasing the steric influence of the ligand. It is possible that this influence encourages the carbene to reside *trans* to phosphine. However, in the case of IEt_2Me_2 this product is the minor product, only seen in a ratio of 1:9 to the major C-H insertion product and therefore was not isolated.

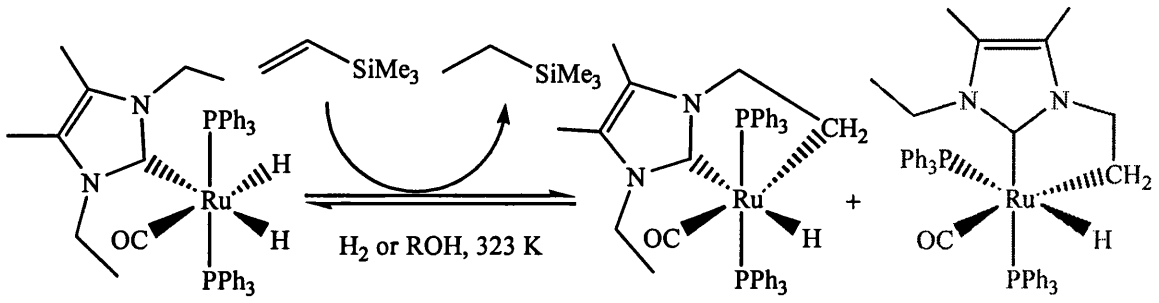

57 Major 85a Minor 85b

Scheme 3.13 *C-H activation of 57.*

The activation process was monitored *in situ* by ^{1}H NMR spectroscopy (benzene-d_6, 400 MHz, 323 K) to examine the rate at which formation of the two isomers **85a** and **85b** occurs. The series of ^{1}H NMR spectra (Figure 3.1) display how the axial activated isomer **85b** forms first but then remains constant. After 1 h, a substantial amount of the alternative isomer **85a** is present but as there is still starting material (**57**) present in addition to isomer **85b** it remains to be established how this isomerisation proceeds. After 5 h little of the starting dihydride **57** could be detected by ^{1}H NMR spectroscopy. Variable temperature (VT) ^{1}H NMR experiments on the mixture of isomers **85a** and **85b** exhibited no change between the ratio of the two isomers at either high or low temperatures.

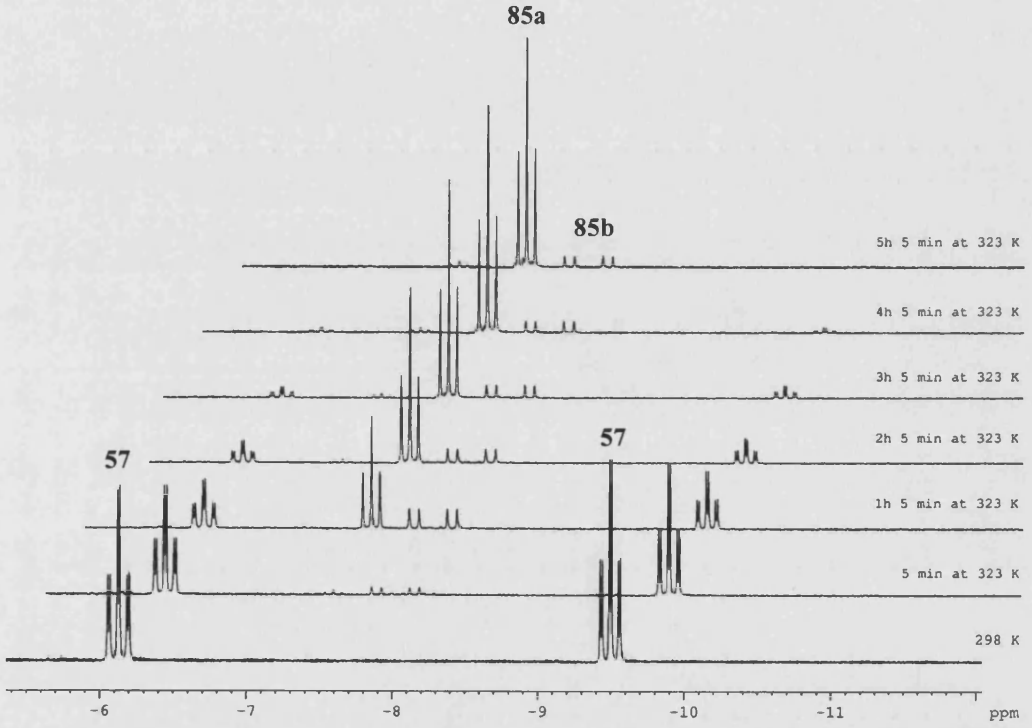

Figure 3.1 *Hydride region of the ^{1}H NMR spectrum (400 MHz, benzene-d_6, 298 K) showing interconversion of **85a**, **85b**, and **57**.*

C-H activation of the ethyl CH_3 group was attempted at *room temperature* with the addition of five equivalents of H_2C=$CHSiMe_3$ but even after four days, no evidence for activation could be detected. This reflects the difference in N-aryl versus N-alkyl C-H

bond insertion. Activation of IMes in $RuH_2(CO)(PPh_3)_2$(IMes) (**51**) occurs at room temperature after only 3 h upon addition of an alkene.[18]

To confirm the structure of the major C-H insertion product $RuH(CO)(PPh_3)_2(IEt_2Me_2')$ **85a**, crystals suitable for X-ray diffraction were grown. The X-ray structure of **85a** (Figure 3.2) displays clearly the metallated five-membered ring of the activated IEt_2Me_2 ligand, with a Ru-C bond length of 2.0900(19) Å and a Ru-C(6)-C(5) angle close to that expected for an unstrained sp^3-hybridised methylene group (109.96(12) °). The Ru-C bond length is shorter than that of the corresponding dihydride complex **57** (2.171(3) Å) due to the metallated group bringing the carbene ligand closer to the metal centre. The P(2)-Ru-P(3) angle is almost identical to that of **57** with activation causing no further distortion to the octahedral geometry. The IR data show a large decrease in CO stretching frequency from 1921 cm^{-1} to 1895 cm^{-1} as the complex is activated.

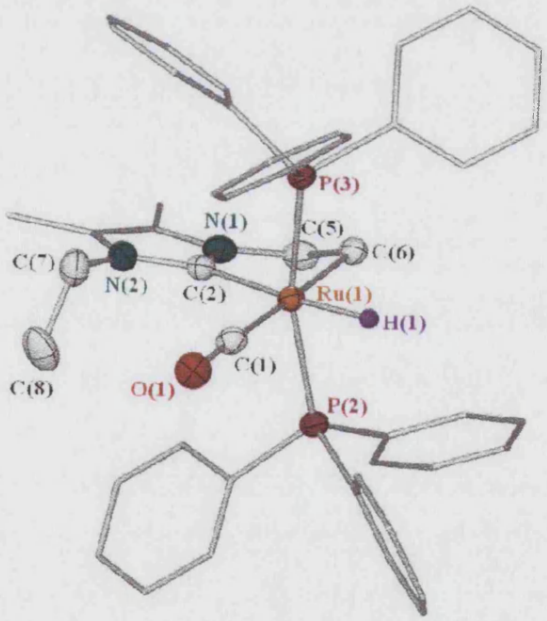

Figure 3.2 *X-ray structure of $RuH(CO)(PPh_3)_2(IEt_2Me_2')$ (**85a**).*

Selected Bond Lengths (Å)		Selected Bond Angles (°)	
Ru-C(1)	1.8646(18)	P(2)-Ru-P(3)	164.785(18)
Ru-C(2)	2.0900(19)	C(1)-Ru-C(2)	98.46(8)
Ru-C(6)	2.2098(18)	C(1)-Ru-C(6)	174.90(8)
Ru-P(2)	2.3218(5)	C(2)-Ru-P(2)	99.83(5)
Ru-(P3)	2.3315(5)	C(2)-Ru-P(3)	94.25(5)
C(7)-C(8)	1.519(3)	C(2)-Ru-C(6)	76.90(7)
N(2)-C(7)	1.461(3)	C(1)-Ru-P(2)	88.26(6)
O(1)-C(1)	1.163(2)	C(6)-Ru-P(2)	90.43(5)
N(1)-C(5)	1.466(3)	C(1)-Ru-P(3)	95.38(5)
C(5)-C(6)	1.535(3)	C(6)-Ru-P(3)	87.15(5)
		N(1)-C(2)-Ru	117.79(13)
		N(1)-C(5)-C(6)	108.79(15)
		C(5)-C(6)-Ru	109.96(12)
		N(2)-C(7)-C(8)	112.10(19)

Table 3.1 *Selected bond lengths and angles for $RuH(CO)(PPh_3)_3(IEt_2Me_2)$ (**85a**).*

C-H activation of **57** was fully reversible upon heating with H_2 or primary or secondary alcohols (Scheme 3.13), showing the potential for **57** to be applied to catalysis.

3.2.1.2 Isomerisation

Unexpectedly, dissolution of **85a** in ethanol resulted in the precipitation of the *trans*-dihydride isomer of $RuH_2(CO)(PPh_3)_2IEt_2Me_2$ (**86**) (Scheme 3.14). Although this complex displayed poor solubility in common NMR solvents (benzene-d_6, THF-d_8), it proved to be more soluble in pyridine-d_5, allowing assignment of the stereochemistry by 1- and 2-D multinuclear NMR. Thus, **86** displayed a single triplet integrating to 2H in the hydride region of the proton spectrum (δ -4.90, J_{HP} = 20.3 Hz) and a singlet in the $^{31}P\{^1H\}$ NMR spectrum (δ 63.2). Due to the rapid isomerisation of **86** in solution, $^{13}C\{^1H\}$ NMR assignments for the carbene (δ 183.6) and carbonyl (δ 209.9) could only be made by an ^1H-$^{13}C\{^1H\}$-HMBC experiment (Figure 3.3). Only one set of signals for the ethyl arms and imidazole backbone methyls appeared in the ^1H NMR spectrum revealing that the carbene rotates freely at room temperature or that there is a time

averaged plane of symmetry. Stirring **85a** with EtOD yielded an isotopic mixture of **86** with deuterium incorporated into one of the ethyl arms of the NHC (δ 0.64) and onto the metal (δ -4.91) to give the hydride deuteride complex (confirmed by ^{2}H NMR spectroscopy).

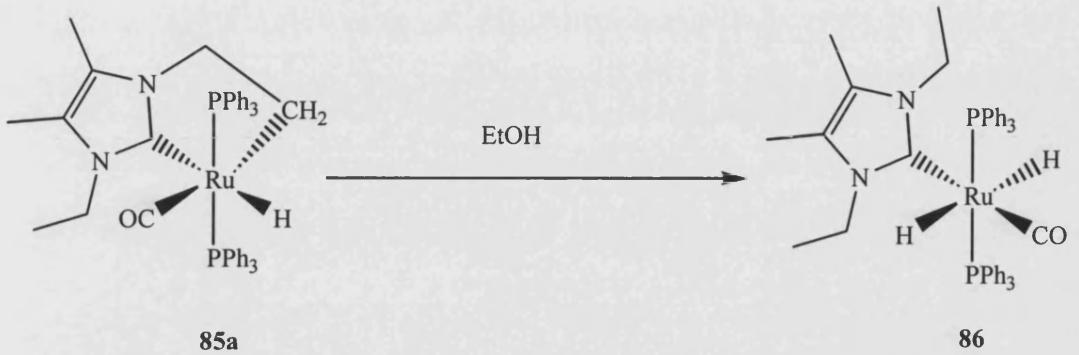

85a **86**

Scheme 3.14 *Formation of the trans hydride isomer,* ***86****.*

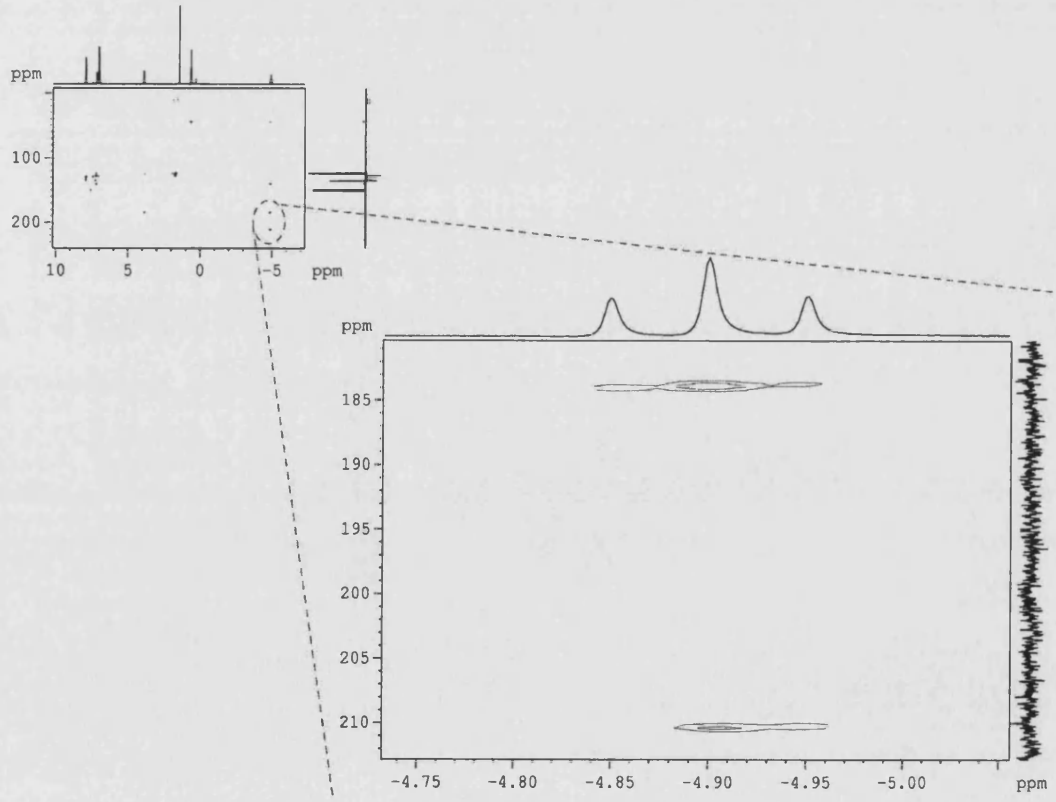

Figure 3.3 *^{1}H-$^{13}C\{^{1}H\}$-HMBC (pyridine-d_5, 400 MHz, 298 K) of* ***86****. The expansion shows cross-peaks to the carbene and CO which cannot be seen in the $^{13}C\{^{1}H\}$ NMR spectrum.*

Complex **86** proved to be thermally unstable in solution and rapidly isomerised (in pyridine-d_5) to a mixture of **85a**, **57**, and the all-*cis* isomer **87** after only 5 min at 323 K (1:1.2:1 ratio respectively) (Scheme 3.15). The geometry of the dihydride **87** paralleled the structure of **51** and had not previously been seen with the IEt_2Me_2 ligand. However, rapid isomerisation occurred and loss of intermediate **87** was observed indicating that **57** is more thermodynamically favoured. It appeared that **86** isomerised through **87** to **57**, however, with all three complexes present in the solution it could not be discounted that **86** also isomerised directly to **57**. After 40 min, **57** was essentially the only hydride species observable in the ^1H NMR spectrum (Figure 3.4).

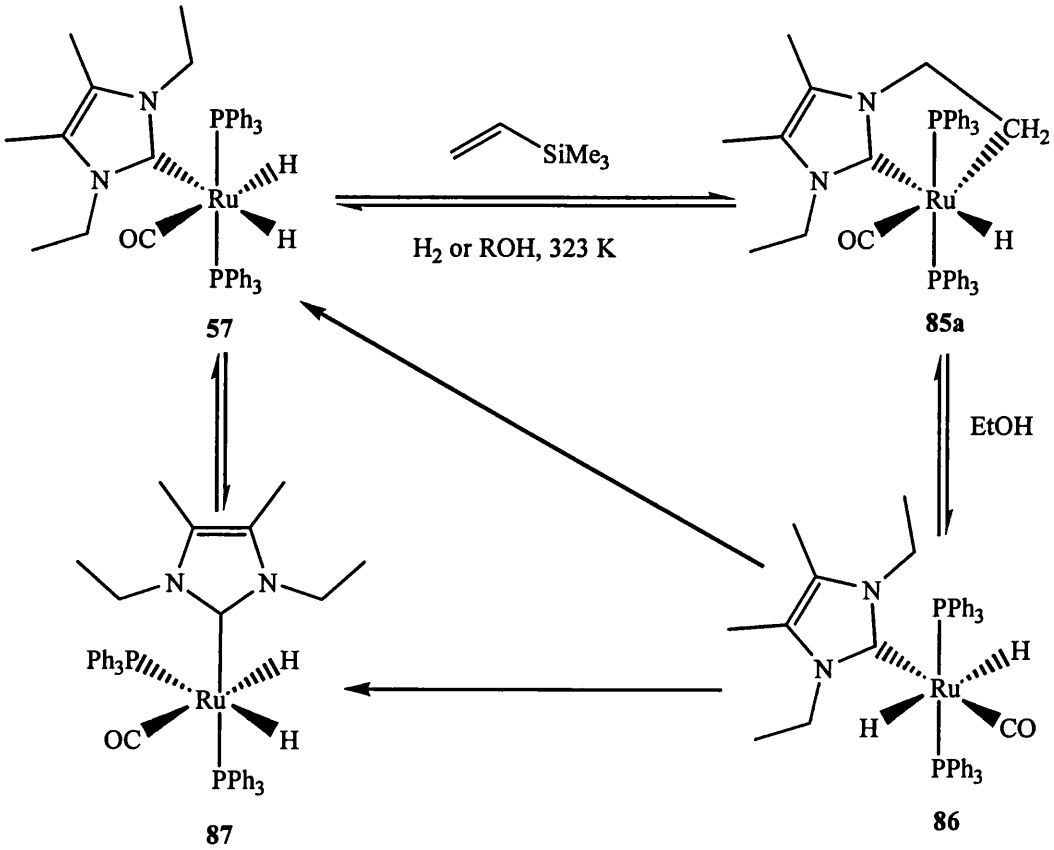

Scheme 3.15 *Interconversion of complexes 57, 85a, 86, and 87.*

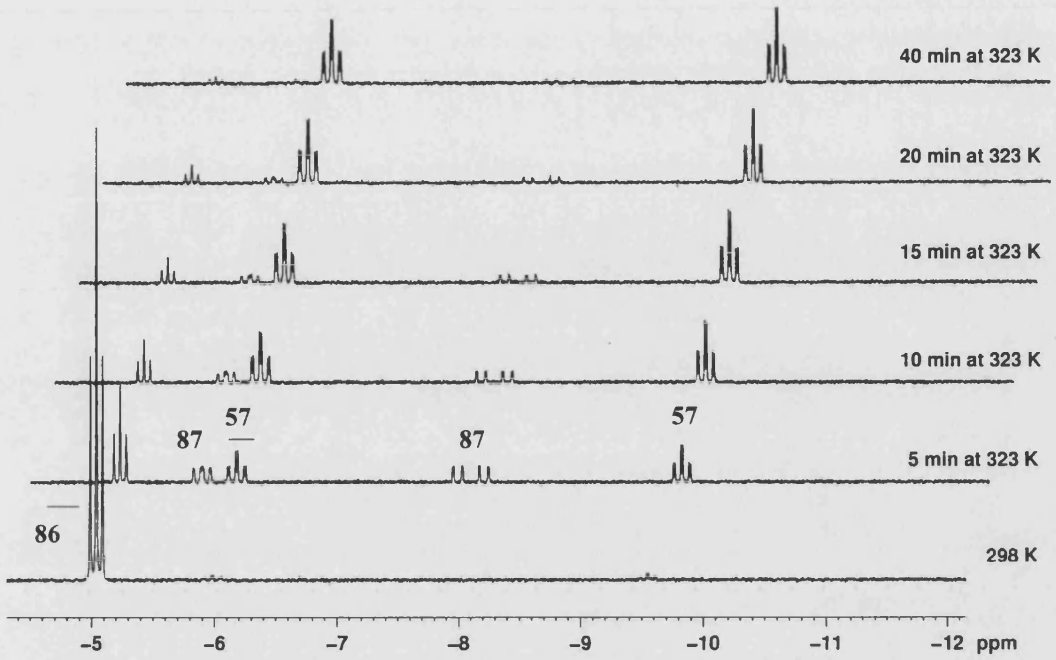

Figure 3.4 *Hydride region of the ^{1}H NMR spectrum (pyridine-d_5, 400 MHz, 323 K) showing interconversion of* ***87***, ***86*** *and* ***57***.

The rate of isomerisation was unaffected by the addition of up to ten equivalents of PPh_3 or by changing the solvent from pyridine to toluene. This is represented in Figure 3.5 where after only 5 min there were approximately a 1:1:1 ratio of isomers (with and without PPh_3) and after 20 min the same relative proportions of isomers were observed in both cases by ^{1}H NMR spectroscopy (**86**:**57**:**87** is 1:9:1.7).

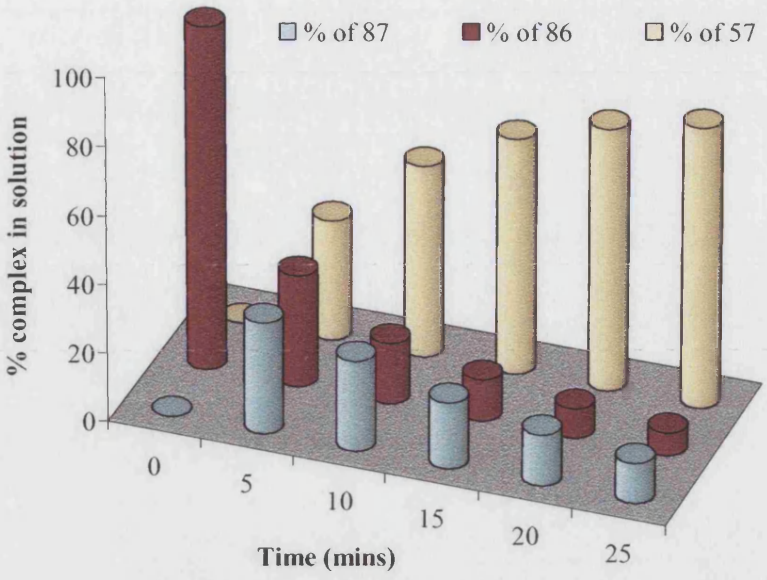

Figure 3.5 *Interconversion of **86**, **87** and **57** with ten equivalents of PPh_3.*

Isolation of **86** only appears to be possible due to its rapid precipitation from solution once formed at room temperature. Formation of the dihydride **57** from the C-H activated product **85a** (Scheme 3.13) was followed by ^{1}H NMR spectroscopy in an attempt to observe **86** as an intermediate. When a sample of **85a** in benzene-d_6/EtOH (**85a**:EtOH = 1:100) was warmed to 323 K, only a mixture of **85a** and **57** was observed with no evidence for either **86** or **87**. Other benzene/alcohol solutions gave similar results, the rate of re-formation of **57** following the order IPA > EtOH > MeOH (^{t}BuOH as expected gave no reaction). Production of acetone could be detected upon reaction with IPA. With MeOH or EtOH, we were unable to detect either acetaldehyde or formaldehyde as the expected products of the alcohol dehydrogenation reaction, although the appearance of a new doublet hydride resonance at δ -17.24 (J_{HP} = 22.0 Hz) in the proton NMR spectrum suggested that aldehydes may undergo reaction with **57**. Indeed when benzaldehyde or propionaldehyde was added to **57**, the same doublet was observed in the ^{1}H NMR spectrum. Attempts to crystallise this compound from the solutions gave several X-ray structures such as **88**, shown in Figure 3.6, although dissolution of the crystals in benzene-d_6 gave no matches to the hydride signal at δ -17.24 by ^{1}H NMR spectroscopy. It is thought that a range of complexes of this type is

formed upon addition of an aldehyde to **57**, including one containing a hydride ligand exhibiting the highfield doublet which was not isolated. The proposed structure **89** is shown in Figure 3.6. This was deduced from the knowledge gained from other complexes isolated and from ^{1}H and $^{31}P\{^{1}H\}$ NMR spectroscopy.

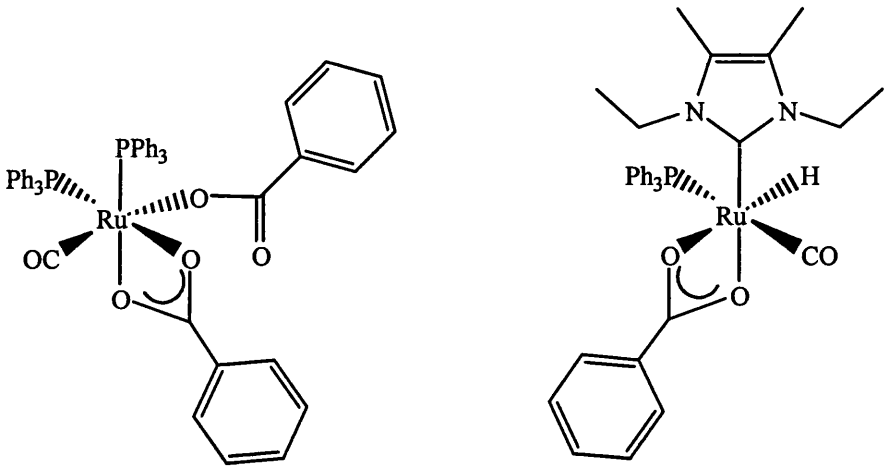

88 **89**

Figure 3.6 *Isolated (88) and proposed (89) structures from reactions of 57 with benzaldehyde.*

3.2.2 $RuH_2(CO)(PPh_3)_2(I^iPr_2Me_2)$ (61)

3.2.2.1 Synthesis of $RuH(CO)(PPh_3)_2(I^iPr_2Me_2')$ (62a)

Attempts to produce the mono $I^iPr_2Me_2$ dihydride complex $RuH_2(CO)(PPh_3)_2(I^iPr_2Me_2)$ (**61**) by the general method used in Chapter 2 were unsuccessful. A ^{1}H NMR spectrum of a mixture of $I^iPr_2Me_2$ (six equivalents) and **52** after heating at 70 °C in toluene for 20 h showed complete conversion of **52** to a mixture of the bis-carbene dihydride complex, $RuH_2(CO)(PPh_3)(I^iPr_2Me_2)_2$ (**90**), identified by the appearance of two doublet of doublets at δ -7.52, and a singlet at δ -6.06 suspected (but not proven) to be a tris-carbene complex, $RuH_2(CO)(I^iPr_2Me_2')_3$ (**91**) with one of the isopropyl arms activated. Trace amounts of the tris-carbene complex $RuH_2(CO)(I^iPr_2Me_2)_3$ (**92**) could also be detected (Figure 3.7). Removal of the toluene *in vacuo* gave a brown oily residue, which upon addition of ethanol immediately turned red and evolved H_2. The solution was left to stir overnight by which time a white precipitate had formed. The mixture was filtered

and the white solid washed with hexane to give the C-H activated mono carbene complex $RuH(CO)(PPh_3)_2(I^iPr_2Me_2')$ (**62a**) in 66% yield.

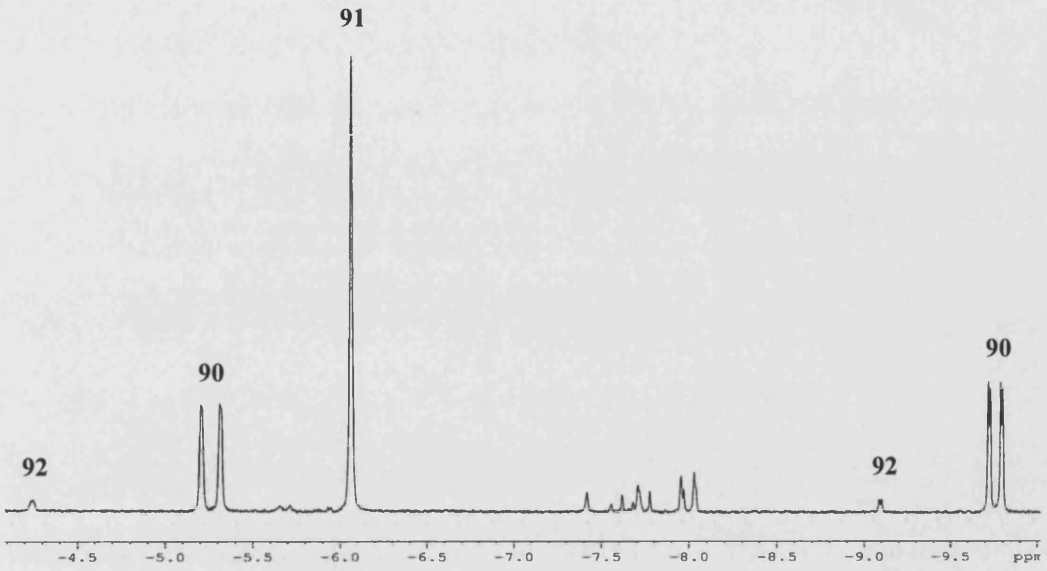

Figure 3.7 *Hydride region of the ^1H NMR spectrum (benzene-d_6, 400 MHz, 298 K) following the reaction of $I^iPr_2Me_2$ (six equivalents) with* ***52*** *in toluene after 20 h at 70 °C.*

The ^1H NMR spectrum of the complex in benzene-d_6 displayed a doublet of doublets (δ -7.72, J_{HP} = 104.8 Hz, J_{HP} = 28.0 Hz) with *trans* and *cis* couplings to phosphine. The N-C-N carbon resonance (δ 187.8, J_{CP} = 10.1 Hz, J_{CP} = 82.7 Hz) in the $^{13}C\{^1H\}$ NMR spectrum also exhibited *cis* and *trans* couplings to phosphine, showing that the carbene must sit *trans* to a phosphine as with **51**. Trace amounts of the activated complex with the carbene residing *trans* to hydride could be detected in the same solution, exhibited as a triplet (δ - 7.47, J_{HH} = 24.7 Hz) in the ^1H NMR spectrum. This is the reverse to the favoured geometry that was observed with **57**. Presumably the extra steric bulk of ^{i}Pr versus Et causes a preference for the carbene to reside *trans* to phosphine.

Separate signals are observed for the methyl groups on the unactivated isopropyl arm in the ^1H and $^{13}C\{^1H\}$ NMR spectra. Unlike the activated ethyl complex **85a**, **62a** displays separate resonances for the diastereotopic CH_2 protons on the activated arm of the

carbene, the assignment of which were confirmed by ^{1}H-NOESY correlation (Figure 3.8). Both H_C and H_F correlate to the hydride indicating that the methyl group on the activated isopropyl arm orients itself to minimise steric interactions with the bulky PPh_3 ligands. The $^{31}P\{^{1}H\}$ NMR spectrum confirms the inequivalent nature of the two phosphines by displaying two doublets at δ 56.5 and 35.8.

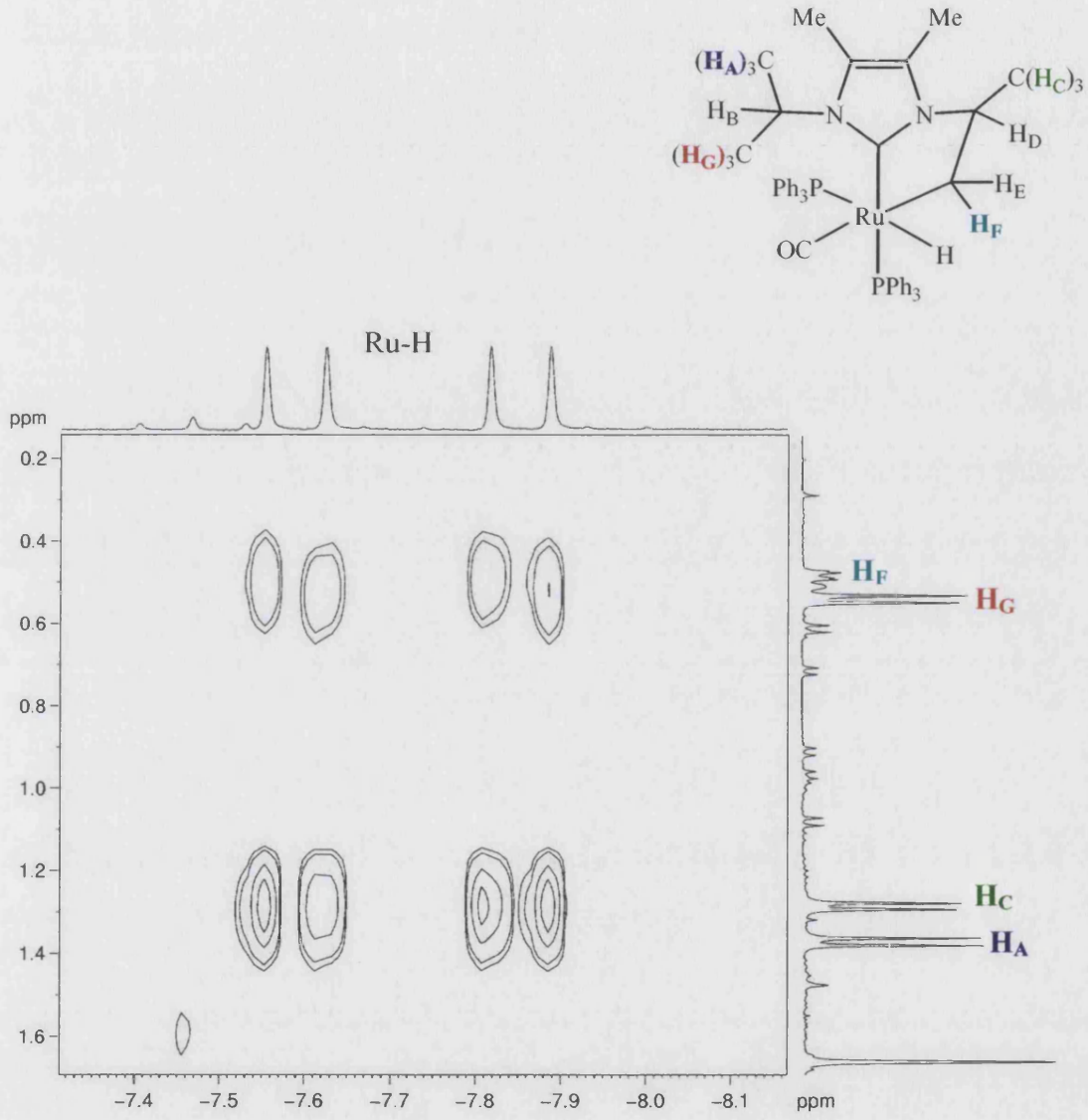

Figure 3.8 *^{1}H-NOESY spectrum (benzene-d_6, 400 MHz, 298 K) of **62a** showing correlations from the hydride.*

To confirm unequivocally the geometry of **62a**, the X-ray crystal structure was determined, illustrated in Figure 3.9. The five-membered ring formed by the activated arm can be seen clearly with a Ru-C bond length of 2.2100(16) Å; this is larger than the

comparable distance in the aryl carbene complex **51** (2.0786(19) Å) and in **85a** where the alkyl carbene sits in the equatorial position (2.0900(19) Å). The angle at the sp^2 hybridised CH_2 of the activated arm (N(1)-C(5)-C(6) = 107.45(12) °) is more acute than of the free ^{i}Pr arm (N(2)-C(8)-C(9) = 112.94(16) °) but the angle at C(5)-C(6)-Ru (110.50(10) °) is close to the expected tetrahedral angle at a methylene group.

Selected Bond Lengths (Å)		Selected Bond Angles (°)	
Ru-C(1)	1.8626(17)	P(1)-Ru-P(2)	102.152(15)
Ru-C(2)	2.0594(16)	C(2)-Ru-P(2)	162.97(4)
Ru-C(6)	2.2100(16)	C(2)-Ru-P(1)	92.97(4)
Ru-P(1)	2.4357(4)	C(2)-Ru-C(1)	97.63(7)
Ru-P(2)	2.3445(4)	C(2)-Ru-C(6)	76.72(6)
N(2)-C(8)	1.468(2)	C(1)-Ru-C(6)	165.25(7)
C(5)-C(7)	1.523(2)	C(1)-Ru-P(1)	103.40(5)
C(8)-C(9)	1.517(3)	C(1)-Ru-(P2)	86.52(5)
N(1)-C(5)	1.476(2)	C(6)-Ru-(P1)	90.59(4)
C(5)-C(6)	1.534(2)	C(6)-Ru-P(2)	95.15(4)
		C(5)-C(6)-Ru	110.50(10)
		N(1)-C(5)-C(6)	107.45(12)
		C(8)-N(2)-C(2)	121.85(14)
		N(2)-C(8)-C(9)	112.94(16)

Table 3.2 *Selected bond lengths and angles for* ***62a****.*

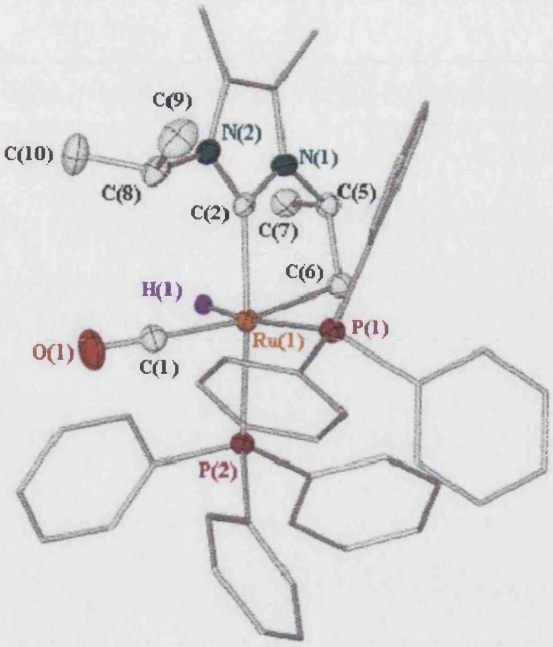

Figure 3.9 *X-ray structure of* ***62a****.*

As described in Chapter 2, the mono-NHC dihydride species **61** was obtained *via* the addition of H_2 or IPA to a heated benzene solution of the activated complex **62a**. Interestingly the activated complex **62a** isomerises in this hydrogenation process so that the carbene sits *trans* to a hydride to form the dihydride species **61**, with the same geometry as with the other mono alkyl-NHC complexes synthesised. Unexpectedly, thermolysis of **61** at 50 °C for 16 h with five equivalents of $H_2C{=}CHSiMe_3$ generated two C-H activated isomers, **62a** and **62b** (Scheme 3.16).

Variable temperature (VT) ^{1}H NMR experiments were carried out on **62a** in toluene-d_8 (Figure 3.10). As the complex was heated to 343 K, interconversion of **62a** and **62b** was rapid. An equilibrium was reached and the quantities of **62a** and **62b** remained the same, in the ratio of 2:1 of axial:equatorial isomers, even upon further heating to 373 K. Upon cooling the same reaction mixture down to 233 K, the relative ratio of isomers did not alter.

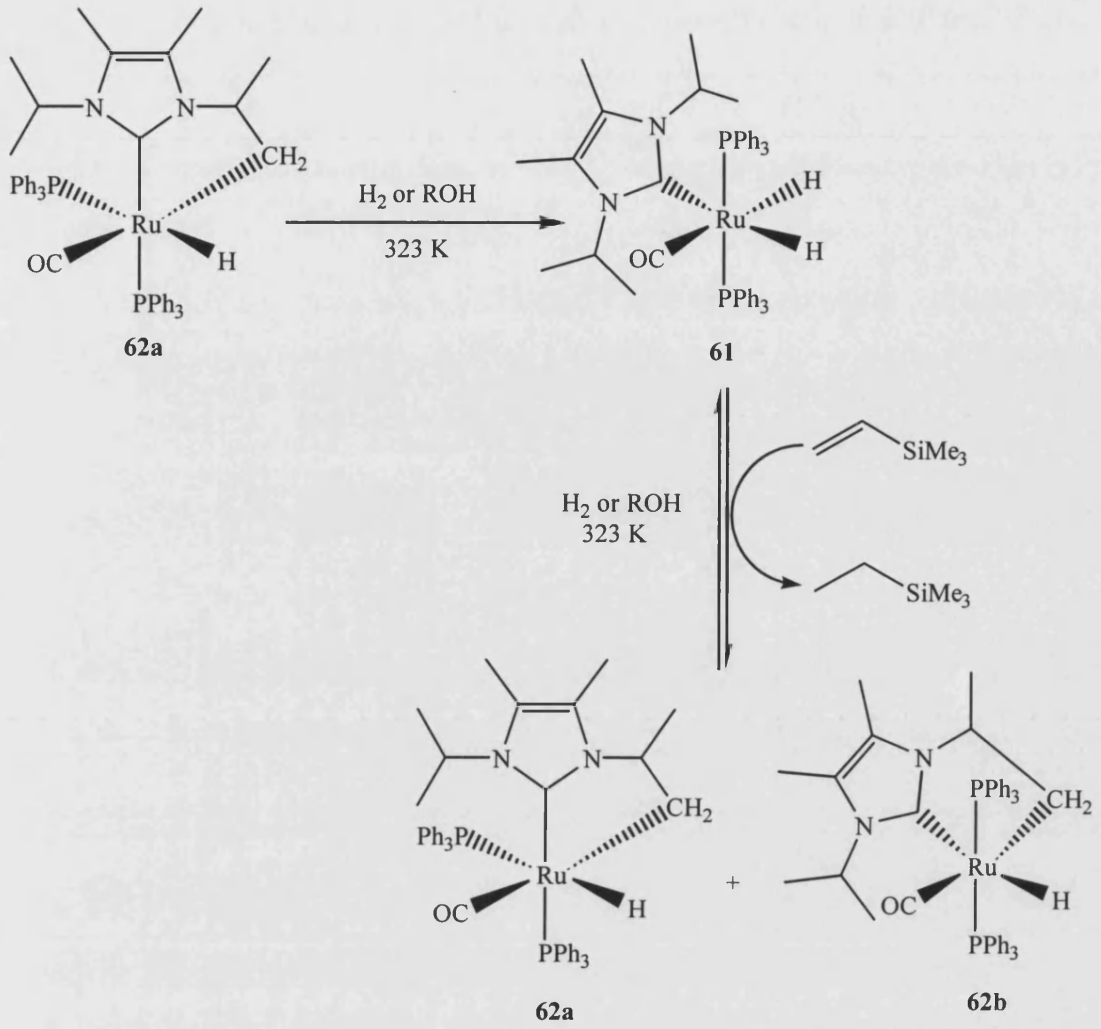

Scheme 3.16 *Reversible C-H activation of* ***62a****.*

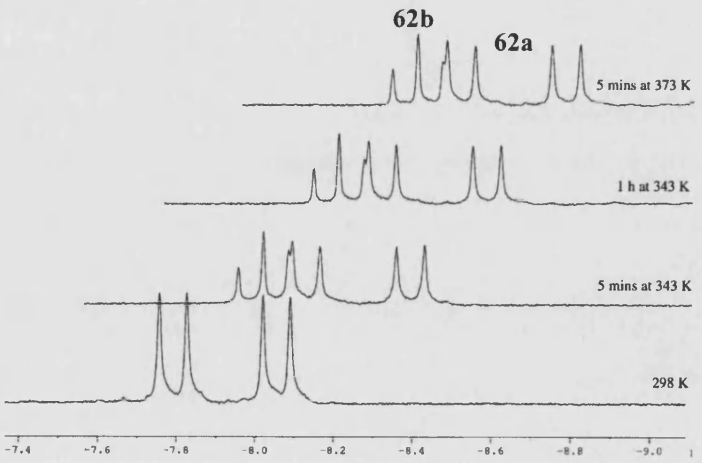

Figure 3.10 *^{1}H NMR spectra (toluene-d_8, 400 MHz, 298 K-373 K) showing interconversion of* ***62a*** *and* ***62b*** *upon heating.*

The C-H activation reaction of **61** with H_2C=CHSiMe$_3$ was then performed again, this time at *room temperature* to see if the axial product, **62a** alone would form. The reaction was slow but after two days with five equivalents of H_2C=CHSiMe$_3$, both C-H activated isomers could be detected by ^{1}H NMR. The reaction took a total of eight days to go to completion to give both C-H activated isomers in a 3:1 ratio of **62a**:**62b**. Since the activation of **61** seemed so facile, a benzene solution of **61** alone was heated to 70 °C. Both C-H activated isomers (in a 2:1 ratio) were observed in the ^{1}H NMR spectrum after 3 h; loss of H_2 had occurred in the absence of a hydrogen acceptor. This had not been seen in any other of our Ru-NHC complexes, either aryl or alkyl substituted. The ease with which **61** activates indicates that the C-H activation step must have a small activation barrier.

3.2.3 RuH$_2$(CO)(PPh$_3$)$_2$(I^{i}Pr) (58)

Unlike **61**, thermolysis of RuH$_2$(CO)(PPh$_3$)$_2$(I^{i}Pr) **58** with H_2C=CHSiMe$_3$ resulted in C-H activation of the ^{i}Pr arm to form only one species **93**, with the Ru-NHC bond *trans* to hydride (Scheme 3.17). This tells us that in addition to the bulky ^{i}Pr substituents on the N atoms, it is the methyl groups on the backbone of the imidazole ring that force the NHC ligand into the axial position in the case of **62a**. The ^{1}H NMR spectrum of **93** displayed a triplet (δ-7.20, J_{HP} = 24.7 Hz) indicating coupling of the hydride to two equivalent phosphines. However, the ^{31}P{^{1}H} NMR spectrum showed an AB pattern (J_{PP} = 294.04 Hz) indicating that the phosphines were now slightly chemically inequivalent. This was confirmed by a simulation using *g*NMR (Figure 3.11).

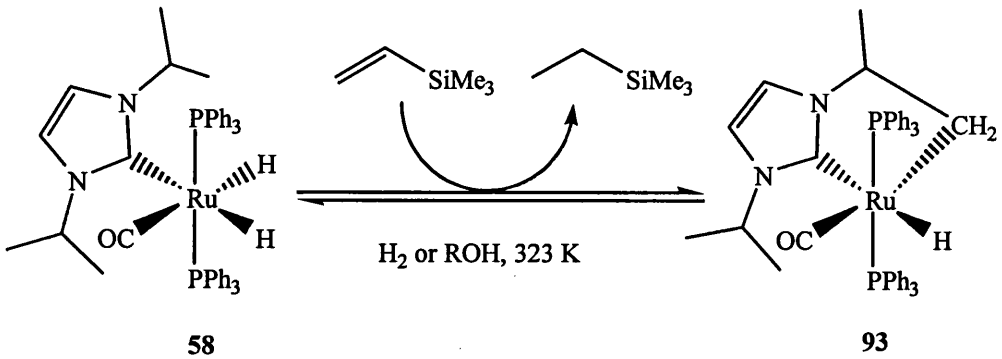

58 93

Scheme 3.17 *C-H activation of RuH$_2$(CO)(PPh$_3$)$_2$(I^{i}Pr) (58).*

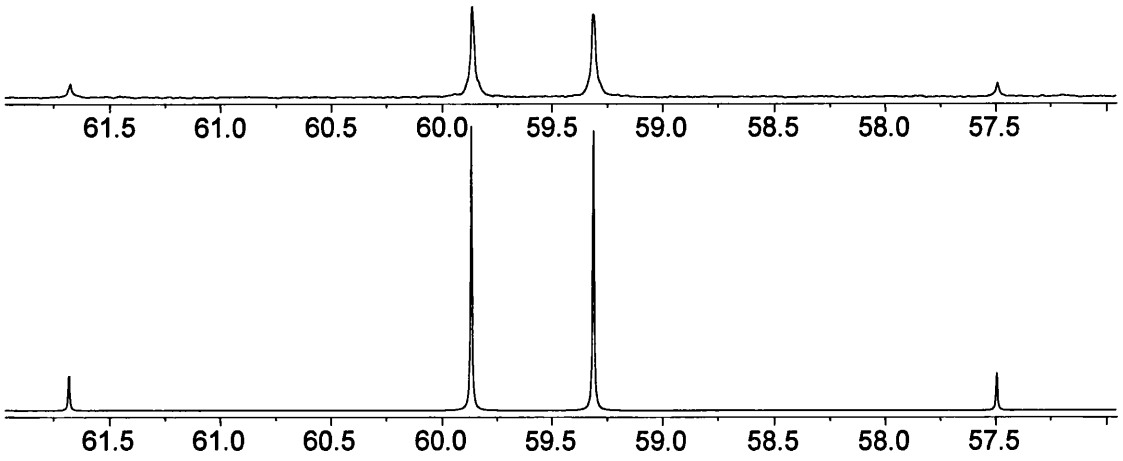

Figure 3.11 *$^{31}P\{^{1}H\}$ NMR spectra (400 MHz, benzene-d_6, 298 K) of* ***58****, real and simulated by gNMR.*

There was no detection of the other C-H activated isomer as had been seen with the IEt_2Me_2 and $I^iPr_2Me_2$ analogues.

Room temperature activation of **58** was attempted with the addition of $H_2C{=}CHSiMe_3$ (five equivalents). However, unlike **62a**, no activation was observed. With no room temperature activation observed with **57** either, it was clear that both the bulky ^{i}Pr N-substituents and the backbone methyls were required for the facile C-H activation to take place.

3.2.4 $RuH_2(CO)(PPh_3)_2(I^nPr)$ (65)

Upon thermolysis of $RuH_2(CO)(PPh_3)_2(I^nPr)$ (**65**) with $H_2C{=}CHSiMe_3$ at 50 °C for 16 h, it was anticipated that C-H activation of either the ^{n}Pr CH_2 or CH_3 group would occur. Activation of a CH_2 group had not previously been observed, and a six-membered cyclometallated ring had only been seen in the activation of the aryl NHC IMes. Unexpectedly, however, **65** did not undergo activation of either the carbene or the

phosphine (Scheme 3.18). Orthometallation of the phosphine ligand has been seen in the ruthenium precursor **52**.[33] A preference for activation of a phosphine ligand over the NHC ligand has been observed in both the ICy and IMe_4 derived complexes **64** and **54** respectively.

An indication as to why C-H bond activation of the carbene ligand was not observed was provided from the X-ray structure of **65** (Figure 3.12).[34] It was evident that the CH_3 group could not be brought within a reasonable, bond forming distance to the metal centre, and orientation of the CH_2 group would cause the CH_3 group to collide with either the carbonyl group on one side, or the hydride on the other. It is not yet fully understood why orthometallation of the phosphine ligand does not occur. It is possible that the I^{n}Pr ligand also interferes sterically to inhibit close approach of the phosphine Ph.

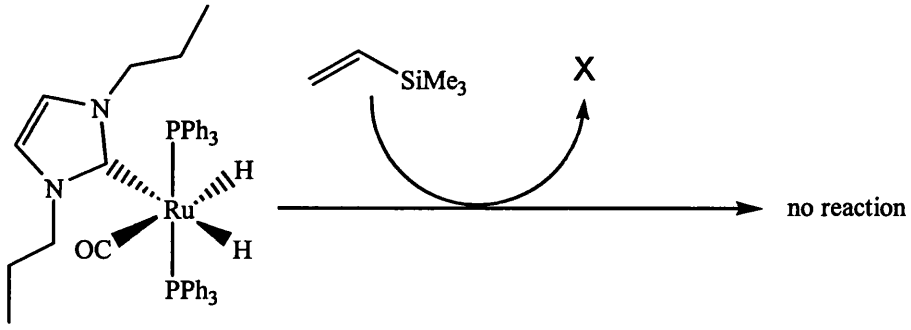

65

Scheme 3.18 *Attempted C-H activation of $RuH_2(CO)(PPh_3)_2(I^nPr)$ 65.*

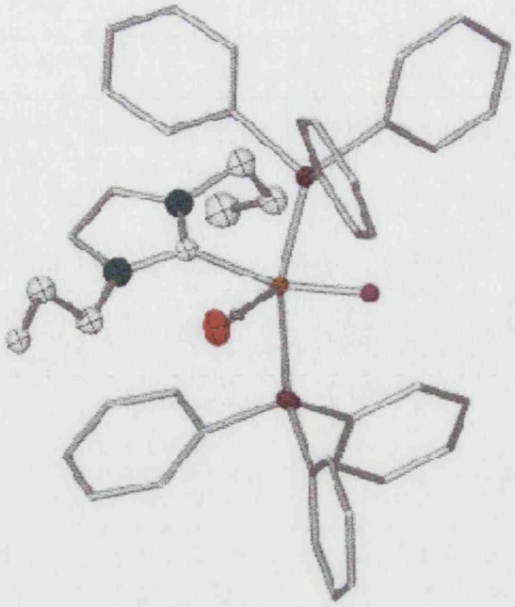

Figure 3.12 *X-ray structure of $RuH_2(CO)(PPh_3)_2(I^nPr)$ (65).*[34]

3.2.5 $RuH_2(CO)(PPh_3)_2I^*$ (59a)

Upon addition of H_2C=$CHSiMe_3$ to RuI* (**59a**) in benzene-d_6, activation of one C-H bond of one of the methyl groups occurred (Scheme 3.19) to afford $RuH(CO)(PPh_3)_2(I^{*\prime})$ (**94a**) as a yellow solid. Multinuclear 1-D NMR in addition to 2-D ^{1}H-COSY and ^{1}H-^{13}C{^{1}H}-HMQC experiments were used to fully characterise **94a**, in particular for the assignment of the aromatic protons and the N-CH protons. Aromatic protons furthest downfield in the ^{1}H NMR spectrum (δ 7.94-7.82 and 7.62-7.52) were assigned to PPh_3 groups by the use of ^{1}H{^{31}P} NMR spectroscopy. The NHC phenyl resonances were identified by a ^{1}H-COSY experiment and shown to overlap with the remaining PPh_3 signals. This 2-D correlation also allowed the assignment of the N-CH protons. In the corresponding dihydride complex, **59a**, these protons were shifted downfield to the aromatic region underneath the PPh_3 peaks. With the C-H insertion complex, **94a**, the proton on the metallated arm was shifted upfield to δ 4.37-4.26 in the ^{1}H NMR spectrum and the proton on the free arm was also shifted slightly downfield to δ 6.05.

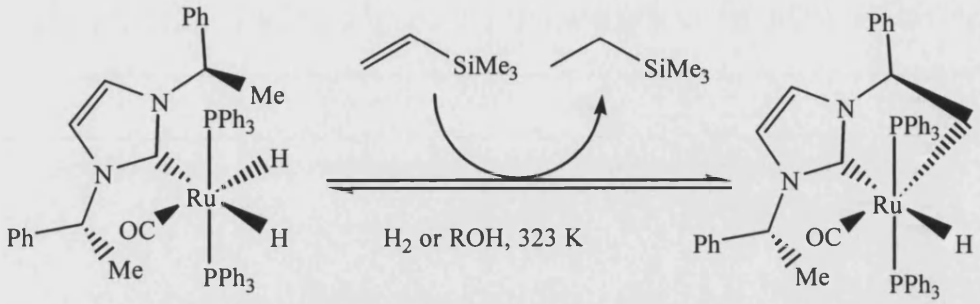

59a **94a**

Scheme 3.19 *C-H activation of* ***59a***.

As discussed in Chapter 2, a second order $^{31}P\{^{1}H\}$ NMR spectrum containing an AB quartet was seen for the dihydride complex **59a**. The $^{31}P\{^{1}H\}$ spectrum of the activated product **94a** showed two singlets indicating that the chemically inequivalent phosphines appear not to couple (Figure 3.13).

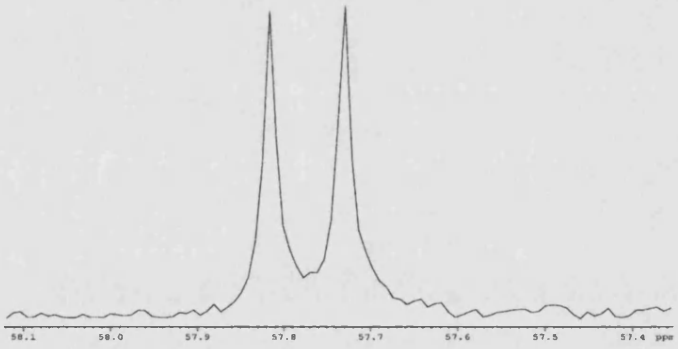

Figure 3.13 *$^{31}P\{^{1}H\}$ NMR spectrum of C-H activated complex* ***94a***.

As previously discussed in section 2.3.3.6.1, when synthesising **59a**, an unknown complex with similar NMR patterns was also produced. An excess of $H_2C{=}CHSiMe_3$ was added to the mixture of complexes: **59a** and the unidentified complex **59b**. The ^{1}H NMR spectrum exhibited two individual triplets indicating that both complexes activated independently to give two complexes **94a** and **94b** (Figure 3.14). The reaction was fully reversible with no change to the relative ratio of the two isomers.

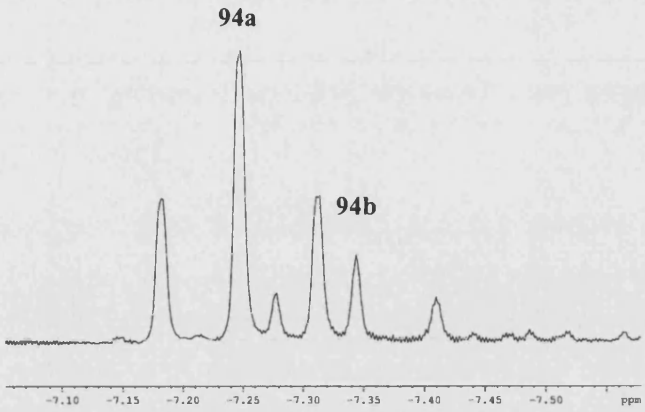

Figure 3.14 *Hydride region of the ^{1}H NMR spectrum (benzene-d_6, 400 MHz, 298 K) showing C-H activation of both **59a** and **59b**.*

3.2.6 $RuH_2(CO)(PPh_3)_2(IMe_4)$ (54)

Heating a THF solution of **54** at 50 °C with five equivalents of H_2C=$CHSiMe_3$ resulted in a colour change from pale yellow to deep green. After 36 h, the ^{1}H NMR spectrum showed that **54** had been converted quantitatively to a product (**95**) resulting from orthometallation of one of the triphenylphosphine C-H bonds rather than C-H activation of the N-CH_3 group (Scheme 3.20). It is likely that the N-CH_3 group is unable to get close enough to the metal centre for activation; similarly, activation would yield a highly strained four-membered ruthenacycle. Interestingly, however, C-H activation of 1,3-dimethylimidazol-2-ylidene (IMe_2) on a ruthenium cluster has very recently been reported by Cabeza and co-workers (Scheme 3.12).[32]

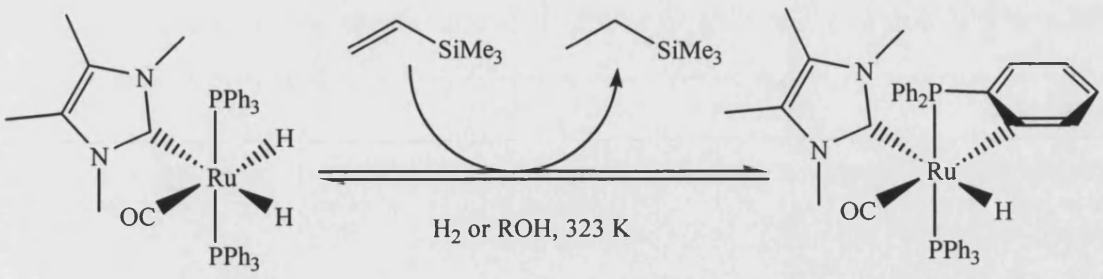

54 **95**

Scheme 3.20 *Orthometallation of* ***54****.*

Evidence for the activated product was shown in the ^{1}H NMR spectrum, which exhibited a single triplet at δ -2.68 (J_{HP} = 25.3 Hz). This is further downfield than the hydride shifts of the C-H insertion products of all Ru-NHC complexes (~ δ -7) where activation of the carbene occurs. The $^{31}P\{^{1}H\}$ NMR spectrum of **95** displayed resonances characteristic of orthometallated species,[33] most tellingly the doublet at δ -21.8 (J_{PP} = 20.6 Hz) (Figure 3.15). The second phosphorus appeared as a doublet at a typical chemical shift expected for a coordinated PPh_3 group (δ 50.3 J_{PP} = 20.6 Hz). Orthometallation of PPh_3 ligands has also been observed in the ruthenium precursor **52**[33] and in the cyclohexyl carbene complex **64**,[35] both exhibiting similar NMR shifts. Orthometallation of **54** is fully reversible with addition of either H_2, primary or secondary alcohols at 50 °C.

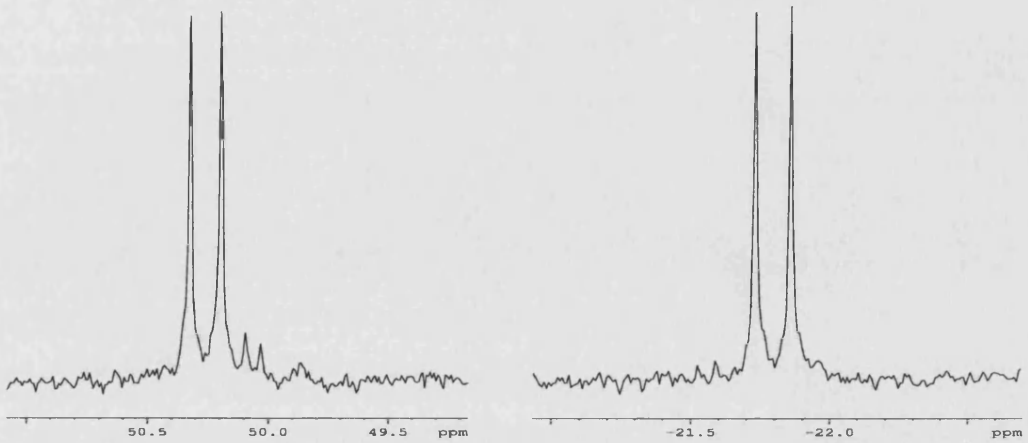

Figure 3.15 *$^{31}P\{^{1}H\}$ NMR Spectrum (THF-d_8, 400 MHz, 298 K) of* ***95****.*

When the activation of **54** was carried out in benzene-d_6, the conversion was very slow and took several days at 50 °C to go to completion. When the temperature was raised to 70 °C, trace amounts of the phosphine C-H activated product could be detected in the ^1H and $^{31}P\{^1H\}$ NMR spectra along with other unwanted side products. When the temperature was raised to 70 °C in THF, the reaction was faster but additional unwanted products appeared.

3.3 Discussion

3.3.1 Activation

The rare C-H activation of N-alkyl carbenes has been shown for a variety of ruthenium complexes. Activation appears to be a result of combined steric and electronic influence. In the case of the complex **61**, which contains sterically demanding *iso*-propyl groups in addition to electron donating methyl groups on the backbone of the imidazole ring, activation is facile. In contrast, the complex **65** did not undergo activation, even under forcing conditions. The ease of activation of alkyl Ru-NHC complexes appears to follow the order $I^iPr_2Me_2$ > IEt_2Me_2 ≥ I^iPr > I* > ICy > IMe_4 > I^nPr.

Activation of alkyl NHC groups is slower than with aryl NHC groups. C-H insertion of the mesityl-CH_3 group in **51** occurred at room temperature within 3 h upon addition of H_2C=$CHSiMe_3$, whereas activation of most alkyl NHC groups required thermolysis at 50 °C with the alkene. The complex **61** bearing the $I^iPr_2Me_2$ ligand was found to have a lower activation barrier than the other alkyl carbenes and activation did occur at room temperature, although the reaction took eight days to go to completion. In the case of the mixed aryl/alkyl nature of the ligand I*, activation of the alkyl CH_3 occurs rather than of the phenyl group. Orthometallation of the phenyl would create a strained six-membered ring. Upon activation of Ru-NHC complexes, only four- and five-membered ruthenacycles were formed.

Preferential C-H activation of the PPh_3 phenyl groups was observed with **54** and **66**. This orthometallation process was slower than C-H insertion reactions that occurred at carbenes. The orthometallated products could be detected by ^1H NMR spectroscopy

upon thermolysis with alkene overnight but both reactions required further heating to go to completion. The orthometallated species could also be detected by their deep green colouration. Addition of H_2 to the deep green solutions gave an immediate colour change to yellow.

All C-H activation processes were reversible upon addition of either H_2 or primary or secondary alcohols indicating that these complexes have the potential for their application as catalysts for organic synthesis. This concept is explored in the following chapter.

3.3.2 Isomerisation

Activation of **57** resulted in formation of the expected C-H activated product **85a**, where carbene remained *trans* to hydride as with the starting dihydride, in addition to trace amounts of the geometrical isomer **85b**, where carbene is *trans* to phosphine. The same isomerisation was observed with activation of **61**, although now the major isomer had become the isomerised product. Interestingly, activation of the Ru-NHC complexes bearing carbenes without methyl groups on the backbone of the imidazole showed no isomerisation. However, $^{31}P\{^1H\}$ NMR spectroscopy revealed that the phosphines had become chemically inequivalent, indicating the greater steric influence of the I^{i}Pr ligand upon activation.

Further isomerisations were seen in the case of **57** where a *trans* hydride species was isolated. Analogous complexes with other alkyl carbenes were not seen. The *trans* hydride species **86** proved to be highly insoluble in regular solvents and once dissolved in pyridine proved to be unstable, rapidly isomerising back to the *cis* dihydride **57**.

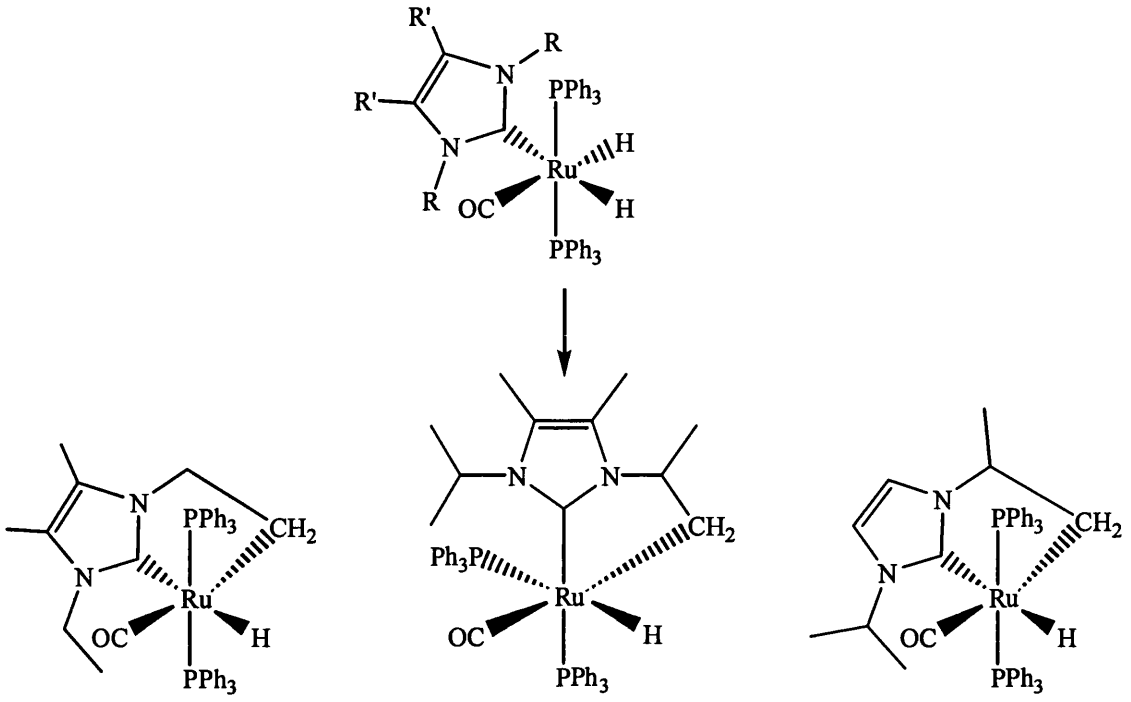

85a major product

62a major product

93 only product

Figure 3.16 *Steric and electronic influence of carbene ligands on the formation of geometrical isomers.*

3.4 Chapter summary

- C-H activation of the range of synthesised Ru-NHC complexes was attempted and all successful C-H activated and isomerisation products were isolated and fully characterised using NMR spectroscopy, IR spectroscopy and X-ray crystallography.

- Metallation of terminal CH_3 protons of the alkyl NHCs on **57**, **61**, **58** and **59a** was observed. Preferential activation of the PPh_3 phenyl groups was observed with **54** and **64**. No C-H activated product could be synthesised with **65**.

- C-H activation of **61** proved to be more facile than with all other alkyl Ru-NHC complexes.

- Isomerisations of complexes were seen upon C-H activation with **57** and **61**. Further isomerisation reactions were seen with **57**.

3.5 References

[1]Shilov, A. E.; Shul'pin, G. B. *Chem. Rev.* **1997**, *97*, 2879-2932.

[2]Rybtchinski, B.; Milstein, D. *Angew. Chem. Int. Edit.* **1999**, *38*, 870-883.

[3]Labinger, J. A.; Bercaw, J. E. *Nature* **2002**, *417*, 507-514.

[4]Kakiuchi, F.; Chatani, N. *Adv. Synth. Catal.* **2003**, *345*, 1077-1101.

[5]Guari, Y.; Sabo-Etienne, S.; Chaudret, B. *Eur. J. Inorg. Chem.* **1999**, 1047-1055.

[6]Crabtree, R. H. *J. Chem. Soc. Dalton Trans.* **2001**, 2437-2450.

[7]Crabtree, R. H. *J. Organomet. Chem.* **2004**, *689*, 4083-4091.

[8]Janowicz, A. H.; Bergman, R. G. *J. Am. Chem. Soc.* **1982**, *104*, 352-354.

[9]Bergman, R. G.; Foo, T. *Organometallics* **1992**, *11*, 1801-1810.

[10]Jones, W. D.; Feher, F. J. *Organometallics* **1983**, *2*, 562-563.

[11]Jones, W. D.; Feher, F. J. *J. Am. Chem. Soc.* **1984**, *104*, 1650-1663.

[12]Baker, M. V.; Field, L. D. *J. Am. Chem. Soc.* **1987**, *109*, 2825-2826.

[13]Kakiuchai, F.; Murai, S. *Acc. Chem. Res.* **2002**, *35*, 826-834.

[14]Ritleng, V.; Sirlin, C.; Pfeffer, M. *Chem. Rev.* **2002**, *102*, 1731-1769.

[15]Gandelman, M.; Shimon, L. J. W.; Milstein, D. *Chem. Eur. J.* **2003**, *9*, 4295-4300.

[16]Bennett, M. A.; Milner, D. L. *Chem. Commun.* **1967**, 581-582.

[17]Abdur-Rashid, K.; Fedorkiw, T.; Lough, A. J.; Morris, R. H. *Organometallics* **2004**, *23*, 86-94.

[18]Jazzar, R. F. R.; Macgregor, S. A.; Mahon, M. F.; Richards, S. P.; Whittlesey, M. K. *J. Am. Chem. Soc.* **2002**, *124*, 4944-4945.

[19]Crudden, C. M.; Allen, D. P. *Coord. Chem. Rev.* **2004**, *248*, 2247-2273.

[20]Hitchcock, P. B.; Lappert, M. F.; Pye, P. L. *J. Chem. Soc. Chem. Commun.* **1977**, 196-198.

[21]Hitchcock, P. B.; Lappert, M. F.; Terreros, P. *J. Organomet. Chem.* **1982**, *239*, C26-C30.

[22]Trnka, T. M.; Morgan, J. P.; Sanford, M. S.; Wilhelm, T. E.; Scholl, M.; Choi, T. L.; Ding, S.; Day, M. W.; Grubbs, R. H. *J. Am. Chem. Soc.* **2003**, *125*, 2546-2558.

[23]Huang, J. K.; Stevens, E. D.; Nolan, S. P. *Organometallics* **2000**, *19*, 1194-1197.

[24]Herrmann, W. A.; Goosen, L. J.; Spiegler, M. *Organometallics* **1998**, *17*, 2162.

[25]Chilvers, M. J.; Jazzar, R. F. R.; Mahon, M. F.; Whittlesey, M. K. *Adv. Synth. Catal.* **2003**, *345*, 1111-1114.

[26]Danopoulos, A. A.; Winston, S.; Hursthouse, M. B. *J. Chem. Soc. Dalton Trans.* **2002,** 3090-3091.

[27]Crabtree, R. H. *Dalton Trans* **2001,** 2437-2450.

[28]Crabtree, R. H. *The Organometallic Chemistry of the Transition Metals*; 3rd ed.; Wiley-Interscience, 2001.

[29]Prinz, M.; Grosche, M.; Herdtweck, E.; Herrmann, W. A. *Organometallics* **2000,** *19,* 1692-1694.

[30]Dorta, R.; Stevens, E. D.; Nolan, S. P. *J. Am. Chem. Soc.* **2004,** *126,* 5054-5055.

[31]Scott, N. M.; Dorta, R.; Stevens, E. D.; Correa, A.; Cavallo, L.; Nolan, S. P. *J. Am. Chem. Soc.* **2005,** *127,* 3516-3526.

[32]Cabeza, J. A.; del Rio, I.; Sanchez-Vega, M. G. *Chem. Commun.* **2005,** 3956-3958.

[33]Jazzar, R. F. R. "PhD thesis," University of Bath, **2003.**

[34]Brown, V. "M. Chem. Report.," University of Bath, **2005.**

[35]Burling, S. *Personal communication.*

Chapter 4

Chapter 4: Ru-NHC hydrogenation reactions and their use in tandem catalysis

4.1 Introduction

Until recently, the application of ruthenium catalysis to non-metathesis formation of carbon-carbon bonds was a relatively unexplored field.[1] In the early 1970s the chemistry of ruthenium catalysis was far behind that of other transition metal complexes, such as rhodium and palladium.[2] However, with recent progress in organometallic chemistry, organic synthesis catalysed by ruthenium complexes has attracted much attention. Ruthenium complexes for oxidation and reduction reactions are well known due to their low redox potential and readily interchangeable oxidation states. The work in this Chapter combines the efficiency of ruthenium to catalyse transfer hydrogenation reactions along with C=C bond forming reactions in a one-pot tandem process to achieve indirect formation of C-C bonds from alcohols.

4.2 Overview of C=C bond formation

Alkenes are often important intermediates or synthetic targets and a valuable approach to prepare them is *via* a C=C bond forming reaction whereby a carbonyl component and a suitable reagent are combined to generate the alkene. Reagents derived from phosphorus are perhaps the most useful. Phosphorane ylides, phosphonate esters and phosphine oxides are used in three of the most useful C=C bond forming reactions; the Wittig,[3] Wadsworth-Emmons[4] and Horner[5] reactions respectively. The strong phosphorus-oxygen bonds that form in the by-product provides the thermodynamic driving force for the reaction. Many other non-phosphorus based C=C bond forming methods are available, such as the Peterson elimination and Julia coupling reactions.[6] These provide valuable techniques for the synthesis of alkenes although, unlike the Wittig reaction, proceed in more than one step and for that reason are not so widely used.

4.2.1 The Wittig reaction

The Wittig reaction (Figure 4.1) is possibly the most important way of making alkenes. In this reaction a carbonyl compound and a phosphorane ylide are combined to generate an alkene. The stereoselectivity of the Wittig reaction can be controlled by the nature of the substituent on the carbon atom of the ylide. With stabilised ylides, that is ylides whose anion is stabilised by further conjugation, usually with R^2 as carbonyl group, the Wittig reaction is *E*-selective. With unstabilised ylides (R^2 = alkyl) the Wittig reaction is *Z*-selective. While stabilised ylides are air and moisture stable, unstabilised ylides rapidly decompose when exposed to air/moisture and must be stored under an inert atmosphere.

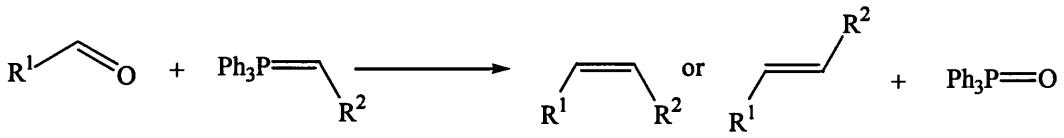

Figure 4.1 *The Wittig reaction.*

The Wittig reaction is valuable for the homologation of substrates, whereby one or more extra carbons can be introduced. The reaction of ketones is sometimes slow; in fact all but the most reactive ketones are unreactive towards Wittig reagents. However, the reaction of aldehydes is much faster although another problem arises, in that aldehydes are difficult to prepare, unstable and prone to oxidation, in addition to the fact that relatively few are commercially available.

4.2.1.1 Mechanism of the Wittig reaction

Despite the incredible amount of research that has been undertaken into the Wittig reaction, the exact mechanism by which it proceeds is still unclear. The generally accepted mechanism is depicted in Scheme 4.1. The reaction generates a negatively charged oxygen that attacks the positively charged phosphorus atom to give an unstable four membered oxaphosphetane (**96**). The ring collapses to form two double bonds, the alkene product along with phosphine oxide.

The *cis*-oxaphosphetane is thought to be the kinetic product. If the ylide and carbonyl compound react together to give the oxaphosphetane in one step, they will do so by

approaching one another at right angles to produce a transition state whereby the oxaphosphetane will have *syn* stereochemistry (Scheme 4.2). The more stable *trans*-oxaphosphetane with two bulky groups on opposite sides of the ring can be formed when using stabilised ylides. The extra stability given to the ylide starting materials makes the reaction leading to the oxaphosphetane reversible and the reaction is therefore now thermodynamically controlled.

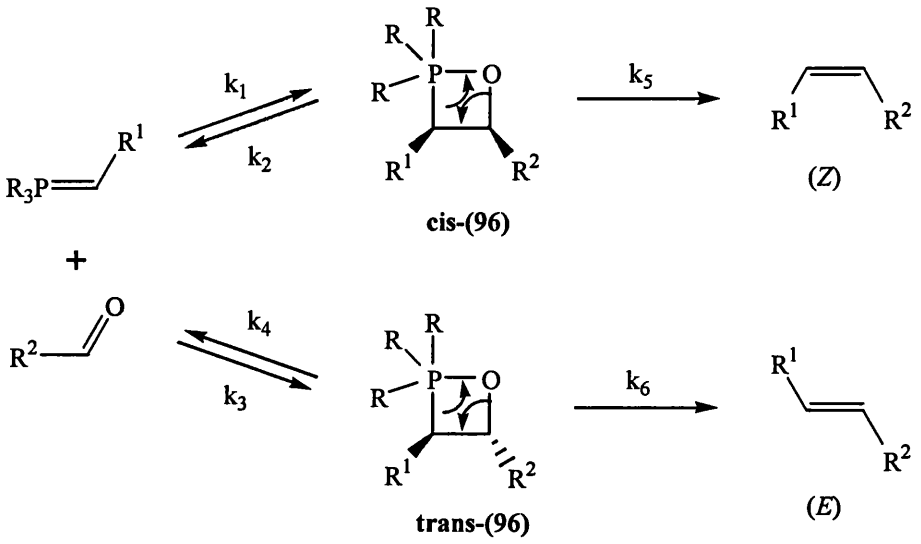

Scheme 4.1 *Mechanism of the Wittig reaction.*

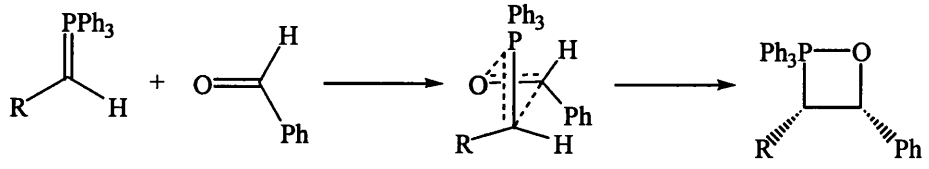

Scheme 4.2 *Formation of syn oxaphosphetane.*

4.2.2 Preparation of phosphorane ylides

There are three major routes to the preparation of ylides: deprotonation of a phosphonium salt,[7-9] transylidation[10] and Umpolung substitution.[11,12] The salt method is the most widely used method and is the process we used for generation of phosphorane ylides (section 4.5). The phosphonium salt precursor is prepared from phosphine and an alkyl halide and subsequent deprotonation generates the ylide.

4.3 Project overview

Research within the Williams group established the concept of Catalytic Electronic Activation (CAE), whereby "*temporary enhancement of the electronic nature of a functional group to a given reaction allows an otherwise unfeasible reaction to take place.*" Ketones and aldehydes are able to undergo many reactions that the corresponding alcohols are incapable of achieving. A protocol involving "borrowing hydrogen" in order to form the ketone or aldehyde from the alcohol precursor allows carbonyl derivatisation chemistry to be effected prior to the return of hydrogen. This principle was first applied to the one-pot indirect addition of nucleophiles to allylic alcohols (Scheme 4.3).[13] The unreactive allylic alcohol is temporarily converted into an electronically activated α,β-unsaturated ketone, which can undergo facile conjugate addition. The indirect addition is completed by restoration of the alcohol functional group. The oxidation and reduction steps are mediated by an aluminium catalysed MPV-Oppenauer transfer hydrogenation system. Addition of methylmalononitrile to cyclohexen-2-ol was achieved in 90% yield.

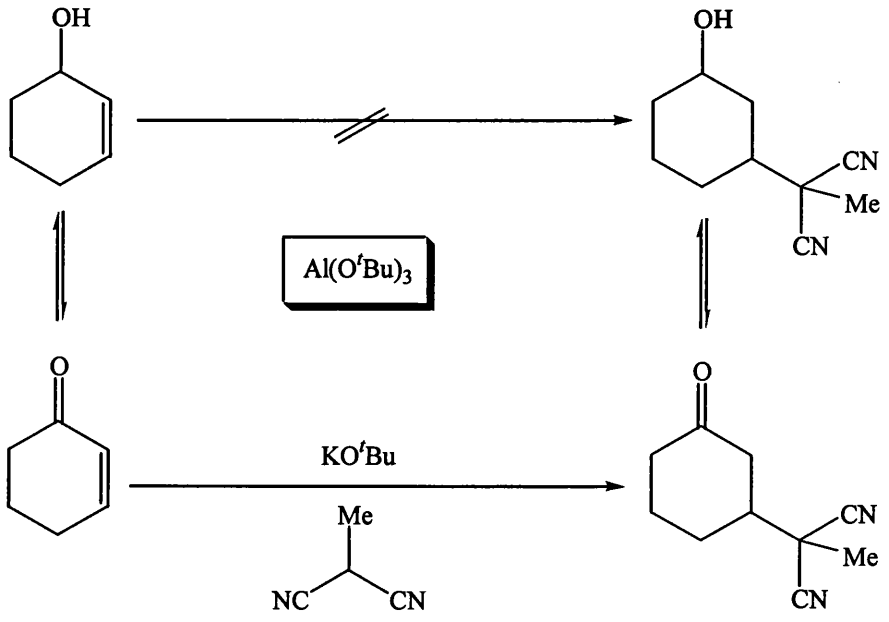

Scheme 4.3 *Indirect addition of nucleophiles to allylic alcohols.*

The concept of Catalytic Electronic Activation was extended to the indirect formation of C-C bonds from alcohols. C=C bond forming reactions readily occur with carbonyl compounds but not with alcohols. The alcohol can therefore be temporarily oxidised to the carbonyl compound allowing the facile C=C bond forming reaction to proceed affording an intermediate alkene. The hydrogen is then returned to the alkene to yield the alkane product, longer in chain length than the starting alcohol (Scheme 4.4). The one-pot sequence offers an alternative to the traditional route involving conversion of alcohol into alkyl halides, malonate substitution and subsequent decarboxylation.[6]

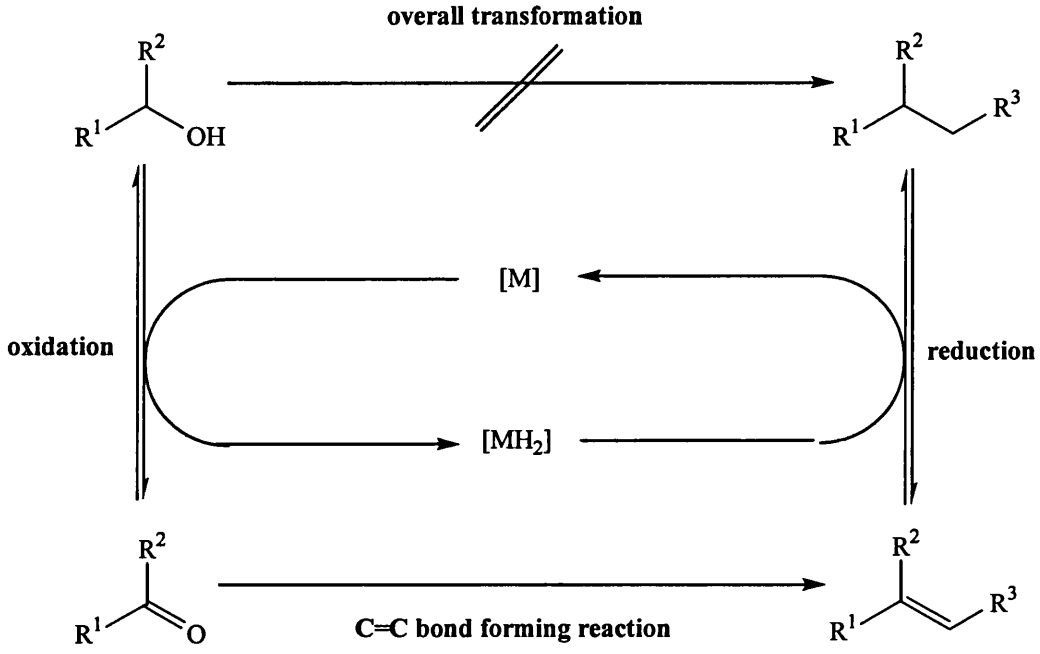

Scheme 4.4 *Indirect C-C bond formation from alcohols.*

Several of the popular methods to form the crucial C=C bond were discounted on the basis of compatibility. Thus reactions that are incompatible with alcohols e.g. Tebbe reaction and reactions that require multiple steps, e.g. Julia coupling were eliminated. The Wadsworth-Emmons (WE) and Wittig reactions looked to be the two most promising methods. Since more phosphonates are commercially available than the comparative phosphorane ylide, initially the WE reaction was employed with a modified Ishii[14] iridium system (Scheme 4.5). Although the successful isolation of alkane products was achieved, significant amounts of aldehyde and alkene intermediates remained. The system was thought to be prevented from progressing through the

domino sequence due to incompatibility of WE phosphonoacetates with the iridium catalyst causing deactivation.[15]

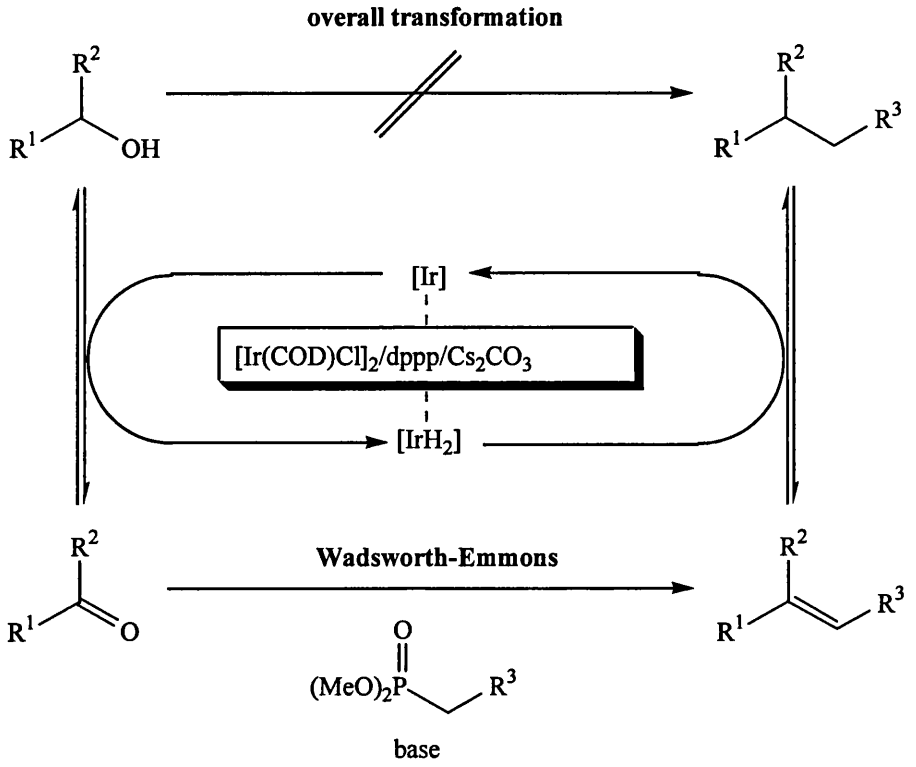

Scheme 4.5 *The envisaged domino crossover transfer hydrogenation (CTH) WE processes.*

It was established that an alternative method of C=C bond formation was required for the successful completion of the domino reaction process. Thus the Wittig reaction was employed and the iridium system was shown to be compatible with phosphorane ylides allowing the three-step transformation of alcohol substrates to alkanes[16] (Scheme 4.6). The reaction was found to be very concentration dependent; when the system is either too dilute or too concentrated the reaction is slower. Employment of benzyl alcohol and a cyano ylide with the homogeneous iridium system produced the desired alkane with 79% conversion.

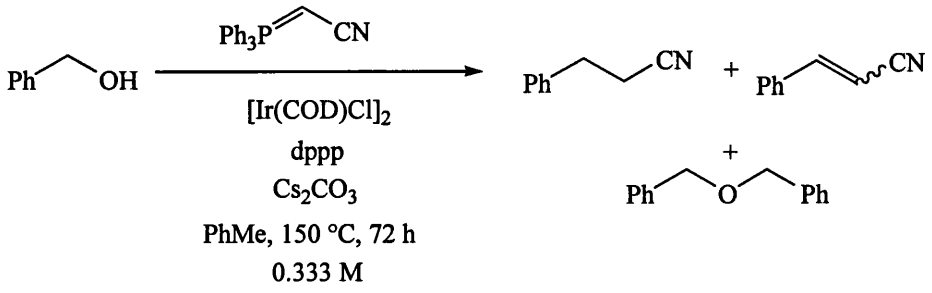

Scheme 4.6 *Three-step transformation of alcohol substrates using Ishii's iridium catalyst with phosphorane ylides.*

Despite the success of the three-step domino sequence, the iridium system had shown weaknesses. The forcing conditions required (150 °C, 72 h) led to transesterification products in addition to uncatalysed reaction pathways and hydrogen loss. The development of an improved system was required. A more active catalyst should allow the use of milder reaction conditions reducing the problems associated with high temperature.

4.4 Hydrogenations: proof of concept

4.4.1 Direct hydrogenations

The key to the three-step tandem process is the ability of the catalyst to shuttle hydrogen between substrates. As discussed in Chapter 3, all synthesised mono Ru-NHC complexes, excluding **65**, underwent reversible C-H activation upon addition of an alkene. Subsequently the alkene is reduced to form the corresponding alkane suggesting a potential for these complexes to act as hydrogenation catalysts.

Initially $RuH_2(CO)(PPh_3)_2(IMes)$ **51** was tested for its ability to hydrogenate alkenes upon direct addition of hydrogen. The experiments were performed on small scale in sealed Young's NMR tubes with 2 mol% catalyst and 1 atm H_2 (Scheme 4.7). Conversions were calculated from integrations measured from ^1H NMR spectra.

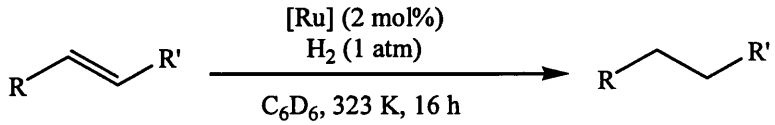

Scheme 4.7 *Hydrogenation of alkenes using **51**.*

The array of alkenes and alkynes used in the hydrogenation reactions is illustrated in Figure 4.2. H_2C=$CHSiMe_3$ was chosen as the initial test since we had already seen reduction of this alkene in the C-H activation chemistry. This alkene should be reduced easily with the assistance of the electron donating $SiMe_3$ group. As shown in Table 4.1 (Entry 1) 67% of alkene was converted into the desired alkane product. To achieve 100% conversion the NMR tube had to be degassed prior to further addition of H_2 gas followed by heating. Other alkenes were not reduced so easily. However, reduction of substrate was observed in all but two cases (Entries 4 and 8). In the case of substrate **100**, evidence for the reduced product propionamide could be seen by ^1H NMR spectroscopy. However, an accurate conversion could not be obtained due to poor solubility of acrylamide (**100**) in all NMR solvents. Upon further addition of H_2, it was only β-bromostyrene (Entry 4) that showed no evidence for reduction.

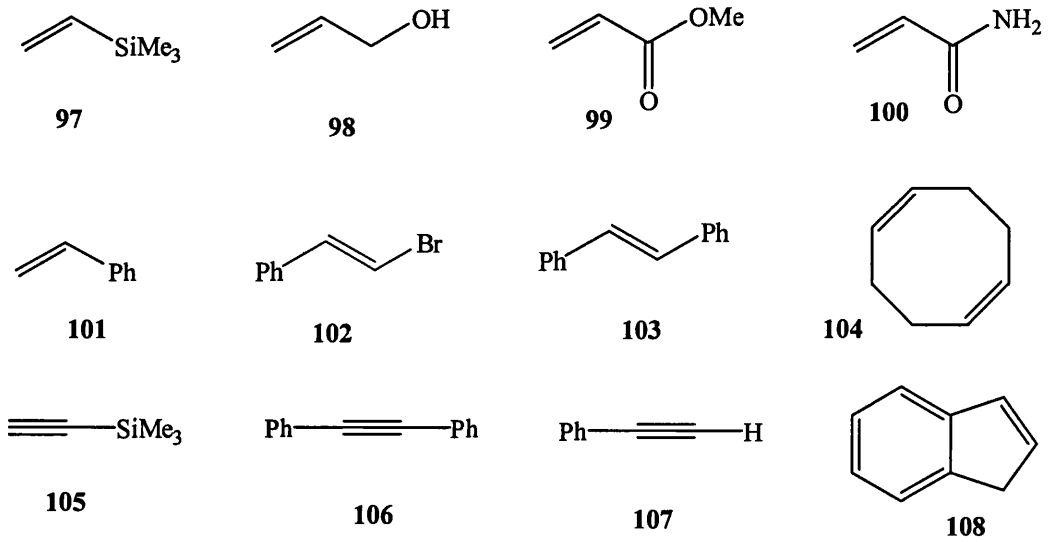

Figure 4.2 *Substrates used in hydrogenation reactions.*

Entry	Substrate	Conversion with 1 atm H_2 (%)		
		Starting material	**Partially reduced**	**Product**
1	**97**	33	-	67
2	**99**	87	-	13
3	**101**	94	-	6
4	**102**	100	-	0
5	**103**	96	-	4
6	**104**	95	5	0
7	**105**	21	50	29
8	**106**	100	0	0
9	**107**	42	49	9
10	**108**	89	-	11

Table 4.1 *Direct hydrogenations of alkenes using **51** (benzene-d_6, 2 mol%,50 °C, 16 h).*

Oxidation in addition to reduction was seen in the case of allyl alcohol, giving a mixture of products. In fact under a pressure of 1 atm H_2, reaction of any of the complexes with allyl alcohol (**98**) produced only small amounts of the desired product, 1-propanol (less than 10% conversion). The ^{1}H NMR spectrum exhibited an aldehyde resonance (δ 9.26) and it was suspected that this product was irreversibly binding to the metal centre.

Allyl alcohol was added to **57** and heated at 50 °C for 16 h. The resulting solution was concentrated and layered with hexane to grow X-ray quality crystals. The crystal structure obtained is shown below and illustrates how acrolein has coordinated to the ruthenium using the binding site of the PPh_3 ligand in addition to the hydride sites. (Figure 4.3). The complexation of aldehydes to Ru-NHC complexes was previously discussed in Chapter 3 (section 3.1.2.2). It is thought that this is one of many complexes that may form.

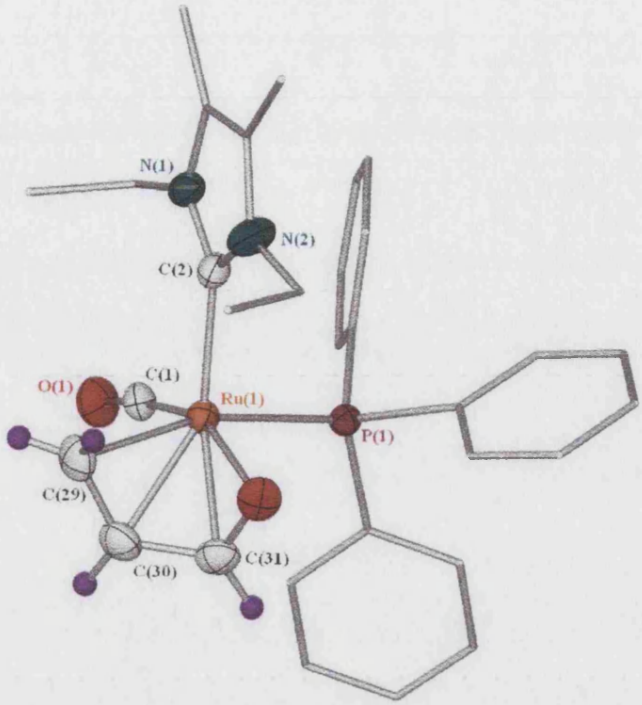

Figure 4.3 *X-ray structure of an acrolein-ruthenium complex.*

Since the surface of solution in the Young's NMR tube is small, the experimental set-up was perhaps not as efficient as it could have been. The need for further additions of H_2 gas was inconvenient and it was decided that reactions would be performed whereby high pressures of hydrogen could be applied in an autoclave. The larger vessel meant that all components in the reaction could be mixed more easily to create a homogeneous solution. Conditions were as according to Figure 4.4, and were optimised so that catalyst loadings were reduced down to 0.4 mol% in a 5 M solution of benzene and reaction temperatures were increased to 70 °C. The conversions obtained are depicted in Table 4.2. Compounds **97** and **105** were not tested since their products $H_2C{=}CHSiMe_3$ and $CH_3CH_2SiMe_3$, were too volatile to allow accurate analysis with the given experimental set-up.

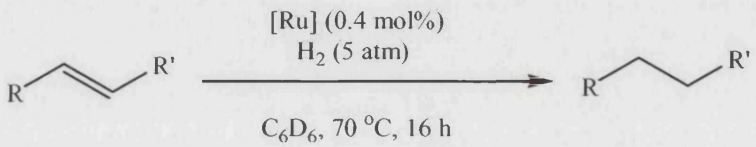

Figure 4.4 *Direct hydrogenation carried out in the autoclave with* ***51****.*

Entry	Substrate	Conversion with 5 atm H_2 (%)		
		Starting material	Partially reduced	Product
1	**98**	12	-	88
2	**100**	0	-	100
3	**101**	0	-	100
4	**102**	100	-	0
5	**103**	0	-	100
6	**104**	0	0	100
7	**105**	Overlapping	resonances	53
8	**106**	0	0	100
9	**107**	66	-	34

Table 4.2 *Direct hydrogenation carried out in the autoclave with **51** (conditions: benzene, 5 M, 0.4 mol% loading, 70 °C, 16 h).*

Higher conversions were achieved under the autoclave conditions for most of the alkenes. In many cases (Entries 2, 3, 5, 6 and 8) 100 % conversion was achieved. However, still no reduction was observed with *β*-bromostyrene (Entry 6). This is perhaps due to the electron withdrawing power of the bromide producing an electron poor, and thus unreactive alkene.

The reaction with allyl alcohol **98** (Entry 1) was clean and went in 88% conversion to 1-propanol, where previously a mixture of products had been produced (Table 4.1, Entry 2). Under the more forcing conditions with 5 atm H_2, oxidation of the alcohol does not occur and only the desired 1-propanol is produced. The reaction with methyl acrylate **99** was analysed by GC rather than ^{1}H NMR (due to the low boiling point of the desired product methyl propionate) and GC analysis revealed total consumption of methyl acrylate and the formation of two unidentified products. These products are most likely from production of methyl propionate in addition to the fully reduced product 1-propanol. The solubility issues previously encountered with acrylamide were eliminated since the substrate was totally consumed and the product was soluble in $CDCl_3$. Diphenylacetylene **106** (Entry 7) did not go to completion in the reaction time. In comparison with the terminal alkyne, phenylacetylene **107** (Entry 8), the reaction was slower. This is most likely due to the steric bulk of the added phenyl group. In addition,

the alkyne **106** is less electron rich than the terminal alkyne. Reduction of indene **108** (Entry 9) also did not go to completion. This is most likely due to the steric bulk of this substrate. Alkene binding is probably difficult slowing the reduction process down. In these reactions, $RuH_2(CO)(PPh_3)_2$(IMes) **51** has shown itself to be an effective direct hydrogenation catalyst. The next step was to test if it was capable of transfer hydrogenations.

4.4.2 Transfer hydrogenations

The hydrogenations that had previously been attempted *via* direct addition of hydrogen were repeated in reactions with 2-propanol (IPA) as the hydrogen donor to identify if **51** could be utilised as a transfer hydrogenation catalyst as well as a direct hydrogenation catalyst. 2 mol% of **51** with substrate and IPA was heated in benzene-d_6 at 70 °C for 16 h (Scheme 4.8). Initially two equivalents of IPA to substrate were used but it was found that better conversions were achieved upon addition of a total of five equivalents of IPA. The conversions obtained are displayed in Table 4.3.

100% conversion into alkane was obtained in the case of H_2C=CHSiMe_3 (Entry 1) proving that **51** functions well as a transfer hydrogenation catalyst. Problems arose again with the allyl alcohol where evidence of aldehyde formation could be seen in the ^{1}H NMR spectrum of the reaction mixture. Reaction with methyl acrylate produced too many products to identify by ^{1}H NMR spectroscopy. In the reduction of acrylamide, the product could be detected *via* the appearance of a quartet (δ 1.98) and a triplet (δ 0.92) in the ^{1}H NMR spectrum. However, as with the direct hydrogenation reaction, poor substrate solubility prevented calculation of an accurate conversion. Not surprisingly, no reduction of the vinyl bromide **102** was observed. Reduction of styrene was good compared to stilbene. This presumably reflects the increased ability of styrene to bind to ruthenium due to decreased steric bulk.

Alkyne conversions (Entries 6, 7 and 8) were poor. For Entry 7, conversion was calculated from the IPA to acetone (ratio 13:1) since the ^{1}H NMR resonances of diphenylacetylene and stilbene overlap. No alkane was detected.

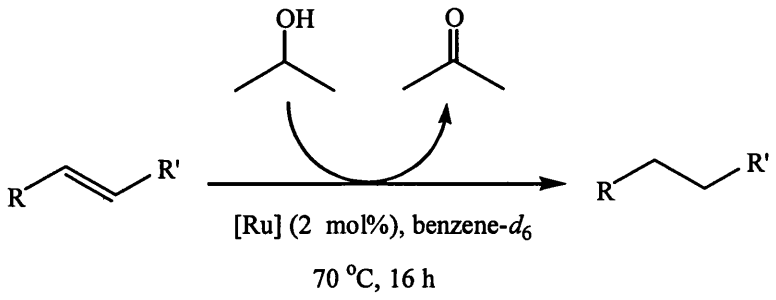

Scheme 4.8 *$RuH_2(CO)(PPh_3)_2(IMes)$ (51) catalysed transfer hydrogenation of alkenes with IPA.*

Entry	Substrate	Conversion with five equivalents IPA (%)		
		Starting material	Partially reduced	Product
1	97	0	-	100
2	101	31	-	69
3	102	100	-	0
4	103	74	-	26
5	104	0	74	26
6	105	100	0	0
7	106	93	7	0
8	107	90	10	0
9	108	93	-	7

Table 4.3 *Transfer hydrogenations of alkenes using 51 (conditions: benzene-d_6, 2 mol%, 5 equiv. IPA, 70 °C, 16 h).*

4.4.3 Crossover transfer hydrogenations (CTH)

Crossover transfer hydrogenations were carried out to hydrogenate the C=C double bond of the α,β-unsaturated ester benzyl cinnamate (**109**). Benzyl alcohol (**110**) and *sec*-phenethyl alcohol (**111**) were used as hydrogen donors respectively. The substrates were heated together at 70 °C in benzene-d_6 with 5 mol% of **51** (Scheme 4.9). With benzyl alcohol, only 45% of benzyl dihydrocinnamate (**112**) could be observed and very little aldehyde was present. The hydride region revealed that a new hydride species had formed (δ -16.48, d, J_{HH} = 23.4 Hz). It became apparent that once the aldehyde is

formed it complexes to the ruthenium, concomitantly deactivating the catalyst. This did not bode well for the indirect Wittig process where an intermediate aldehyde would be produced. However, the Wittig reaction is rapid so it was hoped that the aldehyde would be removed rapidly from the system allowing the tandem cycle to proceed. To validate the process where aldehyde is not present, *sec*-phenethylalcohol was used under the same conditions and 100% conversion of both alkene and alcohol starting materials was observed.

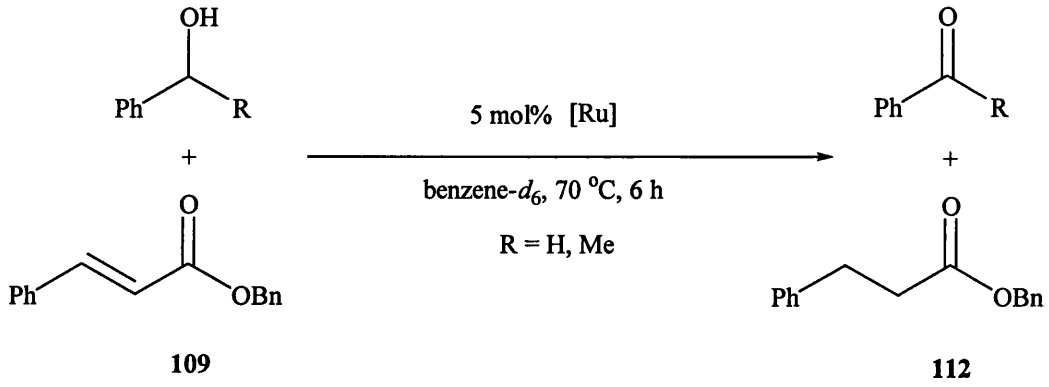

109 **112**

Scheme 4.9 *Crossover transfer hydrogenations (CTHs).*

The success of the transfer hydrogenation and crossover transfer hydrogenation reactions is crucial for the three-step tandem process to succeed. With the results obtained, the transformation illustrated in Scheme 4.10 could be envisaged.

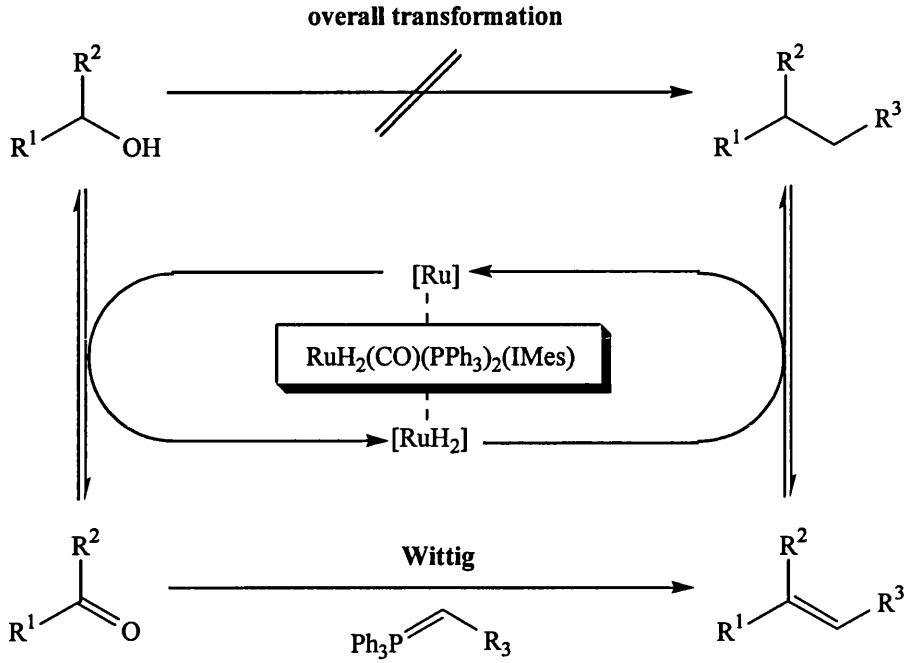

Scheme 4.10 *Three-step domino process envisaged for the ruthenium catalysts.*

4.5 Preparation of phosphorane ylides

4.5.1 Phosphonium salt preparation

The salts required for the synthesis of the phosphorane ylides were prepared from reaction of triphenylphosphine and the relevant commercially available alkyl halide precursor (Scheme 4.11). Salts **113-116** were obtained in good yields (Table 4.4)

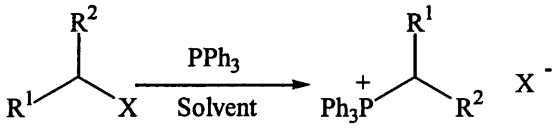

Scheme 4.11 *Preparation of phosphonium salt precursors.*

Entry	Compound Number	Salt			Yield (%)
		R^1	R^2	X^-	
1	113	CN	H	Br^-	93
2	114	CO_2Bn	H	Br^-	90
3	115	$CO_2{}^tBu$	H	Br^-	95
4	116	$C(O)CO_2Et$	H	Br^-	*a*

[a] A hygroscopic residue was obtained. The residue was carried through to the next step without further purification.

Table 4.4 *Preparation of phosphonium salt precursors.*

4.5.2 Phosphorane ylide preparation

Deprotonations of the phosphonium salts yielded the desired phosphonium ylides **117-120** in good yields (Scheme 4.12, Table 4.5).

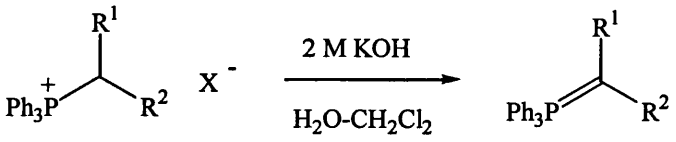

Scheme 4.12 *Preparation of phosphorane ylides.*

Entry	Compound number	Ylide			Yield (%)
		R^1	R^2	X^-	
1	117	CN	H	Br^-	98
2	118	CO_2Bn	H	Br^-	97
3	119	$CO_2{}^tBu$	H	Br^-	51
4	120	$C(O)CO_2Et$	H	Br^-	33

Table 4.5 *Preparation of phosphorane ylides.*

In addition, (triphenylphosphoranylidene)acetone (**121**), N,N-dimethyl (triphenylphosphoranylidene)acetamide (**122**) and N-methyl,N-methoxy

(triphenylphosphoranylidene)acetamide (**123**) had been previously synthesised in the group.

4.6 Indirect Wittig reactions

4.6.1 Initial results

Reactions were set up in a Radley carousel synthesiser according to the conditions depicted in Scheme 4.13. $RuH_2(CO)(PPh_3)_2(IMes)$ **51** was compared with the non-NHC complexes $RuH_2(CO)(PPh_3)_3$ **52** and $RuH_2(PPh_3)_4$. The small quantity of sacrificial alkene was added in order to remove the initial hydrogen from the catalyst to allow dehydrogenation of the alcohol to occur (see Scheme 3.6) The reactions were stirred at 80 °C for 24 h and the results obtained are listed in Table 4.6.

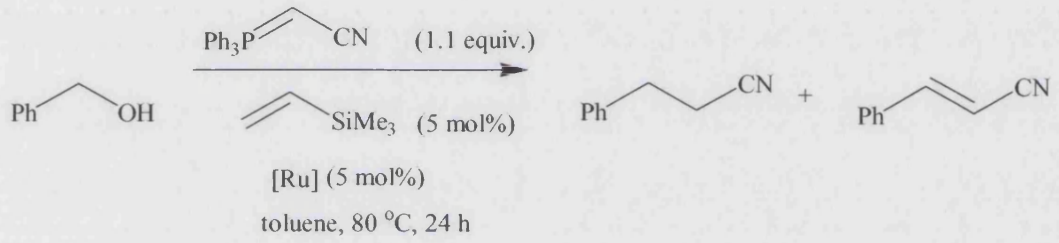

Scheme 4.13 *Indirect Wittig reaction employing [Ru].*

Entry	Catalyst	Total Conversion (%)	Alkene (%)	Alkane (%)
1	$RuH_2(PPh_3)_4$	51	13	38
2	$RuH_2(CO)(PPh_3)_3$	50	1	49
3	$RuH_2(CO)(PPh_3)_3$(IMes)	87	6	81

Table 4.6 *Indirect Wittig reaction employing [Ru] (conditions: 1 mL, toluene, 5 mol% loading, 80 °C, 24 h).*

The results demonstrate that the introduction of a NHC into the complex improved the reactivity (Entry 3). $RuH_2(CO)(PPh_3)_3$(IMes) (**51**) gave an 81% conversion into the

desired alkane product. Comparing Entries 1 and 2, the substitution of a phosphine ligand for a carbonyl does not affect the alcohol oxidation step since total conversion from the alcohol is essentially the same. However, in the case of Entry 1, dehydrogenation (loss of H_2) is faster.

Already a great improvement in reaction time and temperature had been achieved from the previous iridium system used (150 °C, 72 h).[15] The presence of the NHC ligand clearly improved reactivity and so it was important to test all of the Ru-NHC complexes that had been developed. Both catalytic steps of the tandem reaction were investigated individually and results plotted so that the reactivity of each complex synthesised (including **64** and **65** prepared by other members of the group) could be compared.

4.6.2 Oxidation of 4-fluoro-α-methylbenzylalcohol (124) with acetone

The first requirement of the one-pot Wittig reaction is the oxidation of an alcohol. Oxidation of a series of secondary alcohols into ketones by transfer hydrogenation with **51** using acetone as a hydrogen acceptor has been investigated by Burling *et al.*[17] 4-Fluoro-α-methylbenzylalcohol (**124**) was shown to be readily oxidised to the corresponding ketone reaching the equilibrium position of 86% after 5 h. This alcohol was chosen as the substrate to compare complex reactivity.

Treatment of 2 mol% ruthenium-NHC pre-catalyst with five equivalents of acetone to the substrate in 0.6 mL benzene-d_6 at 50 °C was monitored by ^{1}H NMR spectroscopy over 14 h. The conversions determined from the ^{1}H NMR integrals are plotted against time on the graph shown below (Figure 4.5).

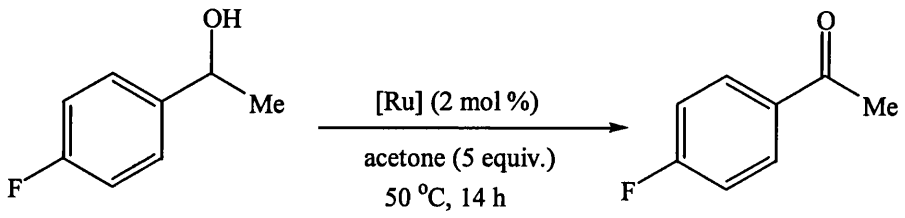

Scheme 4.14 *Oxidation of 4-fluoro-α-methylbenzylalcohol (124) with acetone.*

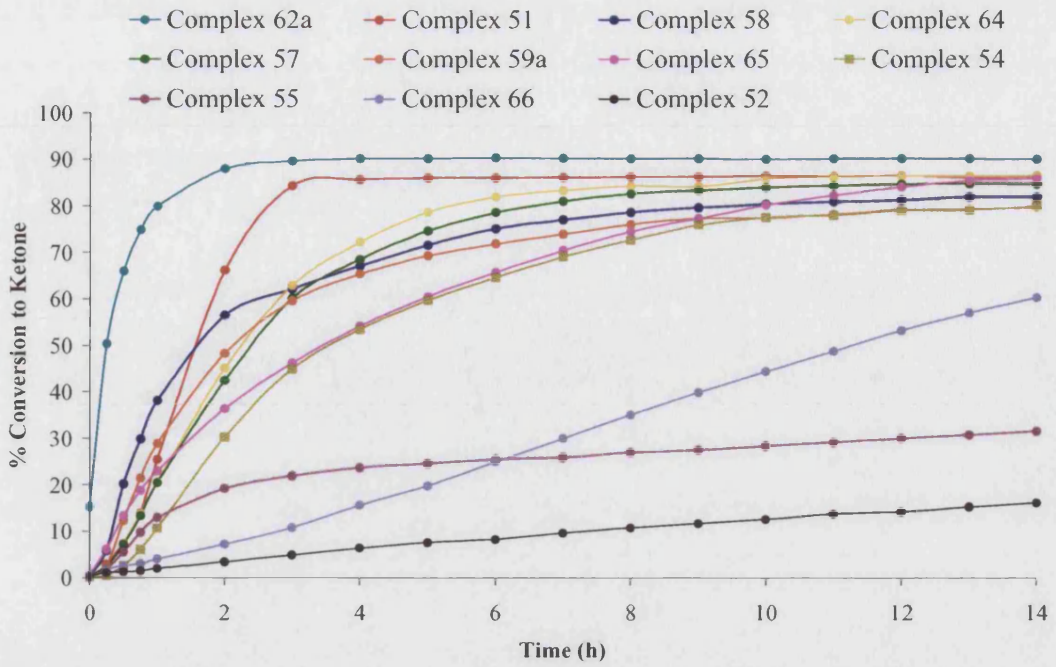

Figure 4.5 *Oxidation of 4-fluoro-α-methylbenzylalcohol (**124**) with acetone (conditions: benzene-d6, 2 mol% [Ru], 323 K, 14 h).*

The plot illustrates clearly how the addition of NHC ligands vastly improves the rate of transformation. The one non-NHC complex employed ($RuH_2(CO)(PPh_3)_3$) **52** only achieves 16% conversion into ketone product after 14 h. All complexes show their ability to be used as transfer hydrogenation catalysts. The range of mono Ru-NHC complexes all reach a similar end point after 14 h, although some reach their equilibrium points faster than others. **51** remains an excellent catalyst; however, the most striking is **62a** which reaches 88% conversion to ketone after just 2 h. This can clearly be compared in this reaction to **58** where the backbone methyls are absent. After just 1 h, **62a** has converted 80% of alcohol to the corresponding ketone compared to **58** where only 38% has been converted. The significant difference between **62a** and all other complexes may be related to C-H activation. Chapters 2 and 3 describe the ease at which C-H activation of **61** occurs. In fact, it is the only complex that spontaneously C-H activates in the absence of a hydrogen acceptor.

65 and **54** have different shaped curves to the other mono-NHC complexes. This may be because these are the two complexes that do not C-H activate the NHC upon addition of

a hydrogen acceptor. Although **54** was seen to undergo orthometallation of a PPh_3 ligand, this process was slow (see Chapter 3). In fact, unlike the other ruthenium-NHC complexes, no C-H insertion product was observed in any of the spectra recorded in the 14 h time period. Only the starting dihydride complex could be detected in the ^1H NMR spectrum. These results indicate that C-H activation of the complex is not essential for the transfer hydrogenation reaction, although may improve reactivity. The complexes that do undergo C-H activation have faster rate curves than for **65** and **54**.

Inspection of the hydride regions of the ^1H NMR spectra at the end of the 14 h time period revealed the state of the catalysts. Only the complexes with NHC ligands of aryl character, namely **51** and **59a**, showed some decomposition to $RuH_2(CO)(PPh_3)_3$.

The bis-carbene complexes **55** and **66** display lower reactivities than their corresponding mono Ru-NHC complexes **54** and **64** respectively. The lower activity of bis-carbene complexes has also been observed by others.

4.6.3 Reduction of trimethylvinylsilane (97)

The last requirement of the one-pot Wittig reaction is the reduction of an alkene. Previous transfer hydrogenation results using **51** (Section 4.4.2) showed reduction of $H_2C{=}CHSiMe_3$ with IPA to be rapid. The transfer hydrogenations in Section 4.4.2 were performed at 70 °C but for a comparison with the alcohol oxidation step the temperature was reduced to 50 °C.

Treatment of 2 mol% [Ru] with five equivalents of IPA to the substrate was monitored by ^1H NMR spectroscopy in benzene-d_6 over a period of 14 h at 50 °C. The conversions measured from the ^1H NMR spectra were plotted against time as shown below (Figure 4.6). Integrations of the CH and CH_2 groups were taken for the alkene and alkane respectively.

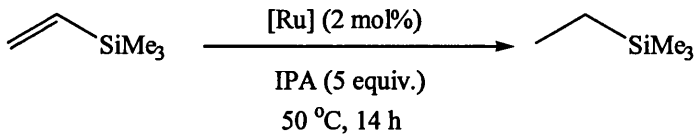

Scheme 4.15 *Reduction of trimethylvinylsilane (97).*

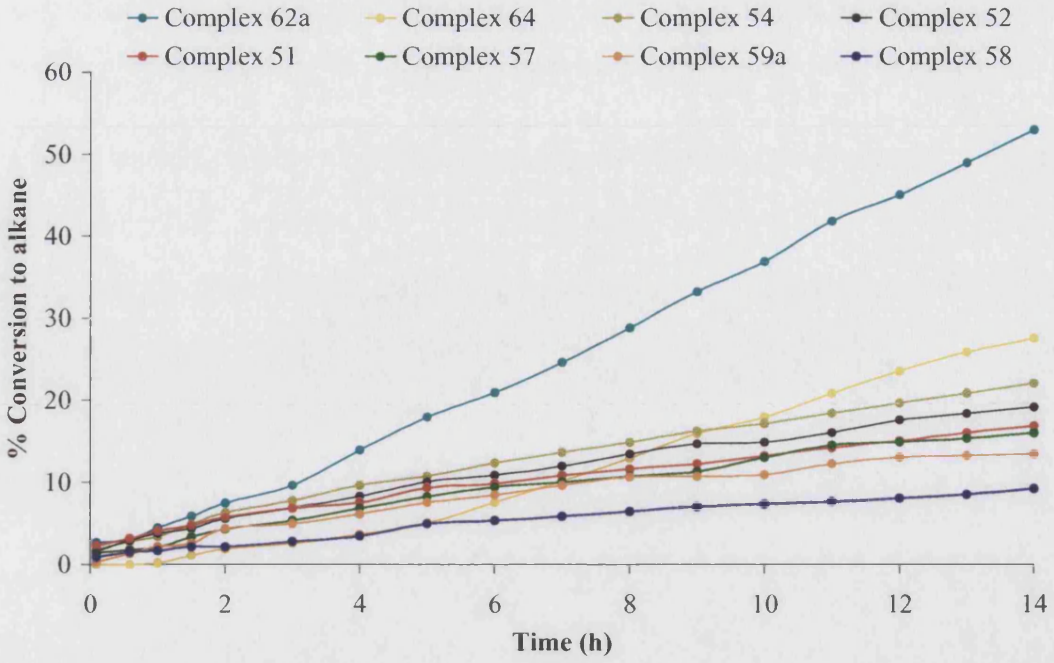

Figure 4.6 *Reduction of trimethylvinylsilane with IPA (2 mol% ruthenium catalyst, 50 °C, 14 h).*

The initial point to notice is how the graph illustrates that alkene reduction is a slower step than alcohol oxidation. With alcohol oxidation, most complexes had converted 80-90% to ketone after just 8 h. Reduction of $H_2C{=}CHSiMe_3$ to the corresponding alkane had gone to a maximum of 53% but only after 14 h.

62a performs much better than all of the other tested catalysts again. This result paired with the alcohol oxidation result indicates that this complex should catalyse the one-pot tandem process more efficiently than **51**.

There is no significant difference between the other catalysts. The bis-Ru-NHC, mono-Ru-NHC complexes and the catalyst omitting an NHC ligand (**52**) perform much the same as catalysts for alkene transfer hydrogenation.

The hydrogenations were repeated under the same conditions but with an elevated temperature of 70 °C to obtain a greater disparity in the results. Rate curves were recorded as illustrated in Figure 4.7.

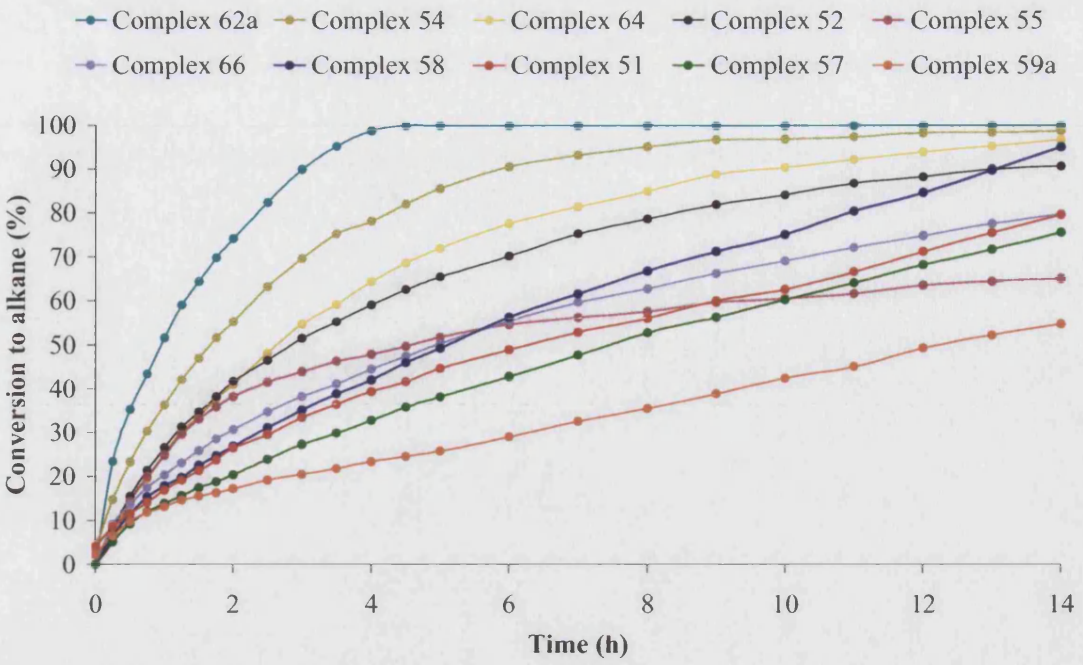

Figure 4.7 *Reduction of trimethylvinylsilane with IPA (2 mol% ruthenium catalyst, 70 °C, 14 h).*

After just 4 h, **62a** had converted 100% of H_2C=CHSiMe$_3$ into the corresponding alkane. Unlike the alcohol oxidation reaction, surprisingly the Ru-NHC complexes **54** and **64** bearing the ICy and IMe$_4$ ligands, which preferentially undergo C-H activation of the phosphine ligand rather than the carbene, are very efficient catalysts for this process. In addition the non-NHC complex **52** also performs better than most of the complexes with NHC ligands. These results were very surprising but nonetheless, all complexes did reduce alkene **97** and were tested in further reactions for their potential application to the three-step tandem process.

4.6.4 Crossover transfer hydrogenations (CTH)

All complexes were also tested in the crossover transfer hydrogenations carried out previously with **51**. The C=C double bond of the α,β-unsaturated ester benzyl cinnamate (**109**) was hydrogenated with benzyl alcohol (**110**) and *sec*-phenethyl alcohol (**111**) respectively as hydrogen donors. The substrates were heated together at 70 °C in benzene-d_6 with 5 mol% of each of the prepared ruthenium catalysts (Scheme 4.16). The results obtained for the two reactions are shown in Table 4.7. The conversions in both cases were calculated from the **109** to benzyl dihydrocinnamate (**112**) because once

the aldehyde is formed it coordinates to the ruthenium, concomitantly deactivating the catalyst.

Table 4.7 illustrates that when **110** was used as substrate, irreversible complexation of benzaldehyde and thus deactivation of the catalyst poses a problem for most of the complexes. However **62a** still achieves high conversion. Looking at the hydride region of the ^{1}H NMR spectra recorded at the end of the reaction time revealed the formation of new hydride species from all complexes, including **62a**. It may be that **62a** performs the CTH before complexation occurs. When the reaction of **62a** with benzyl alcohol was heated for a further 20 h), no additional alkane product was produced, proving that the catalyst had indeed been deactivated at this point.

When the hydrogen donor substrate was changed to *sec*-phenethyl alcohol, conversions of alkene to alkane were generally improved. Surprisingly **62a** converted less alkene than other complexes, although a good conversion was still obtained. At the end of the reactions, new hydride complexes were observed in the ^{1}H NMR spectra of all complexes. However, in all cases except for **51** and **62a** some starting dihydride complex was still present. This suggests that complexation of the carbonyl species and subsequent deactivation of **51** and **62a** is more rapid than with the other complexes, reflecting their increased reactivity.

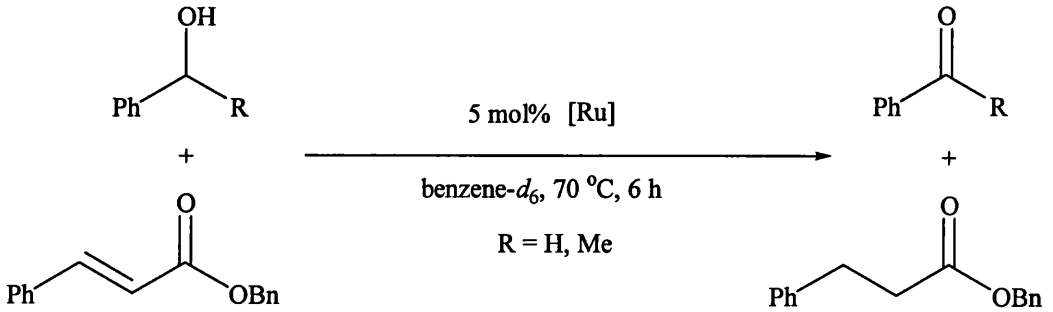

Scheme 4.16 *CTH of benzyl cinnamate with benzyl alcohol (110) and sec-phenethyl alcohol (111).*

Entry	Catalyst precursor	Conversion to 112 (%) R=H	Conversion to 112 (%) R=Me
1	$RuH_2(CO)(PPh_3)_3$	46	83
2	$RuH_2(CO)(PPh_3)_2$**(IMes)**	45	100
3	$RuH_2(CO)(PPh_3)_2$**(IMe_4)**	28	100
4	$RuH_2(CO)(PPh_3)_2$**(IEt_2Me_2)**	46	98
5	$RuH(CO)(PPh_3)_2$**(I^iPrMe_2')**	80	78
6	$RuH_2(CO)(PPh_3)_2$**(I^iPr)**	44	92
7	$RuH_2(CO)(PPh_3)_2$**(I*)**	38	93
8	$RuH_2(CO)(PPh_3)_2$**(ICy)**	32	71

Table 4.7 *Conversion of CTH reactions.*

4.7 One-pot tandem process

4.7.1 Activity of Ru-NHC complexes

Now that the crossover transfer hydrogenations of each of the individual catalysts had been examined, the Ru-NHC complexes were compared in the overall one-pot tandem process. Reactions were set up as before (Scheme 4.13) using a Fisher carousel synthesiser with 5 mol% [Ru] in 1 mL toluene at 80 °C for 24 h. The results obtained are presented in Table 4.8.

Both bis- and mono- Ru-NHC complexes gave significantly higher conversions than the complex **52** lacking an NHC ligand (Entry 1). With the exception of **65**, the complexes containing alkyl NHCs in general gave conversions of about 10% higher than the two NHC-complexes containing aromatic groups ($RuH_2(CO)(PPh_3)_2$(IMes) **51** and $RuH_2(CO)(PPh_3)_2$(I*) **59a**). This is probably due to the stability of the complexes; those containing the aromatic NHCs have been shown to degrade over time and form **52**, which is a less reactive catalyst. The lower conversion obtained using **65** (Entry 4) as a catalyst may be a reflection of the inability for the complex to C-H activate. Complex **62a** containing the C-H activated $I^iPr_2Me_2$ carbene ligand afforded the highest conversion with the desired alkane product being the only detectable species in the ^1H NMR spectrum.

Complex **62a** repeatedly gave the best results so it was thought perhaps the activation of the carbene played a part. The mono dihydride complex **61** was prepared and compared to the activated complex but no difference in activity was observed. As discussed in Chapter 3, C-H activation of **61** is rapid upon heating and hence it became apparent that it does not make a difference if starting from the dihydride or activated complex.

Entry	Catalyst	Total Conversion (%)	Alkene (%)	Alkane (%)
1	$RuH_2(CO)(PPh_3)_3$	50	1	49
2	$RuH_2(CO)(PPh_3)_3$**(IMes)**	87	6	81
3	$RuH_2(CO)(PPh_3)_2$**(I*)**	83	4	79
4	$RuH_2(CO)(PPh_3)_2$**(I^nPr)**	81	6	75
5	$RuH_2(CO)(PPh_3)_2$**(IMe_4)**	92	4	88
6	$RuH_2(CO)(PPh_3)_2$**(IEt_2Me_2)**	92	2	90
7	$RuH_2(CO)(PPh_3)_2$**(ICy)**	96	7	89
8	$RuH_2(CO)(PPh_3)_2$**(I^iPr)**	91	4	87
9	$RuH(CO)(PPh_3)_2$**($I^iPr_2Me_2'$)**	100	0	100
10	$RuH_2(CO)(PPh_3)$**(IMe_4)$_2$**	83	4	79
11	$RuH_2(CO)(PPh_3)$**(ICy)$_2$**	95	8	87

Table 4.8 *Indirect Wittig reaction catalysed by a range of Ru-NHC complexes (conditions: 1 mL toluene, 5 mol% loading, 80 °C, 24 h).*

Reactions were also compared with and without the addition of H_2C=$CHSiMe_3$ **97** and results did not vary. Therefore the addition of "sacrificial" alkene was eliminated in all further reactions.

The reaction times and temperatures were gradually reduced. It became clear that the reaction catalysed by **62a** had reached completion long before the 24 h reaction time that had been used previously. Conditions were optimised according to Scheme 4.17. Catalyst **62a** achieved high conversions even at these decreased temperatures (70 °C) and times (3 h) (Table 4.9). **51** proved to be the next best catalyst surpassing the

remaining alkyl substituted Ru-NHC complexes. The rate of reaction of **51** appears to be faster than all alkyl substituted NHCs (except **62a**) although its stability over time is poor. The bis Ru-NHC complexes **55** and **66** (Entries 10 and 11) and **65** (Entry 2) gave low conversions, only marginally surpassing that of **52** (Entry 1).

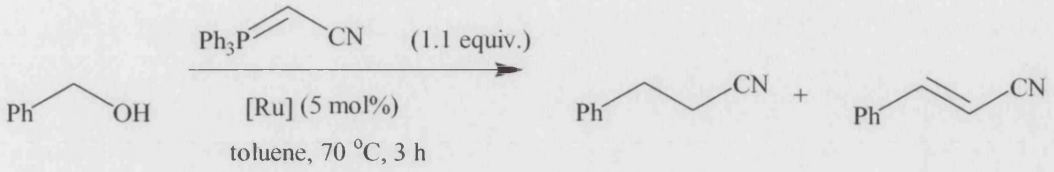

Scheme 4.17 *One-pot Wittig reaction run under conditions of reduced temperature (70 °C) and reaction time (3 h).*

Entry	Catalyst	Total Conversion (%)	Alkene (%)	Alkane (%)
1	$RuH_2(CO)(PPh_3)_3$	6	2	4
2	$RuH_2(CO)(PPh_3)_2$**(I^nPr)**	13	4	9
3	$RuH_2(CO)(PPh_3)_2$**(IMe_4)**	20	4	16
4	$RuH_2(CO)(PPh_3)_2$**(ICy)**	25	3	22
5	$RuH_2(CO)(PPh_3)_2$**(I*)**	27	4	23
6	$RuH_2(CO)(PPh_3)_2$**(I^iPr)**	27	3	24
7	$RuH_2(CO)(PPh_3)_2$**(IEt_2Me_2)**	29	2	26
8	$RuH_2(CO)(PPh_3)_2$**(IMes)**	56	3	53
9	$RuH(CO)(PPh_3)_2$**($I^iPr_2Me_2'$)**	99	2	97
10	$RuH_2(CO)(PPh_3)$**(IMe_4)$_2$**	19	4	15
11	$RuH_2(CO)(PPh_3)$**(ICy)$_2$**	6	3	3

Table 4.9 *One-pot Wittig reaction run under conditions of reduced temperature (70 °C) and reaction time (3 h).*

4.7.2 *In situ* preparation of Ru-NHC catalysts

To avoid the isolation of the Ru-NHC catalysts, reactions were set up in attempt to synthesise the catalysts *in situ* in the one-pot tandem process. The conditions are illustrated in Scheme 4.18. The reactions were heated for 20 h at 70 °C, the reaction conditions used to synthesise the alkyl Ru-NHC complexes. Upon addition of 5 mol% loading of the free carbenes (1:1 **52**:NHC), improved conversions were achieved in comparison to addition of no carbene (Table 4.10). Addition of 5 mol% IMes gave parallel results to the standard (Entry 1). Synthesis of **51** required heating for two weeks at 70 °C for the total consumption of **52**. Thus in the 20 h reaction period it is likely that only trace amounts of the catalyst **51** were present, resulting in negligible improvement in conversion. Addition of 5 mol% $I^iIPr_2Me_2$ (Entry 8) achieved good conversions to the desired alkane product. This reflects the rapid complexation of the carbene to the ruthenium in addition to the reactivity of the catalyst once formed. Only trace amounts of the starting benzyl alcohol (1%) and intermediate alkene (2%) could be detected by ^1H NMR spectroscopy. **59a** and **57** gave moderate conversions. Complexation of these carbenes is rapid but they are less active catalysts.

Increased loadings (15 mol%, 1:3 **52**:NHC) of NHCs had a detrimental affect in comparison to the presence of 5 mol% carbene. This is presumably due to the formation of the bis- and tris- carbene complexes which we have found to be less active catalysts.

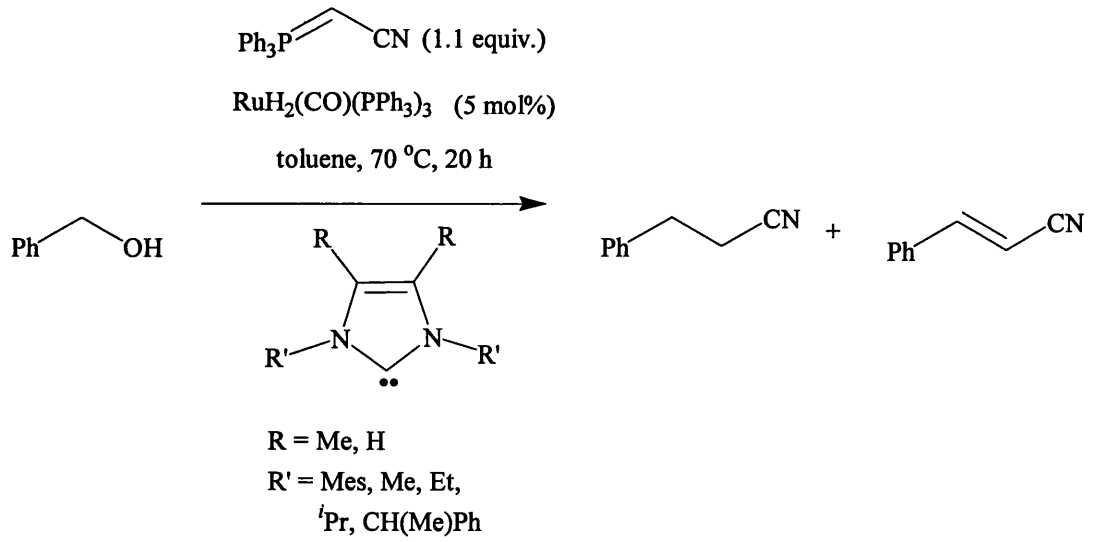

Scheme 4.18 *In situ preparation of Ru-NHC complexes.*

Entry	Catalyst precursor	Additive	Loading (mol %)	Total Conversion (%)	Alkene (%)	Alkane (%)
1	$RuH_2(CO)(PPh_3)_3$	-	-	5	2	3
2	$RuH_2(CO)(PPh_3)_3$	**IMes**	5	6	1	5
3	$RuH_2(CO)(PPh_3)_3$	**IMes**	15	4	0	4
4	$RuH_2(CO)(PPh_3)_3$	**I***	5	21	2	19
5	$RuH_2(CO)(PPh_3)_3$	**I***	15	20	3	17
6	$RuH_2(CO)(PPh_3)_3$	**IEt_2Me_2**	5	41	5	36
7	$RuH_2(CO)(PPh_3)_3$	**IEt_2Me_2**	15	9	2	7
8	$RuH_2(CO)(PPh_3)_3$	**$I^iPr_2Me_2$**	5	81	2	79
9	$RuH_2(CO)(PPh_3)_3$	**$I^iPr_2Me_2$**	15	42	2	40

Table 4.10 *In situ preparation of Ru-NHC complexes in the one-pot Wittig reaction (conditions: 1 mL toluene, 5 mol% **52**, 5-15 mol% NHC, 70 °C, 20 h).*

4.7.3 Effect upon variation of ylide

62a had now been established as a very effective catalyst in the one-pot process using the cyano ylide $Ph_3P{=}CHCN$ (**117**). To establish whether the catalyst could be applied to other systems, a range of phosphorane ylides was synthesised and tested with **62a** (Scheme 4.19, Table 4.11). Successful synthesis of alkane products with varied functionality would result in the accessibility to a wide range of chemistry. While the cyano ylide proved by far to be the most successful reagent for this particular system, reasonable conversions were obtained with other ylides . In the case of the acetone ylide **121** (Entry 2) and the pyruvate ylide **120** (Entry 5) only starting material could be detected by ^{1}H NMR spectroscopy. In these cases it was suspected that the ylides were irreversibly complexing to the ruthenium. Treatment of **62a** with ylides **117-123** in benzene-d_6 at 70 °C for 3 h confirmed the formation of new hydride species. An example is shown in Figure 4.8 upon reaction of **62a** with the Weinreb ylide **123**, which leads to the complete loss of hydride signals from **62a** and formation of a new unidentified hydride containing product at δ -16.8. In the case of the cyano ylide **117**, however, only signals for **62a** were observed in the ^{1}H NMR spectrum, with no formation of high field doublets as seen upon addition of other ylides. **117** is the only

ylide of the ones tested that was insoluble in benzene and toluene. It is possible that this slows the rate of complexation to the ruthenium catalyst and allows for the reaction to take place before deactivation occurs. It seems that the one-pot tandem process becomes a competing reaction between rate of reaction versus complexation of the ylide and subsequent deactivation of the catalyst. The deactivated species were not identified.

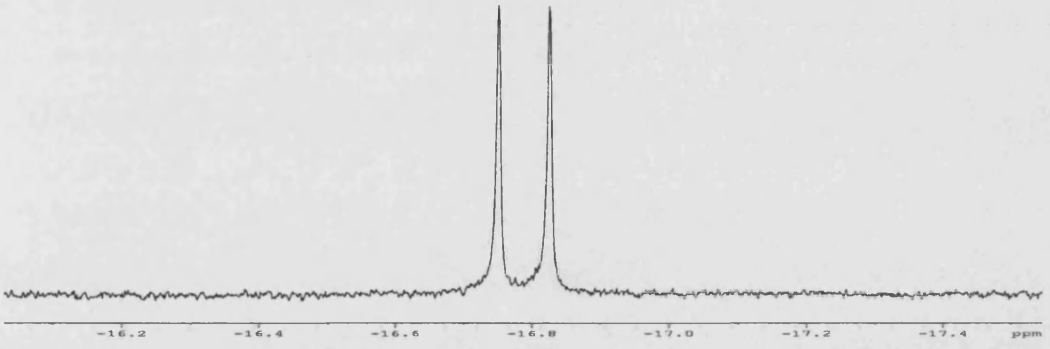

Figure 4.8 *^{1}H NMR (benzene-d_6, 300 MHz, 298 K) showing the formation of a new hydride species upon complexation of the Weinreb ylide to* ***62a****.*

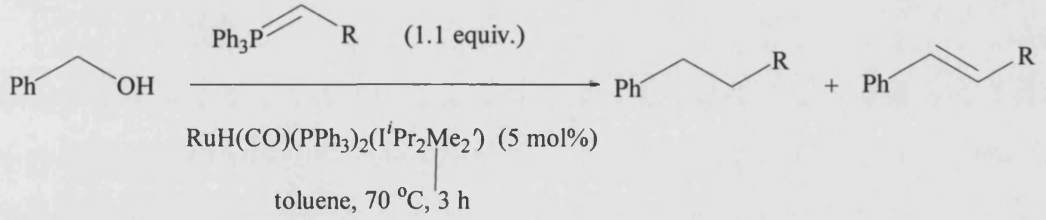

Scheme 4.19 *One-pot Wittig reaction using* ***62a*** *with a range of ylides.*

Entry	Ylide		Total Conversion (%)	Alkene (%)	Alkane (%)
1	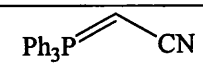	**117**	99	2	97
2	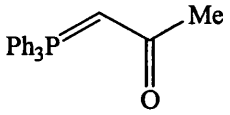	**121**	0	0	0
3	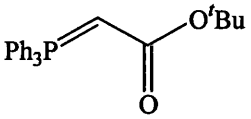	**119**	53	8	45
4	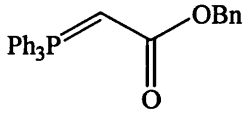	**118**	33	3	30
5	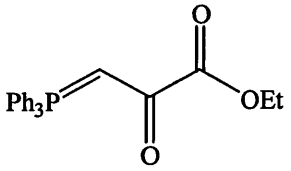	**120**	0	0	0
6	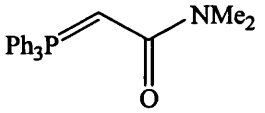	**122**	37	15	22
7	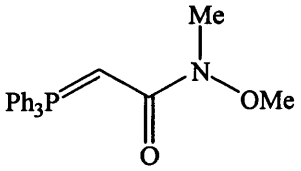	**123**	23	15	8

Table 4.11 *Range of ylides utilised in the one-pot tandem process with benzyl alcohol and* ***62a*** *(conditions: 1 mL toluene, 5 mol% loading, 70 °C, 3h).*

51 was also used to catalyse the process with the range of ylides. Although catalyst **62a** is far superior when employing the cyano ylide (99% compared to 56% with **62a** and **51** respectively), it was anticipated that **51** may give better conversions with other ylides since complexation of the ylide to **51** may be slower than to **62a**. It has already been shown that deactivation of **51** is slower than **62a** in the crossover transfer hydrogenation of benzyl cinnamate with *sec*-phenethyl alcohol where **51** was a superior catalyst to **62a**.

Table 4.12 shows that in fact similar conversions were found in reactions employing the ester ylides in Entries 3 (53% and 56%) and 4 (33% and 46%) for **62a** and **51** respectively. Entry 6 with **122** shows an interesting result and actually gives a higher conversion to the desired alkane product (73%) than the cyano ylide **117** (56%), a value twice as large as was seen when employing **62a** as a catalyst. Still no reaction was seen with the pyruvate ylide **120** (Entry 5) and only trace amounts of products were observed for the acetone ylide **121** (Entry 2).

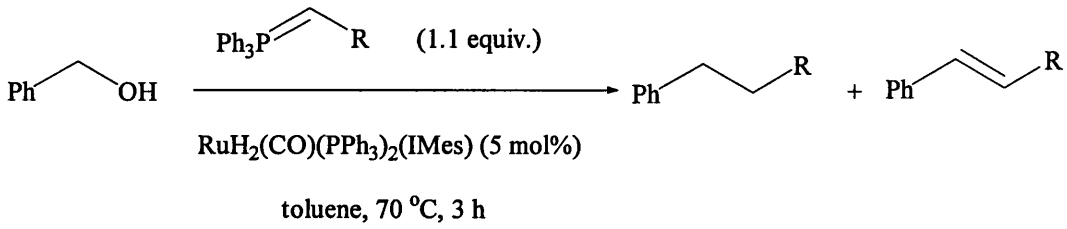

Scheme 4.20 *One-pot Wittig using **51** with a range of ylides.*

Entry	Ylide		Total Conversion (%)	Alkene (%)	Alkane (%)
1	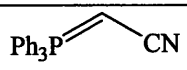	**117**	56	3	53
2	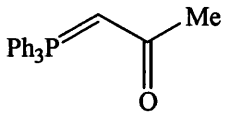	**121**	6	4	2
3	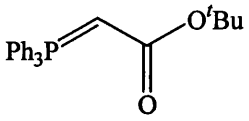	**119**	52	2	50
4	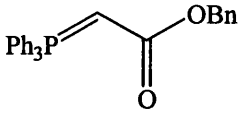	**118**	46	3	43
5	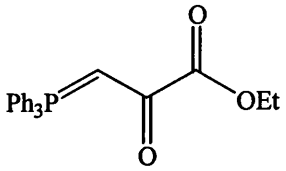	**120**	0	0	0
6	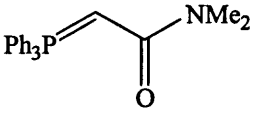	**122**	74	1	73
7	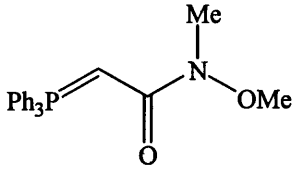	**123**	9	1	8

Table 4.12 *Effect of varying ylide in the Wittig reaction of benzyl alcohol catalysed by* ***51*** *(conditions: toluene, 70 °C, 3 h, 5 mol% loading).*

4.7.4 Effect upon variation of alcohol substrate

To test the scope of the Wittig reaction for a range of alcohol substrates, the most successful system of catalyst (**62a**) paired with ylide (**117**) was used (Scheme 4.21). The reaction showed versatility for the application of different substrates (Table 4.13). The reactions were initially run at 70 °C for 6 h.

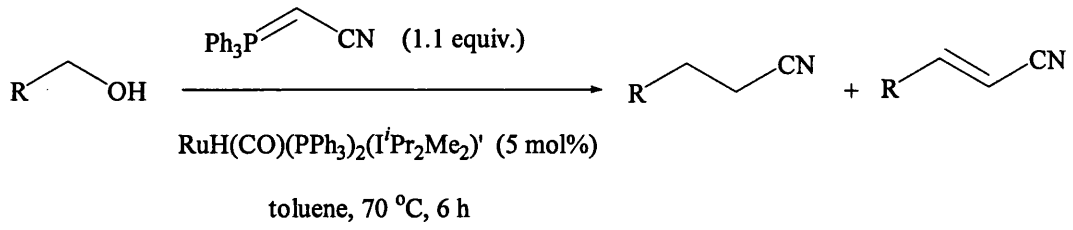

Scheme 4.21 *One-pot Wittig reaction using* ***62a*** *with a range of alcohol substrates.*

Entry	Alcohol		Conversion	Alkene	Alkane
1	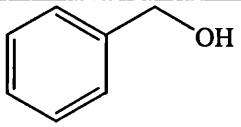	**110**	100	0	100
2	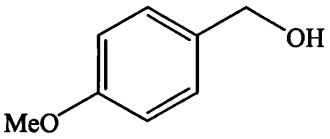	**125**	95	9	86
3	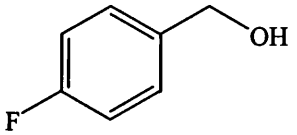	**124**	100	1	99
4	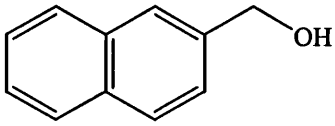	**126**	100	0	100
7	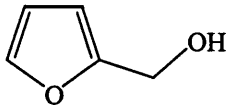	**127**	87	1	86
9	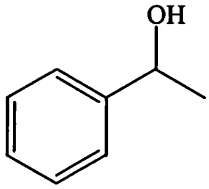	**111**	0	0	0

Table 4.13 *Effect of varying alcohol substrate in the Wittig reaction using* ***117*** *catalysed by* ***62a*** *(conditions: toluene, 70 °C, 6 h, 5 mol% loading).*

Reaction of simple benzyl alcohols (Entries 1-4) proceeded to afford the desired dihydrocinnamonitrile alkane products in 86-100% conversion. The presence of the electron donating methoxy group allows for a more reactive oxidation step compared

with benzyl alcohol and 4-fluoro-benzylalcohol, but a subsequently less reactive reduction step. Hence more alkene intermediate is detected in the reaction mixture of **125** (9%) than with **110** and **126** (0 and 1% respectively). The oxidation reactions of 4-methoxy-α-methylbenzylalcohol (**125**) and 4-fluoro-α-methylbenzylalcohol (**124**) in addition to the reduction of their corresponding ketones using **51** were previously compared.[17] Rates of oxidation were very similar although **125** reached a higher conversion than **124**. A greater difference was seen between the two substrates in the reduction reactions. Reduction of **125** was considerably slower than reduction of **124**.

The reaction was also extended to heteroaryl alcohols, furfuryl alcohol **127** (Entry 7) and 3-indole ethanol **128** (tryptophol). **127** gave a good conversion (86%) to the desired alkane. However analysis of the ^{1}H NMR spectrum of tryptophol **128** revealed the production of unidentifiable aliphatic products. This is due to the alcohol functional group being further removed from the aromatic ring. The same problem arose with 3-phenyl-1-propanol **129** and the aliphatic amyl alcohol **130** and thus conversions were not obtained. As expected, the secondary alcohol **111** (Entry 9) underwent no reaction. The intermediate ketone that would be produced would be unable to proceed through the Wittig reaction. Only starting material could be detected upon analysis of the ^{1}H NMR spectrum.

The best alcohol substrates from Table 4.13 were taken and the reaction time was reduced to 2 h (Scheme 4.22). The results illustrated in Table 4.14 show that **62a** catalyses the tandem process for a wide range of alcohol substrates, some matching the high reactivity found with the initial substrate, benzyl alcohol.

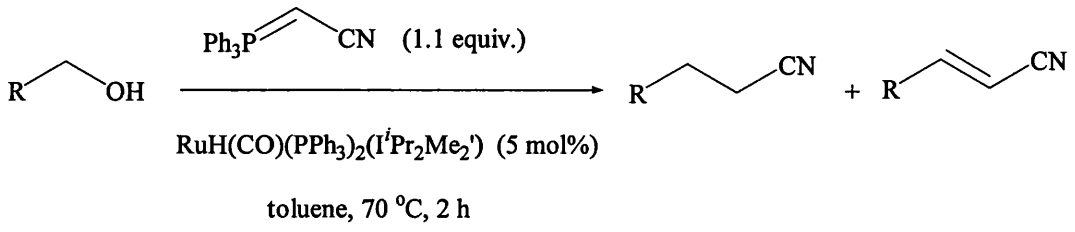

Scheme 4.22 *Reduced times for **62a** catalysed reaction of reactive alcohol substrates.*

Entry	Alcohol		Conversion	Alkene	Alkane
1	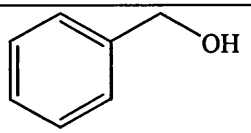	**110**	87	2	85
2	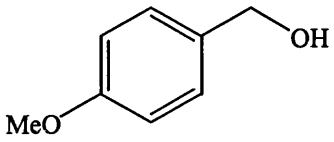	**125**	61	7	54
3	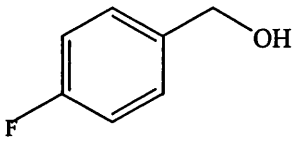	**124**	88	2	86
4	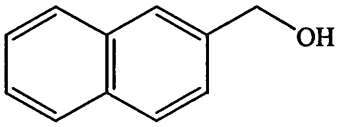	**126**	85	2	83
5	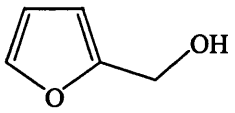	**127**	65	1	64

Table 4.14 *Reduced times (2 h) for* ***62a*** *catalysed reaction of reactive alcohol substrates (conditions: 1 mL toluene, 5 mol%, 70 °C, 2 h).*

4.8 Discussion

The complex **51** was established as an effective catalyst for the three-step tandem process converting alcohol substrate to alkane product. Reaction temperatures and times were reduced dramatically from the Ishii iridium system that was previously used for this chemistry. The reactivity of the new alkyl Ru-NHC complexes that had been developed in Chapters 2 and 3 were compared with that of **51** in a series of one-pot Wittig reactions. Whilst all alkyl Ru-NHC complexes showed their applicability to this chemistry, only the C-H activated complex **62a** proved to be superior to **51**. The high reactivity of the complex allowed for further reductions and in reaction temperatures and times. Furthermore, the Ru-NHC systems do not require the addition of base. The progress made for this indirect Wittig reaction is highlighted in Scheme 4.23. Catalyst **62a** also gave high conversions for a range of alcohol substrates although its limitations were met when varying the phosphorane ylide.

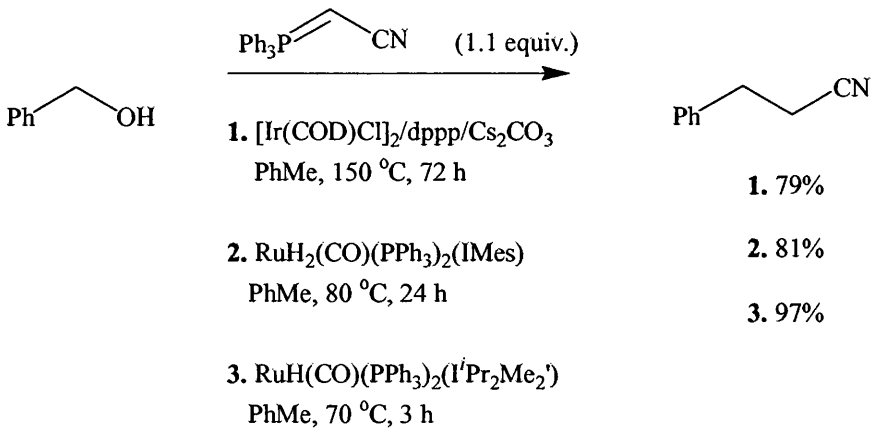

Scheme 4.23 *Progress made in the three-step tandem reaction.*

4.9 Chapter summary

- **51** was shown to be an effective direct and transfer hydrogenation catalyst for a range of alkenes.

- The range of synthesised alkyl Ru-NHC complexes were shown to be effective catalysts for the transfer hydrogenation for alcohols and alkenes and subsequently for the one-pot Wittig reaction.

- Reaction temperatures and times were reduced from 150 °C for 72 h to 70 °C for 3 h with the employment of the catalyst **62a** achieving superior conversions to the desired alkane product.

- **62a** was shown to be versatile for a number of different alcohol substrates although limitations became apparent in the use of different phosphorane ylides.

4.10 References

[1]Trost, B. M.; Toste, F. D.; Pinkerton, A. B. *Chem. Rev.* **2001**, *101*, 2067-2096.

[2]Murahashi, S.-I. *Ruthenium in Organic Synthesis*; Wiley-VCH, 2004.

[3]Wittig, G.; Geissler, G. *Liebigs. Ann. Chem.* **1953**, *580*, 44.

[4]Wadsworth, W. S.; Emmons, W. D. *J. Am. Chem. Soc.* **1961**, *83*, 1733.

[5]Horner, L.; Hoffmann, H.; Wipel, H. C.; Klahre, G. *Chem. Ber.* **1959**, *92*, 2499.

[6]Clayden, J.; Greeves, N.; Warren, S.; Wothers, P. *Organic Chemistry*; Oxford University Press Inc., 2001.

[7]Michaelis, G.; Gimborn, H. V. *Chem. Ber.* **1894**, *28*, 272.

[8]Zhang, X. M.; Bordwell, F. G. *J. Am. Chem. Soc.* **1994**, *116*, 968.

[9]Trippett, S.; Ross, S. T. *J. Org. Chem.* **1962**, *27*, 998.

[10]Bestmann, H. J.; Arnason, B. *Chem. Ber.* **1962**, *95*, 1513.

[11]Huang, Z. Z.; Yu, X. C.; Huang, X. *Tetrahedron Lett.* **2002**, *43*, 6823.

[12]Huang, Z. Z.; Yu, X. C.; Huang, X. *J. Org. Chem.* **2002**, *67*, 8261.

[13]Black, P. J.; Harris, W.; Williams, J. M. J. *Angew. Chem. Int. Edit.* **2001**, *40*, 4475.

[14]Sakuguchi, S.; Yamaga, T.; Ishii, Y. *J. Org. Chem.* **2001**, *66*, 4710-4712.

[15]Edwards, M. G. "PhD thesis," University of Bath, **2003**.

[16]Edwards, M. G.; Williams, J. M. J. *Angew. Chem. Int. Edit.* **2002**, *41*, 4740-4743.

[17]Burling, S.; Whittlesey, M. K.; Williams, J. M. J. *Adv. Synth. Catal.* **2005**, *347*, 591-594.

Chapter 5

Chapter 5: Experimental

5.1 General Procedures

All reactions and manipulations were carried out under argon using standard Schlenk line techniques or under nitrogen in a moisture free glovebox unless otherwise stated. Glassware was ovendried at 140 °C overnight and subsequently flame dried under vacuum.

Solvents were purchased from Fisher, dried, distilled, and degassed prior to use: hexane, benzene and THF were distilled from purple solutions of sodium dispersion benzophenone and a few additional drops of ethylene glycol in the case of hexane. Toluene was dried over sodium and ethanol, methanol and 1-hexanol were distilled from magnesium turnings and iodine. Deuterated solvents were purchased from Sigma-Aldrich and dried over potassium (benzene-d_6, toluene-d_8 and THF-d_8), or calcium hydride ($CDCl_3$ and DCM-d_2), and subsequently vacuum-transferred into ampoules. H_2 (BOC, 99.99%) was used as received. $RuCl_3.3H_2O$ was kindly donated by Johnson-Matthey.

5.2 Physical and analytical measurements

NMR spectra were recorded on Bruker Avance 300 and 400 MHz spectrometers. The ^1H NMR spectra were referenced to the chemical shifts of the relevant solvent [benzene-d_5 (δ 7.15), toluene-d_7 (δ 2.10), THF-d_7 (δ 3.60), pyridine-d_4 (8.72), chloroform (δ 7.26), DCM-d_2 (δ 5.31), DMSO-d_5, (2.49)]. The $^{13}C\{^1H\}$ NMR spectra were referenced to benzene-d_6 (δ 128.7), toluene-d_8 (δ 21.1), THF-d_8 (δ 20.4), $CDCl_3$ (δ 77.7) and pyridine-d_5 (149.5). The $^{31}P\{^1H\}$ NMR chemical shifts were referenced externally to 85% H_3PO_4 (δ 0.0).

GC analyses were performed using a Fisons GC 8000 series using an HP Ultra 2 Column, crosslinked 5% Ph Me silicone stationary phase (25 m, 0.32 mm, 0.52 μm film thickness) under the following conditions: injector, 250 °C; detector, 250 °C; oven, 40 °C (isothermal).

IR spectra were recorded on a Nicolet Nexus FTIR spectrometer as nujol mulls or as benzene-d_6 solutions. Elemental analyses were performed at the University of Bath and at Elemental Microanalysis Ltd., Okehampton, Devon. Crystal structures were recorded on a Nonius KappaCCD diffractometer. Structural calculations and drawings were carried out using the SHELX suite of programs.

5.3 Syntheses of N-heterocyclic carbenes

5.3.1 Preparation of 1,3-bis(2,4,6-trimethylphenyl)imidazol-2-ylidene (IMes) (L17)

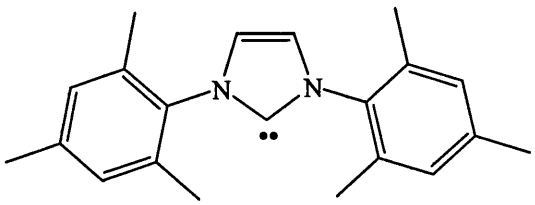

IMes was prepared from a method adapted from the literature.[1]

5.3.1.1 Preparation of glyoxal-bis(2,4,6-trimethylphenyl)imine

To a 1000 mL round-bottomed flask was added 2,4,6-trimethylphenylamine (135.2 g, 1.0 mol), a 40 % aqueous solution of glyoxal (72.6 g, 0.5 mol) and undried but degassed EtOH (500 mL). The mixture was stirred for 12 h at room temperature, during which time a thick yellow precipitate formed. The precipitate was isolated by filtration and then washed with cold EtOH (3 x 50 mL). The product was finally dried under vacuum for 6 h or left to dry in air. Yield: 212.0 g (73%); ^{1}H NMR ($CDCl_3$, 300 MHz, 298 K): δ 8.13 (s, 2H, *H*C=C*H*), 6.93 (s, 4H, *m*-C*H*), 2.32 (s, 6H, *p*-CH_3), 2.19 (s, 12H, *o*-CH_3).

5.3.1.2 Preparation of 1,3-bis(2,4,6-trimethylphenyl)imidazolium chloride

To an undried toluene solution of bis-(2,4,6-trimethylphenyl)-diazabutadiene (20.0 g, 68.5 mmol), paraformaldehyde (2.0 g, 0.7 mmol) was added. The reaction mixture was heated to reach 100 °C and then cooled to 40 °C, after which time HCl (16.5 mL, 4 M in dioxane) was introduced. The reaction was maintained at 70 °C for 5 h and

allowed to cool to room temperature and stirred for a further 36 h. The product was collected by filtration and washed with THF (3 x 50 mL). Yield: 15.6 g (69 %); ^{1}H NMR ($CDCl_3$, 300 MHz, 293 K): δ 10.31 (s, 1H, C*H*), 7.65 (s, 2H, *H*C=C*H*), 6.88 (s, 4H, *m*-C*H*), 2.22 (s, 6H, *p*-CH_3), 2.04 (s, 12H, *o*-CH_3).

5.3.1.3 Preparation of 1,3-bis(2,4,6-trimethylphenyl)imidazol-2-ylidene (IMes) (L17)

1,3-bis(2,4,6-trimethylphenyl)imidazolium chloride (10.0 g, 28.0 mmol) was placed into a flame dried Schlenk tube and left under vacuum for approximately 16 h. Potassium *tert*-butoxide (4.0 g, 36.0 mmol) was added and the mixture cooled to -70 °C in an isopropanol/dry-ice bath, before adding THF (100 mL). The mixture was stirred vigorously and kept at 0-5 °C for 30 min. The reaction was warmed to room temperature and stirred for a further 30 min. The solvent was removed *in vacuo* and the residue pumped to dryness. (NB: complete dryness of the residue is crucial for the successful isolation of the final product). The residue was dissolved in toluene (100 mL) and filtered through a glass-fibred filter cannular. The filtrate was pumped down to a dry residue before hexane (50 mL) was added. The mixture was stirred until a precipitate formed and then cooled down to -30 °C to enforce precipitation of the product. Yield: 6.5 g (73 %); ^{1}H NMR (benzene-d_6, 300 MHz, 298 K): δ 6.80 (s, 4H, *m*-C*H*), 6.51 (s, 2H, *H*C=C*H*), 2.16 (s, 6H, *p*-CH_3), 2.14 (s, 12H, *o*-CH_3).

5.3.2 Preparation of 1,3-bis(2,4,6-trimethylphenyl)imidazolin-2-ylidene (SIMes) (L18)

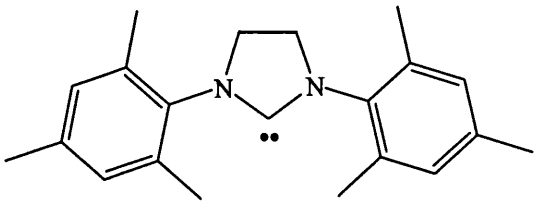

SIMes was prepared from a method adapted from the literature.[1]

5.3.2.1 Preparation of N,N-bis(2,4,6-trimethylphenylamino)ethane dichloride

A suspension of glyoxyl-bis-(2,4,6-trimethylphenyl)imine (29.5 g, 100.0 mmol) in THF (400 mL) was treated at 0 °C with $NaBH_4$ (16.0 g) in portions of 1.0 g over a

period of 1 h. The mixture was stirred for 16 h at 23 °C and heated subsequently for 2 h under reflux. To the mixture was added ice-water (300 mL) followed by hydrochloric acid (HCl, 3 M). A white solid precipitated and was collected by filtration and dried *in vacuo*. Yield: 32.4 g (87%); ^{1}H NMR (DMSO-d_6, 300 MHz, 298 K): δ 6.97 (s, 4H, *m*-C*H*),), 3.67 (s, 4H, NH_2), 2.44 (s, 12H, *o*-CH_3), 2.23 (s, 6H, *p*-CH_3).

5.3.2.2 Preparation of 1,3-bis(2,4,6-trimethylphenylamino)imidazolium chloride

A mixture of *N,N'*-bis-(2,4,6-trimethylphenylamino)ethane dihydrochloride (8.4 g, 22.8 mmol), triethyl orthoformate (75 mL), and formic acid (two drops, 96%) was heated in a distillation apparatus until the EtOH distillation ceased. The temperature of the reaction mixture reached 130 °C. Upon cooling to room temperature a white solid precipitated which was collected by filtration, and dried *in vacuo*. Yield: 6.1 g (78%); ^{1}H NMR (DMSO-d_6, 300 MHz, 298 K) δ 9.02 (s, 1H, im-C*H*), 7.09 (s, 4H, *m*-C*H*), 4.44 (s, 4H, H_2C-CH_2), 2.34 (s, 12H, *o*-CH_3), 2.29 (s, 6H, *p*-CH_3).

5.3.2.3 Preparation of 1,3-bis(2,4,6-trimethylphenyl)imidazolin-2-ylidene (SIMes) (L18)

To 0.2 g of a ca. 35% suspension of potassium hydride in mineral oil (corresponding to 1.7 mmol KH) was added a suspension of 1,3,-bis-(2,4,6-trimethylphenyl)imidazolium chloride (0.5 g, 1.3 mmol) in THF (30 mL). Immediately a moderate evolution of gas was observed. The mixture was stirred for 2 h at room temperature until the evolution of gas had ceased, filtered through a frit covered with celite, and evaporated. Recrystallisation from hexane at –25 °C gave the product as a pale yellow solid. Yield: 0.2 g (58%); ^{1}H NMR (benzene-d_6, 300 MHz, 298 K): δ 6.83 (s, 4H, *m*-C*H*), 3.26 (s, 4H, H_2C-CH_2), 2.29 (s, 12H, *o*-CH_3), 2.16 (s, 6H, *p*-CH_3).

5.3.3 Preparation of 1,3,4,5-tetramethylimidazol-2-ylidene (IMe$_4$) (L2)

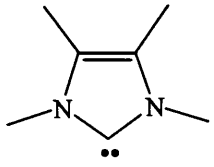

IMe_4 was prepared from a method adapted from the literature.[2]

5.3.3.1 Preparation of 1,3,4,5-tetramethylimidazole-2(3H)-thione (48)

A stirred 1-hexanol (250 mL) solution of 1,3-dimethyl-2-thiourea **45** (10.4 g, 0.1 mol) and 3-hydroxy-2-butanone (8.8 g, 0.1 mol) was refluxed (158 °C) for 12 h. The solvent was removed *in vacuo*. The residue was washed with H_2O (2 x 30 mL) and Et_2O (3 x 20 mL) and finally recrystallised from EtOH/H_2O (1:1). Compound **48** was obtained as colourless needles. Yield: 9.0 g (58%); ^{1}H NMR (CD_2Cl_2, 300 MHz, 298 K): δ 3.47 (s, 6H, N-CH_3), 2.05 (s, 6H, H_3CC=CCH_3). ^{13}C {^{1}H}: δ 160.9 (s, *C*=S), 120.8 (s, *C*=*C*), 32.0 (s, N-*C*H_3), 9.4 (s, H_3*C*C=C*C*H_3).

5.3.3.2 Preparation of 1,3,4,5-tetramethylimidazol-2-ylidene (IMe_4) (L2)

Chopped pieces of potassium metal (0.5 g, 12.8 mmol) were added at 0 °C to a solution of 1,3,4,5-tetramethylimidazole-2(3H)-thione **48** (0.8 g, 5.0 mmol) in THF (30 mL) and refluxed under argon for 4 h. The filtered solution was evaporated to dryness to give a yellow solid (**L2**). Yield: 0.6 g (91%); ^{1}H NMR (benzene-d_6, 300 MHz, 298 K): δ 3.36 (s, 6H, N-CH_3), 1.57 (s, 6H, CH_3C=CCH_3). ^{13}C{^{1}H}: δ 211.3 (s, N*C*N), 122.6 (s, *C*=*C*), 35.5 (s, N-*C*H_3), 9.0 (s, H_3C=C*C*H_3).

5.3.4 Preparation of 1,3-diethyl-4,5-dimethylimidazol-2-ylidene (IEt_2Me_2) (L20)

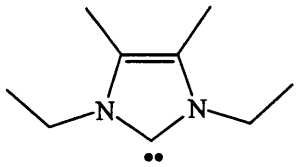

IEt_2Me_2 was prepared from a method adapted from the literature.[2]

5.3.4.1 Preparation of 1.3-diethyl-4,5-dimethylimidazole-2(3H)-thione (49)

A stirred 1-hexanol solution (250 mL) of 1,3-diethyl-2-thiourea **46** (13.2 g, 0.1 mol) and 3-hydroxy-2-butanone (8.8 g, 0.1 mol) was refluxed (158 °C) for 12 h. The solvent was removed *in vacuo*. The residue was washed with H_2O (2 x 30 mL) and Et_2O (3 x 20 mL) and finally recrystallised from EtOH/H_2O (1:1). Yield: 8.7 g (47%); ^{1}H NMR ($CDCl_3$, 300 MHz, 298 K): δ 4.06 (q, J_{HH} = 7.2 Hz, 4H, N-

CH_2CH_3), 2.07 (s, 6H, $H_3CC{=}CCH_3$), 1.24 (t, J_{HH}=7.2 Hz, 6H, N-CH_2CH_3). $^{13}C\{^1H\}$: δ 159.3 (s, *C*=S), 120.8 (s, *C*=*C*), 40.2 (N-CH_2CH_3), 14.3 (N-CH_2CH_3), 9.3 ($H_3CC{=}CCH_3$).

5.3.4.2 Preparation of 1,3-diethyl-4,5-dimethylimidazol-2-ylidene (IEt_2Me_2) (L20)

Chopped pieces of potassium metal (1.0 g, 25.6 mmol) were added at 0 °C to a solution of 1.3-diethyl-4,5-dimethylimidazole-2(3H)-thione **49** (1.8 g, 10.0 mmol) in THF (60 mL) and refluxed under argon for 4 h. The filtered solution was evaporated to dryness to give a white solid (**L20**). Yield: 2.5 g (83%); ^1H NMR (benzene-d_6, 400 MHz, 298 K): δ 3.79 (q, J_{HH} = 7.1 Hz, 2H, CH_2CH_3), 1.69 (s, 6H, $H_3C{=}CCH_3$), 0.44 (t, J_{HH} = 7.1 Hz, 6H, CH_2CH_3). $^{13}C\{^1H\}$: δ 211.5 (s, NCN), 122.6 (s, *C*=*C*), 43.7 (s, N-CH_2CH_3), 18.0 (s, N-CH_2CH_3), 9.5 (s, $H_3CC{=}CCH_3$).

5.3.5 Preparation of 1,3-diisopropyl-4,5-dimethylimidazol-2-ylidene ($I^iPr_2Me_2$) (L6)

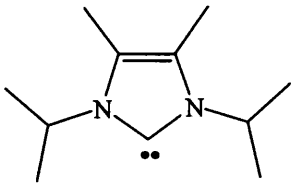

$I^iPr_2Me_2$ was prepared from a method adapted from the literature.[2]

5.3.5.1 Preparation of 1.3-diisopropyl-4,5-dimethylimidazole-2(3H)-thione (50)

A stirred 1-hexanol solution (250 mL) of 1,3-diisopropyl-2-thiourea **47** (16.0 g, 0.1 mol) and 3-hydroxy-2-butanone (8.8 g, 0.1 mol) was refluxed (158 °C) for 12 h. The solvent was removed *in vacuo*. The residue was washed with H_2O (2 x 30 mL) and Et_2O (3 x 20 mL) and finally recrystallised from EtOH/H_2O (1:1). Compound **50** was obtained as colourless needles. Yield: 15.0 g (93%); ^1H NMR (benzene-d_6, 300 MHz, 298K): δ 5.61 (sept, J_{HH} = 6.9 Hz, 2H, $CH(CH_3)_2$), 2.16 (s, 6H, $H_3CC{=}CCH_3$), 1.40 (d, J_{HH} = 6.9 Hz, 12H, $CH(CH_3)_2$). $^{13}C\{^1H\}$: δ 160.2 (s, *C*=S), 121.2 (s, *C*=*C*), 48.9 (s, N-$CH(CH_3)_2$), 20.3 (s, N-$CH(CH_3)_2$), 10.1 (s, $H_3CC{=}CCH_3$).

5.3.5.2 Preparation of 1,3-diisopropyl-4,5-dimethylimidazol-2-ylidene ($I^iPr_2Me_2$) (L6)

Chopped pieces of potassium metal (1.0 g, 25.6 mmol) were added at 0 °C to a solution of 1.3-diisopropyl-4,5-dimethylimidazole-2(3H)-thione **50** (2.1 g, 10.0 mmol) in THF (60 mL) and refluxed under argon for 4 h. The filtered solution was evaporated to dryness to give a white solid (**L6**). Yield: 0.9 g (86%); ^{1}H NMR (benzene-d_6, 400 MHz, 298 K): δ 3.94 (sept, J_{HH} = 6.9 Hz, 2H, C*H*$(CH_3)_2$), 1.72 (s, 6H, H_3CC=CCH_3), 1.47 (d, J_{HH} = 6.9 Hz, 12H, N-CH(CH_3)$_2$). ^{13}C {^{1}H}: δ 206.4 (s, NCN), 121.5 (s, *C*=*C*), 48.6 (s, N-*C*H$(CH_3)_2$), 24.64 (s, N-CH(*C*H_3)$_2$), 8.9 (s, H_3*C*C=C*C*H_3).

5.3.6 Preparation of 1,3-diisopropylimidazol-2-ylidene (I^iPr) (L4)

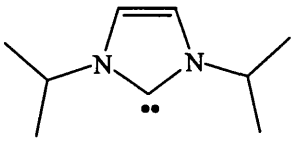

I^iPr was prepared from a method adapted from the literature.[31]

5.3.6.1 Preparation of 1,3-diisopropylimidazolium chloride

A 500 mL round-bottomed flask was charged with isopropylamine (8.5 mL, 0.1 mol) in toluene (100 mL), and paraformaldehyde (3.0 g, 0.1 mol) was added under intense stirring. After 30 min at room temperature, the flask was cooled to 0 °C, and another equivalent of isopropylamine (8.5 mL, 0.1 mol) was added. The solution was stirred at 0 °C for a further 10 min followed by a dropwise addition of 4 M HCl in dioxane (25 mL, 0.1 mol) The solution was allowed to warm to room temperature, and 40 % aqueous glyoxal (14.5 mL, 0.1 mol) was added. The resulting cloudy mixture was stirred at 34-38 °C for 36 h. After the mixture had cooled to room temperature, Et_2O (100 mL) and saturated Na_2CO_3 solution (50 mL) were added, and the layers separated. The phase between the organic and aqueous layers was kept with the organic phase and the aqueous layer washed with Et_2O (3 x 100 mL). The volatiles were removed *in vacuo*, and the residue extracted with dry DCM (50 mL), dried over $MgSO_4$, and filtered. After removal of the solvents, the solid residue was broken

down to a pale brown hygroscopic powder by treatment with Et_2O (50 mL). Yield: 10.1 g (54%); ^1H NMR ($CDCl_3$, 400 MHz, 298 K): δ 10.74 (br s, 1H, im-C*H*), 7.55 (s, 1H, *H*C=CH), 7.54 (s, 1H, HC=C*H*), 4.83 (sept, J_{HH} = 6.7 Hz, 2H, C*H*$(CH_3)_2$), 1.50 (d, J_{HH} = 6.7 Hz, 12H, CH(C$H_3)_2$).

5.3.6.2 Preparation of 1,3-diisopropylimidazol-2-ylidene (I^iPr) (L4)

A solution of 1,3-diisopropylimidazolium chloride (1.0 g, 5.3 mmol) and potassium *tert*-butoxide (0.7 g, 6.8 mmol) in THF (15 mL) was stirred at <0 °C for 1 h. The solvent was removed *in vacuo* and the resulting oily residue redissolved in toluene (15 mL), filtered and pumped to dryness. Hexane (20 mL) was added, the mixture filtered and the solvent removed *in vacuo* to yield a yellow oil. Yield: 0.66 g (81%); ^1H NMR (benzene-d_6, 400 MHz, 298 K): δ 6.57 (s, 2H, *H*C=C*H*), 4.40 (sept, J_{HH}=6.7 Hz, 2H, C*H*$(CH_3)_2$), 1.26 (d, J_{HH}=6.7 Hz, CH(C$H_3)_2$). $^{13}C\{^1H\}$ NMR: δ 210.5 (s, *C*:), 128.7 (s, *C*=*C*), 52.8 (s, *C*H$(CH_3)_2$), 24.9 (s, CH(*C*$H_3)_2$).

5.3.7 Preparation of 1,3-bis((S)1-phenylethyl)imidazol-2-ylidene (I*) (L19)

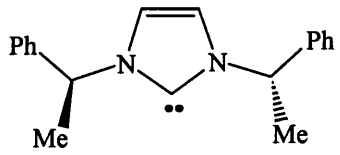

I* was prepared from a method adapted from the literature.[1,4]

5.3.7.1 Preparation of 1,3Bis((*S*)1-phenylethyl)imidazolium Chloride

A 500 mL round-bottomed flask was charged with (*S*)-1-phenylethylamine (5.0 mL, 42.0 mmol) in toluene (50 mL), and paraformaldehyde (1.3 g, 42.0 mmol) was added under intense stirring. After 30 min at room temperature the flask was cooled to 0 °C, and another equivalent of (*S*)-1-phenylethylamine (5.0 mL, 42.0 mmol) was added. The solution was stirred at 0 °C for 10 min, followed by a dropwise addition of 4 M HCl in dioxane (10.5 mL, 42.0 mmol). The solution was allowed to warm to room temperature, and 40 % aqueous glyoxal (6.1 mL, 42 mmol) was added. The resulting cloudy mixture was stirred at 34-38 °C for 36 h. After the mixture had cooled to room temperature, Et_2O (100 mL) and a saturated Na_2CO_3 solution (50

mL) were added, and the layers separated. The phase between the organic and aqueous layers was kept with the organic phase and the aqueous layer washed with Et_2O (3 x 100 mL). The volatiles were removed *in vacuo*, and the residue extracted with dry DCM (50 mL), dried over $MgSO_4$, and filtered. After removal of the solvents, the solid residue was broken down to a pale yellow hygroscopic powder by treatment with Et_2O (50 mL). Yield: 6.3 g (48%); ^1H NMR ($CDCl_3$, 400 MHz, 298 K): δ 11.63 (br s, 1H, im-C*H*), 7.49-7.42 (m, 4H, Ph), 7.39-7.28 (m, 6H, Ph), 7.11 (s, 1H, *H*C=CH), 7.10 (s, 1H, HC=C*H*), 6.07 (q, J_{HH} = 7.1 Hz, 2H, C*H*(CH_3)Ph), 1.99 (d, J_{HH} = 7.1 Hz, 6H, CH(C*H*$_3$)Ph). ^{13}C {^1H}: δ 138.3 (s, Ph), 137.9 (s, im-*C*), 129.7 (s, Ph), 129.6 (s, Ph), 127.4 (s, Ph), 120.3 (s, *C*=*C*), 60.1 (s, *C*H(CH_3)Ph), 21.4 (s, CH(*C*H$_3$)Ph).

5.3.7.2 Preparation of 1,3-bis((S)1-phenylethyl)imidazolin-2-ylidene (I*) (L19)

An Et_2O solution (20 mL) of 1,3-bis((S)1-phenylethyl)imidazolium chloride (1.0 g, 3.2 mmol) and potassium tert-butoxide (0.5 g, 4.5 mmol) was stirred for 30 min at room temperature. The solvent was removed *in vacuo* and the resulting residue redissolved in toluene (20 mL). The mixture was filtered and after removal of the solvent, the brown/orange residue was dissolved in hexane (20 mL) and filtered. The solvent was removed *in vacuo* to yield a yellow solid. Yield: 0.73 g (83%); ^1H NMR (benzene-d_5, 400 MHz, 298 K): δ 7.28-7.18 (m, 4H, Ph), 7.12-5.94 (m, 5H, Ph), 5.43 (s, *H*C=C*H*), 5.45 (q, J_{HH} = 7.1 Hz, 2H, C*H*(CH_3)Ph), 1.78 (d, J_{HH} = 7.1 Hz, CH(C*H*$_3$)Ph). ^{13}C {^1H}: δ 214.0 (s, im-*C*), 144.9 (s, Ph), 128.0 (s, Ph), 129.3 (s, Ph), 127.5 (s, Ph), 118.5 (s, *C*=*C*), 50.5 (s, *C*H(CH_3)Ph), 23.5 (s, CH(*C*H$_3$)Ph).

5.3.8 Preparation of 1,3-bis(cyclohexyl)-imidazol-2-ylidene (ICy) (L21)

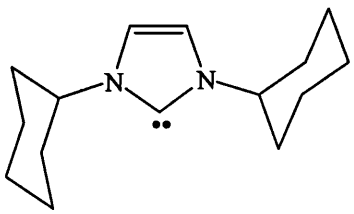

The synthesis for ICy was provided by Steve Nolan and Rohit Singh, University of New Orleans.[5]

5.3.8.1 Preparation of 1,3-bis(cyclohexyl)imidazolium tetrafluoroborate

A suspension of paraformaldehyde (3.0 g) in toluene (15 mL) was cooled in an ice bath. Cyclohexylamine (23 mL, 0.2 mol) was added dropwise over an hour. HCl (25 mL, 4 M in dioxane) was then added dropwise over 30 min, maintaining the temperature below 25 °C. The white cloudy mixture was allowed to warm to room temperature before adding glyoxal (11.5 mL). The mixture was stirred for 1 h and then toluene (30 mL) was added. Water (10.8 cm^3) was removed from the reaction mixture using a Dean-Stark trap. The volatiles were removed from the remaining mixture *in vacuo* affording the imidazolium chloride as a brown sticky solid. This was dissolved in water (75 mL) and tetrafluoroboric acid (13 mL) added, immediately precipitating the BF_4 salt as a pale brown solid. Yield: 26.0 g (41%); ^{1}H NMR ($CDCl_3$, 400 MHz, 298 K): δ 8.91 (t, J_{HH} = 1.7 Hz, 1H C-*H*), 7.41 (d, J_{HH} = 1.7 Hz, 2H, *H*C=C*H*), 4.29 (tt, J_{HH} = 11.9 Hz, J_{HH} = 3.8 Hz, 2H, C*H*-Cy), 2.17-2.13 (m, 4H, CH_2-Cy), 1.90-1.87 (m, 4H, CH_2-Cy), 1.73-1.62 (m, 6H, CH_2-Cy), 1.50-1.39 (m, 4H, CH_2-Cy), 1.30-1.18 (m, 2H, CH_2-Cy). ^{13}C{^{1}H}: δ 133.2 (s, im-*C*), 120.2 (s, H*C*=*C*H), 60.0 (s, *C*H-Cy), 33.2 (s, *C*H_2-Cy), 24.9 (s, *C*H_2-Cy), 24.5 (s, *C*H_2-Cy).

5.3.8.2 Preparation of 1,3-bis(cyclohexyl)-imidazol-2-ylidene (ICy) (L21)

NaH (0.3 g, 12.5 mmol) and NaO^{t}Bu (30.0 mg, 0.3 mmol) were added to ICy.HBF_4 (2.0 g, 5.2 mmol) in a Schlenk flask and dried under vacuum for several hours. THF (20 mL) was added at room temperature and the mixture stirred for 4 h. The volatiles were removed *in vacuo* producing a solid brown residue. Sublimation at 100 °C for 1 h afforded ICy as an air-sensitive white solid (turned orange rapidly). Yield: 0.8 g (66%); ^{1}H NMR (benzene-d_6, 400 MHz, 298 K): δ 6.61 (s, 2H, *H*C=C*H*), 4.10 (tt, J_{HH} = 11.8 Hz, J_{HH} = 3.7 Hz, 2H, C*H*-Cy), 2.06 (m, 4H, CH_2-Cy), 1.69-1.62 (m, 8H, CH_2-Cy), 1.49-1.46 (m, 2H, CH_2-Cy), 1.30-1.01 (m, 6H, CH_2-Cy). ^{13}C{^{1}H}: δ 211.7 (s, *C*:), 114.9 (s, H*C*=*C*H), 59.0 (s, *C*H($C_{10}H_5$)), 34.2 (s, *C*H_2-Cy), 24.9 (s, *C*H_2-Cy), 24.8 (s, *C*H_2-Cy).

5.3.9 Synthesis of 1,3-bis(*n*-propyl)-imidazol-2-ylidene (L22)

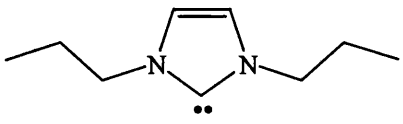

I^{n}Pr was prepared from a method adapted from the literature.[3 1]

5.3.9.1 Synthesis of 1,3-bis(*n*-propyl) imidazolium chloride

A 500 mL round-bottomed flask was charged with *n*-propylamine (3.6 mL, 50 mmol) in toluene (100 mL), and paraformaldehyde (1.5 g, 50 mmol) was added under intense stirring. After 30 min at room temperature, the flask was cooled to 0 °C, and another equivalent of *n*-propylamine (3.6 mL, 50 mmol) was added. The solution was stirred at 0 °C for a further 10 min followed by a dropwise addition of 4 M HCl in dioxane (12.5 mL, 50 mmol) The solution was allowed to warm to room temperature, and 40 % aqueous glyoxal (7.3 mL, 50 mmol) was added. The resulting cloudy mixture was stirred at 34-38 °C for 36 h. After the mixture had cooled to room temperature, Et_2O (50 mL) and saturated Na_2CO_3 solution (25 mL) were added, and the layers separated. The phase between the organic and aqueous layers was kept with the organic phase and the aqueous layer washed with Et_2O (3 x 50 mL). The volatiles were removed *in vacuo*, and the residue extracted with dry CH_2Cl_2 (25 mL), dried over $MgSO_4$, and filtered. After removal of the solvents, the oily residue was broken down to a pale yellow hygroscopic solid by treatment with Et_2O (25 mL). Yield: 5.48 g (58%); ^{1}H NMR (CD_2Cl_2, 400 MHz, 298K): δ 10.92 (s, 1H, NC*H*N), 7.42 (s, 2H, im-C*H*), 4.29 (t, 4H, J_{HH} = 7.3 Hz, N-CH_2), 1.93 (m, 4H, CH_3-CH_2), 0.97 (t, 6H, J_{HH} = 7.3 Hz, CH_3). ^{13}C{^{1}H}: δ 138.9 (s, NCHN), 122.5 (s, im-CH), 52.1 (s, N-CH_2), 24.4 (s, CH_3-CH_2), 11.2 (s, CH_3).

5.3.9.2 Synthesis of 1,3-bis(*n*-propyl)imidazol-2-ylidene (I^{n}Pr) (L22)

A solution of 1,3-bis(*n*-propyl)imidazolium chloride (1.0 g, 5.3 mmol) and potassium *tert*-butoxide (0.7 g, 6.8 mmol) in THF (15 mL) was stirred at <0 °C for 1 h. The solvent was removed *in vacuo* and the resulting oily residue redissolved in toluene (15 mL), filtered and pumped to dryness. Hexane (20 mL) was added, the mixture filtered and the solvent removed *in vacuo* to yield a yellow oil. Yield: 0.38 g (47%); ^{1}H NMR (benzene-d_6, 400 MHz, 298K): δ 6.45 (s, 2H, im-C*H*), 3.79 (t, 4H, J_{HH} = 7.2 Hz, N-CH_2), 1.62 (m, 4H, CH_3-CH_2), 0.73 (t, 6H, J_{HH} = 7.2 Hz, CH_2-CH_2). ^{13}C{^{1}H} NMR (benzene-d_6, 100 MHz, 298K): δ 215.5 (s, NCN), 119.1 (s, im-CH), 53.3 (s, N-CH_2), 25.9 (s, CH_3-CH_2), 11.9 (s, CH_3).

5.4 Syntheses of Ruthenium Precursors

5.4.1 Synthesis of $RuH_2(CO)(PPh_3)_3$ (52)

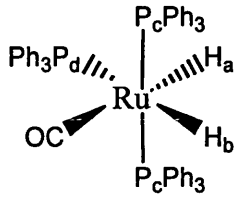

Three Schlenk tubes were prepared: (1) was charged with hydrated ruthenium trichloride (2.1 g, 8.0 mmol) and EtOH (80 mL); (2) was charged with aqueous formaldehyde (80 mL, 40 % w/v solution) which was subsequently degassed by argon bubbling; (3) was charged with potassium hydroxide (2.4 g, 40.0 mmol) and EtOH (80 mL). (1), (2), (3) were quickly added in that order to a boiling EtOH solution (280 mL) of triphenylphosphine (12.6 g, 48.0 mmol). The solution was heated under reflux for 25 min and then cooled in an ice bath. The resulting grey precipitate was washed with EtOH (2 x 50 mL), deionised water (50 mL) and hexane (50 mL). The crude powder was dissolved in benzene and passed through neutral alumina. The solution was reduced *in vacuo* and layered with methanol to produce a precipitate which was filtered to yield a white solid (**52**). Yield: 5.0 g (68 %); ^{1}H NMR (benzene-d_6, 300 MHz, 293 K): δ -6.53 (ddt, 1H, Ru-H_a, $J_{Pc\text{-}Ha}$ = 30.5 Hz, $J_{Pd\text{-}Ha}$ = 15.3 Hz, $J_{Ha\text{-}Hb}$ = 6.1 Hz), -8.29 (ddt, 1H, Ru-H_b, $J_{Pd\text{-}Hb}$ = 74.5 Hz, $J_{Pc\text{-}Hb}$ = 28.1 Hz, $J_{Ha\text{-}Hb}$ = 6.1 Hz). ^{31}P{^{1}H}: δ 58.2 (d, $J_{Pc\text{-}Pd}$ = 16.8 Hz), 46.1 (t, $J_{Pd\text{-}Pc}$ = 16.8 Hz). IR (nujol, cm^{-1}): 1960 (ν_{CO}).

5.5 Syntheses of Ruthenium-NHC Complexes

5.5.1 Syntheses of Ru(IMes) complexes

All syntheses of Ru(IMes) complexes used the method of Rudolf Jazzar.[6]

5.5.1.1 Synthesis of $RuH_2(CO)(PPh_3)_2(IMes)$ (51)

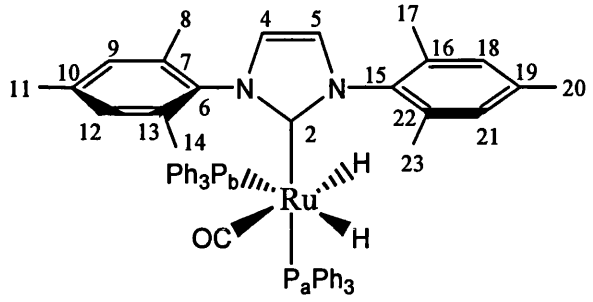

Toluene (30 mL) was added to **52** (1.0 g, 1.1 mmol) and IMes (1.0 g, 3.3 mol) and was heated at 80 °C with stirring for 4 days. The solvent was removed *in vacuo* to afford a dark oily residue, which was subsequently washed with EtOH (1 x 30 mL, 2 x 10 mL) and hexane (1 x 30 mL) to give the product **51** as a white solid. Yield: 0.6 g (59%); ^{1}H NMR (benzene-d_6, 400 MHz, 298 K) δ 7.42-7.30 (m, 12H, PPh_3), 6.93 (m, 18H, PPh_3), 6.86 (br s, 2H, C9&18-C*H*), 6.82 (br s, 2H, C12&21-C*H*), 6.25 (br s, 2H, C4&5-C*H*), 2,26 (s, 6H, C11&20-CH_3), 2.20 (s, 6H, C8&17-CH_3), 1.82 (s, 6H, C14&23-CH_3), -6.36 (ddd, J_{HPb} = 26.8, J_{HPa} =23.6, J_{HH} = 6.0 Hz, 1H, Ru-*H*), -8.08 (ddd, J_{HPb} = 81.2, J_{HPa} = 33.6, J_{HH} = 6.0 Hz, 1H, H_a). $^{31}P\{^1H\}$: δ 59.0 (d, P_a, J_{PP} = 14.8 Hz), 47.8 (d, P_b, J_{PP} = 14.8 Hz). $^{13}C\{^1H\}$: δ 205.2 (t, J_{CP} = 8.8 Hz, Ru-*C*O), 197.7 (dd, J_{CPa} = 75.5, J_{CPb} = 6.7 Hz, *C*2), 142.2 (br d, PPh_3), 142.1 (br d, PPh_3), 140.1 (br s, *C*6&15), 137.7 (br s, *C*7&16), 134.6 (d, J_{CP} = 5.4 Hz, *C*H-PPh_3), 134.4 (d, J_{CP} = 6.7 Hz, *C*H-PPh_3), 129.4 (br s, C9&18), 127.9 (s, *C*H-PPh_3), 127.4 (d, J_{CP} = 8.4 Hz, *C*H-PPh_3), 127.0 (d, J_{CP} = 8.9 Hz, *C*H-PPh_3), 122.4 (br s, *C*4&5), 21.4 (s, *C*8,11,14,17,20&23). IR (benzene-d_6, cm^{-1}): 1941 (ν_{CO}).

5.5.1.2 Synthesis of $RuH(CO)(PPh_3)_2(IMes')$ (72)

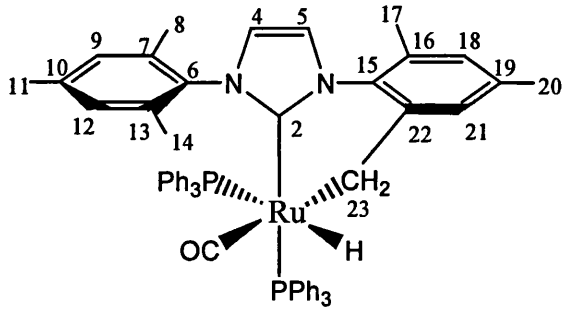

Trimethylvinylsilane (twenty equivalents) was added to $RuH_2(CO)(PPh_3)_2(IMes)$ (15 mg) dissolved in benzene-d_6 (0.6 mL). The sample was heated at 50 °C for 16 hours. The solvent was removed *in vacuo* affording a yellow solid which was subsequently dissolved in toluene (0.5 mL) and layered with hexane (1.5 mL) to obtain pale yellow crystals of **72**. Yield: 13.6 mg (92%); ^{1}H NMR (benzene-d_6, 400 MHz, 298 K): δ -7.97 (dd, 1H, J_{HP} = 102.4 Hz, J_{HP} = 30.8 Hz, Ru-H). $^{31}P\{^1H\}$ NMR: δ 53.7 (d, J_{PP} = 18.1 Hz, PPh_3), 28.4 (d, J_{PP} = 18.1 Hz, PPh_3). IR (nujol, cm^{-1}): 1919 (ν_{CO}).

5.5.2 Syntheses of $RuIMe_4$ Complexes

5.5.2.1 Synthesis of $RuH_2(CO)(PPh_3)_2(IMe_4)$ (54)

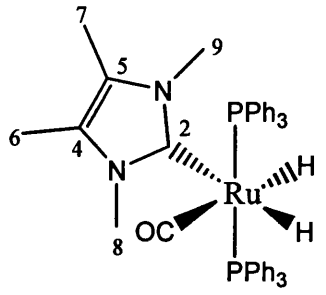

Toluene (30 mL) was added to IMe_4 (0.6 g, 4.9 mmol) and **52** (1.5 g, 1.6 mmol). The mixture was heated at 80 °C with stirring for 2 weeks. The resulting solution was reduced *in vacuo* to precipitate a yellow solid. The mixture was filtered by cannular under argon and the filtrate taken to dryness *in vacuo*. The resulting residue was washed with EtOH (2 x 10 mL) to afford **54** as a white solid. Yield: 0.65 g (51%); ^{1}H (benzene-d_6, 400 MHz, 298K): δ 8.00-7.90 (m, 12H, PPh_3), 7.07-6.89 (m, 18H, PPh_3), 3.10 (s, 3H, C8-CH_3), 2.69 (s, 3H, C9-CH_3), 1.37 (s, 3H, C6-CH_3), 1.17 (s, 3H, C7-CH_3), -5.92 (dt, J_{HP} = 26.9 Hz, J_{HH} = 5.5 Hz, 1H, Ru-*H*), -9.03 (dt, J_{HP} = 23.1 Hz, J_{HH} = 5.5 Hz, 1H, Ru-*H*). $^{31}P\{^1H\}$: δ 65.0 (s, PPh_3). $^{13}C\{^1H\}$: δ 210.2 (t, J_{CP} = 9.6 Hz, *C*O), 194.1 (t, J_{CP} = 9.6 Hz, *C*2), 142.0 (t, J_{CP} = 20.0 Hz, PPh_3), 134.9 (t, J_{CP} = 6.4 Hz, *C*H-PPh_3), 128.6 (s, *C*H-PPh_3), 128.2 (t, J_{CP} = 4.8 Hz, *C*H-PPh_3), 123.8 (s, *C*5), 123.7 (s, *C*4), 37.2 (s, *C*9), 37.0 (s, *C*8), 10.4 (s, *C*6), 10.3 (s, *C*7). IR (nujol, cm^{-1}): 1917 (ν_{CO}). Analysis for $RuC_{44}H_{44}N_2OP_2$ [found (calculated)]: C, 67.71 (67.77); H, 5.79 (5.69); N, 3.62 (3.59).

5.5.2.2 Synthesis of RuH(CO)(PPh$_3$')(PPh$_3$)(IMe$_4$) (95)

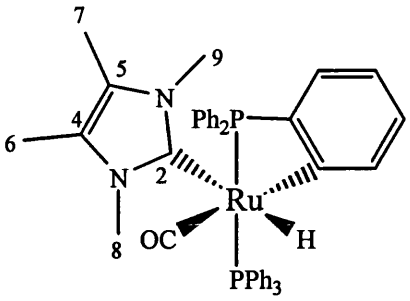

Trimethylvinylsilane (twenty equivalents) was added to **54** (15 mg, 20 μmol) dissolved in THF (0.6 mL). The sample was heated at 50 °C for 36 h to give the title compound **95** in quantitative yield. ^{1}H (benzene-d_6, 298K): δ 8.08-7.30 (m, 11H, PPh$_3$), 7.12-6.76 (m, 18H, PPh$_3$), 3.64 (s, 3H, C8-CH_3), 3.21 (s, 3H, C9-CH_3), 2.63 (s, 3H, C7-CH_3), 1.13 (s, 3H, C6-CH_3), -2.68 (t, J_{HP} = 25.3 Hz, Ru-*H*). ^{31}P{^{1}H}: δ 50.3 (d, J_{PP} = 20.6 Hz, *P*Ph$_3$), - 21.8 (d, J_{PP} = 20.6 Hz, *P*Ph$_2$C$_6$H$_4$). ^{13}C{^{1}H}: δ 208.7 (dd, J_{CP} = 15.5 Hz, J_{CP} = 7.8 Hz, CO), 189.9 (dd, J_{CP} = 80.2 Hz, J_{CP} = 7.8 Hz, C2), 165.8 (dd, J_{CP} = 68.1 Hz, J_{CP} = 12.1 Hz, PPh$_3$), 130-129 (m, PPh$_3$), 128.3-127.8 (m, PPh$_3$), 133.4 (dd, J_{CP} = 57.8 Hz, J_{CP} = 10.3 Hz, PPh$_3$), 132.2 (d, J_{CP} = 2.6 Hz, PPh$_3$), 126.4 (d, J_{CP} = 5.2 Hz *C*5), 124.4 (d, J_{CP} = 1.7 Hz, *C*4), 38.2 (s, *C*8), 37.0 (s, *C*9), 34.8 (s, *C*7), 9.0 (s, *C*6).

5.5.2.3 Synthesis of RuH$_2$(CO)(PPh$_3$)(IMe$_4$)$_2$ (55)

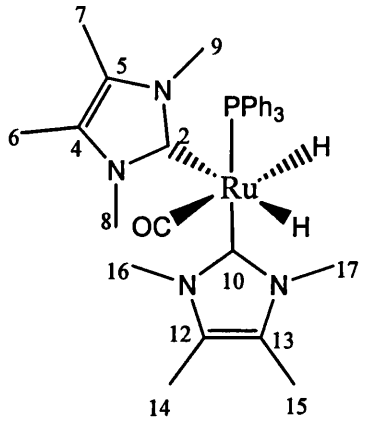

Toluene (30 mL) was added to IMe$_4$ (0.6 g, 4.9 mmol) and **52** (1.5 g, 1.6 mmol). The mixture was heated at 80 °C with stirring for 2 weeks. The resulting solution was

reduced down to precipitate a yellow solid. The mixture was filtered and the resulting residue washed with hexane (2 x 10 mL) to yield a pale yellow solid (**55**). Yield: 0.45 g (43%); ^{1}H NMR (THF-d_8, 400 MHz, 298K): δ 7.25-7.13 (m, 6H, PPh_3), 6.81-6.60 (m, 9H, PPh_3), 3.17 (s, 6H, C16&17-CH_3), 3.00 (s, 3H, C8–CH_3), 2.62 (s, 3H, C9–CH_3), 1.66 (s, 6H, C14&15-CH_3), 1.47(s, 3H, C6–CH_3), 1.45 (s, 3H, C7–CH_3), -6.37 (dd, J_{HP} = 37.3 Hz, J_{HH} = 4.9 Hz, Ru-*H*), -9.75 (dd, J_{HP} = 26.3 Hz, J_{HH} = 4.9 Hz, 1H, Ru-*H*). ^{31}P{^{1}H}: δ 65.0 (s, *P*Ph_3). ^{13}C{^{1}H}: δ 209.6 (d, J_{CP} = 9.2 Hz, *C*O), 197.2 (d, J_{CP} = 9.2 Hz, *C*2), 193.3 (d, J_{CP} = 82.7, *C*10), 144.0 (d, J_{CP} = 33.1 Hz, PPh_3), 134.4 (d, J_{CP} = 11.9 Hz, *C*H, PPh_3), 127.7 (s, *C*H, PPh_3), 127.1 (d, J_{CP} = 8.3 Hz, *C*H, PPh_3), 123.5 (s, *C*5), 123.3 (s, *C*12&13), 123.3 (s, *C*4), 37.0 (s, *C*16&17), 36.2 (s, *C*8), 35.9 (s, *C*9), 9.6 (s, C14&15), 9.6 (s, *C*7), 9.5 (s, *C*6). IR (nujol, cm^{-1}): 1886 (ν_{CO}).

5.5.3 Syntheses of $RuIEt_2Me_2$ Complexes

5.5.3.1 Synthesis of $RuH_2(CO)(PPh_3)_2(IEt_2Me_2)$ (57)

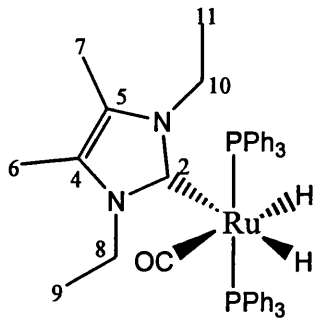

Toluene (30 mL) was added to IEt_2Me_2 (0.7 g, 4.6 mmol) and **52** (1.4 g, 1.5 mmol). The mixture was heated at 70 °C with stirring for 20 h. The volatiles were removed *in vacuo* and the red/brown oily residue was washed with EtOH (1 x 30 mL) and filtered. The resulting solid was dissolved in benzene (5 mL) and heated at 70 °C for 1 h. The volatiles were removed *in vacuo* and the resulting solid dissolved in THF (10 mL) and layered with hexane (20 mL) affording **57** as a white crystalline solid. Yield: 0.6 g (49%); ^{1}H NMR (THF-d_8, 400 MHz, 298K): δ 7.62-7.48 (m, 12H, PPh_3), 7.25-7.07 (m, 18H, PPh_3), 3.69 (q, J_{HH} = 6.6 Hz, 2H, C8-CH_2), 3.28 (q, J_{HH} = 6.6 Hz, 2H, C10-CH_2), 2.00 (s, 3H, C6-CH_3), 1.72 (s, 3H, C7-CH_3), 1.01 (t, J_{HH} = 6.6

Hz, 3H, C9-CH_3), 0.34 (t, J_{HH} = 6.6 Hz, 3H, C11-CH_3), -6.38 (dt, J_{HP} = 26.3 Hz, J_{HH} = 5.5 Hz, 1H, Ru-*H*), -9.99 (dt, J_{HP} = 24.7 Hz, J_{HH} = 5.5 Hz, 1H, Ru-*H*). $^{31}P\{^1H\}$: δ 63.7 (s, *P*Ph_3). $^{13}C\{^1H\}$: δ 208.3 (t, J_{CP} = 9.2 Hz, *C*O), 191.1 (t, J_{CP} = 8.3 Hz, *C*2), 141.6 (t, J_{CP} = 19.3 Hz, PPh_3), 134.6 (t, J_{CP} = 6.4 Hz, PPh_3), 128.6 (s, *C*H-PPh_3), 127.6 (t, J_{CP} = 4.6 Hz, *C*H-PPh_3), 124.2 (s, *C*4), 124.1 (s, *C*5), 43.9 (s, *C*10), 43.7 (s, *C*8), 15.9 (s, *C*9), 14.2 (s, *C*11), 9.6 (s, *C*7), 9.4 (s, *C*6). IR (benzene-d_6, cm^{-1}): 1921 (ν_{CO}). Analysis for $RuC_{46}H_{48}N_2OP_2$ [found (calculated)]: C, 68.6 (68.39); H, 6.08 (5.99); N, 3.46 (3.47).

5.5.3.2 Synthesis of $RuH(CO)(PPh_3)_2(IEt_2Me_2')$ (85a)

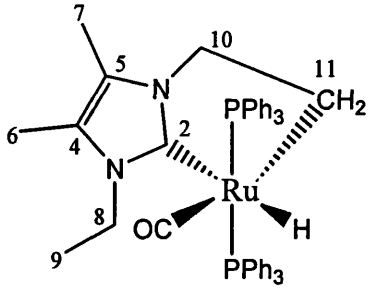

Trimethylvinylsilane (248 μL, 100 equivalents) was added to **57** (15 mg) dissolved in THF (0.6 mL). The sample was heated at 50 °C for 16 h. $^{31}P\{^1H\}$ NMR spectroscopy indicated complete conversion to the C-H activated complex. The solvent was removed *in vacuo* affording a yellow solid. Yellow crystals for X-ray analysis were grown by layering a THF solution with hexane. ^1H NMR (benzene-d_6, 400 MHz, 298 K): δ 7.96-7.84 (m, 12H, PPh_3), 7.11-6.87 (m, 18H, PPh_3), 3.28 (q, J_{HH} = 7.1 Hz, 2H, C8-CH_2), 2.67-2.78 (m, 2H, C10-CH_2), 1.50 (s, 3H, C6-CH_3), 1.34(s, 3H, C7-CH_3), 1.28-1.16 (m, 2H, C11-CH_2), 0.73 (t, J_{HH} = 7.1 Hz, 3H, C9-CH_3), -7.01 (t, J_{HP} = 23.1 Hz, 1H, Ru-*H*). $^{31}P\{^1H\}$: δ 61.1 (s, *P*Ph_3). $^{13}C\{^1H\}$: δ 206.4 (t, J_{CP} = 11.7 Hz, *C*O), 191.7 (t, J_{CP} = 8.8 Hz, Ru-*C*2), 139.3 (t, J_{CP} = 19.0 Hz, PPh_3), 134.3 (t, J_{CP} = 5.9 Hz, PPh_3), 128.4 (s, *C*H-PPh_3), 127.6 (t, J_{CP} = 4.4 Hz, *C*H-PPh_3), 122.3 (m, *C*4&5), 50.2 (s, *C*10), 42.9 (s, *C*8), 15.7 (s, *C*9), 9.5 (s, *C*7), 8.9 (s, *C*6), 8.3 (t, J_{CP} = 11.0 Hz, *C*11). IR (benzene-d_6, cm^{-1}): 1895 (ν_{CO}). Analysis for $RuC_{46}H_{46}N_2OP_2$ [found (calculated)]: C, 68.7 (68.56); H, 6.38 (5.75); N, 3.20 (3.48).

5.5.3.3 Synthesis of *trans*-$RuH_2(CO)(PPh_3)_2(IEt_2Me_2)$ (86)

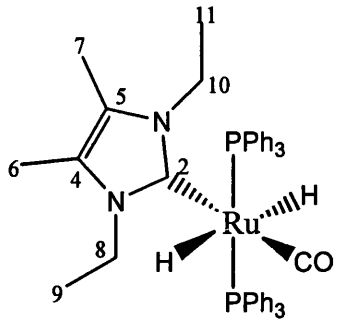

85a (0.50 g, 0.62 mmol) was stirred in EtOH (10 mL) for 16 h at room temperature. The resulting green precipitate was filtered and washed with THF (10 mL), affording **86** as a white solid. Yield: 0.37 g (74%); ^{1}H NMR (pyridine-d_5, 400 MHz, 298 K): δ 7.51-7.40 (m, 12H, PPh_3), 7.39-7.30 (m, 18H, PPh_3) 3.93 (q, J_{HH} = 7.1 Hz, 4H, C8&10-CH_2), 1.76 (s, 6H, C6&7-CH_3), 0.67 (t, J_{HH}=7.1 Hz, 6H, C9&11-CH_3), -4.90 (t, J_{HP} = 20.3 Hz, 2H, Ru-*H*). ^{31}P{^{1}H}: δ 63.2 (s, *P*Ph_3). ^{13}C{^{1}H}: δ 209.9 (*C*O*), 183.6 (Ru-*C*2*), 139.5 (t, J_{CP} = 19.2 Hz, PPh_3), 134.3 (m, PPh_3), 128.6 (m, PPh_3), 127.3 (m, PPh_3), 124.4 (s, *C*4&5), 43.2 (s, *C*8&10), 14.3 (s, *C*6&7), 9.3 (s, *C*9&11). IR (nujol, cm^{-1}): 1905 (ν_{CO}). Analysis for $RuC_{46}H_{48}N_2OP_2$ [found (calculated)]: C, 68.2 (68.39); H, 6.00 (5.99); N, 3.51 (3.47).

* Due to low solubility and rapid isomerisation, ^{13}C shifts obtained by ^{13}C-^{1}H HMBC spectroscopy.

5.5.3.4 Synthesis of $RuH_2(CO)(PPh_3)(IEt_2Me_2)_2$ (60)

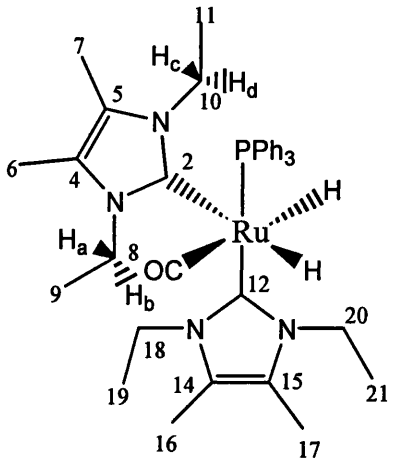

Toluene (15 mL) was added to **52** (0.54 g, 0.58 mmol) and IEt_2Me_2 (0.46 g, 2.3 mmol) and heated at 70 °C for 20 h. The reaction was cooled to room temperature to precipitate a white solid from a red solution. The mixture was filtered and the red solution reduced to an oily residue, washed with hexane (3 x 5 mL) to yield **60** as a pale purple solid. Yield: 0.12 g (29%) ^{1}H NMR (benzene-d_6, 298 K): δ 8.04-7.94 (m, 6H, PPh_3), 7.13-7.05 (m, 3H, PPh_3), 7.04-6.97 (m, 3H, PPh_3), 5.17 (dq, J_{HaHb} = 14.3 Hz, J_{HH} = 7.1 Hz, 1H, C8-CH_b), 4.58 (m, 4H, C18&20-CH_2), 4.33 (dq, J_{HcHd} = 14.3 Hz, J_{HH} = 7.1 Hz, 1H, C10-CH_d), 3.45 (dq, J_{HcHd} = 14.3 Hz, J_{HH} = 7.1 Hz, 1H, C10-CHc), 3.01 (dq, J_{HaHb} = 14.3 Hz, J_{HH} = 7.1 Hz, 1H, C8-CH_a), 1.67 (s, 6H, C16&17-CH_3), 1.59 (s, 3H, C6-CH_3), 1.57 (s, 3H, C7-CH_3), 1.30 (t, J_{HH} = 7.1 Hz, 3H, C9-CH_3), 1.16 (t, J_{HH} = 7.1 Hz, 6H, C19&21-CH_3), 0.54 (t, J_{HH} = 7.1 Hz, 3H, C11-CH_3), -5.52 (dd, J_{HP} = 39.5 Hz, J_{HH} = 4.9 Hz, 1H, Ru-*H*), -8.93 (dd, J_{HP} = 26.9 Hz, J_{HH} = 4.9 Hz, 1H, Ru-*H*). ^{31}P{^{1}H}: δ 63.4 (s, *P*Ph_3). ^{13}C{^{1}H}: δ 210.2 (d, J_{CP} = 8.3 Hz, *C*O), 196.2 (d, J_{CP} = 8.3 Hz, *C*2), 191.4 (d, J_{CP} = 80.9 Hz, 144.7 (d, J_{CP} = 34.0 Hz, PPh_3), 129.5 (d, J_{CP} = 6.4 Hz, *C*H-PPh_3), 129.0 (s, *C*H-PPh_3), 127.8 (d, J_{CP} = 8.3 Hz, *C*H-PPh_3), 123.9 (s, *C*5), 123.8 (s, *C*4), 123.7 (s, *C*14&15), 45.0 (s, *C*18&20), 44.5 (s, *C*8), 44.0 (s, *C*10), 16.5 (s, *C*7), 15.3 (s, *C*16&17), 14.9 (s, *C*6), 10.1 (s, *C*19&21), 9.4 (s, *C*11), 8.0 (s, *C*9). IR (nujol, cm^{-1}): 1874 (ν_{CO}).

5.5.4 Syntheses of Ru$I^iPr_2Me_2$ Complexes

5.5.4.1 Synthesis of $RuH(CO)(PPh_3)_2(I^iPr_2Me_2')$ (62a)

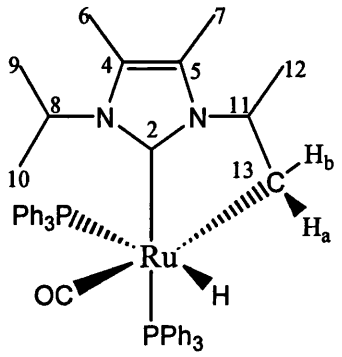

Toluene (30 mL) was added to $I^iPr_2Me_2$ (0.8 g, 4.4 mmol) and **52** (1.0 g, 1.1 mmol) in a Schlenk flask under argon. The mixture was stirred at 70 °C for 20 h. The solution was removed *in vacuo* and EtOH (20 mL) was added. The resulting red

solution was stirred overnight to afford an off-white precipitate. The mixture was filtered and the solid washed with hexane (2 x 10 mL) to yield the C-H activated product **62a** as a white solid. Yield: 0.6 g (66%); ^{1}H NMR (benzene-d_6, 400 MHz, 298 K): δ 7.76-7.60 (m, 6H, PPh_3), 7.41-7.28 (m, 6H, PPh_3), 7.08-6.91 (m, 18H, PPh_3), 5.50 (sept, J_{HH} =7.1 Hz, 1H, C8-C*H*), 4.28 (m, 1H, C11-C*H*), 2.06-1.90 (m, 1H, C13-CH_b), 1.76 (s, 3H, C6-CH_3), 1.66 (s, 3H, C7-CH_3), 1.37 (d, J_{HH} = 7.1 Hz, 3H, C9-CH_3), 1.28 (d, 6.0 Hz, 3H, C12-CH_3), 0.54 (d, J_{HH} = 7.1 Hz, 3H, C10-CH_3), 0.50-0.42 (m, 1H, C13-CH_a), -7.72 (dd, J_{HP} = 104.8 Hz, J_{HP} = 28 Hz, 1H, Ru-*H*). ^{31}P{^{1}H}: δ 56.49 (d, J_{PP} = 16.7 Hz, *P*Ph_3), 35.79 (d, J_{PP} = 16.7 Hz, *P*Ph_3). ^{13}C{^{1}H}: δ 207.4 (dd, J_{CP} = 5.5 Hz, J_{CP} = 13.8 Hz, *C*O), 187.8 (dd, J_{CP} = 10.1 Hz, J_{CP} = 82.7 Hz, *C*2), 140.3 (dd, J_{CP} = 34.9 Hz, J_{CP} = 1.8 Hz, PPh_3), 140.0 (dd, J_{CP} = 23.0 Hz, J_{CP} = 1.8 Hz, PPh_3), 135.5 (d, J_{CP} = 11.0 Hz, *C*H-PPh_3), 134.8 (d, J_{CP} = 11.0 Hz, *C*H-PPh_3), 129.4-129.0 (m, PPh_3), 128.4-128.1 (m, PPh_3), 124.0 (s, *C*4), 123.2 (s, *C*5), 59.1-58.8 (m, *C*11), 54.0 (s, *C*8), 24.5 (t, J_{CP} = 7.4 Hz, *C*13), 23.9 (s, *C*9), 22.4 (s, *C*12), 21.4 (s, *C*10), 11.3 (s, *C*7), 10.0 (s, *C*6). IR (benzene-d_6, cm^{-1}): 1884 (ν_{CO}). Analysis for $RuC_{48}H_{50}N_2OP_2$ [found (calculated)]: C, 68.57 (69.13); H, 6.40 (6.04); N, 3.25 (3.15).

5.5.4.2 Synthesis of $RuH_2(CO)(PPh_3)_2(I^iPr_2Me_2)$ (61)

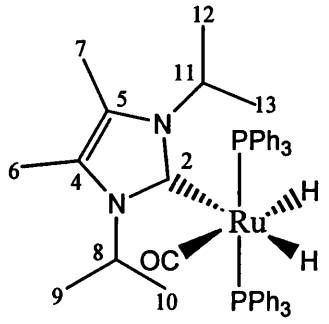

Method 1: 62a (0.50 g, 0.6 mmol) was dissolved in the minimum amount of warm benzene (10-15 mL) and H_2 was bubbled through for 2 h at 50 °C. The solution was cooled to room temperature to precipitate a white solid. The solvent was removed by filtration and the white solid further purified by washing with hexane. Yield: 0.47 g (93%). **Method 2: 62a** (0.50 g, 0.6 mmol) was dissolved in the minimum amount of warm benzene (10-15 mL) and IPA (12 mmol, 919 μL) was added and the reaction

heated at 70 °C for 2 h. The solution was cooled to room temperature to precipitate a white solid. The solvent was removed by filtration and the white solid further purified by layering a THF solution with hexane. Yield: 0.28 g (56%); ^{1}H NMR (benzene-d_6, 400 MHz, 298 K): δ 7.73-7.93 (m, 12H, PPh_3), 6.94-7.11 (m, 18H, PPh_3), 6.36 (sept, J_{HH} = 7.1 Hz, 1H, C8-C*H*), 6.08 (sept, J_{HH} = 7.1 Hz, 1H, C11-C*H*), 1.82 (s, 3H, C6-CH_3), 1.70 (s, 3H, C7-CH_3), 1.08 (d, J_{HH} = 7.1 Hz, 6H, C9&10-CH_3), 0.48 (d, J_{HH} = 7.1 Hz, 6H, C12&13-CH_3), -5.79 (dt, 1H, J_{HH} = 6.0 Hz, J_{HP} = 26.9 Hz, Ru-*H*), -9.98 (dt, 1H, J_{HH} = 6.0 Hz, J_{HP} = 26.9 Hz, Ru-*H*). ^{31}P{^{1}H}: δ 61.3 (s, *P*Ph_3). ^{13}C{^{1}H}: δ 208.2 (t, J_{CP} = 9.2 Hz, *C*O), 195.8 (t, J_{CP} = 8.3 Hz, *C*2), 142.6 (t, J_{CP} = 19.3 Hz, PPh_3), 135.1 (t, J_{CP} = 6.4 Hz, *C*H-PPh_3), 129.2 (s, *C*H-PPh_3), 128.3 (t, J_{CP} = 4.6 Hz, *C*H-PPh_3), 126.2 (s, *C*5), 125.9 (s, *C*4), 54.5 (s, *C*11), 54.3 (s, *C*8), 22.6 (s, *C*9&10), 21.4 (s, *C*12&13), 11.5 (s, *C*6&7). IR (benzene-d_6, cm^{-1}): 1917 (ν_{CO}). Analysis for $RuC_{48}H_{52}N_2OP_2$ [found (calculated)]: C, 68.97 (69.00); H, 6.27 (6.07); N, 3.35 (3.03).

5.5.5 Syntheses of Ru(I^{i}Pr) Complexes

5.5.5.1 Synthesis of $RuH_2(CO)(PPh_3)_2$(I^{i}Pr) (58)

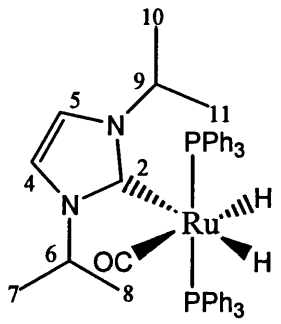

Toluene (30 mL) was added to I^{i}Pr (0.7 g, 4.4 mmol) and **52** (1.0 g, 1.1 mmol). The mixture was stirred at 70 °C for 20 h. The solution was removed *in vacuo* and EtOH (20 mL) was added. The resulting red solution was stirred overnight to afford an off-white precipitate. The mixture was filtered and the solid washed with hexane. Yield: 0.48 g (55%); ^{1}H NMR (benzene-d_6, 400 MHz, 298 K): δ 7.87-7.73 (m, 12H, PPh_3), 7.11-6.94 (m, 18H, PPh_3), 6.47 (d, J_{HH} = 1.6 Hz, 1H, C4-C*H*), 6.30 (d, J_{HH} = 1.6 Hz, 1H, C5-C*H*), 5.56 (sept, J_{HH} = 6.6 Hz, 1H, C6-C*H*), 5.31 (sept, J_{HH} = 6.6 Hz, 1H, C9-

C*H*), 0.96 (d, J_{HH} = 6.6 Hz, C7&8-CH_3), 0.38 (d, J_{HH} = 6.6 Hz, 6H, C10&11-CH_3), -5.89 (dt, J_{HP} = 26.9 Hz, J_{HH} = 6.0 Hz, 1H, Ru-*H*), -9.46 (dt, J_{HP} = 26.9 Hz, J_{HH} = 6.0 Hz, 1H, Ru-*H*). ^{31}P {^{1}H}: δ 61.4 (s, *P*Ph$_3$). ^{13}C{^{1}H}: δ 208.5 (t, J_{CP} = 9.2 Hz, *C*O), 194.7 (t, J_{CP} = 8.3 Hz, *C*2), 142.3 (t, J_{CP} = 20.2 Hz, PPh$_3$), 135.0 (t, J_{CP} = 6.4 Hz, *C*H, PPh$_3$), 129.2 (s, *C*H-PPh$_3$), 128.4 (t, J_{CP} = 4.6 Hz, *C*H-PPh$_3$), 117.1 (s, *C*5), 116.8 (s, *C*4), 52.8 (s, *C*9), 52.5 (s, *C*6), 24.0 (s, *C*7&8), 22.9 (s, *C*10&11). IR (nujol, cm^{-1}): 1930 (ν_{CO}). Analysis for $RuC_{46}H_{48}N_2OP_2$ [found (calculated)]: C, 68.17 (68.38); H, 6.09 (5.89); 3.39 (3.47).

5.5.5.2 Synthesis of RuH(CO)(PPh$_3$)$_2$(I^{i}Pr′) (93)

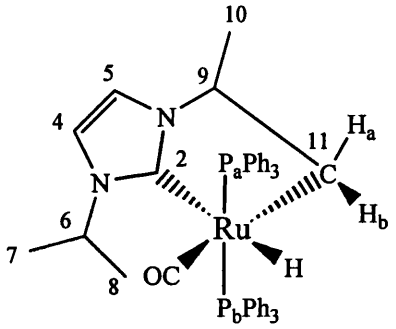

Trimethylvinylsilane (50 equivalents) was added to **58** (15 mg) dissolved in benzene-d_6 (0.6 mL). The sample was heated at 50 °C for 16 h. ^{31}P{^{1}H} NMR spectroscopy indicated complete conversion to the C-H activated complex. The solvent was removed *in vacuo* affording the title compound **93** as an orange solid in quantitative yield. ^{1}H NMR (benzene-d_6, 400 MHz, 298 K): δ 7.91-7.69 (m, 12H, PPh$_3$), 7.13-6.87 (m, 18H, PPh$_3$), 6.26 (d, J_{HH} = 1.6 Hz, 1H, C4-C*H*), 6.20 (d, J_{HH} = 1.6 Hz, 1H, C5-C*H*), 4.61 (sept, J_{HH} = 6.6 Hz, 1H, C6-C*H*), 3.29-3.15 (m, 1H, C9-C*H*), 1.37-1.22 (m, 1H, C11-CH_b), 1.01-0.87 (m, 1H, C11-CH_a), 0.77 (d, J_{HH} = 6.6 Hz, 3H, C8-CH_3), 0.72 (d, J_{HH} = 6.6 Hz, 3H, C11-CH_3), 0.64 (d, J_{HH} = 6.6 Hz, 3H, C7-CH_3), -7.20 (t, J_{HP} = 24.7 Hz, 1H, Ru-*H*). ^{31}P {^{1}H}: δ 60.7 (d, J_{PP} = 294.9 Hz, *P*Ph$_3$), 58.4 (d, J_{PP} = 294.9 Hz, *P*Ph$_3$). ^{13}C{^{1}H}: δ 207.0 (t, J_{CP} = 12.9 Hz, *C*O), 195.8 (t, J_{CP} = 8.3 Hz, *C*2), 140.3 (dd, J_{CPa} = 22.1 Hz, J_{CPb} = 9.2 Hz, PPh$_3$), 140.0 (J_{CPb} = 22.1 Hz, J_{CPa} = 9.2 Hz, PPh$_3$), 135.1 (dd, J_{CPa} = 20.2 Hz, J_{CPb} = 2.8 Hz, *C*H-PPh$_3$), 135.0 (dd, J_{CPb} = 20.2 Hz, J_{CPa} = 2.8 Hz, *C*H-PPh$_3$), 129.2 (d, J_{CP} = 12.9 Hz, *C*H-PPh$_3$), 128.5 (d, J_{CP} = 12.9 Hz, *C*H-PPh$_3$), 118.0 (s, *C*5), 116.0 (s, *C*4), 60.9 (s, *C*9), 52.0 (s, *C*6), 25.4 (s, *C*10), 24.1 (t,

J_{CP} = 11.0 Hz, *C*11), 24.0 (s, *C*7), 22.9 (s, *C*10).

5.5.6 Syntheses of Ru(I*) Complexes

5.5.6.1 Synthesis of $RuH_2(CO)(PPh_3)_2(I^*)$ (59a)

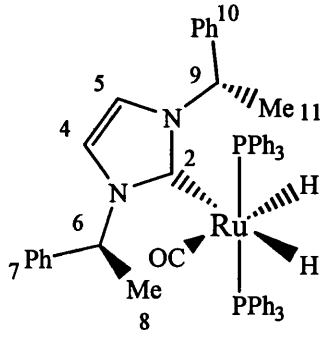

Toluene (20 mL) was added to I^* (0.6 g, 2.2 mmol) and **52** (0.5 g, 0.5 mmol). The mixture was stirred at 70 °C for 20 h. The solution was removed *in vacuo* and EtOH (20 mL) was added. The resulting red solution was stirred for one week to afford an off-white precipitate. The mixture was filtered and the solid washed with hexane (2 x 10 mL) to yield the mono carbene complex, **59a**, as a white solid. Yield: 0.23 g (46%); ^{1}H NMR (benzene-d_6, 400 MHz, 298 K): δ 7.83-7.72 (m, 6H, PPh_3), 7.68-7.50 (m, 6H, PPh_3), 7.05 (m*, C9-C*H*), 7.03-6.95 (m, 28 H, PPh_3 and C7&10-Ph), 6.84 (m*, C6-C*H*), 6.67 (s, 2H C4&5-C*H*), 0.97 (d, J_{HH} = 7.1 Hz, 3H, C8-CH_3), 0.58 (d, J_{HH} = 7.1 Hz, 3H, C11-CH_3), -5.72 (ddd, J_{HP} = 28.0 Hz, J_{HP} = 22.0 Hz, J_{HH} = 5.5 Hz, 1H, Ru-*H*), -9.81 (dt, J_{HP} = 28.0 Hz, J_{HH} = 5.5 Hz, 1H, Ru-*H*). ^{31}P{^{1}H}: δ 63.7 (d, J_{PP} = 245.9 Hz, *P*Ph_3), 57.6 (d, J_{PP} = 245.9 Hz, *P*Ph_3). ^{13}C{^{1}H}: δ 208.2 (t, J_{CP} = 9.2 Hz, *C*O), 198.0 (t, J_{CP} = 8.3 Hz, *C*2), 144.2 (s, Ph), 143.8 (s, Ph), 142.9 (dd, J_{CP} = 37.7 Hz, J_{CP} = 2.8 Hz, PPh_3), 141.8 (dd, J_{CP} = 37.7 Hz, J_{CP} = 2.8 Hz, PPh_3), 135.2 (d, J_{CP} = 11.9 Hz, PPh_3), 134.8 (d, J_{CP} = 11.9 Hz, PPh_3), 133.1 (s, Ph), 133.0 (s, Ph), 132.2 (2 x s, Ph), 129.4-129.0 (m, PPh_3 and Ph), 128.4-127.9 (m, PPh_3 and Ph), 119.1 (2 x s, *C*4&5), 60.0 (s, *C*9), 59.9 (s, *C*6), 23.1 (s, *C*11), 22.8 (s, *C*8). IR (nujol, cm^{-1}): 1942 (ν_{CO}).

*C9 and C6 were assigned from the COSY spectrum. The resonances were not defined enough to assign couplings.

5.5.6.2 Synthesis of RuH(CO)(PPh_3)$_2$($I^{*\prime}$) (94a)

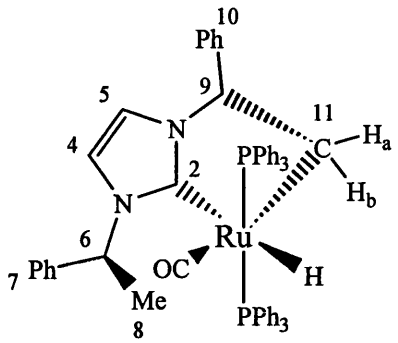

Trimethylvinylsilane (twenty equivalents) was added to **59a** (15.0 mg) dissolved in benzene-d_6 (0.6 mL). The sample was heated at 50 °C for 16 h. $^{31}P\{^1H\}$ NMR spectroscopy indicated complete conversion to the C-H activated complex. The solvent was removed *in vacuo* affording the title complex **94a** as a yellow solid in quantitative yield. ^1H NMR (benzene-d_6, 400 MHz, 298 K): δ 7.94-7.82 (m, 6H, PPh_3), 7.62-7.52 (m, 6H, PPh_3), 7.21-6.78 (m, 28 H, PPh_3 and C7&10-Ph), 6.15 (d, J_{HH} = 1.6 Hz, 1H, C5-C*H*), 6.05 (q, J_{HH} = 7.1 Hz, 1H, C6-C*H*), 4.37-4.26 (m, 1H, C9-C*H*), 1.52-1.41 (m, 1H, C11-CH_a), 1.30-1.23 (m, 1H, C11-H_b), 0.94 (d, J_{HH} = 7.1 Hz, 3H, C8-CH_3), -7.20 (t, J_{HP} = 26.3 Hz, 1H, Ru-*H*). $^{31}P\{^1H\}$: δ 57.8 (s, *P*Ph_3), 57.7 (s, *P*Ph_3).* $^{13}C\{^1H\}$: δ 207.6 (t, J_{CP} = 12.2 Hz, *C*O), 198.4 (t, J_{CP} = 8.0 Hz, *C*2), 148.5 (s, *C*10-Ph), 143.1 (s, *C*7-Ph), 140.1 (dd, J_{CP} = 32.2 Hz, J_{CP} = 13.8 Hz, PPh_3), 135.5 (dd, J_{CP} = 7.4 Hz, J_{CP} = 4.6 Hz, CH-PPh_3), 135.0 (dd, J_{CP} = 7.4 Hz, J_{CP} = 4.6 Hz, *C*H-PPh_3), 129.8-129.1 (m, PPh_3 and Ph), 128.4-127.3 (m, PPh_3 and Ph), 120.3 (s, *C*5), 118.1 (s, *C*4), 72.5 (s, *C*9), 60.4 (s, *C*6), 29.0 (t, J_{CP} = 10.1 Hz, *C*11), 23.1 (s, *C*8). IR (benzene-d_6, cm^{-1}): 1895 (ν_{CO}).

* The outer resonances of the AB system could not be detected in the ^{31}P NMR spectrum.

5.5.7 Syntheses of Ru(ICy) Complexes

All syntheses of Ru(ICy) complexes were provided by Suzanne Burling.[7]

5.5.7.1 Synthesis of $RuH_2(CO)(PPh_3)_2(ICy)$ (64)

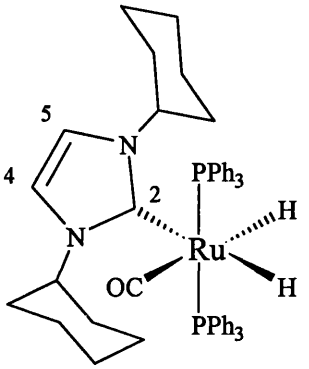

Toluene (20 mL) was added to ICy (0.2 g, 0.9 mmol) and **52** (0.4 g, 0.4 mmol) in a Schlenk flask under argon. The mixture was heated at 70 °C with stirring for 16 h. The volatiles were removed *in vacuo* and the residue washed with EtOH (2 x 10 mL) and filtered. The resulting cream solid was dissolved in THF and layered with hexane affording **64** as fine cream-coloured crystals. Yield: 0.2 g (51%); ^{1}H NMR (benzene-d_6, 400 MHz, 298K): δ 7.85-7.80 (m, 12H, PPh_3), 7.09-6.99 (m, 18H, PPh_3), 6.58 (d, J_{HH} = 1.6 Hz, 1H, C4-C*H*), 6.38 (d, J_{HH} = 1.6 Hz, 1H, C5-C*H*), 5.18 (m, 1H, C*H*-Cy), 4.80 (m, 1H, C*H*-Cy), 1.73 (m, 2H, CH_2-Cy), 1.49-0.57 (m, 18H, Cy), -5.93 (dt, J_{HP} = 26.3, J_{HH} = 6.0 Hz, 1H, Ru-*H*), -9.49 (dt, J_{HP} = 26.9, J_{HH} = 6.0 Hz, 1H, Ru-*H*). ^{31}P{^{1}H}: δ 62.8 (s, *P*Ph_3). ^{13}C{^{1}H}: δ 206.6 (t, J_{CP} = 9.5 Hz, *C*O), 193.1 (t, J_{CP} = 7.8 Hz, *C*2), 140.5 (t, J_{CP} = 19.8 Hz, PPh_3), 133.4 (t, J_{CP} = 6.0 Hz, PPh_3), 127.6 (s, PPh_3), 126.7 (t, J_{CP} = 4.3 Hz, PPh_3), 116.0 (s, *C*5), 115.4 (s, *C*4), 58.5 (s, *C*H-Cy), 58.2 (s, *C*H-Cy), 33.3 (s, *C*H_2-Cy), 32.0 (s, *C*H_2-Cy), 25.1 (s, *C*H_2-Cy), 25.0 (s, *C*H_2-Cy), 24.9 (s, *C*H_2-Cy), 24.7 (s, *C*H_2-Cy). IR (nujol, cm^{-1}): 1931 (ν_{CO}). Analysis for $C_{52}H_{56}N_2OP_2Ru$ [found (calculated)]: C, 70.3 (70.33); H, 6.30 (6.36); N, 3.32 (3.15).

5.5.7.2 Synthesis of $RuH_2(CO)(PPh_3)(ICy)_2$ (66)

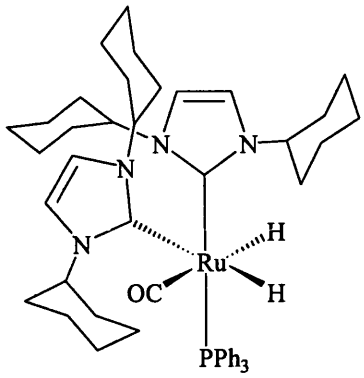

Toluene (20 mL) was added to ICy (230 mg, 1.0 mmol) and **52** (300 mg, 0.33 mmol) in a Schlenk flask under argon. The mixture was heated at 70 °C with stirring for 16 h. The volatiles were removed *in vacuo* and the residue was washed with hexane (3 x 10 mL) and filtered. The resulting cream solid was dissolved in THF and layered with hexane affording **66** as small cream-coloured crystals. Yield: 175.0 mg (62%); ^{1}H NMR (benzene-d_6, 400 MHz, 298K): δ 7.88 (m, 6H, PPh_3), 7.12 (m, 6H, PPh_3), 7.04 (m, 3H, PPh_3), 6.63 (br s, 2H, im-C*H*), 6.59 (d, J_{HH} = 2.2 Hz, 1H, im-C*H*), 6.56 (d, J_{HH} = 2.2 Hz, 1H, im-C*H*), 5.93 (br s, 2H, C*H*-Cy), 5.48 (m, 1H, C*H*-Cy), 5.28 (m, 1H, C*H*-Cy), 2.91 (m, 1H, C*H*-Cy), 2.37 (m, 2H, CH_2-Cy), 1.87-0.77 (m, 37H, Cy), -5.39 (dd, J_{HP} = 40.1, J_{HH} = 4.4 Hz, 1H, Ru-*H*), -9.10 (dd, J_{HP} = 30.2, J_{HH} = 4.4 Hz, 1H, Ru-*H*). ^{31}P{^{1}H}: δ 60.8 (s, *P*Ph_3). ^{13}C{^{1}H}: δ 207.3 (d, J_{CP} = 8.6 Hz, *C*O), 197.7 (d, J_{CP} = 6.9 Hz, Ru-*C*), 192.4 (d, J_{CP} = 82.8 Hz, Ru-*C*, *trans*-PPh_3), 144.0 (d, J_{CP} = 34.5 Hz, PPh_3), 134.0 (d, J_{CP} = 11.2 Hz, PPh_3), 127.6 (s, PPh_3), 127.1 (d, J_{CP} = 8.6 Hz, PPh_3), 116.1 (s, im-*C*H), 116.0 (s, im-*C*H), 59.3 (s, *C*H-Cy), 59.2 (s, *C*H-Cy), 58.0 (s, *C*H-Cy), 36.1 (s, *C*H_2-Cy), 34.0 (s, *C*H_2-Cy), 33.1 (s, *C*H_2-Cy), 32.4 (s, *C*H_2-Cy), 25.7 - 25.4 (7 x *C*H_2-Cy). IR (nujol, cm^{-1}): 1865 (ν_{CO}). Analysis for $C_{49}H_{65}N_4OPRu$ [found (calculated)]: C, 68.2 (68.58); H, 7.53 (7.63); N, 6.28 (6.53).

5.5.8 Synthesis of $RuH_2(CO)(PPh_3)_2(^nPr)$ (65)

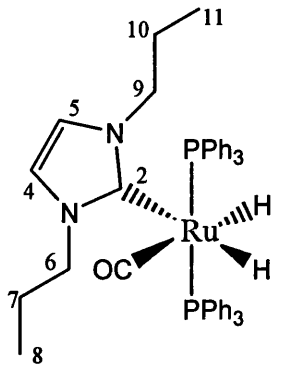

Toluene (30 mL) was added to I^{n}Pr (0.45 g, 2.97 mmol) and **52** (0.45 g, 0.50 mmol). The mixture was stirred at 70 °C for 20 h. The solution was removed *in vacuo* and EtOH (20 mL) was added. The resulting red solution was stirred over 3 days to afford an off-white precipitate. The mixture was filtered and the solid washed with hexane. Yield: 0.10 g (25%); ^{1}H NMR (benzene-d_6, 400 MHz, 298K): δ 7.85-7.80 (m, 12H, PPh_3), 7.09-6.98 (m, 18H, PPh_3), 6.15 (d, 1H, J_{HH} = 2.2 Hz, im-C*H*), 5.96 (d, 1H, J_{HH} = 2.2 Hz, im-C*H*), 3.59 (m, 2H, N-CH_2), 3.31 (m, 2H, N-CH_2), 1.45 (m, 2H, CH_2-CH_3), 0.84 (m, 2H, CH_2-CH_3), 0.67 (t, 3H, J_{HH} = 7.1 Hz, CH_2-CH_3), 0.45 (t, 3H, J_{HH} = 7.1 Hz, CH_2-CH_3), -6.02 (dt, 1H, J_{HH} = 6.6 Hz, J_{HP} = 25.8 Hz, Ru-*H*), -9.15 (dt, 1H, J_{HH} = 6.6 Hz, J_{HP} = 25.2 Hz, Ru-*H*). ^{31}P{^{1}H} NMR (benzene-d_6, 161.9 MHz, 298K): δ 63.8 (s, *P*Ph_3).

5.6 Direct hydrogenations of alkenes and alkynes

5.6.1 Direct hydrogenations in Young's NMR tubes: general procedure 1

The relevant alkene/alkyne (0.5 mmol) was added to a benzene-d_6 solution of $RuH_2(CO)(PPh_3)_2$(IMes) (**51**) (0.01 mmol, 10 mg). Solutions were subsequently degassed and put under a pressure of 1 atm H_2. Reaction mixtures were placed in a water bath set to 50 °C for 16 h.

5.6.1.1 Synthesis of ethyltrimethylsilane (131)

58 µl of trimethylvinylsilane **97** was used according to general procedure 1 affording 67% conversion into **131**. ^{1}H NMR (benzene-d_6): δ 1.09 (s, 9H, $(CH_3)_3$), 0.91 (t, 3H, J_{HH} = 7.7 Hz, CH_3), 0.43 (q, 2H, J_{HH} = 7.7 Hz, CH_2).

5.6.1.2 Attempted synthesis of 1-propanol (132)

35 µl of allyl alcohol **98** was used according to general procedure 1. Multiple products could be detected by ^{1}H NMR spectroscopy along with the desired 1-propanol **132**. ^{1}H NMR (benzene-d_6, 300 MHz, 298 K): δ 0.79 (t, 2H, J_{HH} = 7.5 Hz, $CH_3CH_2CH_2$), 1.36 (td, 2H, J_{HH} = 7.2 Hz, J_{HH} = 14.4 Hz, $CH_3CH_2CH_2$), 2.06 (s, 1H, O*H*), 3.33 (t, 3H, J_{HH} = 6.5 Hz, $CH_3CH_2CH_2$).

5.6.1.3 Synthesis of methyl propionate (133)

47 µl of methyl acrylate **99** was used according to general procedure 1 affording 13% conversion into **133**. ^{1}H NMR (benzene-d_6, 300 MHz, 298 K): δ 0.92 (t, 3H, J_{HH} = 7.4 Hz, CH_2CH_3), 1.98 (q, 2H, J_{HH} = 7.4 Hz, CH_2), 3.34 (s, 3H, CH_3).

5.6.1.4 Synthesis of propionamide (134)

37 mg acrylamide **100** were used according to general procedure 1. An accurate conversion could not be obtained due to insolubility of the starting material, although conversion to the product **134** could be detected by ^{1}H NMR spectroscopy. ^{1}H NMR (benzene-d_6, 300 MHz, 298 K): δ 0.92 (t, 3H, J_{HH} = 7.5 Hz, CH_3), 1.98 (q, 2H, J_{HH} = 7.4 Hz, CH_2).

5.6.1.5 Synthesis of ethylbenzene (135)

60 µl of styrene **101** were used according to general procedure 1 affording 6% conversion into **135**. ^{1}H NMR (benzene-d_6, 300 MHz, 298 K): δ 1.06 (t, 3H, J_{HH} = 7.5 Hz, CH_3), 2.42 (q, 2H, J_{HH} = 7.7 Hz, CH_2), 6.96-7.38 (m, 5H, Ph).

5.6.1.6 Attempted synthesis of phenethyl bromide (136)

62 µL of β-bromostyrene **102** were used according to general procedure 1. No reduction to **136** was observed.

5.6.1.7 Synthesis of dibenzyl (137)

94 mg of *trans*-stilbene **103** were used according to general procedure 1 affording 4% conversion to **137**. ^{1}H NMR (benzene-d_6, 300 MHz, 298 K): δ 2.90 (s, 4H, (CH_2)$_2$), 7.20-7.50 (m, Ph).

5.6.1.8 Synthesis of cyclooctene (138)

64 µl of 1,5-cyclooctadiene (COD) **104** were used according to general procedure 1 affording 5% conversion to cycloocetene **138** only. ^{1}H NMR (benzene-d_6, 300 MHz, 298 K): δ 1.40 (m, 8H, CH_2), 2.11 (m, 4H, CH_2), 5.57 (m, 2H, C*H*).

5.6.1.9 Synthesis of trimethylvinylsilane (97) and ethyltrimethylsilane (131)

118 µL (trimethylsilyl)acetylene were used according to general procedure 1 affording 50% conversion to **97** and 29% conversion to **131**. ^{1}H NMR (benzene-d_6, 300 MHz, 298 K) **131**: δ 5.65 (dd, 1H, J_{HaHb} = 4.0 Hz, J_{HaHc} = 19.5, CH_a(H$_b$)CH$_c$SiMe$_3$), 5.90 (dd, 1H, J_{HcHb} = 4.2 Hz, $J_{Hc,Ha}$ = 19.2 Hz, CH$_a$(H$_b$)CH_cSiMe$_3$), 6.16 (dd, 1H, J_{HbHc} = 6.6 Hz, J_{HbHa} = 3 Hz, CH$_a$(H_b)CH$_c$SiMe$_3$). Data for **97** as recorded in 5.6.1.1.

5.6.1.10 Attempted synthesis of stilbene (103)and dibenzyl (139)

89 mg diphenylacetylene **106** were used according to general procedure 1. No reduction to the **103** or **139** was observed.

5.6.1.11 Synthesis of styrene (101) and ethylbenzene (135)

55 µL phenylacetylene were used according to general procedure 1 affording 49% conversion to **101** and 9% conversion to **135**. ^{1}H NMR (benzene-d_6, 300 MHz, 298 K) **101**: δ 7.32-7.00 (m, 5H, Ph), 6.62 (dd, 1H, JH$_b$H$_c$ = 17.6 Hz, JH$_a$H$_c$ = 10.9 Hz, CH$_a$(H$_b$)CH_cPh), 5.65 (dd, 1H, JH$_b$H$_c$ = 17.6 Hz, JH$_a$H$_b$ = 1.0 Hz, CH$_a$(H_b)CH$_c$Ph), 5.12 (dd, 1H, JH$_a$H$_c$ = 10.9 Hz, JH$_a$H$_b$ = 1.0 Hz, CH_a(H$_b$)CH$_c$Ph), Data for **135** as recorded in 5.6.1.5.

5.6.1.12 Synthesis of indan (140)

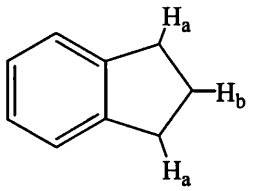

58 μL of indene **108** were used according to general procedure 1 affording 11% conversion to **140**. ^{1}H NMR ($CDCl_3$-d_1, 300 MHz, 298 K): δ 7.41-7.02 (m, 4H, Ph), 2.82 (t, 2H, J_{HaHb} = 7.5 Hz, H_a), 1.97 (quintet, 1H, J_{HaHb} = 7.5 Hz, H_b).

5.6.2 Direct hydrogenations of alkenes and alkynes using an autoclave: general procedure 2

Benzene (10 mL) was added to **51** (19.2 mg, 0.4 mmol) in an autoclave. The required alkene (5 mmol) was subsequently added, the autoclave sealed and pressurised to 5 atm with H_2. The reaction was heated for 16 h at 70 °C and cooled to room temperature. The solvent was removed *in vacuo* and the residue dissolved in $CDCl_3$ and analysed by ^{1}H NMR spectroscopy.

5.6.2.1 Table of results

Substrate	Amount of substrate used	Product	Conversion (%)[a]
allyl alcohol	340 μL	1-propanol	88
acrylamide	359 mg	propionamide	100
styrene	573 μL	ethylbenzene	100
β-bromostyrene	641 μL	phenethyl bromide	0
trans-stilbene	901 mg	bibenzyl	100
COD	622 μL	cyclooctane	100
diphenylacetylene	891 mg	dibenzyl	53
phenylacetylene	549 μL	ethylbenzene	100
indene	583μL	indan	34

[a] ^{1}H NMR data as recorded in 5.6.1. ^{1}H NMR (benzene-d_6, 300 MHz, 298 K) cyclooctane: δ 1.50 (s, 16H, CH_2). 45 μl of methyl acrylate was used and was analysed by GC.

Table 5.1 *Direct hydrogenation of alkenes using 51.*

5.7 Transfer hydrogenations of alkenes and alkynes

5.7.1 General procedure 3

The relevant alkene/alkyne (0.5 mmol) and IPA* was added to a benzene-d_6 solution of $RuH_2(CO)(PPh_3)_2(IMes)$ **51** (0.01 mmol, 10 mg). Reaction mixtures were placed in an oil bath set to 70 °C for 16 h.

* Initially two equivalents of IPA were used and the conversions obtained are shown in Table 5.2. Subsequent reactions were performed with the addition of five equivalents of IPA.

5.7.2 Transfer hydrogenations of alkenes and alkynes with two equivalents of IPA

According to general procedure 3 with two equivalents (1.0 mmol, 77 μL) of IPA, conversions according to Table 5.2 were obtained.

Entry	Substrate	Amount substrate used	Conversion with 2 equivalents IPA (%)[a]		
			Starting material	Partially reduced	Product
1	A	73 μL	0	-	100
2	C	45 μL	89	-	11
3	E	57 μL	87	-	13
4	F	62 μL	100	-	0
5	G	90 mg	98	-	2
6	H	61 μL	0	97	3
7	I	71 μL	100	0	0
8	J	89 mg	90	10	0
9	K	55 μL	89	11	0
10	L	58 μL	98	98	2

[a] ^{1}H NMR data as recorded in 5.6.1. and 5.6.2.

Table 5.2 *Transfer hydrogenations of alkenes using* ***51****.*

5.7.3 Transfer hydrogenations of alkenes and alkynes with five equivalents of IPA

According to general procedure 3 with five equivalents (2.5 mmol, 191 μL) IPA, conversions according to Table 5.3 were obtained.

Substrate	Amount of substrate used	Product	Conversion (%)[a]
trimethylvinylsilane	73 μL	ethyltrimethylsilane	100
styrene	57 μL	ethylbenzene	69
β-bromostyrene	62 μL	phenethyl bromide	0
trans-stilbene	90 mg	dibenzyl	26
COD	61 μL	cyclooctane	0
trimethylsilylacetylene	71 μL	ethyltrimethylsilane	0
diphenylacetylene	89 mg	dibenzyl	0
phenylacetylene	55 μL	ethylbenzene	7
indene	58 μL	indan	34

[a] ^{1}H NMR data as recorded in 5.6.1. and 5.6.2.

Table 5.3 *Transfer hydrogenations of alkenes with IPA using* ***51****.*

5.7.4 *In situ* transfer hydrogenation reactions monitored inside the 400 MHz NMR spectrometer

5.7.4.1 Oxidation of 4-fluoro-α-methylbezylalcohol (124)

4-fluoro-α-methylbezylalcohol (0.5 mmol, 63 μL) and acetone (2.5 mmol, 175 μL) were added *via* syringe to a benzene solution (0.6 mL) of [Ru] (0.01 mmol, ~10 mg). The reactions were heated to 50 °C in the probe of the NMR spectrometer and ^{1}H NMR spectra recorded every 15 min over a period of 14 h. ^{1}H NMR (benzene-d_6, 400 MHz, 323 K): δ 2.16 (s, CH_3).

5.7.4.2 Reduction of trimethylvinylsilane (97)

Trimethylvinylsilane (0.5 mmol, 73 μL) and IPA (2.5 mmol, 191 μL) were added *via* syringe to a benzene solution (0.6 mL) of [Ru] (0.01 mmol, ~10 mg). The reactions

were heated to 70 °C in the probe of the NMR spectrometer and ^{1}H NMR spectra recorded every 15 min over a period of 14 h. Data as recorded in section 5.6.1.1.

5.8 Crossover transfer hydrogenations (CTH)

5.8.1 General procedure 4

Benzyl alcohol **110** (0.2 mmol, 20.8 μL) **OR** *sec*-phenethyl alcohol **111** (0.2 mmol, 24.1 μL) were added *via* syringe to a benzene solution of benzyl dihydrocinnamate (0.2 mmol, 47.7 mg) and ruthenium precatalyst (0.01 mmol, ~10 mg). Reactions were placed in an oil bath set to 70 °C for 6 h.

5.8.2 Synthesis of benzyl dihydrocinnamate (112)[8]

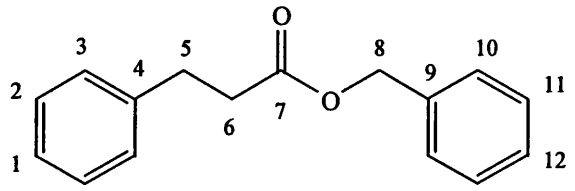

According to general procedure 4, ^{1}H NMR ($CDCl_3$, 400 MHz, 298 K): δ 7.24-7.37 (m, 7H, Ph), 7.16-7.21 (m, 3H, Ph), 5.10 (s, 2H, C8-C*H*$_2$), 2.96 (t, 2H, *J* = 7.4 Hz, C5-C*H*$_2$), 2.67 (t, 2H, *J* = 7.4 Hz, C6-C*H*$_2$).

5.8.3 Synthesis of benzaldehyde

According to general procedure 4, (benzene-d_6, 300 MHz, 298 K): δ 9.72 (s, CO(*H*)).

5.8.4 Synthesis of acetophenone

According to general procedure 4, (benzene-d_6, 300 MHz, 298 K): δ 2.18 (s, C*H*$_3$).

5.9 Syntheses of ylides

5.9.1 Preparation of stabilised phosphorane ylides: general procedure 5

The required phosphonium salt was dissolved in dichloromethane and then extracted with two portions of 2 M potassium hydroxide solution. The collected aqueous

extract was back-extracted with further dichloromethane (25 mL) and then the combined organic layers washed with saturated brine (100 mL), dried ($MgSO_4$), filtered and concentrated *in vacuo* to afford the phosphorane ylide. The ylide thus obtained was further purified as required.

5.9.2 Preparation of (triphenylphosphoranylidene)acetonitrile (117)

The cyano ylide was prepared by adapting a method given in the literature.[9,10]

5.9.2.1 Preparation of (cyanomethyl)triphenylphosphonium bromide (113)

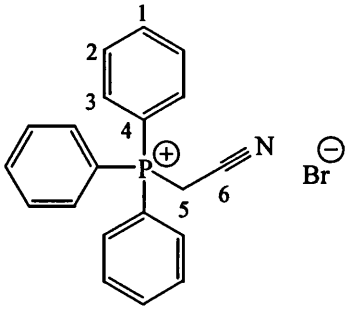

To a solution of bromoacetonitrile (10.0 g, 166.7 mmol) in toluene (150 mL) was added a solution of triphenylphosphine (21.9 g, 166.7 mmol) in toluene (50 mL). The reaction flask was stoppered and set aside for 3 days at room temperature. The white precipitate obtained was collected *via* filtration and washed thoroughly with toluene (2 × 50 mL) and then hexane (3 × 50 mL). Drying under vacuum afforded the title compound **113** as a white powder. Yield: 29.6 g (93%); ^{1}H NMR ($CDCl_3$, 300 MHz, 298 K): δ 6.42 (d, J_{PH} = 15.4 Hz, 2H, C5-CH_2), 7.67-7.71 (m, 6H, C2&3-C*H*), 7.80 (t, J_{HH} = 7.1 Hz, 3H, C1-C*H*), 7.93-8.00 (m, 6H, C2&3-C*H*). ^{31}P{^{1}H}: δ 23.1 (s, *P*Ph$_3$).

5.9.2.2 Preparation of (triphenylphosphoranylidene)acetonitrile (117)

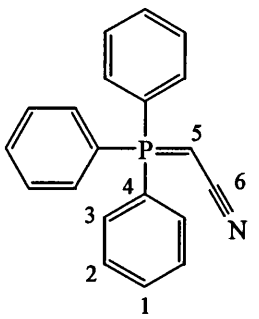

According to general procedure 5 using (cyanomethyl)triphenyl phosphonium bromide (5.0 g, 13.1 mmol, 1 equiv.), dichloromethane (100 mL) and 2 M potassium hydroxide (2 × 50 mL) the title compound **117** was obtained as a cream solid which was recrystallised from the minimum volume of boiling benzene to afford colourless cubes. Yield: 3.9 g (98 %); ^{1}H NMR ($CDCl_3$, 300 MHz, 298 K): δ 7.43-7.54 (m, 7H, C2&5-C*H*), 7.56-7.69 (m, 9H, C1&3-C*H*). $^{31}P\{^{1}H\}$: δ 24.2 (s, *P*Ph$_3$).

5.9.3 Preparation of benzyl (triphenylphosphoranylidene)acetate (118)

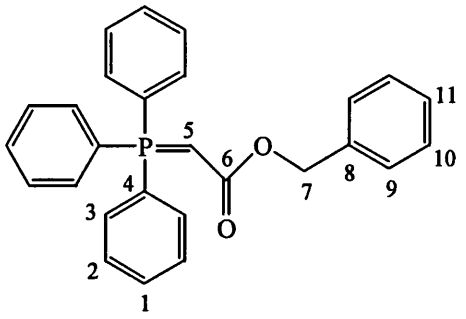

The benzyl ester ylide was prepared by adapting a method given in the literature.[11]

5.9.3.1 Preparation of (benzyloxycarbonylmethyl)triphenylphosphonium bromide (114)

To a solution of benzyl bromoacetate (20.0 g, 87.3 mmol) in toluene (50 mL) was added dropwise a solution of triphenylphosphine (22.9 g, 87.3 mmol) in toluene (50 mL). The reaction flask was then sealed and the mixture stirred vigorously for 16 h at room temperature. The white solid precipitate was collected *via* filtration and washed thoroughly with toluene (2 × 50 mL) followed by hexane (3 × 50 mL). Drying under vacuum afforded the title compound **114** as a white powder. Yield: 38.4 g (90%); ^{1}H NMR ($CDCl_3$, 300 MHz, 298 K): δ 7.72-7.83 (m, 9H, C1&3-C*H*), 7.56-7.62 (m, 6H, C2-C*H*), 7.22-7.31 (m, 3H, C9&11-C*H*), 7.08-7.11 (m, 2H, C10-C*H*), 5.60 (d, J_{PH} = 14.1 Hz, 2H, C5-CH_2), 5.00 (s, 2H, C7-CH_2). $^{31}P\{^{1}H\}$: δ 21.9 (s, *P*Ph$_3$).

5.9.3.2 Preparation of benzyl (triphenylphosphoranylidene)acetate (118)

According to general procedure 5 using (benzyloxycarbonylmethyl)triphenyl phosphonium bromide (12.122 g, 24.67 mmol), CH_2Cl_2 (100 mL) and 2 M potassium

hydroxide (2 × 50 mL) the title compound **118** was obtained as a dense glassy white solid which could be recrystallised from di-*n*-butyl ether to afford colourless needles. Yield: 9.8 g (97%); ^{1}H NMR (benzene-d_6, 300 MHz, 298 K): δ 7.62 (br. s, 6H), 7.43 (br. s, 2H), 6.90-7.00 (br. m, 12H, Ph), 5.38 (br. s, 2H, C7-CH_2), 3.36 (br. d, J_{PH} = 17.2 Hz, 1H, C5-C*H*). ^{31}P{^{1}H}: δ 19.5 (s, *P*Ph$_3$).

5.9.4 Preparation of *tert*-butyl (triphenylphosphoranylidene)acetate (119)

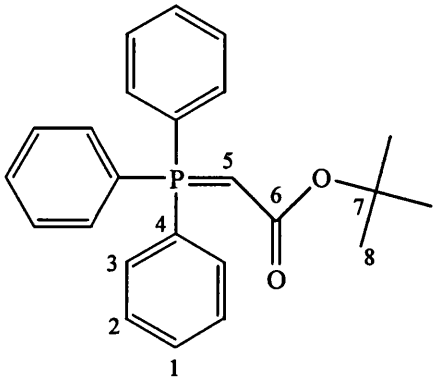

The *tert*-butyl ester ylide was prepared following a method adapted from the literature.[11]

5.9.4.1 Preparation of (*tert*-butyloxycarbonylmethyl)triphenylphosphonium bromide (115)

To a solution of triphenylphosphine (6.72 g, 25.63 mmol, 1 equiv.) in toluene (20 mL) was added dropwise *via* syringe *tert*-butyl bromoacetate (5.00 g, 25.63 mmol, 1 equiv.). The reaction flask was then sealed and the mixture set aside in the fridge (4 °C) for 18 h. The white solid precipitate was collected *via* filtration and washed thoroughly with toluene (2 × 25 mL) followed by hexane (3 × 30 mL). Drying under vacuum afforded the title compound **115** a white powder. Yield: 11.2 g (95%); ^{1}H NMR ($CDCl_3$, 300 MHz, 298 K): δ 7.58-7.84 (15H, m, Ph), 5.21 (d, 2H, J_{PH} = 14.0 Hz, C5-C*H*), 1.11 (s, 9H, C8CH_3). ^{31}P{^{1}H}: δ 22.2 (s).

5.9.4.2 Preparation of *tert*-butyl (triphenylphosphoranylidene)acetate (119)

According to general procedure 5 using (*tert*-butyloxycarbonylmethyl)triphenyl phosphonium bromide (10.08 g, 22.04 mmol, 1 equiv.), dichloromethane (100 mL)

and 2 M potassium hydroxide (2 × 50 mL) the title compound was obtained as dense glassy solid. The crude product was dissolved in the minimum volume of boiling toluene and colourless cubes were grown by allowing the solution to stand at -13 °C for 2 weeks. Yield: 8.45 g (51%); ^{1}H-NMR (DMSO-d_6, 300 MHz, 298 K): δ 7.58-7.66 (m, 15H, C1, C2 and C3-C*H*), 2.66 (d, 1H, J_{PH} = 23.4 Hz, C5-C*H*, 47%), 2.27 (d, 1H, J_{PH} = 23.0 Hz, C5-C*H*, 53%), 1.36 (s, 9H, C8-CH_3, 47%), 0.98 (s, 9H, C8-CH_3, 53%), ^{31}P{^{1}H}: δ 18.7 (s), 17.1 (s).

5.9.5 Preparation of ethyl (triphenylphosphoranylidene)pyruvate (120)[12,13]

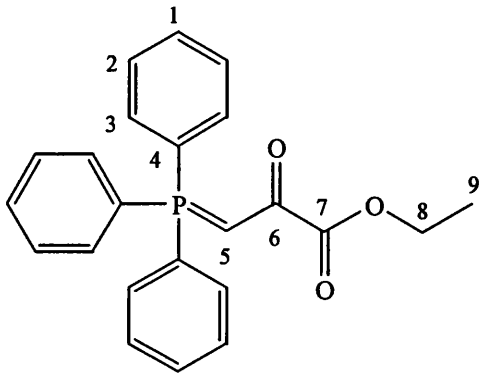

5.9.5.1 Preparation of (2-ethoxycarbonyl-2-oxyethyl)triphenylphosphonium bromide (116)

To a solution of ethyl 2-bromopyruvate (5.00 g, 25.64 mmol, 1 equiv.) in toluene (20 mL) was added a solution of triphenylphosphine (6.724 g, 25.64 mmol, 1 equiv.) in toluene (30 mL). The reaction flask was stoppered and set aside for 3 days at room temperature, resulting in the precipitation of an orange/red gum from solution. Concentration *in vacuo* afforded the crude phosphonium salt, an orange syrup, which was used without further purification Yield: 11.7 g (100%). No characterisation of **116** was attempted.

5.9.5.2 Preparation of ethyl (triphenylphosphoranylidene)pyruvate (120)

According to general procedure 5 using (2-ethoxycarbonyl-2-oxyethyl) triphenyl phosphonium bromide, DCM (100 mL) and 2 M potassium hydroxide (2 × 75 mL) the crude product was obtained as a brown powder. Recrystallisation from acetone afforded the title compound **120** as beige cubes. Yield: 3.17 g (33%); ^{1}H ($CDCl_3$, 400

MHz, 298 K): δ 7.54-7.68 (m, 9H, C1 and C3-C*H*), 7.44-7.50 (m, 6H, C2-C*H*), 4.84 (d, 1H, J_{PH} = 23.6 Hz, C5-C*H*), 4.24 (q, 2H, J = 7.0 Hz, C8-CH_2), 1.35 (t, 3H, J = 7.0 Hz, C9-CH_3). $^{31}P\{^1H\}$: δ 18.3 (s).

5.9.6 Preparation of *N,N*-dimethyl(triphenylphosphoranylidene)acetamide (122)[14]

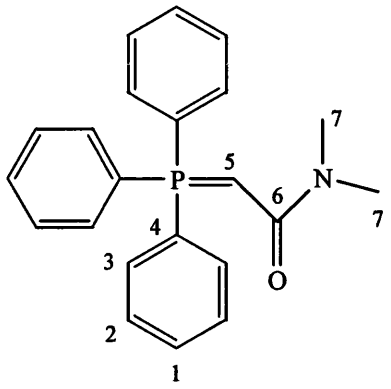

To a solution of (*N,N*-dimethylcarbamoylmethyl)triphenyl phosphonium chloride (8.36 g, 21.82 mmol, 1 equiv.) in anhydrous dichloromethane (100 mL) cooled to 0 °C (ice-bath) was added in six portions sodium hydride [60 w/w% dispersion in mineral oil] (1.81 g, 75.28 mmol, 3.45 equiv.) whilst the mixture was stirred vigorously. Immediate effervescence was observed and stirring continued for 1 hour at 0 °C. The resulting pale green solution was filtered through a celite plug (non-acidic celite 545) and then concentrated *in vacuo* to ~ 10 mL. Anhydrous hexane (500 mL) was added and the mixture allowed to stand. This resulted in the precipitation of a pale yellow powder which was collected by filtration and washed carefully with hexane (2 × 50 mL). Drying under vacuum afforded the title compound as a pale yellow powder. Yield: 5.84 g (79%); ^1H NMR ($CDCl_3$, 300 MHz, 298 K): δ 7.62-7.72 (m, 6H, Ph), 7.38-7.53 (m, 9H, Ph), 2.94 (s, 6H, C7-CH_3), 2.80 (br. d, 1H, J_{PH} = 15.3 Hz, C5-C*H*), $^{31}P\{^1H\}$: δ 18.3 (s).

5.9.7 Preparation of *N*-methyl,*N*-methoxy(triphenylphosphoranylidene) acetamide (123)[15]

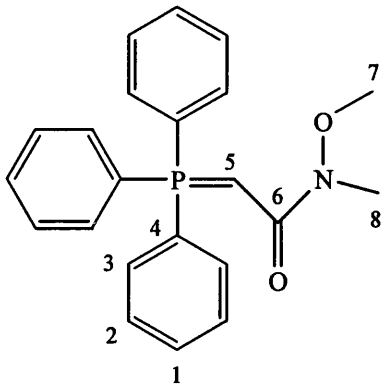

According to general procedure 5 using (*N*-methyl,*N*-methoxycarbamoylmethyl) triphenyl phosphonium chloride (10.80 g, 54.00 mmol, 1 equiv.), dichloromethane (100 mL) and 2 M potassium hydroxide (2 × 50 mL) the title compound **123** was obtained as yellow micro-needles following recrystallisation from 1:1 dichloromethane/ethyl acetate. Yield: 4.80 g (52%); ^{1}H NMR ($CDCl_3$, 400 MHz, 298 K): δ 7.63-7.68 (m, 6H, Ph), 7.48-7.53 (m, 3H, C1-C*H*), 7.39-7.45 (m, 6H, Ph), 3.72 (s, 3H, C7-CH_3), 3.52 (br. s, 1H, C5-C*H*), 3.07 (s, 3H, C8-CH_3). ^{31}P{^{1}H}: δ 19.3 (s).

5.9.8 Preparation of (triphenylphosphoranylidene)acetone (121)[16-18]

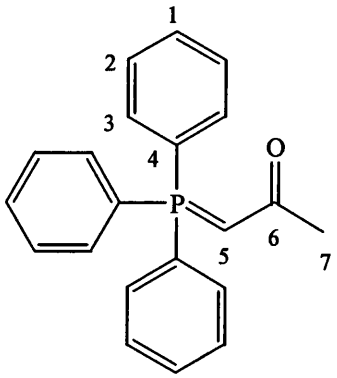

According to general procedure 5 using (2-oxypropyl) triphenylphosphonium chloride (5.09 g, 14.34 mmol), dichloromethane (50 mL) and 2 M potassium hydroxide (2 × 50 mL) the crude product was obtained as a crumbly pale yellow

solid. Recrystallisation from toluene afforded the title compound **121** as colourless needles. Yield: 3.38 g (74%); ^{1}H NMR (DMSO-d_6, 300 MHz, 298 K): δ 7.54-7.67 (15H, m, C1-, C2- and C3-C*H*), 3.63 (1H, d, J_{PH} = 26.9 Hz, C5-C*H*), 1.91 (3H, s, C7-CH_3). ^{31}P{^{1}H} δ 14.9 (s).

5.10 Indirect Wittig reactions

5.10.1 General procedure 6

An oven-dried Young's tube was charged with the required ruthenium catalyst (5 mol%, 25 μmol) and phosphorane ylide (0.55 mmol, 1.1 equiv.). The tubes were placed in a Fisher carrousel synthesiser and purged under argon. Toluene (1 mL) and the required alcohol (0.5 mmol) were added *via* syringe. The reaction was heated for (2 h, 3 h, 6 h or 24 h) before cooling to room temperature. Wet diethyl ether was added to quench the reaction and the mixture was then concentrated *in vacuo* to afford the crude product. Conversion was determined by analysis of the ^{1}H NMR spectrum.

5.10.2 Preparation of benzyl dihydrocinnamate (112)

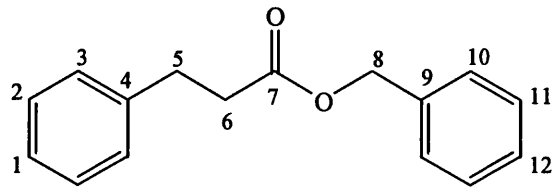

According to general procedure 6 with of benzyl (triphenylphosphoranylidene) acetate (226 mg), benzyl alcohol **110** (52 μL) and either **51** (24 mg) or (20.8 mg), **62a** at 70 °C for 3 h, 33-46% conversion into the title compound was achieved. ^{1}H NMR ($CDCl_3$, 400 MHz, 298 K): δ 7.24-7.37 (m, 7H, Ph), 7.16-7.21 (m, 3H, Ph), 5.10 (s, 2H, C8-CH_2), 2.96 (t, 2H, J_{HH} = 7.4 Hz, C5-CH_2), 2.67 (t, 2H, J_{HH} = 7.4 Hz, C6-CH_2).

5.10.3 Preparation of *tert*-butyl dihydrocinnamate (141)

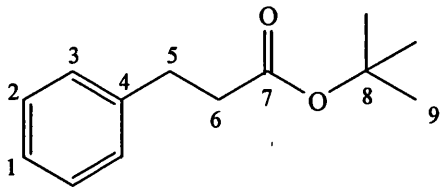

According to general procedure 6 with *tert*-butyl (triphenylphosphoranylidene) acetate (207 mg), benzyl alcohol (52 μL) and either **51** (24 mg) or **62a** (20.8 mg), at 70 °C for 3 h, 52-53% conversion into the title compound was achieved. ^{1}H NMR ($CDCl_3$, 300 MHz, 298 K): δ 7.19-7.23 (2H, m, C2-C*H*), 7.08-7.12 (3H, m, C1- and C3-C*H*), 2.83 (2H, t, J_{HH} = 7.1 Hz, C5-CH_2), 2.46 (2H, t, J_{HH} = 7.1 Hz, C6-CH_2), 1.34 (9H, s, C9-CH_3).

5.10.4 Preparation of 4-phenylbutan-2-one (142)

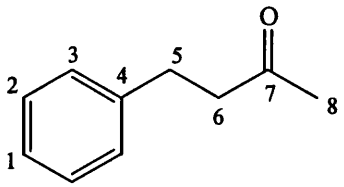

According to general procedure 6 with (triphenylphosphoranylidene)acetone (173 mg), benzyl alcohol (52 μL) and either **51** (24 mg) or **62a** (20.8 mg) at 70 °C for 3 h. Only trace amounts of the title compound (2% conversion) could be detected in the ^{1}H NMR spectrum in accordance with the literature.[19]

5.10.5 Preparation of *N,N*-dimethyl 3-phenylpropionamide (143)

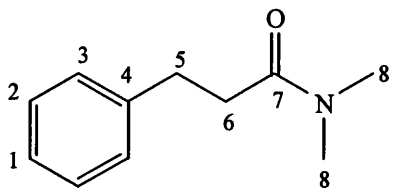

According to general procedure 6 with *N,N*-dimethyl(triphenylphosphoranylidene) acetamide (191 mg), benzyl alcohol **110** (52 μL) and either **51** (24 mg) or **62a** (20.8

mg), at 70 °C for 3 h, 37-74% conversion into the title compound **143** was achieved. ^{1}H NMR ($CDCl_3$, 300 MHz, 298 K) δ 7.19-7.24 (m, 2H, C2-C*H*), 7.11-7.16 (m, 3H, C1- and C3-C*H*), 2.85 (s, 3H, C8-CH_3), 2.87 (s, 3H), 2.85 (partially obscured t, 3H, J_{HH} = 7.5 Hz, C5-CH_2), 2.54 (t, 3H, J_{HH} = 7.5 Hz, C6-CH_2).

5.10.6 Preparation of *N*-methoxyl-*N*-methyl 3-phenylpropionamide (144)

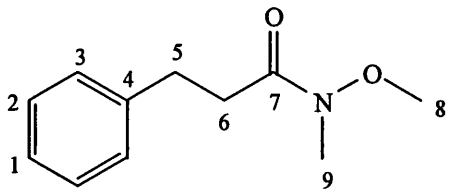

According to general procedure 6 with of *N*-methyl,*N*-methoxy (triphenylphosphoranylidene)acetamide (200 mg), benzyl alcohol (52 μL) and either **51** (24 mg) or **62a** (20.8 mg), at 70 °C for 3 h, 9-23% conversion into the title compound **144** was achieved. ^{1}H NMR ($CDCl_3$, 300 MHz, 298 K). δ 7.20-7.32 (s, 5H, C1-, C2-, C3-C*H*), 3.61 (s, 3H, C9-CH_3), 3.18 (s, 3H, C8-CH_3), 2.97 (t, 2H, J_{HH} = 7.5 Hz, C5-CH_2), 2.74 (2H, t, J_{HH} = 7.5 Hz, C6-CH_2).

5.10.7 Attempted preparation of ethyl 2-oxo-4-phenylbutyrate (144)

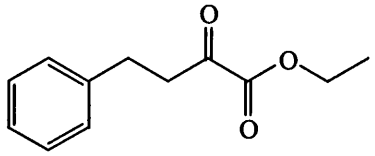

According to general procedure 6 with of benzyl (triphenylphosphoranylidene) acetate (200 mg), benzyl alcohol (52 μL) and either **51** (24 mg) or **62a** (20.8 mg) ethyl(triphenylphosphoranylidene) pyruvate (207 mg), at 70 °C for 3 h, none of the title compound, ethyl 2-oxo-4-phenylbutyrate, and indeed no identifiable components could be detected.

5.10.8 Preparation of dihydrocinnamonitrile (145)

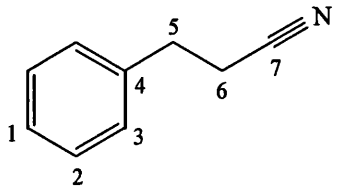

According to general procedure 6 with (triphenylphosphoranylidene)acetonitrile (166 mg), benzyl alcohol **110** (52 μL) and **62a** (20.8 mg), at 70 °C for 6 h, 100% conversion into the title compound **145** was achieved. ^{1}H-NMR ($CDCl_3$, 300 MHz, 298 K): δ 7.22-7.39 (m, 5H, C1-, C2- and C3-C*H*), 2.98 (t, 3H, J_{HH} = 7.4 Hz, C5-CH_2), 2.64 (t, 3H, J_{HH} = 7.4 Hz, C6-CH_2).

5.10.9 Preparation of 3-(naphthalene-2-yl)propionitrile (146)

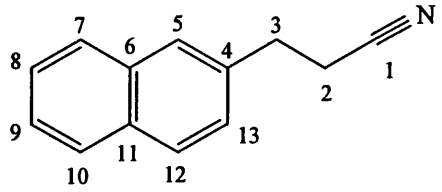

According to general procedure 6 with (triphenylphosphoranylidene)acetonitrile (166 mg), 2-naphthalenemethanol (79 mg) and **62a** (20.8 mg) at 70 °C for 6 h, 100% conversion into the title compound **146** was achieved. ^{1}H NMR ($CDCl_3$, 300 MHz, 298 K) δ 7.83-7.88 (m, 3H, C9-, C10- and C12-C*H*), 7.72 (br. s, 1H, C5-C*H*), 7.47-7.55 (m, 2H, C7- and C8-C*H*), 7.37 (dd, 1H, J_{HH} = 1.5, 8.4 Hz, C13-C*H*), 3.16 (t, 2H, J_{HH} = 7.4 Hz, C3-CH_2), 2.75 (t, 2H, J_{HH} = 7.4 Hz, C2-CH_2).

5.10.10 Preparation of 3-(furan-2-yl)propionitrile (147)

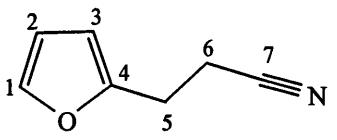

According to general procedure 6 with (triphenylphosphoranylidene)acetonitrile (166 mg), fufuryl alcohol (43 μL) and **62a** (20.8 mg), at 70 °C for 6 h, 86% conversion into the title compound **147** was achieved. ^{1}H NMR (400 MHz, $CDCl_3$, 298 K) δ 7.26 (d, 1H, J_{HH} = 1.5 Hz), 6.23 (app. t, 1H, J_{HH} = 2.7 Hz, C2-C*H*), 6.09 (d, 1H, J_{HH} = 3.1 Hz), 2.93 (t, 2H, J_{HH} = 7.4 Hz, C5-CH_2), 2.60 (t, 2H, J_{HH} = 7.4 Hz, C6-CH_2).

5.11 References

[1]Arduengo, A. J.; Krafczyk, R.; Schmutzler, R.; Craig, H. A.; Goerlich, J. R.; Marshall, W. J.; Unverzagt, M. *Tetrahedron* **1999**, *55*, 14523-14534.

[2]Kuhn, N.; Kratz, T. *Synthesis* **1993**, 561-562.

[3]Herrmann, W. A.; Kocher, C.; Goossen, L. J.; Artus, G. R. J. *Chem. Eur. J.* **1996**, *2*, 1627-1636.

[4]Herrmann, W. A.; Goossen, L. J.; Artus, G. R. J.; Kocher, C. *Organometallics* **1997**, *16*, 2472-2477.

[5]Nolan, S. P.; Singh, R. *Personal communication.*

[6]Jazzar, R. F. R. "PhD thesis," University of Bath, **2003**.

[7]Burling, S. *Personal communication.*

[8]Page, P. C. B.; McKenzie, M. J.; Allin, S. M.; Buckle, D. R. *Tetrahedron* **2000**, *56*, 9683.

[9]Kiddle, J. J. *Tetrahedron Lett.* **2000**, *41*, 1339.

[10]Wilt, J. W.; Ho, A. J. *J. Org. Chem.* **1971**, *36*, 2026.

[11]Aitken, R. A.; Armstrong, J. M.; Drysdale, M. J.; Ross, F. C.; Ryan, B. M. *J. Chem. Soc. Perkin. Trans.* **1999**, *1*, 593.

[12]Ernest, I.; Gosteli, J.; Greengrass, C. W.; Holick, W.; Jackmann, D. E.; Pfaendler, H. R.; Woodward, B. *J. Am. Chem. Soc.* **1978**, 8214.

[13]Aitken, R. A.; Karodia, N. *Liebigs. Ann. Chem.* **1977**, 779.

[14]Vincente, J.; Chicote, M. T.; Lagunas, M. C.; Jones, P. G. *J. Chem. Soc. Dalton Trans.* **1991**, 2579.

[15]Evans, D. A.; Kaldor, S. W.; Jones, T. K.; Clardy, J.; Stout, T. J. *J. Am. Chem. Soc.* **1990**, *112*, 7001.

[16]Schuda, P. F.; Ebner, C. B.; Potlock, S. J. *Synthesis*, 1055.

[17]Facchin, G.; Bertani, R.; Calligaris, M.; Nardin, G.; Mari, M. *J. Chem. Soc. Dalton Trans.* **1987**, 1381.

[18]Bestmann, H. J.; Bomhard, A.; Dostalek, R.; Pichl, R.; Riemer, R.; Zimmermann, R. *Synthesis* **1992**, 787.

[19]Hong, J. E.; Shin, W. S.; Jang, W. B.; Oh, D. Y. *J. Org. Chem.* **1996**, *61*, 2199.

Appendices

Appendix 1: Crystallographic data, bond lengths and angles for 57.

$RuH_2(CO)(PPh_3)_2(IEt_2Me_2)$ (57)	
Empirical formula	$C_{46}H_{48}N_2OP_2Ru$
Formula weight	807.87
Temperature	150(2) K
Wavelength	0.71073 Å
Crystal system	Monoclinic
Space group	C2/c
Unit cell dimensions	a = 23.5760(2)Å $\alpha = 90^o$
	b = 9.9740(1)Å $\beta = 113.239(1)^o$
	c = 18.2220(2)Å $\gamma = 90^o$
Volume	3937.20(7) $Å^3$
Z	4
Density (calculated)	1.363 Mg/m^3
Absorption coefficient	0.517 mm^{-1}
F(000)	1680
Crystal size	0.15 x 0.10 x 0.10 mm
Theta range for data collection	3.58 to 27.49 °
Index ranges	-30<=h<=28; -12<=k<=12; -23<=l<=23
Reflections collected	32590
Independent reflections	8871 [R(int) = 0.0583]
Reflections observed (>2σ)	7674
Data Completeness	0.997
Absorption correction	None
Refinement method	Full-matrix least-squares on F^2
Data / restraints / parameters	8871 / 10 / 497
Goodness-of-fit on F^2	1.031
Final R indices [I>2σ(I)]	R1 = 0.0407 wR2 = 0.0880
R indices (all data)	R1 = 0.0523 wR2 = 0.0925
Absolute structure parameter	0.21(3)
Largest diff. peak and hole	1.142 and -0.799 eÅ-3

Bond Lengths (Å) for $RuH_2(CO)(PPh_3)_2(IEt_2Me_2)$ (57)			
Ru(1)-H(1)	1.6874	Ru(1)-C(1)	1.880(4)
Ru(1)-C(2)	2.171(3)	Ru(1)-P(2)	2.3048(13)
Ru(1)-P(1)	2.3313(13)	P(1)-C(17)	1.843(4)
P(1)-C(23)	1.845(4)	P(1)-C(11)	1.847(5)
P(1)-Ru(1A)	2.291(3)	P(2)-C(35)	1.823(4)
P(2)-C(29)	1.828(5)	P(2)-C(41)	1.845(4)
P(2)-Ru(1A)	2.403(3)	O(1)-C(1)	1.167(5)
N(1)-C(2)	1.368(5)	N(1)-C(3)	1.405(6)
N(1)-C(5)	1.446(5)	N(2)-C(2)	1.359(6)
N(2)-C(4)	1.392(7)	N(2)-C(7)	1.467(5)
C(2)-Ru(1A)	2.185(3)	C(3)-C(4)	1.342(4)
C(3)-C(9)	1.496(7)	C(4)-C(10)	1.495(7)
C(5)-C(6)	1.537(7)	C(7)-C(8)	1.500(7)
C(11)-C(16)	1.379(7)	C(11)-C(12)	1.389(6)
C(12)-C(13)	1.372(8)	C(13)-C(14)	1.395(9)
C(14)-C(15)	1.358(9)	C(15)-C(16)	1.411(8)
C(17)-C(18)	1.382(7)	C(17)-C(22)	1.501(6)
C(18)-C(19)	1.386(7)	C(19)-C(20)	1.378(8)
C(20)-C(21)	1.363(9)	C(21)-C(22)	1.314(8)
C(23)-C(24)	1.360(8)	C(23)-C(28)	1.386(7)
C(24)-C(25)	1.394(7)	C(25)-C(26)	1.384(9)
C(26)-C(27)	1.396(9)	C(27)-C(28)	1.376(7)
C(29)-C(34)	1.393(7)	C(29)-C(30)	1.406(6)
C(30)-C(31)	1.398(9)	C(31)-C(32)	1.351(10)
C(32)-C(33)	1.400(10)	C(33)-C(34)	1.365(8)
C(35)-C(36)	1.399(8)	C(35)-C(40)	1.428(8)
C(36)-C(37)	1.403(8)	C(37)-C(38)	1.343(10)
C(38)-C(39)	1.361(10)	C(39)-C(40)	1.374(8)
C(41)-C(46)	1.124(4)	C(41)-C(42)	1.388(8)
C(42)-C(43)	1.382(7)	C(43)-C(44)	1.361(8)
C(44)-C(45)	1.373(9)	C(45)-C(46)	1.567(5)
Ru(1A)-H(1A)	1.70(5)	Ru(1A)-C(1A)	1.781(16)
O(1A)-C(1A)	1.255(16)		

Bond Angles (°) for $RuH_2(CO)(PPh_3)_2(IEt_2Me_2)$ (57)			
H(1)-Ru(1)-C(1)	87.6	H(1)-Ru(1)-C(2)	172.7
C(1)-Ru(1)-C(2)	99.7(2)	H(1)-Ru(1)-P(2)	83.7
C(1)-Ru(1)-P(2)	89.99(17)	C(2)-Ru(1)-P(2)	96.84(18)
H(1)-Ru(1)-P(1)	83.4	C(1)-Ru(1)-P(1)	98.29(17)
C(2)-Ru(1)-P(1)	94.87(18)	P(2)-Ru(1)-P(1)	164.32(4)
C(17)-P(1)-C(23)	99.6(2)	C(17)-P(1)-C(11)	102.6(2)
C(23)-P(1)-C(11)	101.7(2)	C(17)-P(1)-Ru(1A)	129.38(16)
C(23)-P(1)-Ru(1A)	107.19(17)	C(11)-P(1)-Ru(1A)	112.60(18)
C(17)-P(1)-Ru(1)	116.38(16)	C(23)-P(1)-Ru(1)	119.62(17)
C(11)-P(1)-Ru(1)	114.33(17)	Ru(1A)-P(1)-Ru(1)	14.72(4)
C(35)-P(2)-C(29)	102.3(2)	C(35)-P(2)-C(41)	100.6(2)
C(29)-P(2)-C(41)	101.3(2)	C(35)-P(2)-Ru(1)	112.44(16)
C(29)-P(2)-Ru(1)	114.54(17)	C(41)-P(2)-Ru(1)	122.94(15)
C(35)-P(2)-Ru(1A)	124.68(18)	C(29)-P(2)-Ru(1A)	114.47(18)
C(41)-P(2)-Ru(1A)	110.40(15)	Ru(1)-P(2)-Ru(1A)	14.29(4)
C(2)-N(1)-C(3)	111.8(3)	C(2)-N(1)-C(5)	127.6(4)
C(3)-N(1)-C(5)	120.6(4)	C(2)-N(2)-C(4)	112.3(3)
C(2)-N(2)-C(7)	125.6(4)	C(4)-N(2)-C(7)	122.1(4)
O(1)-C(1)-Ru(1)	174.0(5)	N(2)-C(2)-N(1)	103.0(2)
N(2)-C(2)-Ru(1)	131.4(3)	N(1)-C(2)-Ru(1)	125.6(3)
N(2)-C(2)-Ru(1A)	117.8(3)	N(1)-C(2)-Ru(1A)	138.3(3)
Ru(1)-C(2)-Ru(1A)	15.66(5)	C(4)-C(3)-N(1)	106.1(5)
C(4)-C(3)-C(9)	130.8(6)	N(1)-C(3)-C(9)	123.0(4)
C(3)-C(4)-N(2)	106.8(5)	C(3)-C(4)-C(10)	129.7(6)
N(2)-C(4)-C(10)	123.4(4)	N(1)-C(5)-C(6)	113.7(4)
N(2)-C(7)-C(8)	113.1(4)	C(16)-C(11)-C(12)	119.1(5)
C(16)-C(11)-P(1)	124.6(4)	C(12)-C(11)-P(1)	116.1(3)
C(13)-C(12)-C(11)	121.2(5)	C(12)-C(13)-C(14)	119.2(5)
C(15)-C(14)-C(13)	120.7(6)	C(14)-C(15)-C(16)	119.8(5)
C(11)-C(16)-C(15)	119.9(5)	C(18)-C(17)-C(22)	115.9(4)
C(18)-C(17)-P(1)	123.4(3)	C(22)-C(17)-P(1)	120.7(4)
C(17)-C(18)-C(19)	121.2(4)	C(20)-C(19)-C(18)	121.2(6)
C(21)-C(20)-C(19)	118.4(5)	C(22)-C(21)-C(20)	124.2(5)
C(21)-C(22)-C(17)	119.0(5)	C(24)-C(23)-C(28)	118.5(5)

C(24)-C(23)-P(1)	122.4(4)	C(28)-C(23)-P(1)	118.9(4)
C(23)-C(24)-C(25)	122.3(6)	C(26)-C(25)-C(24)	118.7(6)
C(25)-C(26)-C(27)	119.5(5)	C(28)-C(27)-C(26)	120.1(5)
C(27)-C(28)-C(23)	120.9(5)	C(34)-C(29)-C(30)	118.2(5)
C(34)-C(29)-P(2)	124.8(4)	C(30)-C(29)-P(2)	116.4(4)
C(31)-C(30)-C(29)	120.0(5)	C(32)-C(31)-C(30)	121.1(6)
C(31)-C(32)-C(33)	118.9(6)	C(34)-C(33)-C(32)	121.3(6)
C(33)-C(34)-C(29)	120.5(5)	C(36)-C(35)-C(40)	118.5(5)
C(36)-C(35)-P(2)	118.0(4)	C(40)-C(35)-P(2)	123.4(4)
C(35)-C(36)-C(37)	119.5(6)	C(38)-C(37)-C(36)	120.9(6)
C(37)-C(38)-C(39)	120.3(5)	C(38)-C(39)-C(40)	122.3(6)
C(39)-C(40)-C(35)	118.5(6)	C(46)-C(41)-C(42)	119.9(4)
C(46)-C(41)-P(2)	117.7(4)	C(42)-C(41)-P(2)	122.4(3)
C(43)-C(42)-C(41)	120.9(5)	C(44)-C(43)-C(42)	120.7(6)
C(43)-C(44)-C(45)	119.3(5)	C(44)-C(45)-C(46)	113.1(4)
C(41)-C(46)-C(45)	125.9(4)	H(1A)-Ru(1A)-C(1A)	81(7)
H(1A)-Ru(1A)-C(2)	168(7)	C(1A)-Ru(1A)-C(2)	108.8(7)
H(1A)-Ru(1A)-P(1)	91(7)	C(1A)-Ru(1A)-P(1)	95.7(7)
C(2)-Ru(1A)-P(1)	95.7(2)	H(1A)-Ru(1A)-P(2)	76(7)
C(1A)-Ru(1A)-P(2)	101.9(8)	C(2)-Ru(1A)-P(2)	93.7(2)
P(1)-Ru(1A)-P(2)	156.26(11)	O(1A)-C(1A)-Ru(1A)	171.8(17)

Appendix 2: Crystallographic data, bond lengths and angles for 85a.

$RuH(CO)(PPh_3)_2(IEt_2Me_2')$ (85a)	
Empirical formula	$C_{46}H_{46}N_2OP_2Ru$
Formula weight	805.86
Temperature	150(2) K
Wavelength	0.71073 Å
Crystal system	Monoclinic
Space group	$P2_1/a$
Unit cell dimensions	a = 16.9680(1)Å $\alpha = 90^o$
	b = 10.5800(1)Å $\beta = 109.720(1)^o$
	c = 23.1530(2)Å $\gamma = 90^o$
Volume	3912.60(6) $Å^3$
Z	4
Density (calculated)	1.368 Mg/m^3
Absorption coefficient	0.520 mm^{-1}
F(000)	1672
Crystal size	0.15 x 0.15 x 0.10 mm
Theta range for data collection	3.85 to 27.47°
Index ranges	-22<=h<=22; -13<=k<=13; -29<=l<=30
Reflections collected	58667
Independent reflections	8901 [R(int) = 0.0497]
Reflections observed (>2σ)	7511
Data Completeness	0.995
Absorption correction	None
Refinement method	Full-matrix least-squares on F^2
Data / restraints / parameters	8901 / 5 / 479
Goodness-of-fit on F^2	1.042
Final R indices [I>2σ(I)]	$R^1 = 0.0290$ $wR_2 = 0.0665$
R indices (all data)	$R^1 = 0.0391$ $wR_2 = 0.0710$
Largest diff. peak and hole	0.648 and -0.660 $eÅ^{-3}$

Bond Lengths (Å) for $RuH(CO)(PPh_3)_2(IEt_2Me_2')$ (85a)			
Ru(1)-H(1)	1.6167	Ru(1)-C(1)	1.8646(18)
Ru(1)-C(2)	2.0900(19)	Ru(1)-C(6)	2.2098(18)
Ru(1)-P(2)	2.3218(5)	Ru(1)-P(3)	2.3315(5)
P(2)-C(29)	1.8442(19)	P(2)-C(41)	1.8454(19)
P(2)-C(35)	1.8457(19)	P(3)-C(17)	1.8392(19)
P(3)-C(11)	1.8424(18)	P(3)-C(23)	1.8437(19)
O(1)-C(1)	1.163(2)	N(2)-C(2)	1.356(2)
N(2)-C(4)	1.399(3)	N(2)-C(7)	1.461(3)
N(1)-C(2)	1.360(2)	N(1)-C(3)	1.387(3)
N(1)-C(5)	1.466(3)	C(3)-C(4)	1.350(3)
C(3)-C(9)	1.496(3)	C(4)-C(10)	1.493(3)
C(5)-H(5B)	0.916(10)	C(5)-H(5A)	0.917(9)
C(5)-C(6)	1.535(3)	C(6)-H(6B)	0.9474
C(6)-H(6A)	0.9993	C(7)-C(8)	1.519(3)
C(11)-C(16)	1.390(3)	C(11)-C(12)	1.396(3)
C(12)-C(13)	1.380(3)	C(13)-C(14)	1.386(3)
C(14)-C(15)	1.378(4)	C(15)-C(16)	1.389(3)
C(17)-C(18)	1.390(3)	C(17)-C(22)	1.395(3)
C(18)-C(19)	1.392(3)	C(19)-C(20)	1.378(3)
C(20)-C(21)	1.378(3)	C(21)-C(22)	1.384(3)
C(23)-C(28)	1.392(3)	C(23)-C(24)	1.397(3)
C(24)-C(25)	1.382(3)	C(25)-C(26)	1.381(3)
C(26)-C(27)	1.371(4)	C(27)-C(28)	1.397(3)
C(29)-C(34)	1.387(3)	C(29)-C(30)	1.397(3)
C(30)-C(31)	1.388(3)	C(31)-C(32)	1.379(3)
C(32)-C(33)	1.373(3)	C(33)-C(34)	1.393(3)
C(35)-C(40)	1.395(3)	C(35)-C(36)	1.396(3)
C(36)-C(37)	1.384(3)	C(37)-C(38)	1.383(3)
C(38)-C(39)	1.378(3)	C(39)-C(40)	1.390(3)
C(41)-C(42)	1.377(3)	C(41)-C(46)	1.391(3)
C(42)-C(43)	1.402(3)	C(43)-C(44)	1.362(4)
C(44)-C(45)	1.377(3)	C(45)-C(46)	1.380(3)

Bond Angles (°) for $RuH(CO)(PPh_3)_2(IEt_2Me_2')$ (85a)			
H(1)-Ru(1)-C(1)	89.3	H(1)-Ru(1)-C(2)	172.3
C(1)-Ru(1)-C(2)	98.46(8)	H(1)-Ru(1)-C(6)	95.3
C(1)-Ru(1)-C(6)	174.90(8)	C(2)-Ru(1)-C(6)	76.90(7)
H(1)-Ru(1)-P(2)	80.1	C(1)-Ru(1)-P(2)	88.26(6)
C(2)-Ru(1)-P(2)	99.83(5)	C(6)-Ru(1)-P(2)	90.43(5)
H(1)-Ru(1)-P(3)	85.1	C(1)-Ru(1)-P(3)	95.38(6)
C(2)-Ru(1)-P(3)	94.25(5)	C(6)-Ru(1)-P(3)	87.15(5)
P(2)-Ru(1)-P(3)	164.785(18)	C(29)-P(2)-C(41)	97.84(8)
C(29)-P(2)-C(35)	102.46(9)	C(41)-P(2)-C(35)	102.49(9)
C(29)-P(2)-Ru(1)	116.17(6)	C(41)-P(2)-Ru(1)	117.09(6)
C(35)-P(2)-Ru(1)	117.79(6)	C(17)-P(3)-C(11)	102.40(8)
C(17)-P(3)-C(23)	101.07(9)	C(11)-P(3)-C(23)	102.36(8)
C(17)-P(3)-Ru(1)	116.79(6)	C(11)-P(3)-Ru(1)	114.94(6)
C(23)-P(3)-Ru(1)	116.97(6)	C(2)-N(2)-C(4)	111.50(16)
C(2)-N(2)-C(7)	124.30(16)	C(4)-N(2)-C(7)	124.19(17)
C(2)-N(1)-C(3)	112.10(16)	C(2)-N(1)-C(5)	118.70(16)
C(3)-N(1)-C(5)	129.16(16)	O(1)-C(1)-Ru(1)	176.32(17)
N(2)-C(2)-N(1)	103.63(16)	N(2)-C(2)-Ru(1)	138.53(14)
N(1)-C(2)-Ru(1)	117.79(13)	C(4)-C(3)-N(1)	106.28(17)
C(4)-C(3)-C(9)	130.8(2)	N(1)-C(3)-C(9)	122.9(2)
C(3)-C(4)-N(2)	106.46(17)	C(3)-C(4)-C(10)	131.1(2)
N(2)-C(4)-C(10)	122.4(2)	H(5B)-C(5)-H(5A)	106.9(19)
H(5B)-C(5)-N(1)	107.4(14)	H(5A)-C(5)-N(1)	106.6(14)
H(5B)-C(5)-C(6)	112.0(14)	H(5A)-C(5)-C(6)	114.8(14)
N(1)-C(5)-C(6)	108.79(15)	H(6B)-C(6)-H(6A)	103.3
H(6B)-C(6)-C(5)	105.5	H(6A)-C(6)-C(5)	109.3
H(6B)-C(6)-Ru(1)	117.1	H(6A)-C(6)-Ru(1)	111.2
C(5)-C(6)-Ru(1)	109.96(12)	N(2)-C(7)-C(8)	112.10(19)
C(16)-C(11)-C(12)	118.19(18)	C(16)-C(11)-P(3)	123.75(15)
C(12)-C(11)-P(3)	117.76(14)	C(13)-C(12)-C(11)	121.53(19)
C(12)-C(13)-C(14)	119.4(2)	C(15)-C(14)-C(13)	119.9(2)
C(14)-C(15)-C(16)	120.6(2)	C(15)-C(16)-C(11)	120.3(2)
C(18)-C(17)-C(22)	118.49(18)	C(18)-C(17)-P(3)	122.83(15)
C(22)-C(17)-P(3)	118.58(14)	C(17)-C(18)-C(19)	120.16(19)

C(20)-C(19)-C(18)	120.8(2)	C(19)-C(20)-C(21)	119.3(2)
C(20)-C(21)-C(22)	120.4(2)	C(21)-C(22)-C(17)	120.77(19)
C(28)-C(23)-C(24)	117.96(18)	C(28)-C(23)-P(3)	122.79(16)
C(24)-C(23)-P(3)	119.25(15)	C(25)-C(24)-C(23)	121.2(2)
C(26)-C(25)-C(24)	120.0(2)	C(27)-C(26)-C(25)	119.9(2)
C(26)-C(27)-C(28)	120.4(2)	C(23)-C(28)-C(27)	120.5(2)
C(34)-C(29)-C(30)	118.04(18)	C(34)-C(29)-P(2)	121.73(14)
C(30)-C(29)-P(2)	120.22(15)	C(31)-C(30)-C(29)	120.6(2)
C(32)-C(31)-C(30)	120.4(2)	C(33)-C(32)-C(31)	119.74(19)
C(32)-C(33)-C(34)	120.2(2)	C(29)-C(34)-C(33)	121.04(19)
C(40)-C(35)-C(36)	117.85(18)	C(40)-C(35)-P(2)	123.76(16)
C(36)-C(35)-P(2)	118.33(14)	C(37)-C(36)-C(35)	121.26(19)
C(38)-C(37)-C(36)	120.1(2)	C(39)-C(38)-C(37)	119.7(2)
C(38)-C(39)-C(40)	120.4(2)	C(39)-C(40)-C(35)	120.7(2)
C(42)-C(41)-C(46)	118.30(18)	C(42)-C(41)-P(2)	125.04(16)
C(46)-C(41)-P(2)	116.66(15)	C(41)-C(42)-C(43)	120.2(2)
C(44)-C(43)-C(42)	120.4(2)	C(43)-C(44)-C(45)	120.0(2)
C(44)-C(45)-C(46)	119.7(2)	C(45)-C(46)-C(41)	121.3(2)

Appendix 3: Crystallographic data, bond lengths and angles for 58.

$RuH_2(CO)(PPh_3)_2(I^iPr)$ (58)	
Empirical formula	$C_{46}H_{48}N_2OP_2Ru$
Formula weight	807.87
Temperature	150(2) K
Wavelength	0.71073 Å
Crystal system	Monoclinic
Space group	$P2_1/n$
Unit cell dimensions	a = 9.5160(1)Å $\alpha = 90^o$
	b = 33.3440(3)Å $\beta = 110.250(1)^o$
	c = 13.4570(1)Å $\gamma = 90^o$
Volume	4006.01(6) $Å^3$
Z	4
Density (calculated)	1.339 Mg/m^3
Absorption coefficient	0.508 mm^{-1}
F(000)	1680
Crystal size	0.20 x 0.08 x 0.08 mm
Theta range for data collection	3.70 to 27.47 °.
Index ranges	-12<=h<=12; -43<=k<=43; -17<=l<=17
Reflections collected	40819
Independent reflections	8809 [R(int) = 0.0491]
Reflections observed (>2σ)	7844
Data Completeness	0.959
Absorption correction	Semi-empirical from equivalents
Max. and min. transmission	0.95 and 0.89
Refinement method	Full-matrix least-squares on F^2
Data / restraints / parameters	8809 / 2 / 471
Goodness-of-fit on F^2	1.072
Final R indices [I>2σ(I)]	R1 = 0.0316 wR2 = 0.0683
R indices (all data)	R1 = 0.0398 wR2 = 0.0709
Largest diff. peak and hole	0.411 and -0.844 $eÅ^{-3}$

Bond Lengths (Å) for $RuH_2(CO)(PPh_3)_2(I^iPr)$ (58)			
Ru(1)-C(1)	1.900(2)	Ru(1)-C(2)	2.1604(19)
Ru(1)-P(1)	2.2982(5)	Ru(1)-P(2)	2.3075(5)
P(1)-C(11)	1.845(2)	P(1)-C(23)	1.849(2)
P(1)-C(17)	1.8507(19)	P(2)-C(29)	1.8379(19)
P(2)-C(41)	1.8525(19)	P(2)-C(35)	1.8539(19)
O(1)-C(1)	1.151(2)	N(1)-C(2)	1.378(2)
N(1)-C(3)	1.387(3)	N(1)-C(5)	1.468(2)
N(2)-C(2)	1.369(2)	N(2)-C(4)	1.384(3)
N(2)-C(8)	1.471(2)	C(3)-C(4)	1.338(3)
C(5)-C(6)	1.518(3)	C(5)-C(7)	1.525(3)
C(8)-C(10)	1.517(3)	C(8)-C(9)	1.521(3)
C(11)-C(12)	1.392(3)	C(11)-C(16)	1.394(3)
C(12)-C(13)	1.396(3)	C(13)-C(14)	1.377(4)
C(14)-C(15)	1.382(4)	C(15)-C(16)	1.387(3)
C(17)-C(18)	1.391(3)	C(17)-C(22)	1.395(3)
C(18)-C(19)	1.395(3)	C(19)-C(20)	1.375(3)
C(20)-C(21)	1.385(3)	C(21)-C(22)	1.386(3)
C(23)-C(24)	1.391(3)	C(23)-C(28)	1.393(3)
C(24)-C(25)	1.390(3)	C(25)-C(26)	1.376(4)
C(26)-C(27)	1.383(4)	C(27)-C(28)	1.393(3)
C(29)-C(30)	1.396(3)	C(29)-C(34)	1.399(3)
C(30)-C(31)	1.388(3)	C(31)-C(32)	1.384(3)
C(32)-C(33)	1.389(3)	C(33)-C(34)	1.386(3)
C(35)-C(36)	1.394(3)	C(35)-C(40)	1.396(3)
C(36)-C(37)	1.385(3)	C(37)-C(38)	1.381(3)
C(38)-C(39)	1.380(3)	C(39)-C(40)	1.390(3)
C(41)-C(46)	1.392(3)	C(41)-C(42)	1.398(3)
C(42)-C(43)	1.389(3)	C(43)-C(44)	1.391(3)
C(44)-C(45)	1.374(3)	C(45)-C(46)	1.394(3)

Bond Angles (°) for $RuH_2(CO)(PPh_3)_2(I^iPr)$ (58)			
C(1)-Ru(1)-C(2)	100.10(8)	C(1)-Ru(1)-P(1)	96.90(6)
C(2)-Ru(1)-P(1)	99.03(5)	C(1)-Ru(1)-P(2)	94.13(6)
C(2)-Ru(1)-P(2)	100.42(5)	P(1)-Ru(1)-P(2)	155.549(19)
C(11)-P(1)-C(23)	100.45(9)	C(11)-P(1)-C(17)	101.83(9)
C(23)-P(1)-C(17)	100.01(9)	C(11)-P(1)-Ru(1)	119.18(6)
C(23)-P(1)-Ru(1)	116.06(7)	C(17)-P(1)-Ru(1)	116.26(6)
C(29)-P(2)-C(41)	102.63(8)	C(29)-P(2)-C(35)	97.52(8)
C(41)-P(2)-C(35)	102.34(9)	C(29)-P(2)-Ru(1)	118.50(6)
C(41)-P(2)-Ru(1)	117.10(7)	C(35)-P(2)-Ru(1)	115.72(6)
C(2)-N(1)-C(3)	111.65(16)	C(2)-N(1)-C(5)	126.54(17)
C(3)-N(1)-C(5)	121.81(16)	C(2)-N(2)-C(4)	112.30(16)
C(2)-N(2)-C(8)	124.93(16)	C(4)-N(2)-C(8)	122.53(16)
O(1)-C(1)-Ru(1)	176.19(18)	N(2)-C(2)-N(1)	102.37(16)
N(2)-C(2)-Ru(1)	128.12(13)	N(1)-C(2)-Ru(1)	129.14(13)
C(4)-C(3)-N(1)	106.99(18)	C(3)-C(4)-N(2)	106.68(18)
N(1)-C(5)-C(6)	110.66(18)	N(1)-C(5)-C(7)	110.85(18)
C(6)-C(5)-C(7)	112.26(18)	N(2)-C(8)-C(10)	109.90(16)
N(2)-C(8)-C(9)	110.82(17)	C(10)-C(8)-C(9)	112.11(17)
C(12)-C(11)-C(16)	118.2(2)	C(12)-C(11)-P(1)	124.56(16)
C(16)-C(11)-P(1)	117.26(16)	C(11)-C(12)-C(13)	121.0(2)
C(14)-C(13)-C(12)	119.7(2)	C(13)-C(14)-C(15)	120.1(2)
C(14)-C(15)-C(16)	120.2(2)	C(15)-C(16)-C(11)	120.8(2)
C(18)-C(17)-C(22)	117.67(18)	C(18)-C(17)-P(1)	122.54(16)
C(22)-C(17)-P(1)	119.77(15)	C(17)-C(18)-C(19)	121.0(2)
C(20)-C(19)-C(18)	120.4(2)	C(19)-C(20)-C(21)	119.46(19)
C(20)-C(21)-C(22)	120.1(2)	C(21)-C(22)-C(17)	121.4(2)
C(24)-C(23)-C(28)	118.6(2)	C(24)-C(23)-P(1)	120.63(16)
C(28)-C(23)-P(1)	120.64(17)	C(23)-C(24)-C(25)	120.6(2)
C(26)-C(25)-C(24)	120.6(2)	C(25)-C(26)-C(27)	119.4(2)
C(26)-C(27)-C(28)	120.5(2)	C(23)-C(28)-C(27)	120.4(2)
C(30)-C(29)-C(34)	118.48(17)	C(30)-C(29)-P(2)	115.83(14)
C(34)-C(29)-P(2)	125.25(15)	C(31)-C(30)-C(29)	120.89(18)
C(32)-C(31)-C(30)	120.01(19)	C(31)-C(32)-C(33)	119.73(19)
C(34)-C(33)-C(32)	120.43(18)	C(33)-C(34)-C(29)	120.37(19)

C(36)-C(35)-C(40)	117.75(18)	C(36)-C(35)-P(2)	119.56(15)
C(40)-C(35)-P(2)	122.67(14)	C(37)-C(36)-C(35)	121.04(19)
C(38)-C(37)-C(36)	120.5(2)	C(39)-C(38)-C(37)	119.49(19)
C(38)-C(39)-C(40)	120.17(19)	C(39)-C(40)-C(35)	121.07(18)
C(46)-C(41)-C(42)	118.12(18)	C(46)-C(41)-P(2)	121.58(15)
C(42)-C(41)-P(2)	120.27(15)	C(43)-C(42)-C(41)	120.8(2)
C(42)-C(43)-C(44)	120.2(2)	C(45)-C(44)-C(43)	119.5(2)
C(44)-C(45)-C(46)	120.5(2)	C(45)-C(46)-C(41)	120.88(19)

Appendix 4: Crystallographic data, bond lengths and angles for 62a.

$RuH(CO)(PPh_3)_2(I^iPr_2Me_2')$ (62a)	
Empirical formula	$C_{48}H_{50}N_2OP_2Ru$
Formula weight	833.91
Temperature	150(2) K
Wavelength	0.71073 Å
Crystal system	Monoclinic
Space group	$P2_1/n$
Unit cell dimensions	a = 15.2550(2)Å $\alpha = 90^o$
	b = 17.0150(2)Å $\beta = 107.396(1)^o$
	c = 16.4510(2)Å $\gamma = 90^o$
Volume	4074.77(9) $Å^3$
Z	4
Density (calculated)	1.359 Mg/m^3
Absorption coefficient	0.502 mm^{-1}
F(000)	1736
Crystal size	0.15 x 0.10 x 0.10 mm
Theta range for data collection	3.62 to 30.05°
Index ranges	-21<=h<=21; -23<=k<=23; -23<=l<=23
Reflections collected	75805
Independent reflections	11895 [R(int) = 0.0449]
Reflections observed (>2σ)	9340
Data Completeness	0.996
Absorption correction	Semi-empirical from equivalents
Max. and min. transmission	0.95 and 0.92
Refinement method	Full-matrix least-squares on F^2
Data / restraints / parameters	11895 / 3 / 505
Goodness-of-fit on F^2	1.013
Final R indices [I>2((I)]	R1 = 0.0300 wR2 = 0.0680
R indices (all data)	R1 = 0.0487 wR2 = 0.0748
Largest diff. peak and hole	0.561 and -0.682 eÅ-3

Bond Lengths (Å) for $RuH(CO)(PPh_3)_2(I^iPr_2Me_2)$ (62a)			
Ru(1)-H(1)	1.600(3)	Ru(1)-C(1)	1.8626(17)
Ru(1)-C(2)	2.0594(16)	Ru(1)-C(6)	2.2100(16)
Ru(1)-P(2)	2.3445(4)	Ru(1)-P(1)	2.4357(4)
P(1)-C(25)	1.8408(17)	P(1)-C(19)	1.8479(16)
P(1)-C(13)	1.8555(16)	P(2)-C(43)	1.8328(16)
P(2)-C(37)	1.8456(16)	P(2)-C(31)	1.8482(17)
O(1)-C(1)	1.165(2)	N(1)-C(2)	1.354(2)
N(1)-C(4)	1.391(2)	N(1)-C(5)	1.476(2)
N(2)-C(2)	1.369(2)	N(2)-C(3)	1.404(2)
N(2)-C(8)	1.468(2)	C(3)-C(4)	1.351(3)
C(3)-C(11)	1.496(2)	C(4)-C(12)	1.498(3)
C(5)-C(7)	1.523(2)	C(5)-C(6)	1.534(2)
C(8)-C(9)	1.517(3)	C(8)-C(10)	1.520(3)
C(13)-C(14)	1.397(2)	C(13)-C(18)	1.402(2)
C(14)-C(15)	1.397(2)	C(15)-C(16)	1.378(3)
C(16)-C(17)	1.383(3)	C(17)-C(18)	1.391(2)
C(19)-C(24)	1.392(2)	C(19)-C(20)	1.393(2)
C(20)-C(21)	1.392(3)	C(21)-C(22)	1.377(3)
C(22)-C(23)	1.379(3)	C(23)-C(24)	1.392(2)
C(25)-C(26)	1.395(2)	C(25)-C(30)	1.397(2)
C(26)-C(27)	1.390(3)	C(27)-C(28)	1.379(3)
C(28)-C(29)	1.383(3)	C(29)-C(30)	1.385(3)
C(31)-C(32)	1.394(2)	C(31)-C(36)	1.396(3)
C(32)-C(33)	1.392(3)	C(33)-C(34)	1.387(3)
C(34)-C(35)	1.376(3)	C(35)-C(36)	1.391(3)
C(37)-C(42)	1.389(2)	C(37)-C(38)	1.397(2)
C(38)-C(39)	1.390(2)	C(39)-C(40)	1.378(3)
C(40)-C(41)	1.368(3)	C(41)-C(42)	1.395(3)
C(43)-C(44)	1.396(2)	C(43)-C(48)	1.398(2)
C(44)-C(45)	1.386(2)	C(45)-C(46)	1.388(3)
C(46)-C(47)	1.378(3)	C(47)-C(48)	1.393(2)

Bond Angles (°) for RuH(CO)(PPh_3)$_2$($I^iPr_2Me_2'$) (62a)			
H(1)-Ru(1)-C(1)	86.5(7)	H(1)-Ru(1)-C(2)	81.7(8)
C(1)-Ru(1)-C(2)	97.63(7)	H(1)-Ru(1)-C(6)	79.2(7)
C(1)-Ru(1)-C(6)	165.25(7)	C(2)-Ru(1)-C(6)	76.72(6)
H(1)-Ru(1)-P(2)	82.1(8)	C(1)-Ru(1)-P(2)	86.52(5)
C(2)-Ru(1)-P(2)	162.97(4)	C(6)-Ru(1)-P(2)	95.15(4)
H(1)-Ru(1)-P(1)	169.3(7)	C(1)-Ru(1)-P(1)	103.40(5)
C(2)-Ru(1)-P(1)	92.97(4)	C(6)-Ru(1)-P(1)	90.59(4)
P(2)-Ru(1)-P(1)	102.152(15)	C(25)-P(1)-C(19)	101.81(8)
C(25)-P(1)-C(13)	101.62(7)	C(19)-P(1)-C(13)	98.90(8)
C(25)-P(1)-Ru(1)	115.16(5)	C(19)-P(1)-Ru(1)	119.45(5)
C(13)-P(1)-Ru(1)	116.95(5)	C(43)-P(2)-C(37)	101.15(7)
C(43)-P(2)-C(31)	99.73(7)	C(37)-P(2)-C(31)	101.33(7)
C(43)-P(2)-Ru(1)	120.35(5)	C(37)-P(2)-Ru(1)	112.12(5)
C(31)-P(2)-Ru(1)	119.09(5)	C(2)-N(1)-C(4)	112.11(14)
C(2)-N(1)-C(5)	119.10(13)	C(4)-N(1)-C(5)	128.72(14)
C(2)-N(2)-C(3)	110.84(14)	C(2)-N(2)-C(8)	121.85(14)
C(3)-N(2)-C(8)	127.30(14)	O(1)-C(1)-Ru(1)	172.66(16)
N(1)-C(2)-N(2)	104.01(14)	N(1)-C(2)-Ru(1)	118.57(11)
N(2)-C(2)-Ru(1)	137.37(12)	C(4)-C(3)-N(2)	106.64(15)
C(4)-C(3)-C(11)	128.37(18)	N(2)-C(3)-C(11)	124.91(17)
C(3)-C(4)-N(1)	106.40(15)	C(3)-C(4)-C(12)	130.61(17)
N(1)-C(4)-C(12)	122.94(16)	N(1)-C(5)-C(7)	109.20(13)
N(1)-C(5)-C(6)	107.45(12)	C(7)-C(5)-C(6)	112.28(14)
C(5)-C(6)-Ru(1)	110.50(10)	N(2)-C(8)-C(9)	112.94(16)
N(2)-C(8)-C(10)	111.99(15)	C(9)-C(8)-C(10)	113.18(17)
C(14)-C(13)-C(18)	117.72(15)	C(14)-C(13)-P(1)	122.96(13)
C(18)-C(13)-P(1)	119.30(12)	C(13)-C(14)-C(15)	120.93(17)
C(16)-C(15)-C(14)	120.35(18)	C(15)-C(16)-C(17)	119.69(17)
C(16)-C(17)-C(18)	120.31(18)	C(17)-C(18)-C(13)	120.99(17)
C(24)-C(19)-C(20)	118.16(16)	C(24)-C(19)-P(1)	117.88(13)
C(20)-C(19)-P(1)	123.71(13)	C(21)-C(20)-C(19)	120.62(17)
C(22)-C(21)-C(20)	120.42(18)	C(21)-C(22)-C(23)	119.72(17)
C(22)-C(23)-C(24)	120.08(18)	C(19)-C(24)-C(23)	120.95(17)
C(26)-C(25)-C(30)	117.74(15)	C(26)-C(25)-P(1)	122.10(13)

C(30)-C(25)-P(1)	119.89(12)	C(27)-C(26)-C(25)	120.73(17)
C(28)-C(27)-C(26)	120.70(18)	C(27)-C(28)-C(29)	119.23(18)
C(28)-C(29)-C(30)	120.33(17)	C(29)-C(30)-C(25)	121.22(16)
C(32)-C(31)-C(36)	118.19(16)	C(32)-C(31)-P(2)	118.74(14)
C(36)-C(31)-P(2)	122.97(13)	C(33)-C(32)-C(31)	120.82(19)
C(34)-C(33)-C(32)	120.14(19)	C(35)-C(34)-C(33)	119.63(18)
C(34)-C(35)-C(36)	120.47(19)	C(35)-C(36)-C(31)	120.70(18)
C(42)-C(37)-C(38)	118.15(15)	C(42)-C(37)-P(2)	122.76(13)
C(38)-C(37)-P(2)	119.09(12)	C(39)-C(38)-C(37)	120.78(17)
C(40)-C(39)-C(38)	120.10(18)	C(41)-C(40)-C(39)	119.90(17)
C(40)-C(41)-C(42)	120.54(19)	C(37)-C(42)-C(41)	120.53(18)
C(44)-C(43)-C(48)	118.59(15)	C(44)-C(43)-P(2)	118.40(12)
C(48)-C(43)-P(2)	122.86(12)	C(45)-C(44)-C(43)	120.57(16)
C(44)-C(45)-C(46)	120.31(17)	C(47)-C(46)-C(45)	119.76(16)
C(46)-C(47)-C(48)	120.31(16)	C(47)-C(48)-C(43)	120.44(16)

Appendix 5: Crystallographic data, bond lengths and angles for 59a.

$RuH_2(CO)(PPh_3)_2(I^*)$ (59a)	
Empirical formula	$C_{56}H_{52}N_2OP_2Ru$
Formula weight	932.01
Temperature	396(2) K
Wavelength	0.71073 Å
Crystal system	Monoclinic
Space group	P21
Unit cell dimensions	a = 10.4860(1)Å $\alpha = 90^o$
	b = 22.6220(3)Å $\beta = 92.417(1)^o$
	c = 19.8160(3)Å $\gamma = 90^o$
Volume	4696.46(10) $Å^3$
Z	4
Density (calculated)	1.318 Mg/m^3
Absorption coefficient	0.444 mm^{-1}
F(000)	1936
Crystal size	0.13 x 0.10 x 0.07 mm
Theta range for data collection	3.83 to 27.54 °.
Index ranges	-13<=h<=13; -29<=k<=29; -25<=l<=25
Reflections collected	84248
Independent reflections	21408 [R(int) = 0.0849]
Reflections observed (>2σ)	16125
Data Completeness	0.992
Absorption correction	Semi-empirical from equivalents
Max. and min. transmission	0.96 and 0.89
Refinement method	Full-matrix least-squares on F^2
Data / restraints / parameters	21408 / 5 / 1135
Goodness-of-fit on F^2	1.014
Final R indices [I>2σ(I)]	$R^1 = 0.0421$ $wR_2 = 0.0742$
R indices (all data)	$R^1 = 0.0750$ $wR_2 = 0.0820$
Absolute structure parameter	0.00
Largest diff. peak and hole	0.471 and -0.500 $eÅ^{-3}$

Bond Lengths (Å) for $RuH_2(CO)(PPh_3)_2(I^*)$ (59a)			
Ru(1)-C(1)	1.884(4)	Ru(1)-C(2)	2.136(3)
Ru(1)-P(2)	2.3028(9)	Ru(1)-P(1)	2.3084(9)
P(1)-C(21)	1.833(3)	P(1)-C(27)	1.843(3)
P(1)-C(33)	1.849(4)	P(2)-C(51)	1.835(4)
P(2)-C(45)	1.843(4)	P(2)-C(39)	1.844(4)
O(1)-C(1)	1.162(4)	N(1)-C(3)	1.378(4)
N(1)-C(2)	1.381(4)	N(1)-C(5)	1.484(5)
N(2)-C(2)	1.384(4)	N(2)-C(4)	1.386(5)
N(2)-C(13)	1.479(5)	C(3)-C(4)	1.338(6)
C(5)-C(6)	1.521(5)	C(5)-C(12)	1.528(5)
C(6)-C(7)	1.379(5)	C(6)-C(11)	1.380(5)
C(7)-C(8)	1.392(6)	C(8)-C(9)	1.359(6)
C(9)-C(10)	1.381(6)	C(10)-C(11)	1.387(6)
C(13)-C(20)	1.525(5)	C(13)-C(14)	1.530(5)
C(14)-C(15)	1.384(6)	C(14)-C(19)	1.397(5)
C(15)-C(16)	1.399(6)	C(16)-C(17)	1.356(7)
C(17)-C(18)	1.388(8)	C(18)-C(19)	1.402(7)
C(21)-C(22)	1.381(5)	C(21)-C(26)	1.397(5)
C(22)-C(23)	1.388(6)	C(23)-C(24)	1.378(6)
C(24)-C(25)	1.376(5)	C(25)-C(26)	1.387(5)
C(27)-C(32)	1.386(5)	C(27)-C(28)	1.399(5)
C(28)-C(29)	1.376(5)	C(29)-C(30)	1.372(6)
C(30)-C(31)	1.370(6)	C(31)-C(32)	1.392(5)
C(33)-C(34)	1.383(5)	C(33)-C(38)	1.397(5)
C(34)-C(35)	1.389(6)	C(35)-C(36)	1.371(6)
C(36)-C(37)	1.370(6)	C(37)-C(38)	1.387(5)
C(39)-C(44)	1.390(5)	C(39)-C(40)	1.394(5)
C(40)-C(41)	1.381(5)	C(41)-C(42)	1.360(6)
C(42)-C(43)	1.365(6)	C(43)-C(44)	1.399(6)
C(45)-C(46)	1.396(5)	C(45)-C(50)	1.400(5)
C(46)-C(47)	1.420(5)	C(47)-C(48)	1.371(7)
C(48)-C(49)	1.371(7)	C(49)-C(50)	1.388(5)
C(51)-C(52)	1.380(5)	C(51)-C(56)	1.400(5)
C(52)-C(53)	1.397(5)	C(53)-C(54)	1.382(5)

C(54)-C(55)	1.385(6)	C(55)-C(56)	1.368(5)
Ru(1A)-C(1A)	1.885(4)	Ru(1A)-C(2A)	2.142(3)
Ru(1A)-P(2A)	2.2943(9)	Ru(1A)-P(1A)	2.2999(9)
P(1A)-C(33A)	1.837(3)	P(1A)-C(21A)	1.841(4)
P(1A)-C(27A)	1.844(4)	P(2A)-C(51A)	1.834(4)
P(2A)-C(45A)	1.839(4)	P(2A)-C(39A)	1.846(4)
O(1A)-C(1A)	1.170(4)	N(1A)-C(3A)	1.377(4)
N(1A)-C(2A)	1.380(4)	N(1A)-C(5A)	1.478(5)
N(2A)-C(2A)	1.382(4)	N(2A)-C(4A)	1.388(5)
N(2A)-C(13A)	1.479(5)	C(3A)-C(4A)	1.321(5)
C(5A)-C(6A)	1.492(5)	C(5A)-C(12A)	1.534(5)
C(6A)-C(7A)	1.377(5)	C(6A)-C(11A)	1.403(5)
C(7A)-C(8A)	1.406(6)	C(8A)-C(9A)	1.351(6)
C(9A)-C(10A)	1.374(6)	C(10A)-C(11A)	1.381(6)
C(13A)-C(20A)	1.519(5)	C(13A)-C(14A)	1.524(5)
C(14A)-C(15A)	1.387(5)	C(14A)-C(19A)	1.389(6)
C(15A)-C(16A)	1.390(6)	C(16A)-C(17A)	1.376(6)
C(17A)-C(18A)	1.370(6)	C(18A)-C(19A)	1.392(6)
C(21A)-C(22A)	1.389(5)	C(21A)-C(26A)	1.395(5)
C(22A)-C(23A)	1.375(6)	C(23A)-C(24A)	1.383(6)
C(24A)-C(25A)	1.374(6)	C(25A)-C(26A)	1.390(6)
C(27A)-C(32A)	1.390(5)	C(27A)-C(28A)	1.394(5)
C(28A)-C(29A)	1.382(6)	C(29A)-C(30A)	1.372(6)
C(30A)-C(31A)	1.376(6)	C(31A)-C(32A)	1.385(5)
C(33A)-C(34A)	1.384(5)	C(33A)-C(38A)	1.404(5)
C(34A)-C(35A)	1.399(6)	C(35A)-C(36A)	1.367(6)
C(36A)-C(37A)	1.372(5)	C(37A)-C(38A)	1.374(5)
C(39A)-C(40A)	1.386(5)	C(39A)-C(44A)	1.394(5)
C(40A)-C(41A)	1.389(5)	C(41A)-C(42A)	1.389(6)
C(42A)-C(43A)	1.360(6)	C(43A)-C(44A)	1.397(6)
C(45A)-C(50A)	1.381(5)	C(45A)-C(46A)	1.384(6)
C(46A)-C(47A)	1.389(6)	C(47A)-C(48A)	1.378(7)
C(48A)-C(49A)	1.373(7)	C(49A)-C(50A)	1.386(6)
C(51A)-C(56A)	1.369(5)	C(51A)-C(52A)	1.395(5)
C(52A)-C(53A)	1.394(5)	C(53A)-C(54A)	1.402(6)

C(54A)-C(55A)	1.374(6)	C(55A)-C(56A)	1.425(5)

Bond Angles (°) for $RuH_2(CO)(PPh_3)_2(I^*)$ (59a)			
C(1)-Ru(1)-C(2)	105.87(13)	C(1)-Ru(1)-P(2)	90.13(11)
C(2)-Ru(1)-P(2)	97.93(9)	C(1)-Ru(1)-P(1)	96.53(11)
C(2)-Ru(1)-P(1)	98.09(9)	P(2)-Ru(1)-P(1)	160.24(3)
C(21)-P(1)-C(27)	103.23(15)	C(21)-P(1)-C(33)	101.02(16)
C(27)-P(1)-C(33)	100.20(17)	C(21)-P(1)-Ru(1)	113.43(11)
C(27)-P(1)-Ru(1)	114.15(11)	C(33)-P(1)-Ru(1)	122.23(12)
C(51)-P(2)-C(45)	103.84(17)	C(51)-P(2)-C(39)	98.69(16)
C(45)-P(2)-C(39)	102.37(16)	C(51)-P(2)-Ru(1)	119.01(12)
C(45)-P(2)-Ru(1)	116.12(12)	C(39)-P(2)-Ru(1)	114.17(12)
C(3)-N(1)-C(2)	111.6(3)	C(3)-N(1)-C(5)	122.6(3)
C(2)-N(1)-C(5)	125.7(3)	C(2)-N(2)-C(4)	111.9(3)
C(2)-N(2)-C(13)	126.1(3)	C(4)-N(2)-C(13)	122.1(3)
O(1)-C(1)-Ru(1)	170.9(3)	N(1)-C(2)-N(2)	102.2(3)
N(1)-C(2)-Ru(1)	128.1(2)	N(2)-C(2)-Ru(1)	129.6(2)
C(4)-C(3)-N(1)	107.8(3)	C(3)-C(4)-N(2)	106.5(3)
N(1)-C(5)-C(6)	112.4(3)	N(1)-C(5)-C(12)	110.6(3)
C(6)-C(5)-C(12)	110.5(3)	C(7)-C(6)-C(11)	117.2(3)
C(7)-C(6)-C(5)	120.7(3)	C(11)-C(6)-C(5)	122.0(3)
C(6)-C(7)-C(8)	121.5(4)	C(9)-C(8)-C(7)	120.3(4)
C(8)-C(9)-C(10)	119.6(4)	C(9)-C(10)-C(11)	119.6(4)
C(6)-C(11)-C(10)	121.9(4)	N(2)-C(13)-C(20)	110.4(3)
N(2)-C(13)-C(14)	112.1(3)	C(20)-C(13)-C(14)	112.1(3)
C(15)-C(14)-C(19)	117.5(4)	C(15)-C(14)-C(13)	120.5(4)
C(19)-C(14)-C(13)	121.9(4)	C(14)-C(15)-C(16)	121.9(4)
C(17)-C(16)-C(15)	120.4(5)	C(16)-C(17)-C(18)	119.2(5)
C(17)-C(18)-C(19)	120.8(5)	C(14)-C(19)-C(18)	120.1(5)
C(22)-C(21)-C(26)	117.8(3)	C(22)-C(21)-P(1)	123.6(3)
C(26)-C(21)-P(1)	118.6(3)	C(21)-C(22)-C(23)	121.3(4)
C(24)-C(23)-C(22)	120.3(4)	C(25)-C(24)-C(23)	119.3(4)
C(24)-C(25)-C(26)	120.4(4)	C(25)-C(26)-C(21)	120.9(3)
C(32)-C(27)-C(28)	117.7(3)	C(32)-C(27)-P(1)	122.8(3)

C(28)-C(27)-P(1)	119.5(3)	C(29)-C(28)-C(27)	121.0(4)
C(30)-C(29)-C(28)	120.3(4)	C(29)-C(30)-C(31)	119.9(4)
C(30)-C(31)-C(32)	120.2(4)	C(27)-C(32)-C(31)	120.7(4)
C(34)-C(33)-C(38)	118.4(4)	C(34)-C(33)-P(1)	123.0(3)
C(38)-C(33)-P(1)	118.4(3)	C(33)-C(34)-C(35)	120.9(4)
C(36)-C(35)-C(34)	119.9(4)	C(37)-C(36)-C(35)	120.3(4)
C(36)-C(37)-C(38)	120.2(4)	C(37)-C(38)-C(33)	120.3(4)
C(44)-C(39)-C(40)	117.6(3)	C(44)-C(39)-P(2)	124.8(3)
C(40)-C(39)-P(2)	117.6(3)	C(41)-C(40)-C(39)	121.0(4)
C(42)-C(41)-C(40)	120.3(4)	C(41)-C(42)-C(43)	120.6(4)
C(42)-C(43)-C(44)	119.7(4)	C(39)-C(44)-C(43)	120.7(4)
C(46)-C(45)-C(50)	117.8(4)	C(46)-C(45)-P(2)	125.1(3)
C(50)-C(45)-P(2)	117.0(3)	C(45)-C(46)-C(47)	119.6(4)
C(48)-C(47)-C(46)	120.5(4)	C(49)-C(48)-C(47)	120.6(4)
C(48)-C(49)-C(50)	119.4(4)	C(49)-C(50)-C(45)	122.1(4)
C(52)-C(51)-C(56)	118.4(3)	C(52)-C(51)-P(2)	121.2(3)
C(56)-C(51)-P(2)	120.4(3)	C(51)-C(52)-C(53)	120.4(3)
C(54)-C(53)-C(52)	120.5(3)	C(53)-C(54)-C(55)	118.9(4)
C(56)-C(55)-C(54)	120.7(4)	C(55)-C(56)-C(51)	121.1(4)
C(1A)-Ru(1A)-C(2A)	104.42(14)	C(1A)-Ru(1A)-P(2A)	90.72(11)
C(2A)-Ru(1A)-P(2A)	99.82(9)	C(1A)-Ru(1A)-P(1A)	95.68(11)
C(2A)-Ru(1A)-P(1A)	98.96(9)	P(2A)-Ru(1A)-P(1A)	157.95(3)
C(33A)-P(1A)-C(21A)	100.57(16)	C(33A)-P(1A)-C(27A)	102.46(15)
C(21A)-P(1A)-C(27A)	101.76(17)	C(33A)-P(1A)-Ru(1A)	115.06(11)
C(21A)-P(1A)-Ru(1A)	119.94(12)	C(27A)-P(1A)-Ru(1A)	114.53(11)
C(51A)-P(2A)-C(45A)	101.45(17)	C(51A)-P(2A)-C(39A)	102.77(17)
C(45A)-P(2A)-C(39A)	101.80(16)	C(51A)-P(2A)-Ru(1A)	118.37(12)
C(45A)-P(2A)-Ru(1A)	111.60(12)	C(39A)-P(2A)-Ru(1A)	118.33(12)
C(3A)-N(1A)-C(2A)	112.1(3)	C(3A)-N(1A)-C(5A)	123.7(3)
C(2A)-N(1A)-C(5A)	124.2(3)	C(2A)-N(2A)-C(4A)	111.0(3)
C(2A)-N(2A)-C(13A)	126.5(3)	C(4A)-N(2A)-C(13A)	122.5(3)
O(1A)-C(1A)-Ru(1A)	169.8(3)	N(1A)-C(2A)-N(2A)	102.1(3)
N(1A)-C(2A)-Ru(1A)	128.6(2)	N(2A)-C(2A)-Ru(1A)	129.2(2)
C(4A)-C(3A)-N(1A)	107.0(3)	C(3A)-C(4A)-N(2A)	107.9(3)
N(1A)-C(5A)-C(6A)	113.0(3)	N(1A)-C(5A)-C(12A)	110.2(3)

C(6A)-C(5A)-C(12A)	113.4(3)	C(7A)-C(6A)-C(11A)	117.0(4)
C(7A)-C(6A)-C(5A)	124.0(3)	C(11A)-C(6A)-C(5A)	118.9(3)
C(6A)-C(7A)-C(8A)	121.9(4)	C(9A)-C(8A)-C(7A)	119.1(4)
C(8A)-C(9A)-C(10A)	120.9(4)	C(9A)-C(10A)-C(11A)	120.0(4)
C(10A)-C(11A)-C(6A)	121.0(4)	N(2A)-C(13A)-C(20A)	110.6(3)
N(2A)-C(13A)-C(14A)	111.0(3)	C(20A)-C(13A)-C(14A)	112.4(3)
C(15A)-C(14A)-C(19A)	117.9(4)	C(15A)-C(14A)-C(13A)	121.9(4)
C(19A)-C(14A)-C(13A)	120.3(3)	C(14A)-C(15A)-C(16A)	120.9(4)
C(17A)-C(16A)-C(15A)	120.2(4)	C(18A)-C(17A)-C(16A)	119.8(4)
C(17A)-C(18A)-C(19A)	120.1(4)	C(14A)-C(19A)-C(18A)	121.1(4)
C(22A)-C(21A)-C(26A)	117.2(3)	C(22A)-C(21A)-P(1A)	118.5(3)
C(26A)-C(21A)-P(1A)	124.3(3)	C(23A)-C(22A)-C(21A)	121.8(4)
C(22A)-C(23A)-C(24A)	119.9(4)	C(25A)-C(24A)-C(23A)	120.2(4)
C(24A)-C(25A)-C(26A)	119.4(4)	C(25A)-C(26A)-C(21A)	121.6(4)
C(32A)-C(27A)-C(28A)	117.7(3)	C(32A)-C(27A)-P(1A)	120.2(3)
C(28A)-C(27A)-P(1A)	122.0(3)	C(29A)-C(28A)-C(27A)	120.7(4)
C(30A)-C(29A)-C(28A)	120.7(4)	C(29A)-C(30A)-C(31A)	119.6(4)
C(30A)-C(31A)-C(32A)	120.1(4)	C(31A)-C(32A)-C(27A)	121.1(4)
C(34A)-C(33A)-C(38A)	117.6(3)	C(34A)-C(33A)-P(1A)	123.4(3)
C(38A)-C(33A)-P(1A)	119.1(3)	C(33A)-C(34A)-C(35A)	120.3(4)
C(36A)-C(35A)-C(34A)	120.8(4)	C(35A)-C(36A)-C(37A)	119.6(4)
C(36A)-C(37A)-C(38A)	120.3(4)	C(37A)-C(38A)-C(33A)	121.4(3)
C(40A)-C(39A)-C(44A)	117.9(3)	C(40A)-C(39A)-P(2A)	116.9(3)
C(44A)-C(39A)-P(2A)	125.2(3)	C(39A)-C(40A)-C(41A)	121.3(4)
C(40A)-C(41A)-C(42A)	120.1(4)	C(43A)-C(42A)-C(41A)	119.1(4)
C(42A)-C(43A)-C(44A)	121.2(4)	C(39A)-C(44A)-C(43A)	120.3(4)
C(50A)-C(45A)-C(46A)	117.6(4)	C(50A)-C(45A)-P(2A)	118.3(3)
C(46A)-C(45A)-P(2A)	123.7(3)	C(45A)-C(46A)-C(47A)	121.6(4)
C(48A)-C(47A)-C(46A)	119.7(5)	C(49A)-C(48A)-C(47A)	119.5(4)
C(48A)-C(49A)-C(50A)	120.3(4)	C(45A)-C(50A)-C(49A)	121.3(4)
C(56A)-C(51A)-C(52A)	119.8(3)	C(56A)-C(51A)-P(2A)	119.1(3)
C(52A)-C(51A)-P(2A)	121.1(3)	C(53A)-C(52A)-C(51A)	121.0(3)
C(52A)-C(53A)-C(54A)	119.5(4)	C(55A)-C(54A)-C(53A)	119.2(4)
C(54A)-C(55A)-C(56A)	121.1(4)	C(51A)-C(56A)-C(55A)	119.2(4)

Appendix 6: Crystallographic data, bond lengths and angles for 55.

$RuH_2(CO)(PPh_3)_2(IMe_4)_2$ (55)	
Empirical formula	$C_{33}H_{41}N_4OPRu$
Formula weight	641.74
Temperature	150(2) K
Wavelength	0.71073 Å
Crystal system	Monoclinic
Space group	$P2_1/n$
Unit cell dimensions	a = 24.3590(3)Å $\alpha = 90^o$
	b = 11.1500(2)Å $\beta = 115.417(1)^o$
	c = 25.2540(3)Å $\gamma = 90^o$
Volume	6195.15(15) $Å^3$
Z	8
Density (calculated)	1.376 Mg/m^3
Absorption coefficient	0.590 mm^{-1}
F(000)	2672
Crystal size	0.25 x 0.05 x 0.03 mm
Theta range for data collection	5.48 to 27.49°
Index ranges	-31<=h<=30; -14<=k<=14; -32<=l<=32
Reflections collected	83544
Independent reflections	14033 [R(int) = 0.1033]
Reflections observed (>2σ)	10067
Data Completeness	0.986
Absorption correction	None
Refinement method	Full-matrix least-squares on F^2
Data / restraints / parameters	14033 / 4 / 754
Goodness-of-fit on F^2	1.105
Final R indices [I>2σ(I)]	$R^1 = 0.0484$ $wR_2 = 0.0850$
R indices (all data)	$R^1 = 0.0856$ $wR_2 = 0.1005$
Largest diff. peak and hole	1.106 and -0.699 $eÅ^{-3}$

Bond Lengths (Å) for $RuH_2(CO)(PPh_3)_2(IMe_4)_2$ (55)			
Ru(1)-H(1)	1.662(18)	Ru(1)-H(2)	1.698(18)
Ru(1)-C(1)	1.867(4)	Ru(1)-C(2)	2.086(4)
Ru(1)-C(9)	2.122(4)	Ru(1)-P(1)	2.2930(10)
Ru(2)-H(3)	1.656(18)	Ru(2)-H(4)	1.674(17)
Ru(2)-C(34)	1.889(4)	Ru(2)-C(35)	2.081(3)
Ru(2)-C(42)	2.124(4)	Ru(2)-P(2)	2.2968(9)
P(1)-C(22)	1.841(4)	P(1)-C(16)	1.848(4)
P(1)-C(28)	1.852(4)	P(2)-C(61)	1.846(4)
P(2)-C(49)	1.848(4)	P(2)-C(55)	1.851(4)
O(1)-C(1)	1.165(5)	O(2)-C(34)	1.155(5)
N(1)-C(2)	1.366(4)	N(1)-C(3)	1.399(5)
N(1)-C(5)	1.463(5)	N(2)-C(2)	1.370(5)
N(2)-C(4)	1.396(5)	N(2)-C(8)	1.466(5)
N(3)-C(9)	1.371(4)	N(3)-C(10)	1.400(5)
N(3)-C(12)	1.461(5)	N(4)-C(9)	1.369(5)
N(4)-C(11)	1.397(5)	N(4)-C(15)	1.465(5)
N(5)-C(35)	1.372(4)	N(5)-C(36)	1.401(5)
N(5)-C(38)	1.462(5)	N(6)-C(35)	1.368(4)
N(6)-C(37)	1.402(5)	N(6)-C(41)	1.459(5)
N(7)-C(42)	1.370(5)	N(7)-C(43)	1.398(5)
N(7)-C(45)	1.457(5)	N(8)-C(42)	1.364(4)
N(8)-C(44)	1.390(5)	N(8)-C(48)	1.469(5)
C(3)-C(4)	1.340(5)	C(3)-C(6)	1.504(5)
C(4)-C(7)	1.497(5)	C(10)-C(11)	1.347(5)
C(10)-C(13)	1.491(5)	C(11)-C(14)	1.494(5)
C(16)-C(21)	1.392(5)	C(16)-C(17)	1.398(5)
C(17)-C(18)	1.388(5)	C(18)-C(19)	1.384(6)
C(19)-C(20)	1.387(6)	C(20)-C(21)	1.393(5)
C(22)-C(27)	1.394(5)	C(22)-C(23)	1.399(5)
C(23)-C(24)	1.379(5)	C(24)-C(25)	1.381(6)
C(25)-C(26)	1.379(6)	C(26)-C(27)	1.390(5)
C(28)-C(33)	1.392(5)	C(28)-C(29)	1.395(5)
C(29)-C(30)	1.386(6)	C(30)-C(31)	1.385(6)
C(31)-C(32)	1.391(6)	C(32)-C(33)	1.390(5)

C(36)-C(37)	1.340(5)	C(36)-C(39)	1.492(5)
C(37)-C(40)	1.499(5)	C(43)-C(44)	1.355(6)
C(43)-C(46)	1.506(6)	C(44)-C(47)	1.489(6)
C(49)-C(54)	1.391(5)	C(49)-C(50)	1.396(5)
C(50)-C(51)	1.389(6)	C(51)-C(52)	1.389(6)
C(52)-C(53)	1.386(6)	C(53)-C(54)	1.379(5)
C(55)-C(56)	1.395(5)	C(55)-C(60)	1.398(5)
C(56)-C(57)	1.394(5)	C(57)-C(58)	1.376(6)
C(58)-C(59)	1.384(6)	C(59)-C(60)	1.377(5)
C(61)-C(62)	1.396(5)	C(61)-C(66)	1.398(5)
C(62)-C(63)	1.391(6)	C(63)-C(64)	1.370(7)
C(64)-C(65)	1.389(7)	C(65)-C(66)	1.392(6)

Bond Angles (°) for $RuH_2(CO)(PPh_3)_2(IMe_4)_2$ (55)			
H(1)-Ru(1)-H(2)	84.2(18)	H(1)-Ru(1)-C(1)	172.5(13)
H(2)-Ru(1)-C(1)	88.6(12)	H(1)-Ru(1)-C(2)	80.8(13)
H(2)-Ru(1)-C(2)	85.1(13)	C(1)-Ru(1)-C(2)	96.42(15)
H(1)-Ru(1)-C(9)	87.4(13)	H(2)-Ru(1)-C(9)	171.0(13)
C(1)-Ru(1)-C(9)	99.68(15)	C(2)-Ru(1)-C(9)	90.32(13)
H(1)-Ru(1)-P(1)	90.2(12)	H(2)-Ru(1)-P(1)	84.5(13)
C(1)-Ru(1)-P(1)	91.33(12)	C(2)-Ru(1)-P(1)	166.91(10)
C(9)-Ru(1)-P(1)	98.77(10)	H(3)-Ru(2)-H(4)	83.6(18)
H(3)-Ru(2)-C(34)	172.1(14)	H(4)-Ru(2)-C(34)	88.6(11)
H(3)-Ru(2)-C(35)	83.8(14)	H(4)-Ru(2)-C(35)	85.8(11)
C(34)-Ru(2)-C(35)	94.75(15)	H(3)-Ru(2)-C(42)	88.2(14)
H(4)-Ru(2)-C(42)	171.8(11)	C(34)-Ru(2)-C(42)	99.56(15)
C(35)-Ru(2)-C(42)	93.43(13)	H(3)-Ru(2)-P(2)	88.2(14)
H(4)-Ru(2)-P(2)	84.4(11)	C(34)-Ru(2)-P(2)	91.98(12)
C(35)-Ru(2)-P(2)	167.98(10)	C(42)-Ru(2)-P(2)	95.27(10)
C(22)-P(1)-C(16)	98.87(16)	C(22)-P(1)-C(28)	101.38(17)
C(16)-P(1)-C(28)	99.97(16)	C(22)-P(1)-Ru(1)	115.16(12)
C(16)-P(1)-Ru(1)	119.25(12)	C(28)-P(1)-Ru(1)	118.78(12)
C(61)-P(2)-C(49)	100.91(16)	C(61)-P(2)-C(55)	101.52(16)
C(49)-P(2)-C(55)	99.90(16)	C(61)-P(2)-Ru(2)	117.14(12)

C(49)-P(2)-Ru(2)	119.49(12)	C(55)-P(2)-Ru(2)	114.88(12)
C(2)-N(1)-C(3)	112.4(3)	C(2)-N(1)-C(5)	125.1(3)
C(3)-N(1)-C(5)	122.6(3)	C(2)-N(2)-C(4)	112.4(3)
C(2)-N(2)-C(8)	124.2(3)	C(4)-N(2)-C(8)	123.1(3)
C(9)-N(3)-C(10)	112.7(3)	C(9)-N(3)-C(12)	124.3(3)
C(10)-N(3)-C(12)	123.0(3)	C(9)-N(4)-C(11)	112.7(3)
C(9)-N(4)-C(15)	126.3(3)	C(11)-N(4)-C(15)	120.9(3)
C(35)-N(5)-C(36)	112.2(3)	C(35)-N(5)-C(38)	125.2(3)
C(36)-N(5)-C(38)	122.5(3)	C(35)-N(6)-C(37)	112.2(3)
C(35)-N(6)-C(41)	125.1(3)	C(37)-N(6)-C(41)	122.8(3)
C(42)-N(7)-C(43)	112.3(3)	C(42)-N(7)-C(45)	125.1(3)
C(43)-N(7)-C(45)	122.6(3)	C(42)-N(8)-C(44)	113.4(3)
C(42)-N(8)-C(48)	126.2(3)	C(44)-N(8)-C(48)	120.3(3)
O(1)-C(1)-Ru(1)	175.8(3)	N(1)-C(2)-N(2)	102.3(3)
N(1)-C(2)-Ru(1)	129.4(3)	N(2)-C(2)-Ru(1)	128.1(2)
C(4)-C(3)-N(1)	106.4(3)	C(4)-C(3)-C(6)	130.5(4)
N(1)-C(3)-C(6)	123.0(3)	C(3)-C(4)-N(2)	106.4(3)
C(3)-C(4)-C(7)	130.8(4)	N(2)-C(4)-C(7)	122.7(3)
N(4)-C(9)-N(3)	102.1(3)	N(4)-C(9)-Ru(1)	130.2(2)
N(3)-C(9)-Ru(1)	127.5(3)	C(11)-C(10)-N(3)	106.1(3)
C(11)-C(10)-C(13)	131.0(4)	N(3)-C(10)-C(13)	122.8(3)
C(10)-C(11)-N(4)	106.4(3)	C(10)-C(11)-C(14)	131.1(4)
N(4)-C(11)-C(14)	122.5(3)	C(21)-C(16)-C(17)	118.2(3)
C(21)-C(16)-P(1)	120.6(3)	C(17)-C(16)-P(1)	121.1(3)
C(18)-C(17)-C(16)	120.3(4)	C(19)-C(18)-C(17)	120.7(4)
C(18)-C(19)-C(20)	119.9(4)	C(19)-C(20)-C(21)	119.2(4)
C(16)-C(21)-C(20)	121.6(4)	C(27)-C(22)-C(23)	117.6(3)
C(27)-C(22)-P(1)	124.6(3)	C(23)-C(22)-P(1)	117.8(3)
C(24)-C(23)-C(22)	121.5(4)	C(23)-C(24)-C(25)	120.4(4)
C(26)-C(25)-C(24)	119.0(4)	C(25)-C(26)-C(27)	121.1(4)
C(26)-C(27)-C(22)	120.4(4)	C(33)-C(28)-C(29)	118.5(3)
C(33)-C(28)-P(1)	117.5(3)	C(29)-C(28)-P(1)	124.0(3)
C(30)-C(29)-C(28)	120.6(4)	C(29)-C(30)-C(31)	120.6(4)
C(30)-C(31)-C(32)	119.4(4)	C(31)-C(32)-C(33)	119.9(4)
C(32)-C(33)-C(28)	121.0(4)	O(2)-C(34)-Ru(2)	174.8(4)

N(6)-C(35)-N(5)	102.6(3)	N(6)-C(35)-Ru(2)	129.2(3)
N(5)-C(35)-Ru(2)	128.0(2)	C(37)-C(36)-N(5)	106.5(3)
C(37)-C(36)-C(39)	131.1(4)	N(5)-C(36)-C(39)	122.4(3)
C(36)-C(37)-N(6)	106.6(3)	C(36)-C(37)-C(40)	130.2(4)
N(6)-C(37)-C(40)	123.2(4)	N(8)-C(42)-N(7)	102.1(3)
N(8)-C(42)-Ru(2)	129.6(3)	N(7)-C(42)-Ru(2)	128.2(3)
C(44)-C(43)-N(7)	106.5(3)	C(44)-C(43)-C(46)	130.9(4)
N(7)-C(43)-C(46)	122.6(4)	C(43)-C(44)-N(8)	105.6(3)
C(43)-C(44)-C(47)	131.0(4)	N(8)-C(44)-C(47)	123.4(4)
C(54)-C(49)-C(50)	118.5(3)	C(54)-C(49)-P(2)	120.1(3)
C(50)-C(49)-P(2)	121.4(3)	C(51)-C(50)-C(49)	120.6(4)
C(52)-C(51)-C(50)	120.4(4)	C(53)-C(52)-C(51)	118.9(4)
C(54)-C(53)-C(52)	120.9(4)	C(53)-C(54)-C(49)	120.7(4)
C(56)-C(55)-C(60)	117.9(3)	C(56)-C(55)-P(2)	124.3(3)
C(60)-C(55)-P(2)	117.9(3)	C(57)-C(56)-C(55)	120.3(4)
C(58)-C(57)-C(56)	121.0(4)	C(57)-C(58)-C(59)	119.1(4)
C(60)-C(59)-C(58)	120.4(4)	C(59)-C(60)-C(55)	121.3(4)
C(62)-C(61)-C(66)	117.8(3)	C(62)-C(61)-P(2)	124.7(3)
C(66)-C(61)-P(2)	117.2(3)	C(63)-C(62)-C(61)	121.2(4)
C(64)-C(63)-C(62)	120.4(4)	C(63)-C(64)-C(65)	119.6(4)
C(64)-C(65)-C(66)	120.3(4)	C(65)-C(66)-C(61)	120.7(4)

Appendix 7: Crystallographic data, bond lengths and angles for 60.

$RuH_2(CO)(PPh_3)_2(IEt_2Me_2)_2$ (60)	
Empirical formula	$C_{37}H_{49}N_4OPRu$
Formula weight	697.84
Temperature	150(2) K
Wavelength	0.71073 Å
Crystal system	monoclinic
Space group	P $2_1/n$
Unit cell dimensions	a = 12.7760(2) Å α = 90 deg. b = 18.9650(3) Å β = 103.0120(10) deg. c = 14.7910(3) Å γ = 90 deg.
Volume	3491.79(11) A^3
Z, Calculated density	4, 1.327 Mg/m^3
Absorption coefficient	0.529 mm^-1
F(000)	1464
Crystal size	0.50 x 0.38 x 0.30 mm
Theta range for data collection	3.55 to 30.04 deg.
Limiting indices	-17<=h<=15, -26<=k<=22, -20<=l<=20
Reflections collected / unique	28501 / 10112 [R(int) = 0.0440]
Completeness to theta = 30.04	98.9 %
Max. and min. transmission	0.8575 and 0.7779
Refinement method	Full-matrix least-squares on F^2
Data / restraints / parameters	10112 / 0 / 409
Goodness-of-fit on F^2	1.053
Final R indices [I>2σ(I)]	R1 = 0.0354, wR2 = 0.0801
R indices (all data)	R1 = 0.0504, wR2 = 0.0876
Largest diff. peak and hole	0.744 and -0.692 e.A^-3

Bond Lengths (Å) for $RuH_2(CO)(PPh_3)_2(IEt_2Me_2)_2$ (60)			
Ru-C(19)	1.8615(19)	C(16)-C(17)	1.384(4)
Ru-C(30)	2.0951(18)	C(17)-C(18)	1.387(3)
Ru-C(20)	2.145(2)	C(19)-O	1.167(2)
Ru-P	2.3000(5)	N(1)-C(20)	1.370(2)
Ru-H(1A)	1.64(2)	N(1)-C(23)	1.399(3)
Ru-H(1B)	1.66(3)	N(1)-C(21)	1.456(3)
P-C(1)	1.8416(19)	N(2)-C(20)	1.376(3)
P-C(7)	1.8432(19)	N(2)-C(25)	1.398(3)
P-C(13)	1.8532(19)	N(2)-C(27)	1.465(3)
C(1)-C(6)	1.393(3)	C(21)-C(22)	1.523(3)
C(1)-C(2)	1.402(3)	C(23)-C(25)	1.342(3)
C(2)-C(3)	1.383(3)	C(23)-C(24)	1.490(3)
C(3)-C(4)	1.384(3)	C(25)-C(26)	1.487(3)
C(4)-C(5)	1.381(3)	C(27)-C(28)	1.513(3)
C(5)-C(6)	1.393(3)	N(3)-C(30)	1.376(2)
C(7)-C(8)	1.396(3)	N(3)-C(35)	1.401(2)
C(7)-C(12)	1.398(3)	N(3)-C(37)	1.461(3)
C(8)-C(9)	1.387(3)	N(4)-C(30)	1.369(2)
C(9)-C(10)	1.379(3)	N(4)-C(33)	1.392(2)
C(10)-C(11)	1.384(3)	N(4)-C(31)	1.455(2)
C(11)-C(12)	1.390(3)	C(31)-C(32)	1.504(3)
C(13)-C(18)	1.389(3)	C(33)-C(35)	1.341(3)
C(13)-C(14)	1.392(3)	C(33)-C(34)	1.498(3)
C(14)-C(15)	1.388(3)	C(35)-C(36)	1.496(3)
C(15)-C(16)	1.374(3)	C(37)-C(38)	1.509(3)

Bond Angles (°) for $RuH_2(CO)(PPh_3)_2(IEt_2Me_2)_2$ (60)			
C(19)-Ru-C(30)	93.72(8)	C(15)-C(14)-C(13)	121.4(2)
C(19)-Ru-C(20)	105.40(9)	C(16)-C(15)-C(14)	120.2(2)
C(30)-Ru-C(20)	89.90(7)	C(15)-C(16)-C(17)	119.3(2)
C(19)-Ru-P	99.36(6)	C(16)-C(17)-C(18)	120.4(2)
C(30)-Ru-P	163.30(5)	C(17)-C(18)-C(13)	121.1(2)
C(20)-Ru-P	96.54(5)	O-C(19)-Ru	174.0(2)

C(19)-Ru-H(1A)	168.9(8)	C(20)-N(1)-C(23)	112.08(18)
C(30)-Ru-H(1A)	88.3(8)	C(20)-N(1)-C(21)	124.28(18)
C(20)-Ru-H(1A)	85.5(8)	C(23)-N(1)-C(21)	123.54(18)
P-Ru-H(1A)	76.9(7)	C(20)-N(2)-C(25)	112.21(17)
C(19)-Ru-H(1B)	84.8(9)	C(20)-N(2)-C(27)	125.60(16)
C(30)-Ru-H(1B)	86.8(9)	C(25)-N(2)-C(27)	122.13(18)
C(20)-Ru-H(1B)	169.4(9)	N(1)-C(20)-N(2)	102.50(16)
P-Ru-H(1B)	84.1(9)	N(1)-C(20)-Ru	129.29(14)
H(1A)-Ru-H(1B)	84.4(11)	N(2)-C(20)-Ru	128.07(14)
C(1)-P-C(7)	101.11(9)	N(1)-C(21)-C(22)	113.01(19)
C(1)-P-C(13)	100.48(8)	C(25)-C(23)-N(1)	106.83(18)
C(7)-P-C(13)	99.65(9)	C(25)-C(23)-C(24)	130.1(2)
C(1)-P-Ru	115.21(6)	N(1)-C(23)-C(24)	122.9(2)
C(7)-P-Ru	116.03(6)	C(23)-C(25)-N(2)	106.37(19)
C(13)-P-Ru	121.15(6)	C(23)-C(25)-C(26)	129.4(2)
C(6)-C(1)-C(2)	118.29(18)	N(2)-C(25)-C(26)	124.2(2)
C(6)-C(1)-P	124.07(15)	N(2)-C(27)-C(28)	113.87(18)
C(2)-C(1)-P	117.35(14)	C(30)-N(3)-C(35)	111.89(16)
C(3)-C(2)-C(1)	120.98(19)	C(30)-N(3)-C(37)	125.41(16)
C(2)-C(3)-C(4)	119.8(2)	C(35)-N(3)-C(37)	122.68(16)
C(5)-C(4)-C(3)	120.2(2)	C(30)-N(4)-C(33)	112.27(16)
C(4)-C(5)-C(6)	120.1(2)	C(30)-N(4)-C(31)	125.23(16)
C(5)-C(6)-C(1)	120.5(2)	C(33)-N(4)-C(31)	122.40(16
C(8)-C(7)-C(12)	118.49(18)	N(4)-C(30)-N(3)	102.53(15)
C(8)-C(7)-P	121.89(15)	N(4)-C(30)-Ru	127.60(13)
C(12)-C(7)-P	119.54(15)	N(3)-C(30)-Ru	129.84(13)
C(9)-C(8)-C(7)	120.8(2)	N(4)-C(31)-C(32)	112.15(18)
C(10)-C(9)-C(8)	120.2(2)	C(35)-C(33)-N(4)	106.90(17)
C(9)-C(10)-C(11)	119.8(2)	C(35)-C(33)-C(34)	130.65(19)
C(10)-C(11)-C(12)	120.4(2)	N(4)-C(33)-C(34)	122.39(18)
C(11)-C(12)-C(7)	120.3(2)	C(33)-C(35)-N(3)	106.41(17)
C(18)-C(13)-C(14)	117.58(18)	C(33)-C(35)-C(36)	130.5(2)
C(18)-C(13)-P	118.65(15)	N(3)-C(35)-C(36)	123.05(19)
C(14)-C(13)-P	123.64(16)	N(3)-C(37)-C(38)	113.54(18)

Appendix 8: Crystallographic data, bond lengths and angles for 88.

$C_{54}H_{43}O_5P_2Ru$ (88)	
Empirical formula	$C_{54}H_{43}O_5P_2Ru$
Formula weight	934.89
Temperature	150(2) K
Wavelength	0.71073 A
Crystal system	triclinic
Space group	$P\bar{1}$
Unit cell dimensions	a = 12.3740(3) A α = 68.4310(10) ° b = 13.5060(3) A β = 86.4160(10) ° c = 14.6780(4) A γ = 78.8500(10) °
Volume	2238.10(10) A^3
Z, Calculated density	2, 1.387 Mg/m^3
Absorption coefficient	0.471 mm^{-1}
F(000)	962
Crystal size	0.50 x 0.30 x 0.20 mm
Theta range for data collection	4.11 to 27.52 °
Limiting indices	-15<=h<=16, -17<=k<=17, -19<=l<=19
Reflections collected / unique	39181 / 10074 [R(int) = 0.0663]
Completeness to theta = 30.04	97.6 %
Max. and min. transmission	0.9117 and 0.7986
Refinement method	Full-matrix least-squares on F^2
Data / restraints / parameters	10074 / 0 / 559
Goodness-of-fit on F^2	1.141
Final R indices [I>2σ(I)]	R1 = 0.0604, wR2 = 0.1423
R indices (all data)	R1 = 0.0767, wR2 = 0.1547
Largest diff. peak and hole	1.634 and -0.935 $e.A^{-3}$

Bond Lengths (Å) for $C_{54}H_{43}O_5P_2Ru$ (88)			
Ru-C(51)	1.824(4)	C(19)-C(24)	1.393(6)
Ru-O(4)	2.088(3)	C(19)-C(20)	1.404(6)
Ru-O(3)	2.155(3)	C(20)-C(21)	1.388(6)
Ru-O(2)	2.163(3)	C(21)-C(22)	1.383(7)
Ru-P(1)	2.3289(10)	C(22)-C(23)	1.377(7)
Ru-P(2)	2.3532(11)	C(23)-C(24)	1.402(6)
Ru-C(37)	2.512(4)	C(25)-C(30)	1.399(5)
P(1)-C(1)	1.827(4)	C(25)-C(26)	1.400(6)
P(1)-C(7)	1.831(4)	C(26)-C(27)	1.380(6)
P(1)-C(13)	1.835(4)	C(27)-C(28)	1.389(6)
P(2)-C(31)	1.826(4)	C(28)-C(29)	1.376(7)
P(2)-C(25)	1.827(4)	C(29)-C(30)	1.393(6)
P(2)-C(19)	1.831(4)	C(31)-C(32)	1.396(6)
O(1)-C(51)	1.159(5)	C(31)-C(36)	1.399(6)
O(2)-C(37)	1.279(5)	C(32)-C(33)	1.386(6)
O(3)-C(37)	1.268(5)	C(33)-C(34)	1.376(7)
O(4)-C(44)	1.282(5)	C(34)-C(35)	1.400(7)
O(5)-C(44)	1.231(5)	C(35)-C(36)	1.394(6)
C(1)-C(2)	1.393(6)	C(37)-C(38)	1.479(5)
C(1)-C(6)	1.401(6)	C(38)-C(39)	1.382(6)
C(2)-C(3)	1.399(6)	C(38)-C(43)	1.395(6)
C(3)-C(4)	1.391(8)	C(39)-C(40)	1.389(6)
C(4)-C(5)	1.384(9)	C(40)-C(41)	1.374(7)
C(5)-C(6)	1.392(7)	C(41)-C(42)	1.379(8)
C(7)-C(8)	1.390(6)	C(42)-C(43)	1.388(6)
C(7)-C(12)	1.393(6)	C(44)-C(45)	1.509(6)
C(8)-C(9)	1.401(6)	C(45)-C(46)	1.376(7)
C(9)-C(10)	1.389(7)	C(45)-C(50)	1.382(6)
C(10)-C(11)	1.374(7)	C(46)-C(47)	1.387(8)
C(11)-C(12)	1.405(6)	C(47)-C(48)	1.372(8)
C(13)-C(18)	1.395(6)	C(48)-C(49)	1.359(8)
C(13)-C(14)	1.404(6)	C(49)-C(50)	1.392(6)
C(14)-C(15)	1.403(7)	C(61)-C(62)	1.375(11)
C(15)-C(16)	1.366(8)	C(61)-C(63)#1	1.378(11)

C(16)-C(17)	1.376(7)	C(62)-C(63)	1.373(12)
C(17)-C(18)	1.381(6)	C(63)-C(61)#1	1.378(11)

Symmetry transformations used to generate equivalent atoms: #1 -x+2,-y,-z+1

Bond Angles (°) for $C_{54}H_{43}O_5P_2Ru$ (88)			
C(51)-Ru-O(4)	100.25(15)	C(10)-C(9)-C(8)	120.3(4)
C(51)-Ru-O(3)	103.24(14)	C(11)-C(10)-C(9)	119.9(4)
O(4)-Ru-O(3)	81.35(11)	C(10)-C(11)-C(12)	120.4(4)
C(51)-Ru-O(2)	164.04(14)	C(7)-C(12)-C(11)	119.8(4)
O(4)-Ru-O(2)	80.25(11)	C(18)-C(13)-C(14)	117.3(4)
O(3)-Ru-O(2)	60.93(10)	C(18)-C(13)-P(1)	121.5(3)
C(51)-Ru-P(1)	88.95(12)	C(14)-C(13)-P(1)	121.3(4)
O(4)-Ru-P(1)	86.51(8)	C(15)-C(14)-C(13)	120.5(5)
O(3)-Ru-P(1)	164.10(8)	C(16)-C(15)-C(14)	120.1(5)
O(2)-Ru-P(1)	106.98(8)	C(15)-C(16)-C(17)	120.3(5)
C(51)-Ru-P(2)	92.74(13)	C(16)-C(17)-C(18)	120.1(5)
O(4)-Ru-P(2)	165.37(8)	C(17)-C(18)-C(13)	121.6(4)
O(3)-Ru-P(2)	89.20(8)	C(24)-C(19)-C(20)	119.0(4)
O(2)-Ru-P(2)	85.41(8)	C(24)-C(19)-P(2)	122.5(3)
P(1)-Ru-P(2)	100.53(4)	C(20)-C(19)-P(2)	118.3(3)
C(51)-Ru-C(37)	133.55(15)	C(21)-C(20)-C(19)	120.4(4)
O(4)-Ru-C(37)	79.07(12)	C(22)-C(21)-C(20)	120.1(4)
O(3)-Ru-C(37)	30.32(12)	C(23)-C(22)-C(21)	120.2(4)
O(2)-Ru-C(37)	30.61(11)	C(22)-C(23)-C(24)	120.3(4)
P(1)-Ru-C(37)	136.73(10)	C(19)-C(24)-C(23)	119.9(4)
P(2)-Ru-C(37)	87.12(9)	C(30)-C(25)-C(26)	118.7(4)
C(1)-P(1)-C(7)	104.3(2)	C(30)-C(25)-P(2)	122.5(3)
C(1)-P(1)-C(13)	102.56(19)	O(3)-C(37)-Ru	59.07(19)
C(7)-P(1)-C(13)	103.49(19)	O(2)-C(37)-Ru	59.42(19)
C(1)-P(1)-Ru	114.95(14)	C(38)-C(37)-Ru	179.0(3)
C(7)-P(1)-Ru	117.76(13)	C(39)-C(38)-C(43)	120.0(4)
C(13)-P(1)-Ru	112.05(14)	C(39)-C(38)-C(37)	118.7(4)
C(31)-P(2)-C(25)	103.54(18)	C(43)-C(38)-C(37)	121.3(4)
C(31)-P(2)-C(19)	102.21(18)	C(38)-C(39)-C(40)	120.3(4)
C(25)-P(2)-C(19)	102.27(18)	C(41)-C(40)-C(39)	119.4(5)

C(31)-P(2)-Ru	122.02(13)	C(40)-C(41)-C(42)	121.0(4)
C(25)-P(2)-Ru	115.13(13)	C(41)-C(42)-C(43)	119.9(4)
C(19)-P(2)-Ru	109.27(13)	C(42)-C(43)-C(38)	119.3(4)
C(37)-O(2)-Ru	90.0(2)	O(5)-C(44)-O(4)	125.9(4)
C(37)-O(3)-Ru	90.6(2)	O(5)-C(44)-C(45)	119.8(4)
C(44)-O(4)-Ru	121.6(3)	O(4)-C(44)-C(45)	114.2(4)
C(2)-C(1)-C(6)	119.5(4)	C(46)-C(45)-C(50)	118.5(4)
C(2)-C(1)-P(1)	118.2(3)	C(46)-C(45)-C(44)	120.9(4)
C(6)-C(1)-P(1)	122.2(4)	C(50)-C(45)-C(44)	120.6(4)
C(1)-C(2)-C(3)	120.2(5)	C(45)-C(46)-C(47)	120.7(5)
C(4)-C(3)-C(2)	119.9(5)	C(48)-C(47)-C(46)	119.9(5)
C(5)-C(4)-C(3)	119.9(5)	C(49)-C(48)-C(47)	120.3(5)
C(4)-C(5)-C(6)	120.7(5)	C(48)-C(49)-C(50)	119.9(4)
C(5)-C(6)-C(1)	119.8(5)	C(45)-C(50)-C(49)	120.7(4)
C(8)-C(7)-C(12)	119.8(4)	O(1)-C(51)-Ru	177.2(4)
C(8)-C(7)-P(1)	119.8(3)	C(62)-C(61)-C(63)#1	120.1(9)
C(12)-C(7)-P(1)	120.0(3)	C(63)-C(62)-C(61)	119.3(7)
C(7)-C(8)-C(9)	119.8(4)	C(62)-C(63)-C(61)#1	120.6(9)

Symmetry transformations used to generate equivalent atoms: #1 -x+2,-y,-z+1

Ligands:

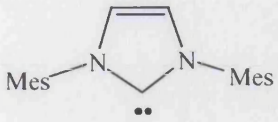

L17 = IMes

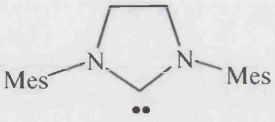

L18 = SIMes

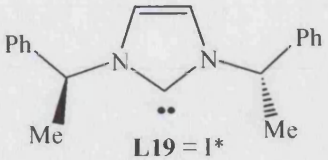

L19 = I*

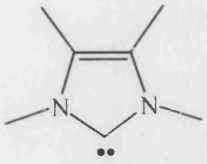

L2 = IMe_4

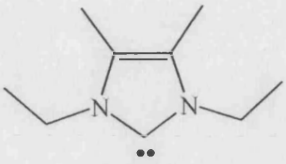

L20 = IEt_2Me_2

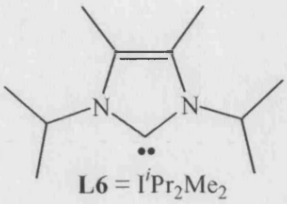

L6 = $I^iPr_2Me_2$

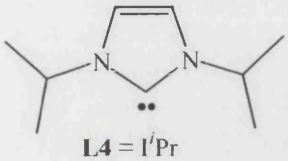

L4 = I^iPr

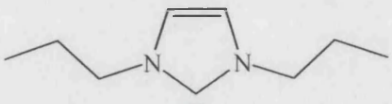

L22 = I^nPr

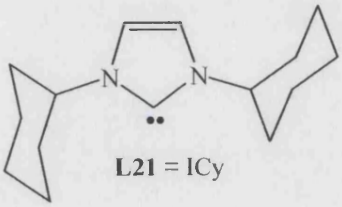

L21 = ICy

Ruthenium Complexes:

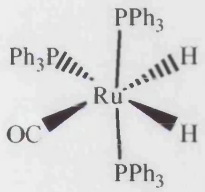

52

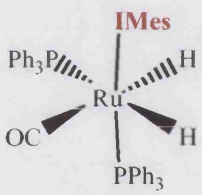

51

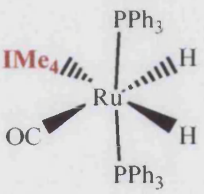

54

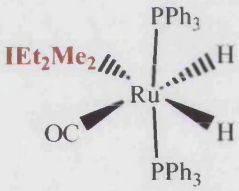

57

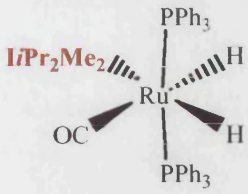

61

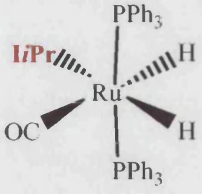

58

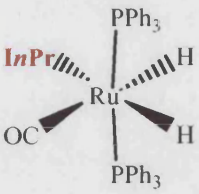

65

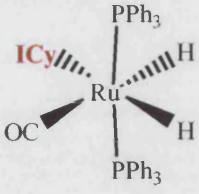

64

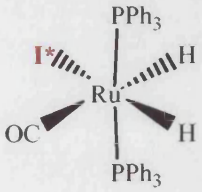

59a

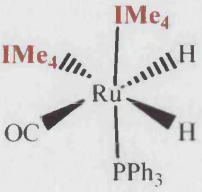

55

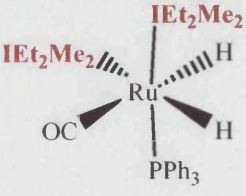

60

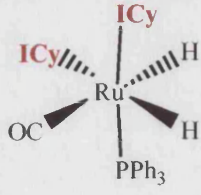

66

86

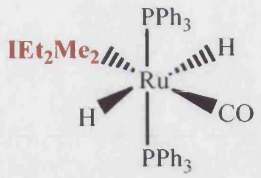

87

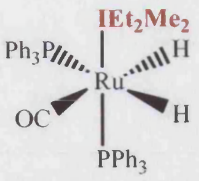

72

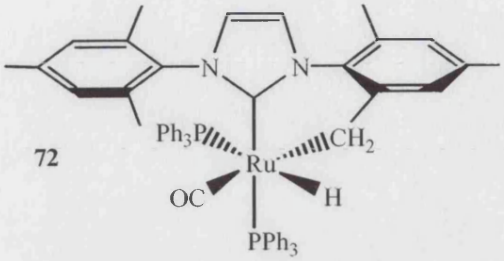

94a

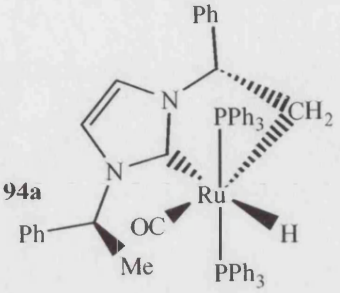

85a

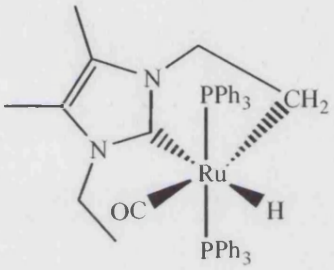

85b

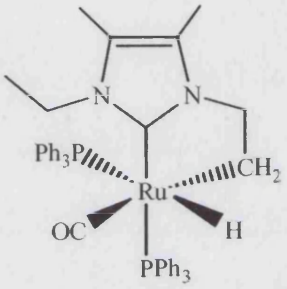

62b

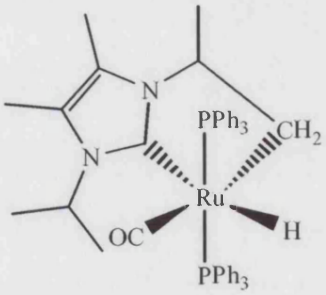

62a

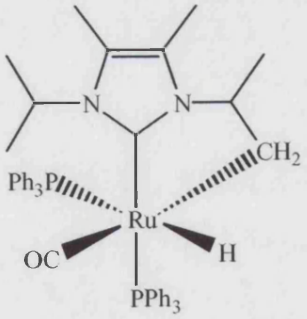

95

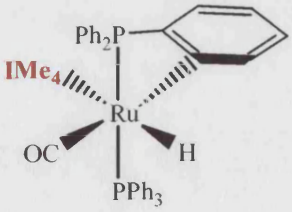
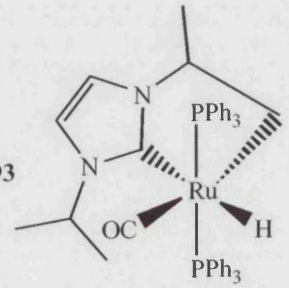
93